CARL
VON
OSSIETZKY
universität OLDENBURG

The influence of ammonia on Fischer-Tropsch synthesis and formation of N-containing compounds

Von der Fakultät für Mathematik und Naturwissenschaften
der Carl von Ossietzky Universität Oldenburg zur Erlangung des Grades und Titels eines
Doctor rerum naturalium
(Dr. rer. nat.)
angenommene Dissertation

von Herrn Robert Henkel
geboren am 27. April 1981 in Demmin

Gutachter: Prof. Dr. Dr. h.c. Frank Rößner

Carl von Ossietzky Universität Oldenburg

Zweitgutachter: Prof. Dr.-Ing. Michael Claeys

Universität Kapstadt, Republik Südafrika

Tag der Disputation: 21.12.2012

Für meinen Großvater

Acknowledgements

The present work was completed from March 2008 until December 2011 in the working group ‘Industrial Chemistry 2’ at the Institute for Pure and Applied Chemistry at the Carl von Ossietzky Universität Oldenburg.

I would like to thank Professor Frank Rößner for the interesting research topic, the supervision of this work and the permanent willingness for discussions. Moreover, I would like to thank him for the opportunities of several research stays in South Africa and Thailand.

I would like to thank Professor Michael Claeys for accepting me in his research group at the University of Cape Town as well as his encouragement on the research topic and his willingness to review this work.

I would like to thank Professor Jatuporn Wittayakun for accepting me in his research group in Korat and for all his kind help.

To all members of the ‘Industrial Chemistry 2’ at the Carl von Ossietzky Universität Oldenburg, thank you very much for the pleasant atmosphere. Special thanks to Stefan ‘Mac Gyver’ Schönen, for his assistance and experience during several repairs (without you, my car would be still damaged) and nice conversations on the balcony. Oliver, Wojtek, Philipp, Elena, both Lennarts, Simon and all others, thank you for an awesome time.

All members of the Department for Chemical Engineering in Cape Town and the Suranaree University of Technology in Korat, thank you for all the help and nice atmosphere. I would like to thank Nico, Nicole, Tawanda, Theresa, Chris, Pongthanawat, Waldo, Joe, Nat, Sek for their help, the braais and parties.

I would like to thank Emilian, Schwichti, Malte and Malte, Sören, Jörn, Jens and Jens, Anja, Lars, Olaf, Philipp, Timo, Heerke, Mareike und many others for their support, excellent music, plenty of funny parties and a beautiful time.

Special thanks to my family, a lot of things would not have been possible without their support and love.

For the financial support of my research stays I would like to thank the BMBF.

Danksagung

Die vorliegende Arbeit entstand in der Zeit von März 2008 bis Dezember 2011 in der Arbeitsgruppe „Technische Chemie 2“ des Institutes für Reine und Angewandte Chemie (IRAC) an der Carl von OssietzkyUniversität Oldenburg.

Herrn Professor Frank Rößner danke ich für die Überlassung des interessanten Themas, der Betreuung der Arbeit und der ständigen Diskussionsbereitschaft. Insbesonders danke ich ihm für die Möglichkeit für diverse Forschungsaufenthalte in Südafrika und Thailand während dieser Zeit.

Herrn Professor Michael Claeys danke ich für die Aufnahme in seinem Arbeitskreis an der Universität Kapstadt sowie seinen Anregungen auf dem Forschungsgebiet und der Bereitschaft zur Begutachtung dieser Arbeit.

Herrn Professor Jatuporn Wittayakun danke ich für die Aufnahme in seine Arbeitsgruppe in Korat und seiner ständigen Hilfsbereitschaft.

Allen Mitarbeitern der „Technischen Chemie 2“ der Carl von Ossietzky Universität Oldenburg danke ich für sehr nette Arbeitsatmosphäre. Stefan „MacGyver“ Schönen danke ich ganz besonders für seine Hilfe und Erfahrung bei diversen Reparaturen (ohne Dich hätte mein Auto noch heute keinen TÜV) und die angenehmen Unterhaltungen auf dem Balkon. Oliver, Wojtek, Philipp, Elena, Lennart , Lennart, Simon und vielen anderen danke ich für eine wundervolle Zeit.

Allen Mitarbeitern des Departments for Chemical Engineering in Kapstadt und der Suranaree University of Technology in Korat danke ich für all die Hilfsbereitschaft und das nette Arbeitsklima. Nico, Nicole, Tawanda, Theresa, Chris, Ponghtanawat, Waldo, Joe, Nat, Sek, vielen Dank für eure Hilfe im und ausserhalb des Labors, die vielen Braais und Parties.

Ich bedanke mich auch bei Emilian, Schwichti, Malte, Malte, Sören, Jörn, Jens, Jens, Anja, Lars, Olaf, Philipp, Timo, Heerke, Mareike und vielen anderen für die Unterstützung, die gute Musik, viele lustige Abende und eine tolle Zeit.

Ein ganz besonderer Dank gilt meiner Familie, ohne deren Rückhalt, Unterstützung und Liebe so vieles nicht möglich gewesen wäre.

Dem BMBF danke ich für die finanzielle Unterstützung meiner Auslandsaufenthalte.

Table of contents

List of figures

List of tables

Nomenclature

Notation		Unit
$A_{MS,I}$, $B_{MS,i}$	Calibration factors of compound i for GC-MS analysis	
A_i	Response area of compound i during gas chromatographic analysis	
CHx	Cyclohexane	
d	Average particle size	nm
$f_{i,FID}$	Response factor of compound i for GC-FID analysis	
$f_{i,TCD}$	Response factor of compound i for GC-TCD analysis	
H^R	Heat of reaction	kJ/mol
k	Debye-Scherer shape factor	
m/z	Mass to charge ratio	
N_C	Number of carbon atoms in a molecule	
n	Carbon number	
$\dot{n}_i$	Molar flow rate of compound i	mol/min
p_g	Chain growth probability	
p_i	Partial pressure of compound i	bar
Pr	Product	
P_{Total}	Total pressure	bar
Sp	Surface species	
S_i	Selectivity of compound i	mol%
t_{NH3}	Time of ammonia addition	min
$\dot{V}_i$	Volumetric flow rate of compound i	mL/min
W_N	Mass fraction of a product consisting of N carbon atoms	wt%

X_i	Conversion of reactant i	C-%, %, area%

Greek letters		Unit
α	Chain growth probability	
χ	Molar concentration	
β	Line broadening at FWHM	radians
λ	Wavelength	nm
ν	Stoichiometry	
θ	Diffraction angle	degree

Abbreviations	
AAS	Atomic Absorption Spectroscopy
ACN	Acetonitrile
ASF	Anderson-Schulz_Flory
CV	Check Valve
DEA	Diethylamine
DFT	Density Functional Theory
DMA	Dimethylamine
FID	Flame Ionization Detector
FT	Fischer-Tropsch
FTS	Fischer-Tropsch Synthesis
FWHM	Full Width at Half Maximum intensity
F	Flow control
GC	Gas Chromatograph

GHSV	Gas Hourly Space Velocity
HCN	Hydrogen cyanide
I.D.	Inner Diameter

Abbreviations	
IS	Internal Standard
LF	Line Filter
MEA	Monomethylamine
MFC	Mass Flow Controller
MMA	Monomethylamine
MS	Mass Spectrometer
MSD	Mass Selective Detector
MV	Magnetic Valve
NIST	National Institute of Standards and Technology
NTP	Normal Temperature and Pressure (0 °C, 1.013 bar)
NV	Needle Valve
O.D.	Outer Diameter
TCD	Thermal Conductivity Detector
TEA	Triethylamine
TEM	Transmission Electron Microscopy
TMA	Trimethylamine
TOF	Time-Of-Flight
TOS	Time On Stream
TPR	Temperature Programmed Reduction
V	one way Valve

XRD	X-Ray Diffraction

1 Introduction

The catalytic synthesis of methane from carbon monoxide (CO) and hydrogen (H_2) was first conducted in 1902 [1]. 20 years later, Franz Fischer and Hans Tropsch successfully synthesized long chain hydrocarbons by reacting synthesis gas (CO plus H_2) over transition metal catalysts at atmospheric pressure, a process which later became known as the Fischer-Tropsch synthesis (FT synthesis). Since these early days, significant research was invested and today the industrial Fischer-Tropsch synthesis represents one big counterpart to the petrochemical industry. Being a polymerization reaction, a wide variety of organic products such as gaseous products, petrol, diesel, olefins, oxygenated compounds or waxes can be obtained from the reaction [2]. Feedstock for the production of CO and H_2, can be coal, natural gas or biomass. Depending on the catalyst metal (e.g. iron, cobalt or ruthenium), reactor type and process parameters such as temperature, pressure, gas hourly space velocity or synthesis gas composition different product distributions can be obtained [2][3]. However, it is not feasible to synthesize a specific organic product with a selectivity of 100 % (with the exception of methane) and the Fischer-Tropsch products have to be separated and worked off after the reaction [4].

Organic nitrogen-containing compounds are of great importance in nature or daily life. Hence the industrial production of nitrogen-containing compounds is an essential branch in chemical industry. With production capacities of several million tons per year amino acids are produced as dietary supplement or pet food [6]. Amines, nitriles or amides are key chemicals and are used as pharmaceuticals, agricultural chemicals, solvents or intermediates in a number of industrial applications [5][6][7][8].

Many production routes to nitrogen-containing compounds such as amines, nitriles or amides are currently available and mostly heterogeneous catalysts are in use [7]. Different reactants based on petrochemical compounds and nitrogen sources such as ammonia, alkyl amines or hydrogen cyanide are employed in the processes [6]. An essential part in the production of amines is the hydroamination of alcohols by ammonia or other amines. Nitriles and organic products such as saturated or unsaturated hydrocarbons are also formed during hydroamination processes as side products [6][9]. This reaction is somewhat related to the Fischer-Tropsch synthesis since similar catalyst are employed and experimentally identified surface reactions as well as hypothesized reaction mechanisms show similarities to the FT synthesis.

The industrial production of nitrogen-containing compounds such as amines, nitriles or amides is based on chemical intermediates and at least two reaction steps are necessary for the whole process. This involves the synthesis of the chemical intermediate in one step and the conversion of this compound to nitrogen-containing products in a consecutive reaction step. Therefore, it would be beneficial from an economical point of view to produce amines, nitriles and amides in one single reaction. It was reported that nitrogen-containing compounds can be formed during the Fischer-Tropsch synthesis in the presence of ammonia or amines as nitrogen sources [10][11][12]. The Fischer-Tropsch process with its huge production capacities could play a key role and more valuable products could be obtained from the reaction. The conventional feedstock, based on limited crude oil reserves, which is required for the industrial production of N-containing products, could be expended or replaced by the use of coal, natural gas or biomass.

The scope of this work is to investigate under which process conditions it is feasible to synthesize organic nitrogen-containing compounds such as amines or nitriles under Fischer-Tropsch conditions in the presence of ammonia. Therefore, a Fischer-Tropsch lab scaled reaction unit, including the possibility of an ammonia co-feed during the reaction, will be realized. The reaction unit consists of a fixed-bed reactor and the experiments are conducted on iron and cobalt catalysts. Furthermore, analytical methods in order to identify and quantify organic products are used. Different gas chromatographic setups and sampling techniques are employed in order to analyze the reactant and product stream during the reactions.

From the results of the experiments it is tried to have an insight onto the reaction behavior during the formation of N-containing products. Based on these findings it is therefore tested if it is possible to increase or steer the product selectivities towards amines or nitriles during Fischer-Tropsch synthesis in the presence of ammonia.

Ammonia is also known as catalyst poison for transition metal catalysts and could affect their catalytic performance [13]. Hence, the influence of ammonia on the formation of conventional Fischer-Tropsch products (e.g. hydrocarbons or oxygenated compounds) as well as reactant conversion is also investigated in this work.

Einleitung

1902 gelang die erste katalytische Darstellung von Methan aus Kohlenmonoxid (CO) und Wasserstoff (H_2) [1]. 20 Jahre später konnten langkettige Kohlenwasserstoffe mittels der sogenannten Fischer-Tropsch Synthese (FT Synthese), benannt nach ihren Erfindern Franz Fischer und Hans Tropsch, hergestellt werden. Die Synthese ist an Übergangsmetallen als Katalysator bei Atmosphärendruck durchgeführt worden. Infolge intensiver Forschung ist die industriell durchgeführte Fischer-Tropsch Synthese in der heutigen Zeit ein wichtiger Gegenpart zu der Petrochemischen Industrie. Als Polymerisationsreaktion ist es möglich eine Vielzahl von organischen Produkten, wie Gase, Benzin, Diesel, Olefine, sauerstoffhaltige Verbindungen und Wachse mittels der Fischer-Tropsch Synthese herzustellen [2]. Das für die Reaktion benötigte Synthesegas (CO und H_2) kann aus Kohle, Erdgas oder Biomasse gewonnen werden. Abhängig von dem Katalysatormetall (Eisen, Kobalt oder Ruthenium), Reaktortyp oder Reaktionsparametern wie Temperatur, Druck, Verweilzeit oder der Synthesegaszusammensetzung ist es möglich die Produktselektivität zu variieren [2][3]. Es ist nicht möglich spezifische Produktselektivitäten von 100 % zu erzielen (die Ausnahme bildet Methan) und aus diesem Grund müssen die aus der Fischer-Tropsch Synthese gewonnen Produkte aufgearbeitet werden [4].

Stickstoffhaltige Verbindungen, zum Beispiel Aminosäuren oder Vitamine, besitzen eine große Bedeutung in der Natur oder dem täglichen Leben und die industrielle Produktion ist ein wichtiger Bestandteil der chemischen Industrie [6]. Aminosäuren werden mit Produktionskapazitäten von mehreren Millionen Tonnen pro Jahr hergestellt. Amine, Nitrile oder Amide sind Schlüsselchemikalien und kommen in der Pharmazie, in der Landwirtschaft, als Lösungsmittel oder chemischen Zwischenstufen in chemischen Industrie zum Einsatz [5][6][7][8].

Es existieren eine Vielzahl an Herstellungsmöglichkeiten für stickstoffhaltige Verbindungen und die Reaktionen sind hauptsächlich heterogen katalysiert [7]. Verschiedenste Edukte auf der Basis von petrochemischen Verbindungen werden hierbei mit Ammoniak, Alkylaminen oder Cyanwasserstoff umgesetzt [6]. Eine wichtige Rolle bei der Herstellung von Aminen nimmt die Hydroaminierung ein, bei der Alkohole mittels Ammoniak oder anderen Aminen an Übergangsmetallkatalysatoren umgesetzt werden. Als Nebenprodukte werden Nitrile und Kohlenwasserstoffe bei dieser Reaktion gebildet [6][9]. Da ähnliche Katalysatoren benutzt werden und einige experimentell bestätigte Oberflächenreaktionen sowie postulierte

Reaktionsmechanismen Gemeinsamkeiten aufweisen, zeigt diese Reaktion in gewisser Weise eine Ähnlichkeit zu der FT Synthese.

Die industrielle Herstellung von Aminen, Nitrilen oder Amiden basiert auf Primärchemikalien und durch deren weiterer Umsetzung sind in der Regel mindestens zwei Reaktionsschritte erforderlich. Aus ökonomischer Sicht ist es aus diesem Grund sinnvoll organische, stickstoffhaltige Verbindungen in einem einzigen Syntheseschritt herzustellen. Diesbezüglich ist in der wissenschaftlichen Literatur über die Herstellung von stickstoffhaltigen Verbindungen unter Fischer-Tropsch Bedingungen in Anwesenheit von Ammoniak oder Aminen berichtet worden [10][11][12]. Die Fischer-Tropsch Industrie mit ihren gewaltigen Produktionskapazitäten und der Unabhängkeit von Rohöl könnte hierbei eine Schlüsselrolle spielen und eine größere Vielzahl an Wertprodukten hergestellt werden. Alternativ zu der petrochemischen Industrie, könnten Kohle, Erdgas oder Biomasse als Ausgangsmaterialien genutzt werden.

Die vorliegende Arbeit widmet sich der Fragestellung, unter welchen Reaktionsbedingungen es möglich ist, stickstoffhaltigen Verbindungen wie zum Beispiel Amine oder Nitrile unter Fischer-Tropsch Bedingungen in der Anwesenheit von Ammoniak herzustellen. Für die katalytischen Fischer-Tropsch Experimente an eisen- und kobalt-haltigen Katalysatoren soll der Aufbau eines Festbettreaktors im Labormaßstab mit der Möglichkeit Ammoniak dem Synthesegas beizumischen, realisiert werden. Um die Zusammensetzung der Produkte quantitativ und qualitativ zu erfassen, werden analytischen Methoden angewandt unter Einbeziehung von verschiedensten gaschromatographischen Techniken.

Basierend auf den Ergebnissen der katalytischen Fischer-Tropsch Experimente unter dem Einfluss von Ammoniak soll ein näherer Einblick auf das Reaktionsgeschehen in Bezug auf die Bildung von N-haltigen Verbindungen erhalten werden. Nachfolgend wird in weiteren Versuchen untersucht, die Produktselektivitäten zu Aminen oder Nitrilen während der Fischer-Tropsch Synthese in Anwesenheit von Ammoniak zu steuern oder zu erhöhen.

Ammoniak ist ebenfalls als Katalysatorgift bekannt und bei chemischen Reaktionen an Übergangsmetallen als Katalysator, können aktive Zentren des Katalysators deaktiviert und die katalytische Aktivität beeinflusst werden [13]. Aus diesem Grund wird der Einfluss von Ammoniak auf den Umsatz der Edukte und die Selektivitäten hin zu konventionellen Fischer-Tropsch Produkten wie zum Beispiel Olefinen oder sauerstoffhaltigen Verbindungen, untersucht werden.

2 Literature review

2.1 Fischer-Tropsch synthesis

The Fischer-Tropsch synthesis (FT synthesis) is a heterogeneous catalyzed reaction of carbon monoxide and hydrogen to organic compounds and was developed in the 1920s by Franz Fischer and Hans Tropsch. Main products of the Fischer-Tropsch process are intermediates for the production of liquid fuels based on feedstock such as coal, natural gas and biomass. Much research was conducted in the recent years to improve catalytic performance or to shed more light on reaction mechanisms.

2.1.1 The Fischer-Tropsch reaction

In the Fischer-Tropsch synthesis, via a hydrogenation reaction of carbon monoxide (CO) and C-C couplings, a wide range of organic products with different chain lengths are formed [14]. The reaction is exothermic (ΔH^R (250 °C) = -158 kJ/mol per C_1 monomer) and water is formed as main co-product:

$$\mathrm{nCO} + 2\mathrm{nH_2} \rightarrow \left(\mathrm{CH_2}\right)_\mathrm{n} + \mathrm{nH_2O} \tag{2.1}$$

The reaction of carbon monoxide and hydrogen is activated by transition metals with iron- and cobalt-containing catalysts being used commercially [15].

Main products of Fischer-Tropsch synthesis are olefins and paraffins which are valuable intermediates for the production of sulphur free diesel, gasoline and specialty chemicals. Depending on catalyst metal, process parameters and reactor type, oxygenated compounds such as alcohols, aldehydes, carboxylic acids or ketones are synthesized, to a smaller extend too [16][17]. These operation conditions can also influence chain lengths of organic products. In general low temperatures (220 – 250°C) are applied for the production of long chain paraffins while at higher temperatures (320 – 350 °C) lighter products are obtained [17].

2.1.2 Formation of carbon dioxide

During the Fischer-Tropsch process the formation of carbon dioxide (CO_2) is possible which results in a low carbon efficiency of the reaction [2][17][18]. On iron catalysts, CO_2 is obtained from carbon monoxide and water in a side reaction, i.e. the Water-Gas Shift reaction (WGS , ΔH^R (250 °C) = -39.5 kJ/mol):

$$CO + H_2O \rightleftharpoons CO_2 + H_2 \tag{2.2}$$

The equilibrium conditions between H_2O and CO_2 can be found at 300 °C [18]. Since hydrogen is formed from the WGS reaction, hydrogen-low synthesis gas compositions (e.g. from coal or biomass) can be used during Fischer-Tropsch reactions on iron catalysts [2][19].

Iron catalysts undergo phase changes during Fischer-Tropsch reactions (section 2.4.3) and it is believed that magnetite phases (Fe_3O_4), which are formed beside iron carbides, are responsible for the formation of carbon dioxide [20].

Carbon dioxide can also be obtained via the disproportionation of CO in the so called Boudouard reaction:

$$2CO \rightleftharpoons C + CO_2 \tag{2.3}$$

This competing reaction is also exothermic (ΔH^R (270 °C) = -172.4 kJ/mol) and surface carbon can be formed which leads to catalyst deactivation [17][128].

While these side reactions can take place during FT synthesis on iron catalysts, cobalt catalysts on the other hand are known for their low CO_2 activity [17][22].

2.2 Proposed Fischer-Tropsch mechanisms

The Fischer-Tropsch synthesis is thought to be a surface polymerization reaction of carbon monoxide and hydrogen. The reactants adsorb onto the catalyst surface, can react further to organic or inorganic products and desorb again and a variety of reaction mechanisms are under discussion which will be presented in this section.

2.2.1 Formation of hydrocarbons

The proposed Fischer-Tropsch reaction pathways such as alkenyl, alkyl, CO insertion and enol mechanisms to the formation of hydrocarbons and oxygenated compounds are shown in Figure 2.1.

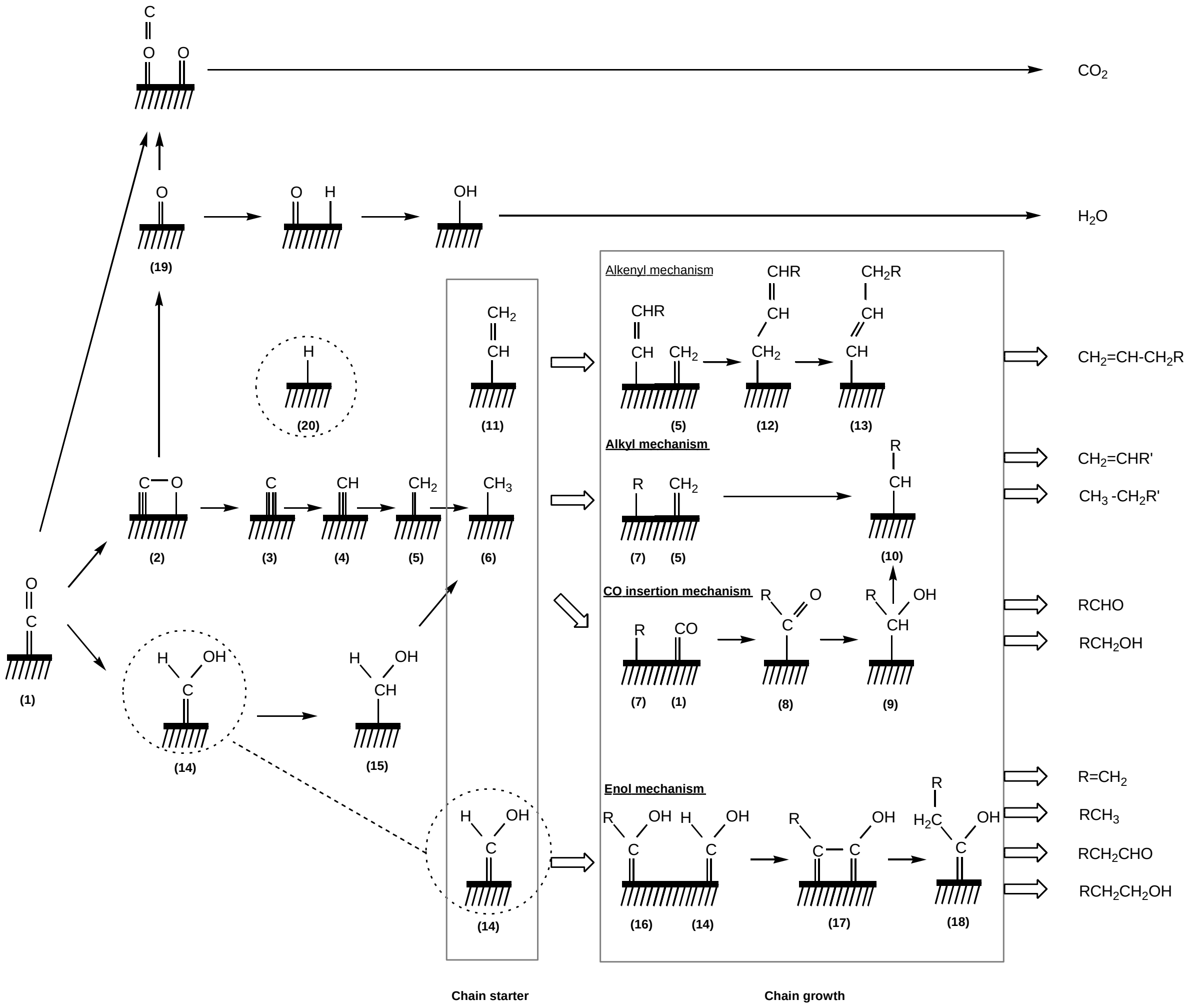

Figure 2.1: Schematic representation of different proposed Fischer-Tropsch reaction pathways (adapted from [23]).

Alkyl surface species (**6**), formed via dissociative adsorption of CO on the catalyst surface ((**2**) and (**3**)) and consecutive hydrogenation with adsorbed hydrogen, are thought to act as chain starter in the most accepted alkyl mechanism [16][24]. According to the CO insertion proposed by Pichler and Schulz [25], the same alkyl species (**6**) act as chain starter for the reaction. While the formation of alkyl surface species (**10**) during the alkyl mechanism takes place via insertion of methylene units (**5**) into a metal-alkyl bond (**7**), the same intermediate (**10**) is obtained from dehydration of surface species (**9**). The formation of *n*-paraffins via hydrogen addition or 1-olefins through β-H elimination results in chain termination. It is not possible to describe the formation of oxygenates with the alkyl reaction pathway and other formation routes are discussed instead (chapter 2.2.2).

During the alkenyl mechanism vinyl surface units (**11**) are formed which could initiate chain growth [26]. Further insertion of CH_2 monomers (**5**) lead to the formation of hydrocarbon with different chain lengths and addition of hydrogen to surface alkenyl species (**13**) lead to the formation of 1-olefins. A disadvantage of this mechanism is that there is no evidence for allyl unit (**12**) and furthermore, only the formation of 1-olefins can be explained.

Storch *et al.* [27] proposed an enolic surface unit (**14**) which is generated via the reaction of hydrogen with chemisorbed CO (enol mechanism). Chain growth takes place when two enolic surface species react and 1-olefins or oxygenate products are formed in a chain termination step. The authors [27] also suggest that enolic species (**14**) can act as a precursor for chain starter (**6**). However, no experimental evidence for these enolic surface units is available in the moment.

Depending on the catalyst used, CO_2 can be formed from chemisorbed carbon monoxide and surface oxygen (**19**). Hydroxyl surface units are obtained from the reaction of surface oxygen with adsorbed hydrogen and water as the main co-product can be formed with additional hydrogen.

2.2.2 Formation of oxygenated compounds

Little is known about the formation of oxygenates, in particular carboxylic acids and methyl-ketones. According to Pichler and Schulz [25], a CO insertion step is involved to produce surface acyl intermediates (**6**) which can be hydrogenated (**3**) as shown in Figure 2.2. A chain termination step via hydrogen addition to these two surface species is yielding aldehydes and alcohols respectively [28][29]. Another route to alcohols was postulated by

Johnston and Joyner [30] where an adsorbed hydroxyl group (**2**) reacts with a surface alkylidene species (**1**) to species (**3**) which can desorb with additional hydrogen to form the corresponding alcohol.

Experiments showed the ability of oxygen-containing compounds not only to re-adsorb but also to interact with other species [15]. In more detail, Cairns [14] showed via co-feeding experiments with C_8 oxygenates (namely 1-octanol, octanal, octanoic acid and 2-octanone) how carboxylic acids and methyl-ketones are linked together with the other oxygenates. He found that that the addition of a hydroxyl or alkyl group to the acyl intermediate (**6**) leads to the formation of carboxylic acids and ketones respectively as it was proposed by Schulz [61] before. Cairns [14] also affirmed that all oxygenates can readily interact reversible and interaction possibly leads through an acyl intermediate (Figure 2.2). An exception here is 2-octanone which can only be converted to a secondary alcohol via a hydrogenation reaction. In contrast to other literature [16], all oxygenates from the co-feeding tests did not hydrogenate to hydrocarbons nor incorporated into the growing chain a. A correlation between CO_2 partial pressure and FT selectivity towards carboxylic acids was described by Dry [31].

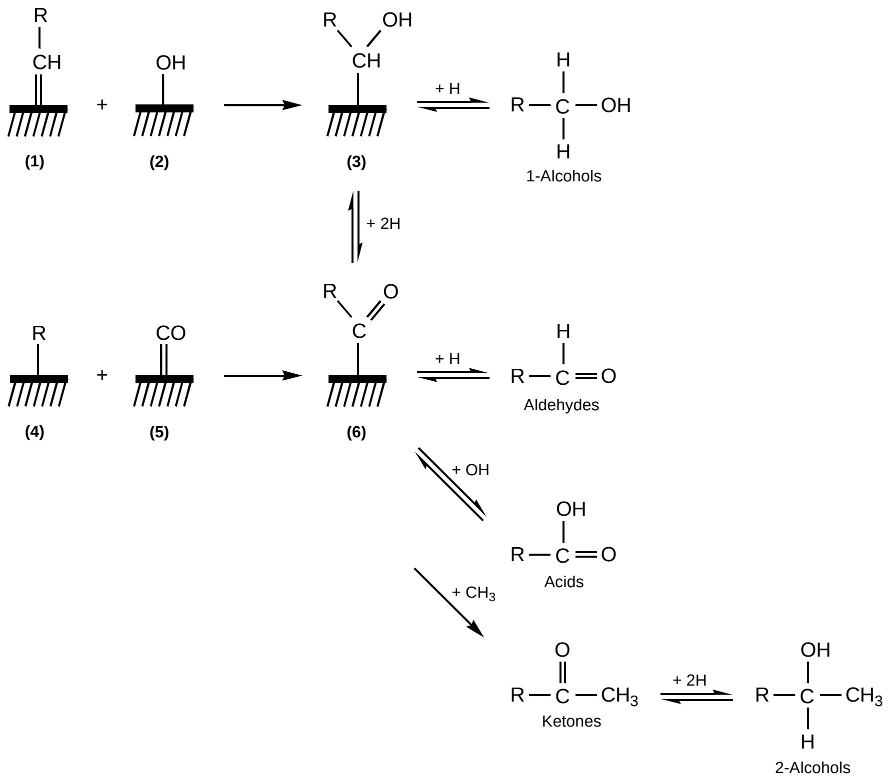

Figure 2.2: Reaction scheme of the formation of alcohols, aldehydes, methyl-ketones and carboxylic acids (adapted from [14]).

Another possible pathway to the formation of organic oxygenated compounds could be the hydroformylation of olefins, which was proven to occur by means of olefin co-feeding experiments with cobalt, iron or ruthenium catalysts [16]. Here, CO insertion on adsorbed olefins takes place but nor the formation of C_1 and C_2 oxygenates in the FT products can be explained with this reaction mechanism.

2.3 Fischer-Tropsch product spectrum

The Fischer-Tropsch synthesis is a polymerization reaction of carbon monoxide and hydrogen. Chain growth is expected to occur via a stepwise addition of C_1 monomer species and result in aliphatic organic products with different chain lengths [32]. Assuming that surface species ‘Sp’ can either desorb from a catalyst surface as a product ‘Pr’ or undergo chain growth g, one can propose a basic chain growth model (Figure 2.3) [15]. Neglecting the formation of oxygenates or branched hydrocarbons, the chain growth probability p_g (α) can be described.

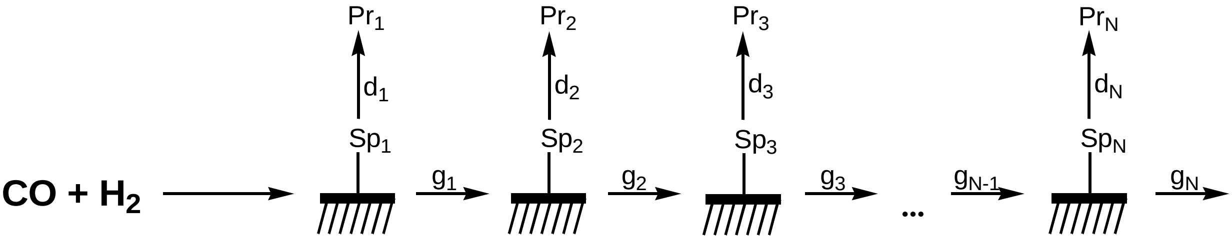

Figure 2.3: Kinetic scheme of chain growth and product desorption (adapted from [3]).

If α is independent of the carbon number, the theoretical chain length distribution can be described by the Anderson-Schulz-Flory (ASF) equation:

$$\lg\left(\frac{W_N}{N}\right) = N \cdot \lg\alpha + \lg\frac{1-\alpha}{\alpha} \qquad (2.4)$$

where W_N represents the mass fraction of a product consisting of N carbon atoms. Equation 2.4 indicates that during Fischer-Tropsch synthesis only methane can be obtained with a selectivity of 100 %. With increasing α values the average molecular weight of the product also increases (Figure 2.4).

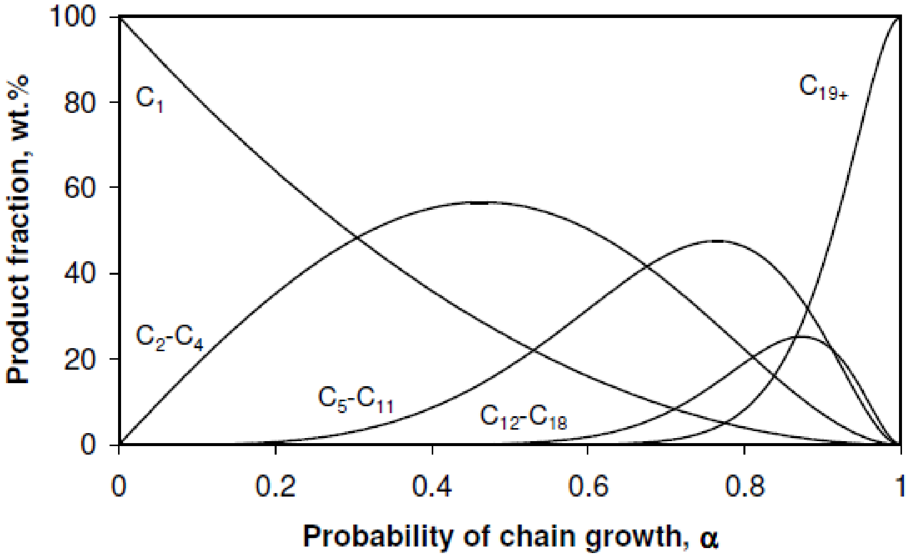

Figure 2.4: Product distribution as function of chain growth probability α on the basis of ideal ASF conditions (adapted from [15]).

2.3.1 Deviations from ideal distributions

When the molar product fraction (W_N/N) is plotted logarithmically against the carbon number, it would result in a straight line for ideal Anderson-Schulz-Flory distributions and the slope represents the chain growth probability [23]. Due to the ease methane formation and active catalytic centers, which only form methane, high mass fractions for C_1 can be observed in general [15][32]. A minimum in the C_2 fractions is often related to the high reactivity of ethene, which can be incorporated to long chain products [15]. In literature [31], a ‘double alpha’ effect after C_{10} products was reported, where in general linear plots are observed. This effect is still under debate and it has been ascribed to either being due to a primary or secondary effect [16]. Different catalysts sites with different chain growth probabilities or two chain growth mechanisms could be responsible for a primary effect [33][34]. Olefins, which are believed to be primary products during Fischer-Tropsch synthesis, can re-adsorb onto the catalyst surface (Figure 4.11) [35]. They can undergo isomerisation reactions to an olefin with an internal double bond, reincorporate into further chain growth or hydrogenate to the corresponding paraffin. Therefore, further chain growth from reinsertion of olefins could be accounted for different ASF deviations in a secondary step due to diffusion or solubility limitations for higher carbon numbers [35][36][37].

2.3.2 Factors affecting product selectivity

There are a variety of process parameters, which can influence the product selectivity in the Fischer-Tropsch synthesis (Table 2.1) [3][23]. Depending on reaction temperature, pressure, synthesis gas composition, residence time or the promotion of an iron catalyst with potassium, different product distributions can be obtained. However, only a few operating conditions and their effects will be described below.

Table 2.1: Effect of process conditions on the Fischer-Tropsch product selectivities: + increase with increasing parameter, - decrease with increasing parameter, ~no clear effect (adapted from [23]).

	Temperature	**Pressure**	**H_2:CO Ratio**	**Residence time**	**K** [1]
Methane selectivity	+	-	+	+	-
Chain growth	-	+	-	~	+
Chain branching	+	-	~	~	-
Olefin selectivity	~	~	-	-	+
Oxygenate selectivity	-	+	-	-	+
Carbon deposition	+	~	-	~	+

[1] Potassium loading of iron catalyst

The production of long chain hydrocarbons, i.e. high alpha values, is preferred at lower temperatures. With increasing temperature, the methane selectivity rises. Short chain hydrocarbons can be obtained with high H_2:CO ratios. Hydrogenation of olefins or Fischer-Tropsch surface intermediates lead to enhanced paraffin formation and lower oxygenate concentrations. Due to secondary reactions the residence time shows similar effects on the product selectivity. Potassium as a chemical promoter (see also chapter 2.4.1) can increase chain growth probabilities and formation of carbon on the catalyst surface. Side reactions are suppressed and higher oxygenate and olefin selectivities can be derived. The degree of chain branching can be lowered due to the presence of potassium on iron catalyst surfaces.

Depending on the catalyst metal which is used during FT synthesis different product compositions can be found, too. However, more detailed information will be given in the next chapter.

2.4 Catalysts for Fischer-Tropsch synthesis

Most of the transition metals are catalytically active for the Fischer-Tropsch synthesis. However, mainly iron- and cobalt-containing catalyst are employed in industrial applications [15][32]. While nickel catalysts show a high methanisation tendency [38], ruthenium shows the highest catalytic activity but is also the most expensive metal [4]. Iron catalysts are cheap, resistant against sulphur and produce high olefin and oxygenate contents. A disadvantage of iron catalysts is the relatively short life time and lower activity compared to cobalt catalysts [4]. Commercially, precipitated and fused iron catalysts are in use and chemical or reduction promoters are to be added [2] which has beneficial effects on the product selectivity (chapter 2.4.1). Due to its high price, cobalt is in general deposited as small particles on SiO_2, Al_2O_3 or other metal oxides in order to gain high surface areas, high thermal and chemical stability and mechanical strength. Cobalt is well suited for hydrogen-rich synthesis gas compositions (H_2:CO = 2:1) whereas iron catalyzes the Water-Gas Shift (WGS) reaction and synthesis gas with lower H_2:CO ratios can be used (chapter 2.1.2).

2.4.1 Chemical promoters

For the Fischer-Tropsch synthesis on iron catalysts, potassium has been used as a chemical promoter for many years in order to obtain more valuable products (e.g. olefins) from the reaction [39][40][63]. Potassium is known to enhance the CO binding strength, it also facilitates CO dissociation while lowering the strength of metal-hydrogen and metal-oxygen bonds [15][128]. As a consequence increased conversion of carbon monoxide to C_{5+} organic products, higher CO_2 selectivities and formation of carbides or free surface carbon can be observed. Undesired side reactions such as olefin isomerisation are suppressed and hydrogenation of olefins to the corresponding paraffins is reduced [3]. Due to the presence of potassium, secondary reactions of oxygenated compounds (e.g. hydrogenation to form a paraffin and incorporation into growing chains) are suppressed and increased selectivities to these compounds can be observed [16][35]. Similar effects on the selectivities are observed for potassium promoted cobalt catalysts [53]. But compared to iron, the catalytic activity of cobalt is reduced and a lower CO conversion was found. It should be noted that promotional effects of potassium are limited and excessive promotion with potassium mainly increases carburization rates [31]. Potassium in high concentrations could also block active sites of the catalyst which leads to catalyst deactivation [41].

2.4.2 Catalyst deactivation

Reactants, products or impurities can chemisorb irreversibly on metal surfaces influencing the activity and/or selectivity for any catalytic surface reaction. Hydrogen sulfide, carbonyl sulfide, arsenic, ammonia and metal carbonyls are the most common poisons for Fischer-Tropsch catalysts [13]. The feed gas quality is often the origin of catalyst poisons. When synthesis gas is derived from coal, poison contents of a few parts per billion can drastically reduce catalyst activity and life time during Fischer-Tropsch synthesis [13][15]. Especially when cobalt is used as catalyst, sulfur-containing compounds have to be removed before the synthesis. Depending on the feed material, the raw synthesis gas can also contain ammonia which has to be removed [42].

When metal catalysts are exposed to high temperatures, their catalytic activity can decrease. Reasons can be the formation of surface carbon [128] or deactivation processes due to sintering effects, which are related to a decrease of the catalyst surface because larger particles are formed [13]. The sintering mechanisms depend on the melting point of the metal and can be described by the Hüttig and Tamman temperature (Table 2.2) [43].

Table 2.2: Melting, Tamman and Hüttig temperatures for iron and cobalt [23][43].

Metal	**$T_{melting}$** (°C)	**T_{Tamman}** (°C)	**$T_{Hüttig}$** (°C)
Fe	1535	631	269
Co	1480	604	253

Upon reaching the Hüttig temperature defect atoms become mobile and can occupy non defect sites (surface recrystallisation). At the Tamman temperature atoms from the bulk will show mobility (bulk recrystallisation). At the melting temperature of the metal, the mobility will be so high that liquid phase behavior is observed. However, this deactivation process is irreversible and needs to be prevented.

2.4.3 Phase changes of catalysts under Fischer-Tropsch conditions

During the Fischer-Tropsch synthesis, transition metal catalysts such as iron or cobalt are exposed to numerous inorganic compounds and phase changes of the catalysts due to gas-solid reactions can be observed. As a consequence, the catalytic performance is affected and changes during the reaction with time on stream (TOS).

Metallic iron is not stable under normal Fischer-Tropsch conditions and undergoes various phase changes. Via oxidation and carburization reactions iron is rapidly converted into a mixture of magnetite (Fe_3O_4) and carbides [32].

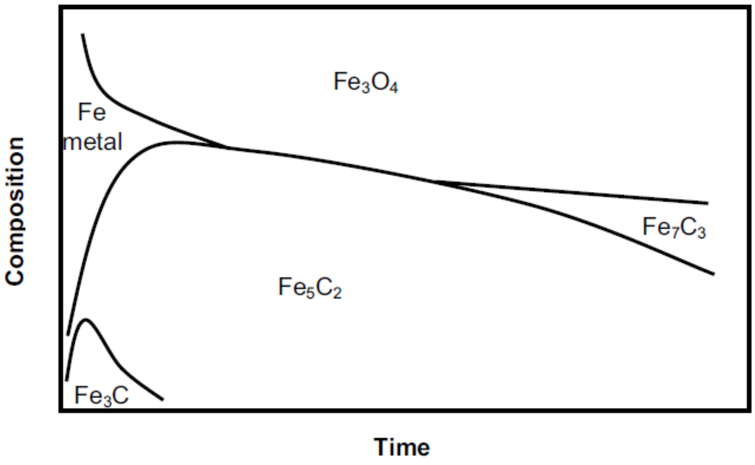

Figure 2.5: Phase composition during iron Fischer-Tropsch synthesis (adapted from [15]).

Figure 2.5 attempts to show the change in phase composition during iron high temperature Fischer-Tropsch synthesis [15]. In the beginning of the reaction metallic iron is present but is converted into the carbide phases Fe_3C (cementite), Fe_5C_2 (Hägg carbide) and with further TOS, Fe_7C_3 (Eckstrom Adcock carbide). Metallic iron and iron carbides are thought to be the active phases during Fischer-Tropsch synthesis while the oxides seem to be inactive for the formation of hydrocarbons [15][20][32][44][45]. As it was already shown in chapter 2.3.2, the promotion of iron catalysts with potassium increases the rate of carburization. Oxidation can occur either from the metallic or carbide phase induced by the reaction by-products H_2O and CO_2 [15][46].

There are some indications that cobalt also can be oxidized by water under Fischer-Tropsch conditions which could lead to catalyst deactivation [46][47][48]. However, it is believed that only small cobalt particles get oxidized [47][48] and oxidation of bulk metallic cobalt is not feasible under commercial FT conditions [23]. The absence of CO_2 during FT synthesis on cobalt catalysts could indicate the absence of the Boudouard as well as the WGS reaction and, therefore the formation of cobalt carbides seems to be unlikely [17].

2.5 Synthesis of nitrogen-containing compounds

Nitrogen-containing compounds such as amines, nitriles or amides are of great importance in nature and daily life [5][6][7][8]. This section attempts to give an overview over the current industrial and alternative production routes towards this compound class.

2.5.1 Amines

The synthesis of amines is part of one of the most important industrial chemical processes. Amines are an important class of compounds which find uses as intermediates in a variety of applications including pharmaceuticals, agricultural chemicals, rubber chemicals, water treatment chemicals and solvents [5]. The global amount for manufactured methylamine exceeds 800.000 Mto per year and the world-wide capacity for lower amines (C_2 - C_4) is greater than 400.000 Mto per year [5][49][50].

The most important industrial routes for amine synthesis depending on reactant feedstock and catalysts used are [6]:

1. **Acid catalyzed amination:** Reaction of alcohols with ammonia or amines on acidic catalysts.
2. **Hydroamination:** Conversion of alcohols with ammonia or amines on metal or supported metal catalysts in hydrogen-rich atmospheres.
3. **Reductive amination:** Reaction of ketones or aldehydes with ammonia or amines on hydrogenation catalysts.
4. **Amination of alkenes:** Reaction of alkenes with ammonia or amines on acidic catalysts.
5. **Amination of halogenated hydrocarbons:** Conversion of alkyl halides with ammonia or amines.
6. **Ritter reaction:** Conversion of hydrogen cyanide with alcohols or alkenes in acidic conditions to secondary or tertiary amines.
7. **Nitrile reduction:** Reaction of nitriles with hydrogen on hydrogenation catalysts.

Most of the catalysts used for reactions 1. - 7. are acidic or transition metal catalysts. In general homogenous hydrogenation catalysts are used for reductive amination and nitrile reduction reactions [51][52]. Homogenous metal complexes (Rh, Ru, Pd, Fe) are used to prepare amines from methyl-ketones, aldehydes (reductive amination) or nitriles (nitrile reduction). Since Fischer-Tropsch synthesis takes place on heterogeneous transition metal catalysts, only the hydroamination of alcohols with ammonia or amines will be described in this chapter.

The hydroamination of alcohols with ammonia or amines was investigated intensively in recent years [6][86][87]. For the reaction transition metal catalysts such as iron, cobalt, nickel or copper can be used [9][92]. During the hydroamination process, an alcohol adsorbs onto the catalyst surface and is consecutively transformed to an amine. It was found that the rate-limiting step for the reaction is the α-H abstraction of the alcohol [92]. A more detailed description of the mechanism was given by Jones *et al.* [9] based on hydroamination experiments of ethanol with ammonia on Ni/SiO_2 and Co/SiO_2 catalysts. From the experiments with isotope marked compounds at temperatures between 110°C and 180 °C, it was found that ethanol is activated via a dissociative reaction step (Figure 2.6). An ethylidene surface species (**2**) is formed after abstraction of the hydroxyl group (**II**). Ammonia is dissociatively chemisorbed and the generated amino group reacts further (**III**) to form a nitrogen-bounded surface species (**3**). This surface group can either desorb to form ethylamine or can be converted via hydrogen abstraction (**IV**) to species (**4**). Further loss of hydrogen leads to the formation of acetonitrile which is a side product during the hydroamination of ethanol with ammonia. Depending on the reaction conditions, another side reaction (**I**) can take place with acetaldehyde as product.

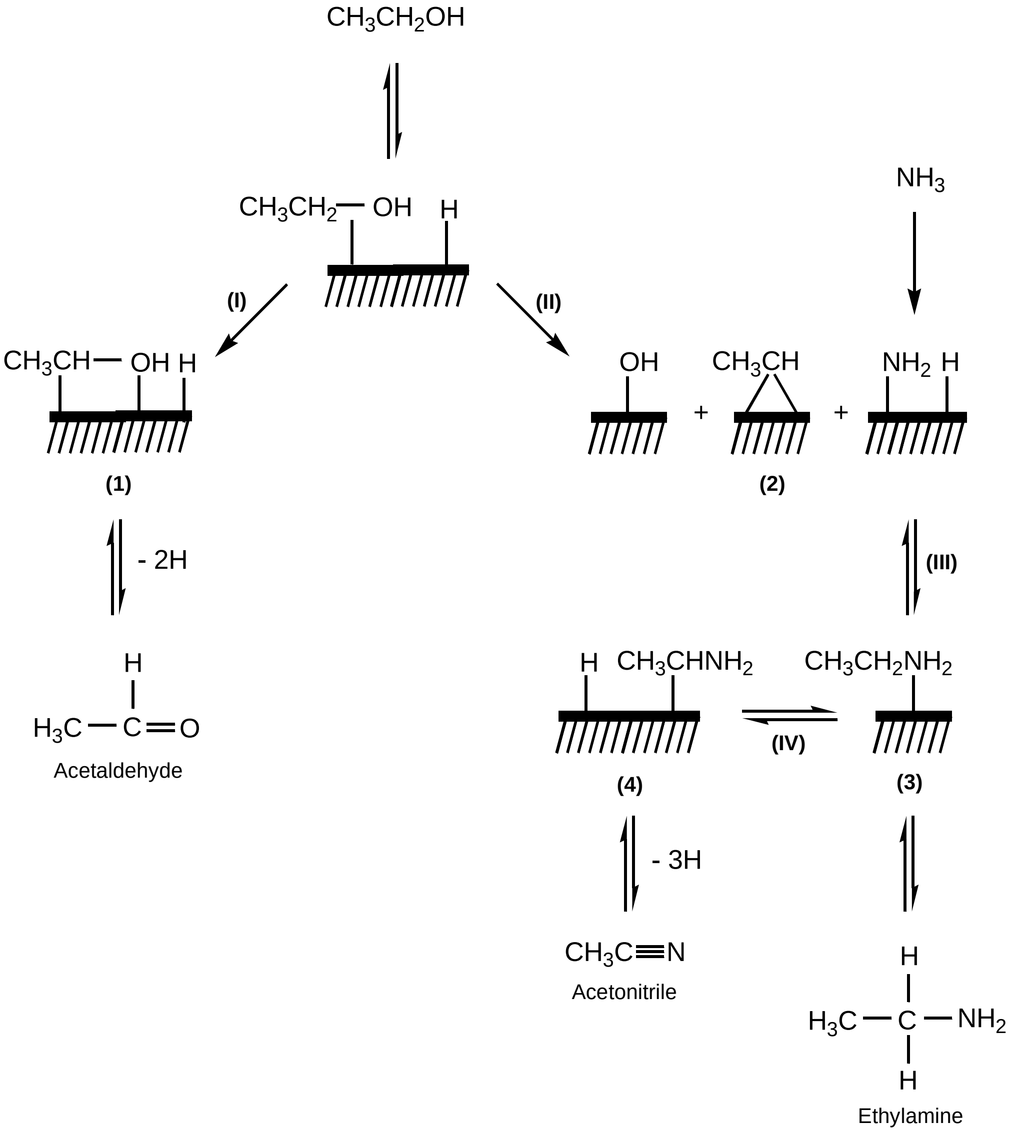

Figure 2.6: Scheme of ethylidene mechanism for the formation of ethylamine, acetonitrile and acetaldehyde during the hydroamination of ethanol with ammonia (adapted from [9]).

During hydroamination experiments, the formation of other side products beside acetaldehyde and acetonitrile (ACN) can occur. Rausch [6] investigated the influence of the reaction parameters on the reaction of ethanol with NH_3 using impregnated Co/SiO_2 catalysts. He observed that with increasing temperature more hydrocarbons such as paraffins or olefins were produced and the highest conversion of ethanol was achieved (Figure 2.7). The selectivity to acetonitrile also increased over a certain temperature range (200 - 280 °C), while the selectivities to amines such as monoethylamine (MEA), diethylamine (DEA) and Triethylamine (TEA) declined. The use of Co/SiO_2 catalysts reduced at higher temperatures (600 °C versus 500°C showed different behavior during the hydroamination experiments. Whereas selectivity to hydrocarbons increase and selectivities to amines decline, acetonitrile was still found in the product (S_{ACN} = 53 mol%) even at highest temperatures.

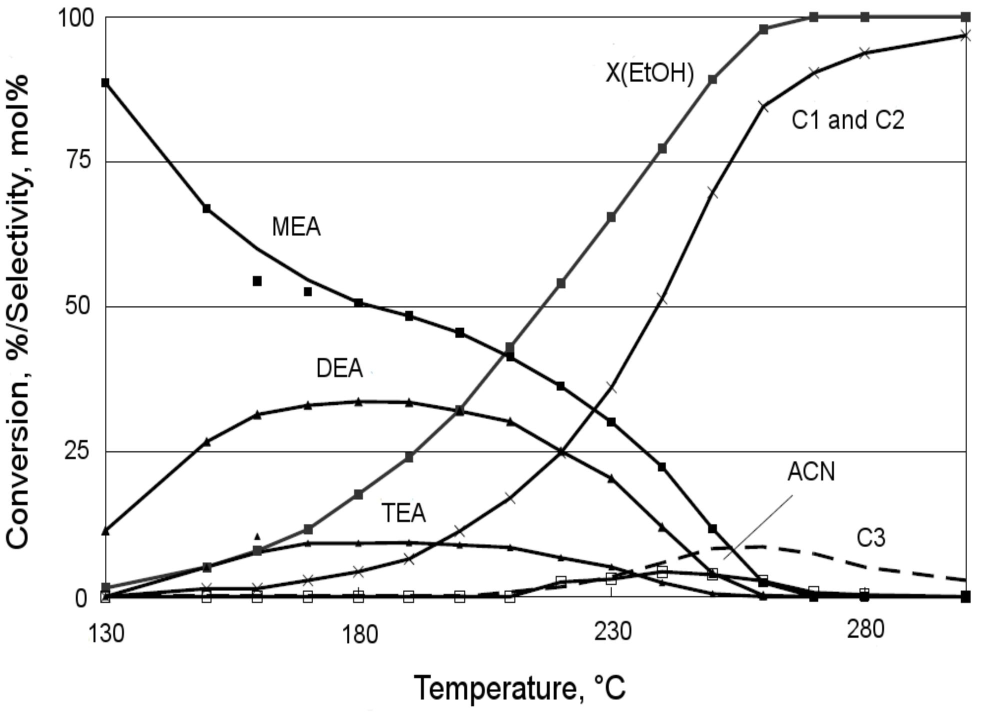

Figure 2.7: Conversion X_{EtOH} (%) and selectivity (mol%) during hydroamination experiments of ethanol with ammonia on 10 wt% Co/SiO_2 catalysts reduced at 500 °C (adapted from [6] and temperatures were changed from K to °C).

From the proposed mechanism in Figure 2.6 it can be seen that hydrogen could affect product selectivities or conversion during hydroamination reactions as well. In hydrogen-rich atmospheres selectivities to amines, especially to higher alkylated amines such as DEA or TEA, can be increased [65]. When increasing ammonia partial pressure, a tendency to the formation of primary amines was observed and less hydrocarbons were produced [6][66]. Sewell *et al.* [65] conducted hydroamination experiments of ethanol with ammonia and observed that monoethylamine is a primary product from the reaction. During their experiments, they changed the weight hourly space velocity (WHSV) and observed that more substituted amines (i.e. di- and triethylamines) were formed with smaller WHSV.

The product composition is also dependent on the catalyst system which is used during hydroamination experiments. Cobalt catalysts were reported to have beneficial effects to produce amines compared to iron catalysts were mainly other nitrogen-containing compounds were found in the organic product.

Since ammonia adsorbs on transition metal surfaces and can dissociate in adsorbed N, N-H or N-H_2 surface species, the formation of nitrogen-containing compounds such as amines is feasible under Fischer-Tropsch conditions. In the 1950s Rottig [10] reported about the presence of N-containing compounds consisting mainly of aliphatic primary amines when adding ammonia to the synthesis gas feed. He used precipitated iron/copper catalysts impregnated with potassium at 30 bar (reaction pressure) and temperatures between 183 - 210 °C. Beside the formation of amines, Rottig [10] also found high selectivities towards oxygenates (chiefly alcohols) of 30 - 35 %. The synthesis of terminal, aliphatic amines was shown by Kölbel and Trapper [11] using iron catalysts doped with potassium. The reaction was carried out in a fixed-bed reactor and hydrogen was replaced by steam to exploit the Water-Gas-Shift (WGS) properties of the catalyst (Kölbel-Engelhardt synthesis conditions). Yields to amines up to 18% were achieved which increased with increasing potassium contents in the catalyst. In the hydrocarbon products oxygenates such as alcohols and carboxylic acids were also found. From the addition of ammonia to the synthesis gas feed during the Fischer-Tropsch synthesis, Sango [111] and Sango *et al.* [12] obtained N-containing compounds such as amines with selectivities between 1.5 - 4.3 % in the carbon number range of C_1 - C_{20}. The authors used potassium promoted bulk iron catalysts and the reactions were carried out in a slurry reactor. However, the selectivity to amines was dependent on the partial pressure of ammonia and mostly primary, aliphatic amines were detected. While the selectivity to amines and other N-containing compounds increased with ammonia partial pressure the selectivity to oxygenates was decreasing. For Sango [111], the reaction pathway towards amines might lead through the same surface intermediate which could be required for the formation of alcohols during the Fischer-Tropsch synthesis. The hydroxyl group is replaced by an adsorbed amino species (**2**) on the catalyst surface and loss of water results in the formation of an amine (Figure 2.8).

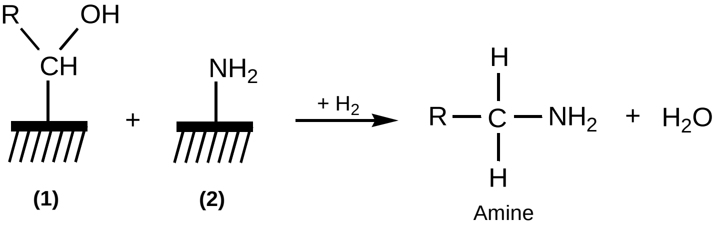

Figure 2.8: Scheme for the formation of an amine from an oxygenate intermediate (adapted from Sango [111])

With the use of supported cobalt catalysts instead of iron, it was possible for Rausch [6] and Knifton *et al.* [88] to produce primary, aliphatic amines during ammonia co-feeding under Fischer-Tropsch conditions.

Based in his findings, Rausch [6] proposed a synthesis route to amines via Fischer-Tropsch intermediates and adsorbed ammonia (Figure 2.9). The surface species (**1**) which is thought to be involved in the enol mechanism can react with adsorbed ammonia to generate intermediate (**3**). The addition of hydrogen then leads to a chain termination which results in the formation of an amine.

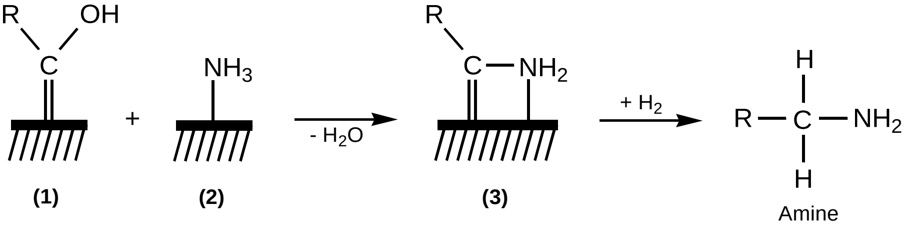

Figure 2.9: Scheme of chain termination step with NH_3 and formation of an amine as proposed by Rausch *et al.* [6].

As it was reported for oxygenated compounds (section 2.2.2), co-feeding experiments could show that amines also have the ability to re-adsorb on a metal catalyst surface. Kölbel *et al.* [89] added monomethylamine (MMA) and dimethylamine (DMA) to Fischer-Tropsch reactions under Kölbel-Engelhardt conditions and beside the conventional FT products, the formation of terminal secondary and terminal tertiary amines was observed. The reactions were conducted on potassium promoted Fe-Cu catalysts and the authors postulated a secondary mechanism with respect to the synthesis of hydrocarbons. The surface species (**1**) in Figure 2.9 is involved and leads to the formation of the amine and water via chain termination.

Secondary and tertiary methylamines were synthesized by Gredig *et al.* [90] under FT conditions in the presence of ammonia using various Al_2O_3 supported metal catalysts (Cu, Ag, Ni, Pt, Co and Fe) and CO_2 instead of CO. On most of the catalysts he was able to obtain a mixture of monomethylamine, dimethylamine and trimethylamine (TMA) from the reaction and Cu/Al_2O_3 catalysts showed the highest methylamine production rates. Increasing ammonia partial pressure in the feed resulted in improved selectivities to monomethylamine and with higher ammonia concentrations, methylamine formation decreased slightly (Figure 2.10). Byproducts from the reaction were methane (high selectivities on Ni, Pt, Co and Fe catalysts), carbon monoxide from the reverse Water-Gas Shift reaction on Cu catalysts and water. On Ag metal catalysts only CO, H_2O and HCN were formed.

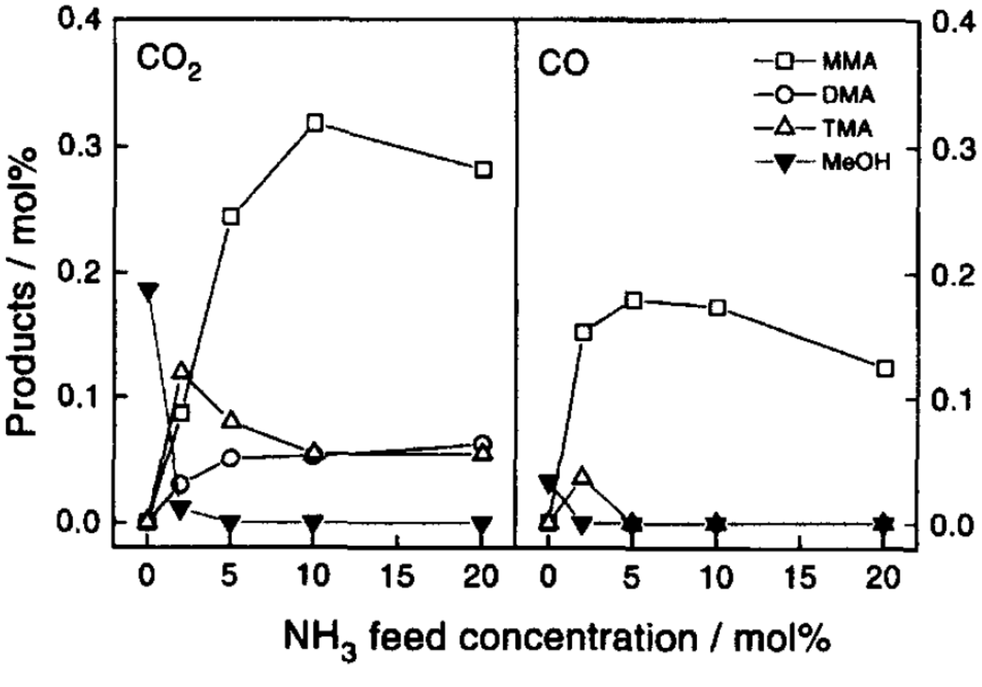

Figure 2.10: Influence of NH_3 concentration on the amine selectivity during the reaction of CO, CO_2, H_2 and NH_3 on Cu/Al_2O_3 catalysts (adapted from [91]).

Further investigations with Cu/Al_2O_3 catalysts showed that the space velocity has little influence on NH_3 conversion and distribution of amines [91]. High temperatures shift the amine selectivity towards the formation of MMA and the replacement of carbon dioxide with carbon monoxide resulted in lower conversions. Since the formation rates of amines were higher compared to the methanol product rates in ammonia-free runs, Gredig *et al.* [91] concluded that amine formation occurs mainly by the reaction of NH_3 with a methanol precursor and not via the hydroamination of methanol with ammonia.

2.5.2 Nitriles

Industrially nitriles are broadly used as solvents or chemical feedstock for production of pharmaceuticals and pesticides [7]. Nitriles are potentially very versatile building blocks that can be used as precursors for amines, isocyanates, amides, carboxylic acids and esters [55]. The most important nitrile in nowadays, however, is acrylonitrile which has the largest commercial production capacities.

A number of synthesis routes towards nitriles are known with a variety of different reactants and catalysts. Acrylonitrile is produced on a large scale by ammoxidation of propylene with ammonia [56][57]. The ammoxidation is a six-electron redox process and complex-mixed catalyst systems, containing metals such as Mo, Fe, Ni, Co, Mg or Mn, are required. The reaction steps involve the activation of propylene through abstraction of an α-hydrogen, followed by NH-insertion, subsequent rearrangements of the chemisorbed activated surface species with additional hydrogen abstraction, and culminating in the desorption of the so formed acrylonitrile from the catalyst surface.

During transition metal-catalyzed alkene hydrocyanation reactions, HCN is added to the C=C double bond of an alkene to form nitriles [55]. When butadiene is used as alkene, the addition of hydrogen cyanide results in the formation of adiponitrile which is a precursor in the hexamethylenediamine production one of the building blocks for the synthesis of nylon 6,6. In the so called DuPont Adiponitrile Process homogeneous nickel-based catalysts are used.

There are patents available which deal with the formation of aliphatic nitriles from the reaction of carboxylic acids with NH_3 [58][59]. The most common catalysts employed are dehydrating catalysts. These include bauxite, aluminum oxide, phosphoric acid or silica gel. During the reaction the corresponding ammonium carboxylate is first formed from the acid and ammonia. After dehydration to an amide, further dehydration takes place to give the nitrile [59]. As an undesirable side reaction, the acid can undergo conversion to a ketone and CO_2.

The formation of acetonitrile during the Fischer-Tropsch synthesis on silica supported catalysts in a fixed-bed reactor was first reported in U.S. patents by Monsanto [94]. From co-feeding experiments with methylamine on molybdenum or partly potassium promoted iron catalysts the authors could show that methylamine decomposes to hydrogen, carbon and ammonia. As a result the presence of acetonitrile (ACN) was observed during the product analysis. When using ammonia as a nitrogen source, acetonitrile was generated in high selectivities by Auvil and Penquite [95] and Gambelli and Auvil [96]. Their experiments were carried out on molybdenum and manganese-containing catalysts supported on SiO_2 or Al_2O_3. The reverse WGS reaction was exploited using a mixture of carbon monoxide and carbon dioxide in the synthesis gas feed and high ratios of CO_2:CO were found to be beneficial for the production of acetonitrile. Additional alkali or alkaline earth metals in the catalysts resulted in a further increase in selectivities towards acetonitrile [96]. In contrast to that, the presence of alkali or alkaline earth metals was not necessary for the formation of acetonitrile in [97]. However, the formation of higher nitriles was also observed in the patents described above but no detailed information is given.

Acetonitrile selectivities up to 96 % were found by Kim and Lane [98] during the NH_3-FT experiments on Mo/SiO_2 catalysts. Beside the formation of nitriles, conventional organic Fischer-Tropsch products were synthesized during the experiments, too. High temperatures and high ammonia concentrations in the feed, increased and decreased the formation rates of organic Fischer-Tropsch products respectively..

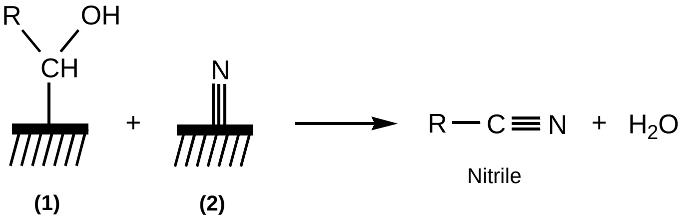

Figure 2.11: Formation of nitriles from an oxygenate intermediate (adapted from Sango [111]).

A more detailed analysis of the organic products especially the N-containing compounds was conducted by Sango [111] and Sango *et al.* [12]. With a gas chromatograph equipped with a mass spectrometer, it was possible to detect long chain nitriles up to carbon number C_{20}. Sango used potassium promoted iron catalysts and the NH_3-FT experiments were carried out in a slurry reactor. When increasing ammonia partial pressure, the nitrile content of all

N-containing compounds was decreased. Since oxygenates such as alcohols, aldehydes and carboxylic acids disappeared during the co-feeding experiments with NH_3, Sango [111] concluded that the formation of nitriles occurs via the same precursor (**1**) which is believed to be a possible pathway to generate alcohols during the Fischer-Tropsch synthesis (Figure 2.11).

2.5.3 Amides

Amides are broadly used in organic synthesis or industrial industry as intermediates and raw materials for detergents and lubricants [67][68]. Feedstock for the production of amides could be nitriles, which can be hydrogenated to the corresponding amide. For example, the hydration of acrylonitrile produces annually more than 2 x 10^5 tons of acrylamide and is the most important technology for the production of this chemical [68].

Important fatty amides are prepared by the reaction of the appropriate fatty acid with anhydrous ammonia. These amides are required as intermediates in the production of water repellents or antislip and antiblock additives for polyethylene films [8].

Rausch [6], Sango [111] and Sango *et al.*[12] showed that it is feasible to obtain amides on cobalt and potassium promoted iron catalysts from NH_3-FT reactions. Their experiments were conducted in a slurry reactor and the authors reported on the presence of long chain amides in small quantities beside other N-containing compounds such as amines and nitriles in the Fischer-Tropsch products.

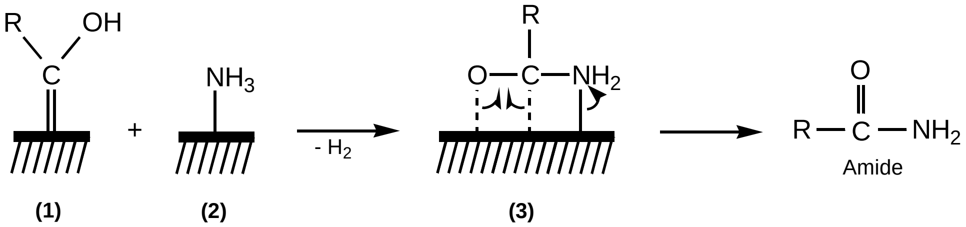

Figure 2.12: Chain termination step with NH_3 and formation of an amide as proposed by Rausch [6].

For the formation of amides, Rausch [6] postulated that the reaction pathway leads over the same surface species ((**1**) in Figure 2.12) which is involved in the amine reaction step (see section 2.5.1, Figure 2.9). Instead of the addition of hydrogen, the chain termination step towards amides occurs via the formation of a C=O bond and back formation of the electron pair of the nitrogen atom (**3**).

During the addition of NH_3 to the synthesis gas feed over potassium promoted iron catalysts, Sango [111] and Sango *et al.* [12] observed that the amount of oxygenates such as alcohols, aldehydes and carboxylic acids decreases with increasing ammonia partial pressure in the system. From his findings he concluded the formation of amides occurs via an acyl intermediate (**1**) as it was proposed by Schulz [61] and Cairns [14] for the formation of carboxylic acids. Instead of the addition of a hydroxyl group the amides are generated due the presence of NH_2 (**2**) species on the catalyst surface (Figure 2.13).

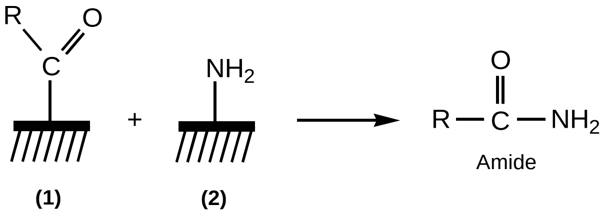

Figure 2.13: Chain termination step with NH_2 and formation of an amide as proposed by Sango [111].

2.5.4 Formation of other N-containing compounds

During the Fischer-Tropsch synthesis on iron catalysts carbon dioxide is formed from the reaction of carbon monoxide with water (WGS reaction). When ammonia is present in the reactor system, it can react between temperatures of 35 - 40 °C with CO_2 and is converted to ammonium carbonate (equation 2.5) [100].

$$2\,NH_3 + CO_2 + H_2O \rightarrow (NH_4)_2\,CO_3 \qquad (2.5)$$

The reaction normally occurs below temperatures of 58 °C as it was reported by Kim and Lane [98]. The authors conducted Fischer-Tropsch experiments in the presence of ammonia in a fixed-bed reactor using Mo/SiO_2 catalysts. Ammonium carbonate can plug the tubing from the reactor equipment and heated transport lines were reported to be beneficial. If exposed to air, ammonium carbonate is readily converted to ammonium bicarbonate (equation 2.6).

$$NH_3 + CO_2 + H_2O \rightarrow (NH_4)HCO_3 \tag{2.6}$$

During Fischer-Tropsch experiments in a slurry reactor with the co-feeding of ammonia, Sango [111] reported the formation of ammonium bicarbonate during his experiments.

In general crystalline ammonium carbonate or ammonium bicarbonate is soluble in water and decompose to CO_2 and NH_3 at higher temperatures [100].

2.6 Ammonia and transition metal catalysts

The reaction of CO and H_2 during the Fischer-Tropsch synthesis in general takes place on transition metal catalysts such as iron, cobalt or ruthenium. These catalyst metals are also active for the production of ammonia in industrial applications and they can facilitate NH_3 decomposition to molecular nitrogen and hydrogen [70][72].

2.6.1 Ammonia synthesis

The reaction steps for the ammonia synthesis on a metal catalyst surface are object of many investigations since 100 years when the synthesis of NH_3 from molecular nitrogen and hydrogen was invented by Fritz Haber and Carl Bosch [69]. In industrial applications the reaction takes place on metal catalysts such as iron (promoted with potassium and alumina oxide) or with more interest today, carbon-supported ruthenium catalysts [70]. It was object of discussions for years if the mechanism for the ammonia synthesis is of associative or dissociative nature. Since it is known that the population of molecular N_2 is very low and the fact that pulsed-laser stimulated field desorption experiments showed the presence of adsorbed N, NH and NH_2 species on the catalyst surface, it is believed that the reaction occurs through dissociative steps [71]. In this context Strongin and Somorjai [72] proposed a model where potassium decreases the concentration of adsorbed NH_3 on an iron catalyst surface via decreasing the adsorption energy of ammonia (determined by means of temperature programmed desorption). Consequently the number of active sites blocked by NH_3 is decreased which leads to a higher activity during the ammonia synthesis. They also found that the rate of dissociative chemisorption of nitrogen over Fe(111) and Fe(100) surfaces is enhanced by additional potassium.

2.6.2 Ammonia decomposition

The ammonia synthesis is reversible and ammonia can be decomposed to its reactants. Today, the catalytic decomposition of ammonia is investigated as a method to produce hydrogen for fuel cell applications [73][78]. The reaction is mildly endothermic ($\Delta H = 46$ kJ/mol) and leads though several surface intermediates similar to the ammonia synthesis (shown in Figure 2.14) [72][73][74].

$$(1) \quad NH_3(g) + * \rightleftharpoons NH_3{-}*$$

$$(2) \quad NH_3{-}* + * \rightleftharpoons NH_2{-}* + H{-}*$$

$$(3) \quad NH_2{-}* + * \rightleftharpoons NH{-}* + H{-}*$$

$$(4) \quad NH{-}* + * \rightleftharpoons N{-}* + H{-}*$$

$$(5) \quad 2N{-}* \rightleftharpoons N_2{-}*$$

$$(6) \quad N_2{-}* \rightleftharpoons N_2(g)$$

$$(7) \quad 2H{-}* \rightleftharpoons H_2(g) + 2*$$

Figure 2.14: Reaction steps for the decomposition of NH_3 to molecular N_2 and H_2 on a catalyst surface where * donates an active site on the catalyst surface (this scheme originally attempts to show reaction steps of the ammonia synthesis [74] and was converted for the purpose of this work**)**.

The rate-limiting step is thought to be temperature-dependent and can be divided in two regions. Tsai and Weinberg [75] reported that on Ru(001) surfaces below a temperature of 377 °C, the re-combinative desorption of atomic N (reaction (6) in Figure 2.14) is the rate limiting step. At higher temperatures, the reaction rate is linearly dependent on the partial pressure of ammonia and independent of the partial pressures of hydrogen and nitrogen. Calculation of the equilibrium conversion by Yin *et al.* [80] at 1 bar shows that ammonia nearly decomposes with a conversion of 100 % at temperatures around 350 °C (Figure 2.15).

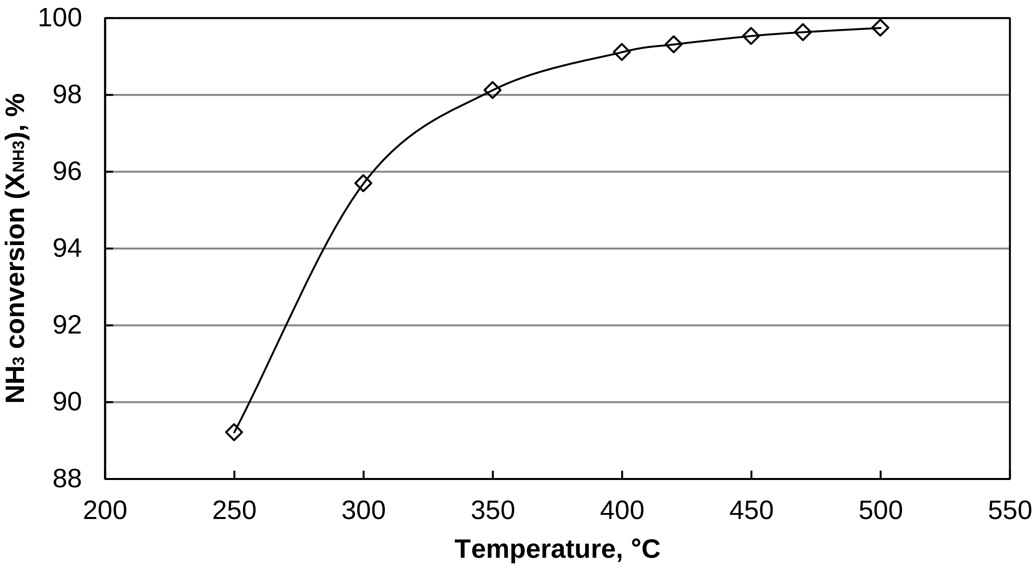

Figure 2.15: Calculated equilibrium conversion of NH_3 at different temperatures at 1 bar for the decomposition to nitrogen and hydrogen (adapted from [80]).

From a thermodynamic point of view, it is feasible to decompose NH_3 and depending on which metal is used during the process, the reaction can result in different ammonia conversions. Ruthenium was reported to show high activities to decompose NH_3 to nitrogen and hydrogen, followed by Iridium and Nickel, whereas the use of iron catalysts seems to be unfavorable since its activity is too low [73][78]. Cobalt can dissociate ammonia as well and compared to its low activity during ammonia synthesis the decomposition rate is reported to be higher than for iron [79]. Despite these findings it is possible to form N_2 and H_2 from ammonia on iron catalysts. The formation rate of N_2 and H_2 can be increased when metal nitrides as catalysts are employed. The use of iron nitrides for the decomposition of ammonia leads to enhanced decomposition rates compared to the use of conventional iron catalysts [85]. In contrast to the ammonia synthesis, potassium has no beneficial effect on the catalytic performance on iron catalysts [84]. The impregnation of iron with potassium results in lower activities in the NH_3 decomposition process. From near-edge X-ray absorption fine-structure (NEXAFS) and X-ray photoelectron spectroscopy (XPS), Strongin and Mowlem [77] reported that when NH_3 is adsorbed on clean iron surfaces, the N-H bond is dilating. If potassium is co-adsorbed this dilation is not observed and the N-H bond length is similar to the N-H distance in condensed ammonia. Arabczyk and Zamlynny [84] also investigated ammonia decomposition rates on iron nitrides and clean iron surfaces. They reported apparent activation energies of the decomposition of ammonia over iron nitrides to be nearly two-fold smaller in comparison to clean iron. From UPS/XPS measurements on Ni(110) surface planes a temperature dependency of different surface species during ammonia synthesis/decomposition could be shown [81]. At temperatures T < -143 °C molecular adsorption of NH_3 is observed and increasing the temperature above -123 °C results in partial dissociation of adsorbed NH_3. The intermediate species were identified by their photoelectron spectra as NH-fragments. At temperatures above 77 °C only atomic nitrogen is observed to populate the surface after NH_3-exposure. In contrast to Grunze *et al.* [81] the evidence for a surface equilibrium between chemisorbed NH_2, NH and H species was found by Gundry *et al.* [82]. The decomposition reaction of ammonia is normally hindered by hydrogen but due to its high heat of adsorption the inhibition by hydrogen on iron catalysts only occurs at low temperatures [85]. Moreover, molecular hydrogen is found to alter the decomposition rate to higher values which for high hydrogen partial pressures is independent of p_{H2}. However, the decomposition of ammonia to hydrogen and nitrogen seems to be a structure sensitive reaction. It was found that the stability of NH_2 and NH species is different on an Fe(111) and Fe(110) surface. While on Fe(111) a mixture of NH_2, NH and atomic nitrogen units populate the surface at 27 °C, only NH species are present under comparable conditions on Fe(110) surfaces [81].

2.6.3 Formation of metal nitrides

The decomposition of ammonia is linked to the process of nitriding of metal catalysts and increases along with the increase of the nitriding potential [76]. The formation of bulk metal nitrides is an endothermic reaction (Figure 2.16) and the process is reversible [108]. Thermodynamic calculations and experimental findings indicate that small amounts of hydrogen are sufficient to suppress the reaction [99][109]. Calculations of equilibrium constants for the nitriding reaction on different metals could show that in case of cobalt and copper the nitriding agent (e.g. ammonia) has to be present in excess [6][106]. This is also affirmed by Löffler and Schmidt [85] and the authors could show that iron catalysts show a higher tendency to form nitrides compared to cobalt and copper.

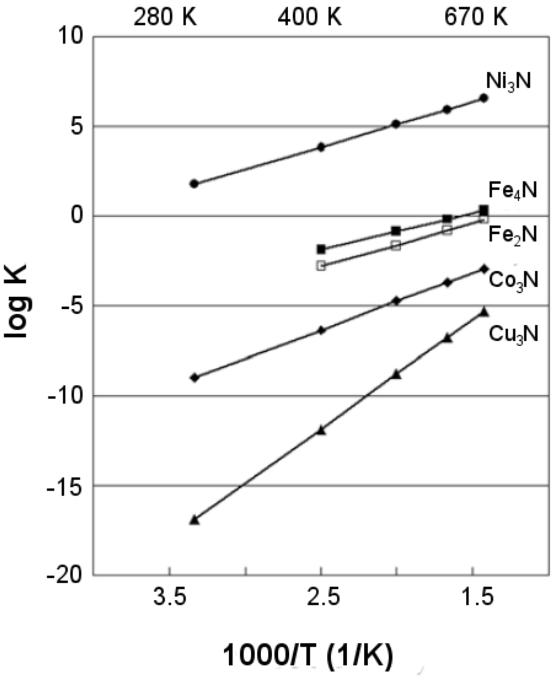

Figure 2.16: Temperature dependency of the formation of metal nitrides (adapted from [99]).

On iron catalysts it was shown by Grabke [83] that for the nitriding process, the dissociative adsorption of ammonia is the rate-limiting step during. Furthermore, the degree of nitriding is only influenced by temperature and partial pressure of ammonia or rather hydrogen and not by the catalyst composition [76][84]. During hydroamination experiments with 1-dodecanol and dimethylamine on a Cu/Al$_2$O$_3$ catalyst, Baiker [104] found that the reaction behavior strongly depends on the presence of hydrogen. By replacing hydrogen with nitrogen, the conversion of 1-dodecanol and the amine selectivity decrease and after switching back to hydrogen this trend was reversible. From the disproportionation of amines in the absence of alcohols copper, nickel and cobalt catalysts, it was found that catalyst deactivation takes place due the formation of metal nitrides [106]. Detailed temperature programmed desorption (TPD) and reduction (TPR) experiments on deactivated catalysts then revealed the formation of metal carbides and nitrides during the process [106][107].

In contrast to catalyst deactivation, nitride formation on iron and cobalt catalysts was reported to have beneficial effects on the catalytic performance during Fischer-Tropsch reactions. Shultz *et al.* [113] prepared iron nitrides by threatening freshly reduced iron based catalysts with ammonia. They reported that ε-iron nitride was formed which is isomorphous with ε-iron carbide. During Fischer-Tropsch experiments, ε-iron nitride catalysts showed higher selectivities to oxygenates, lower chain growth probability as well as improved resistance against oxidation and free carbon deposition. In the further progress of the reaction ε-iron nitride is transformed into carbonitrides due to the carbon monoxide-containing synthesis gas. Iron nitrides were also used by Hummel *et al.* [97] as catalysts for the Fischer-Tropsch synthesis. They observed with Mössbauer spectroscopy that after the reactions no bulk nitrogen atoms were found in the spent catalysts and iron nitride was transferred into iron carbide within minutes under FT reaction conditions.

Different Fischer-Tropsch product selectivities were found by Yeh *et al.* [114] when comparing potassium and nitrogen-containing iron catalysts. They prepared iron nitrides directly after the reduction of iron oxides to the metallic phase by exposing the metal catalyst to NH_3. Both catalysts, the potassium promoted and the iron nitride, have higher olefin and WGS selectivities, lower alcohol yields and a tendency to shift FT products to larger molecular weight compared to pure iron catalysts. On cobalt nitrides as catalyst for the Fischer-Tropsch synthesis, lower methane selectivities, higher chain growth probabilities and higher selectivities towards C_{5+} hydrocarbons were observed by Lapidus *et al.* [105].

Yeh *et al.* [114] concluded that the promotion of iron with nitrogen also leads to an electron donor effect such as the promotion with potassium. They found that the decrease of the iron magnetic moment is higher in case of N neighbors compared to C neighbors from carbides and it is believed that the charge-transfer into the partially filled iron 3d band is larger for interstitial nitrogen than for interstitial carbon [115]. Therefore, promotional effects during the FT synthesis on iron nitrides show similarities to that of potassium promoted iron catalysts.

3 Experimental methods

3.1 Preparation of bulk iron and cobalt catalysts

Unpromoted bulk iron and cobalt catalysts were used during Fischer-Tropsch experiments at ammonia partial pressures of 0.0 and 0.2 bar. Some of the bulk iron catalysts were impregnated with potassium and the preparation methods of the catalyst materials is presented in this chapter.

3.1.1 Precipitation of metal nitrates

Bulk iron and cobalt catalysts were prepared by precipitation from their metal nitrate solutions with ammonium hydroxide. In a 2L glass beaker, an aqueous 1 molar solution of $Fe(NO_3)_3{*}9H_2O$ or $Co(NO_3)_3{*}6H_2O$ was heated to 70 °C under constant stirring. Precipitation was achieved by adding a hot (70 °C) 5 wt% ammonium hydroxide solution until a pH of 7 or 7.5 was reached respectively. The obtained metal hydroxides were filtered off and washed with hot deionized water until the residue was nitrate-free. Subsequent the filter cake was dried at 100 °C for 24 hours and calcined in a muffle furnace at 400 °C with a heating rate of 1 °C/min for 4 hours.

3.1.2 Impregnation with potassium

A portion of the bulk iron catalysts was impregnated with potassium using a 0.03 M solution of KNO_3 (Table 3.1). The aqueous catalyst-potassium solution was heated to 55 °C and the water was evaporated with a vacuum pump. Once again the impregnated catalysts were dried in an oven at 100 °C for 24 hours and calcined at 400 °C for 4 hours with a heating ramp of 1 °C/min. Finally, the formed metal oxides were pressed, crushed and sieved to a mesh size between 200 and 315 µm.

Table 3.1: Bulk iron and cobalt catalyst prepared by precipitation: catalyst names and theoretical potassium content per g_{Fe}.

Catalyst	**Iron** (g)	**Cobalt** (g)	**Potassium** (g)	**Potassium** (wt%)
Fe-0K	1.00	-	0.00	0.00
Fe-2K	0.98	-	0.02	2.00
Fe-5K	0.95	-	0.05	5.00
Co-0K	-	1.00	0.00	0.00

3.2 Catalyst characterization

All promoted/unpromoted bulk iron and cobalt catalyst materials were characterized to determine their composition, reduction behaviour, particle size and morphology. The measurements were conducted at the Carl von Ossietzky Universität Oldenburg (AAS, TPR, chemical analysis of spent catalysts) and at the University of Cape Town (XRD, TEM) as a part of a collaboration between the universities.

3.2.1 Atomic absorption spectroscopy

The potassium loading of the bulk iron was measured by atomic absorption spectroscopy (AAS) using a Varian SpectrAA 300 (measuring inaccuracy is used to be ± 0.1 wt %).

3.2.2 Temperature programmed reduction

The reduction behavior of the unpromoted/promoted bulk iron and cobalt catalysts was investigated by means of temperature programmed reduction (TPR) with hydrogen. The main parts of the experimental TPR equipment (Raczek Analysentechnik GmbH, Hannover) are a quartz U-tube with an oven and a thermal conductivity detector (TCD). For the analysis, 30 g of the metal oxide was mixed with 270 mg of SiO_2 and loaded into the quartz reactor. A detailed outline of the experimental procedure can be found in Table 3.2.

Table 3.2: Cycles for TPR experiments on bulk iron and cobalt catalyst materials and conditions (gas flows at NTP).

	Conditions
Reactor loading	30 mg metal oxide, 270 mg SiO_2
Catalyst pretreatment	50 mL/min Ar, 150 °C isothermal for 60 min
Temperature programmed reduction	50 mL/min H_2/Ar (5 vol% H_2 in Ar), 100 °C to 900 °C at 10 °C/min

As a pretreatment, the catalysts were purged with argon (50 mL/min) for one hour at 150 °C to remove physisorbed water or oxygen. The reactor was then subsequently cooled down to 100 °C. A mixture of hydrogen and argon (5 vol% H_2 in Ar) at 50 mL/min was fed through the reactor while the reactor temperature was increased from 100 °C to 900 °C at a heating ramp of 10 °C/min. Using a thermal conductivity detector, the amount of hydrogen consumed during the reduction was monitored.

3.2.3 X-ray diffraction spectroscopy

The average particle sizes of the calcined bulk iron and cobalt oxides were determined using X-ray diffraction spectroscopy (XRD). Measurements were conducted in a Bruker D8 Advance laboratory X-ray diffractometer equipped with a cobalt source (λ = 0.178897 nm) and a position sensitive detector (Bruker Vantec). The International Centre for Diffraction Data PDF-2 database was used to identify and compare all diffraction patterns. The average particle size d was estimated using the Debye-Scherer equation:

$$d = \frac{k \cdot \lambda}{\beta \cdot \cos\theta} \tag{3.1}$$

where the X-ray wavelength is represented by λ, the shape factor by k (k = 0.9) and the diffraction angle in degrees by θ, while β is the line broadening at the angle’s full width at half maximum intensity (FWHM).

3.2.4 Transmission electron microscopy

To further study the particle’s size and morphology, the prepared metal oxide were investigated by means of high resolution transmission electron microscopy (TEM or HRTEM) using a FEI Technai F20 operated at 220 kV and equipped with a field emission gun as the electron source. Small amounts of the catalyst materials were dispersed in ethanol in an ultrasonic bath for 10 minutes. A drop of the dispersion was placed on a holey carbon copper grid (200 mesh, SPI Supplies) and dried overnight in a desiccator.

3.2.5 Chemical analysis of spent catalysts

In order to investigate the formation of metal nitrides during the Fischer-Tropsch experiments with co-fed NH_3, the spent catalysts were analyzed to determine the nitrogen content with a Vario MAX CNS (Elementar).

3.3 Fischer-Tropsch experiments

The catalytic performance of the unpromoted/promoted bulk iron and cobalt catalysts during Fischer-Tropsch synthesis was investigated in this work. In addition to conventional Fischer-Tropsch experiments, ammonia was added to the synthesis gas feed to study its influence on the Fischer-Tropsch product distribution and the formation of nitrogen-containing compounds. These experiments were performed in a fixed-bed reactor using both *online* and *offline* gas chromatographic analyses.

3.3.1 Experimental setup

Figure 3.1 shows the physical setup of the Fischer-Tropsch apparatus which was build and used in this work. The fixed-bed reactor itself is a U-tube stainless steel pipe (O.D. 1/4 “, I.D. 0.5 mm), which is centered in an aluminum block containing two heating elements at the edges to minimize temperature gradients. Two thermocouples measure and control the temperature of the aluminum block and the reactor. The gas supply consists of the reactants (carbon monoxide, hydrogen and ammonia), as well as nitrogen (pressure gas, balance gas) and a mixture of argon/cyclohexane as an internal standard (0.13 mol % cyclohexane in argon, information to all gases can be found attached in chapter 7 Appendices). All gases are controlled by mass flow controllers (MFC, F-1 - 5) except the nitrogen line which is used to pressurize the reactor. Using a needle valve (NV), a pressure of 4.0 bar was adjusted and the flow rate at the outlet of the reactor (synthesis gas, nitrogen/ammonia, argon/cyclohexane, nitrogen/pressure) was controlled. A 4-way valve (4WV) allows the switching of the synthesis gas/nitrogen/ammonia mixture from running through the reactor or through a bypass line. In order to achieve a constant residence time over the catalyst bed in the experiments with different ammonia concentrations additional nitrogen was used as a balance gas. When the ammonia concentration within the synthesis gas feed was increased, the flow rate of nitrogen was reduced in the same manner. To keep liquid products (C_{5+}) from the Fischer-Tropsch synthesis in the gas phase for the *online* gas chromatographic analyses, all lines after the reactor are heated to 180 °C until the gas chromatograph equipped with a thermal conductivity detector (GC-TCD). A hot trap after the reactor is adjusted at 100 °C to avoid blocking of the 1/16 “ tubes at the gas chromatographs by organic products (C_{12+}) or eventually ammonium carbonate/bicarbonate. In order to minimize damages or fading of the filaments of the thermal conductivity detector (TCD), residue C_{5+} organic products in the gas phase are collected in a cold trap at room temperature before the TCD.

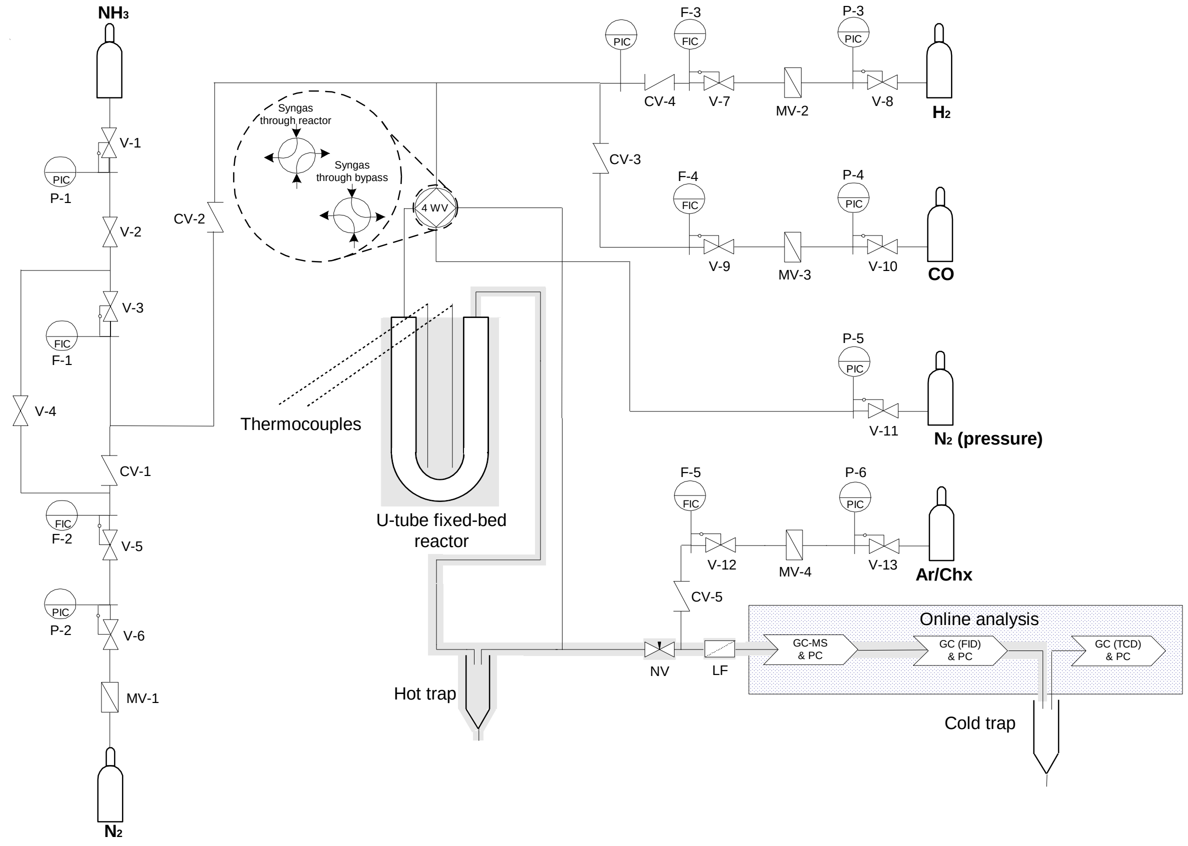

Figure 3.1: Physical set-up of the experimental equipment for the Fischer-Tropsch experiments: CV-1 - 5 check valves, F-1 - 5 flow control, LF line filter, NV needle valve, MV-1 - 4 magnetic valves, V-1 - 13 one way valves, 4WV 4-way valve (shaded areas represent temperature controlled heated zones).

All temperatures (reactor and heated lines), mass flow controllers and magnetic valves were controlled via a reaction control unit which was developed at the Carl von Ossietzky University of Oldenburg (http://www.roessner.chemie.uni-oldenburg.de).

3.3.2 Experimental procedure

For every Fischer-Tropsch synthesis run the catalyst materials (iron and cobalt oxides) were mixed with SiO_2 (pore volume: 0.5 g/cm^3, particle size: 2 - 4 μm, corn fraction: 200 - 315 μm) in a ratio $g_{metal\ oxide}/g_{SiO2}$ = 1.5. By choosing a similar grain size between the catalyst materials and the diluent, pressure drops inside the reactor were avoided. Due to the exothermic nature of the Fischer-Tropsch reaction, this procedure assists in dissipating the heat of the reaction from the catalyst and, thus, minimizing sintering effects as well as temperature “hot spots”. In the further progress of this work the metal (oxide)/diluent mixture will be referred as ‘catalyst’. The isothermal zone of the reactor was determined by heating the aluminum block housing to 300 °C and an external thermocouple was positioned inside the stainless steel U-tube where the temperature was recorded at every centimeter. Along this isothermal zone, the catalyst was placed and the reactor in- and outlet were plugged with glass wool to prevent the catalyst bed from moving during the experiments. It should be noted that different amounts of catalyst were used in chapter 4.2.2.3, where the gas hourly space velocity (GHSV) in the catalyst bed was varied during the experiments.

After the reactor is loaded and before the catalytic experiments the equipment was tested for leaks or a pressure drop inside the catalyst bed. Here the needle valve (NV) was closed and the system was pressurized with pure hydrogen to 4.5 bar. The flow rate of hydrogen was observed using a MFC (F-3). At a flow rate of < 0.5 mL/min of H_2 it was assumed that the system did not show any leaks and the pressure was released again. This was followed by purging the reactor with 60 mL/min H_2 for 15 minutes. If no pressure rise occurred it was assumed that the catalyst bed was efficiently packed.

Table 3.3: Parameter for the *in situ* reduction of bulk iron and cobalt catalysts before the FT experiments (gas flows at NTP).

	Reduction conditions	
	Bulk iron catalysts	Bulk cobalt catalysts
Gas	Hydrogen	Hydrogen
Flow rate	60 mL/min (2880 h^{-1})[1,2]	60 mL/min (2880 h^{-1})[1]
Temperature program	1) RT to 100 °C at 1 °C/min, 60 min isothermal 2) 100 °C to 350 °C at 1 °C/min, 960 min isothermal	1) RT to 100 °C at 1°C/min, 60 min isothermal 2) 100 °C to 350 °C at 1°C/min, 720 min isothermal
Pressure	Atmospheric	Atmospheric

[1] Values in brackets represent the gas hourly space velocity (GHSV).

[2] For the experiments in chapter 4.2.2.3, other H_2 flow rates were used in order to achieve a GHSV = 2880 h^{-1}.

Following this, the oxide phase of the catalyst was reduced *in situ* with 60 mL/min H_2 to the metal phase for the Fischer-Tropsch experiments (Table 3.3). Since both catalysts, Fe_2O_3 and Co_3O_4, show a different reduction behavior two different activation steps were used.

Once the catalysts were reduced, the reactor was prepared for the Fischer-Tropsch experiments. The reactor temperature used during the reduction treatment was decreased to the corresponding reaction temperature (Table 3.4) under 32 mL/min of H_2. The 4-way valve (4WV) was switched to bypass and the system was slowly pressurized to the reaction pressure of 4 bar using a nitrogen pressure line. Here, the needle valve was carefully opened to allow a flow rate of 40 mL/min plus 5 - 10 mL/min N_2 from the pressure line. Once the pressure had reached 4 bar the synthesis gas flow rate/ratio was adjusted to the desired conditions (Table 3.4) by replacing some H_2 with CO. This results in the 4 bar remaining unaffected and with 32 mL/min synthesis gas, 8 mL/min N_2 (balance gas and transport medium for the heat of reaction) and 5 - 10 mL/min N_2 (pressure line) the 4-way valve was switched back to the reactor. This last step represents the start of every Fischer-Tropsch experiment. After 4 hours of time on stream, 2 mL/min of N_2 (balance gas) were replaced with 2 mL/min of NH_3 (5 vol%). All experiments were stopped after 8 hours of time on stream and the reactor was allowed to cool down to room temperature. At the same time the 4-way valve was switched to bypass again and blind runs of the reactant stream were taken on the GC-TCD.

Table 3.4: Reaction parameter for the FT experiments on bulk iron and cobalt catalysts (gas flows at NTP).

	Reaction conditions	
	Bulk iron catalysts	Bulk cobalt catalysts
Total flow rate	40 ml/min (1920 h^{-1})[1, 2]	40 mL/min (1920 h^{-1})[1]
Flow rate CO + H_2	32 mL/min	32 mL/min
H_2:CO ratio	1:1, 2:1, 4:1	1:1
Flow rate N_2	6 – 8 mL/min	6 – 8 mL/min
Flow rate NH_3	0 – 2 mL/min	0 – 2 mL/min
Reactor temperature	250 °C - 300 °C	250 °C
Pressure	4 bar (gauge)	4 bar (gauge)

[1] Values in brackets represent the gas hourly space velocity (GHSV).
[2] For the experiments in chapter 4.2.2.3, other catalyst amounts and consequently other GHSV were used.

Online samples of the gas phase were taken via 6-way valves on top of every gas chromatograph and analyzed using different detectors (see chapter 3.4). A 1 mL sample loop was filled with the product and brought onto the GC column by switching the 6-way valve.

Liquid phase samples were collected after every Fischer-Tropsch experiment from the hot trap and selected samples were analyzed *offline* (chapter 3.4.4).

3.4 Product analysis

This section describes the analytical equipment which was used and the evaluation of the reported data. During the Fischer-Tropsch experiments *online* samples were taken on three different detectors. An internal standard consisting of a mixture of argon and cyclohexane was used to calculate the molar flow rates of the inorganic and organic compounds. Liquid phase samples were taken *offline* after every Fischer-Tropsch experiment and were analyzed by mean of two-dimensional gas chromatography at the University of Cape Town by Mr. Christian de Vries.

3.4.1 Gas chromatographic analysis: GC-TCD (*online*)

The consumption of CO, H_2 and NH_3 as well as the formation of CO_2 and CH_4 were recorded using a HP 5890 gas chromatograph equipped with a thermal conductivity detector (GC-TCD) and nitrogen as a carrier gas. Separation and acquisition of these compounds was performed on two columns both connected to a 10-way valve on top of the HP 5890 gas chromatograph which allows for switching between the columns. The gases in the sample stream leading from the reactor to the 10-way valve were collected previously using a 6-way valve and a 1 mL sample loop as described above.

After the addition of ammonia to the synthesis gas feed, the 10-way valve was switched regularly between a Column 1 and Column 2. Due their characteristic stationary phases of each column, it is possible to calculate the conversion of CO and H_2 and product formation of CO_2 and CH_4 (Column 1: Carbosieve II) as well as NH_3 conversion (Column 2: Porapak P). During the measurements the temperature of the detector was kept constant at 180 °C, while different oven temperatures were used on both columns (Table 3.5).

Table 3.5: Parameter for the analysis of inorganic compounds and methane on a HP 5890 GC-TCD.

Gas chromatograph	Hewlett Packard 5890 (*online*)
Detector	Thermal conductivity detector (TCD) $T_{Detector}$ = 180 °C
Column 1	Packed column (3 m x 1/8’’ O.D.)
Stationary phase	Carbosieve S-II, 80/100
Carrier gas	Nitrogen
Flow rate	15 mL/min
Injector	Splitless
Oven temperature	150 °C isothermal
Analyte	H_2, Ar (internal standard), CO, CH_4, CO_2
Column 2	Packed column (4 m x 1/8’’ O.D.)
Stationary phase	Porapak P, 80/100
Carrier gas	Nitrogen
Flow rate	15 mL/min
Injector	Splitless
Oven temperature	130 °C isothermal
Analyte	NH_3

On column 1, argon acts as an internal standard which allows one to calculate the molar flow rate $\dot{n}_i$ of an inorganic compound and methane from the areas A and the calibration factor $f_{TCD,i}$:

$$\dot{n}_i = f_{TCD,i} \cdot \left(\frac{A_i}{A_{Ar}} \right) \cdot \dot{n}_{Ar} \tag{3.2}$$

with

$$\dot{n}_{Ar} = \frac{\chi_{Ar} \cdot \dot{V}_{IS}}{V_A} \tag{3.3}$$

The molar concentration of argon within the mixture argon/cyclohexane χ_{Ar} and the volumetric flow rate $\dot{V}_{IS}$ are required to calculate the molar flow rate $\dot{n}_{Ar}$. V_A represents the Avogadro volume in equation 3.3.

The TCD was calibrated in constant intervals and the according calibration factor $f_{TCD,i}$ related to argon of a compound i was derived from:

$$f_{TCD,i} = \frac{[i]}{[Ar]} \cdot \frac{A_{Ar}}{A_i} \qquad (3.4)$$

For the determination of the calibration factors a known mixture of CO, CO_2, H_2, Ar and CH_4 was prepared and the flow rates were controlled by mass flow controllers. The obtained calibration factors for the measurements with the GC-TCD are attached in chapter 7.

For column 2, argon as the internal standard could not be separated and the conversion of NH_3 (X_{NH3}) was determined by doing blind runs at the end of every Fischer-Tropsch experiment. Here the ammonia-containing synthesis gas was led through the bypass and the area of NH_3 detected by the TCD is consistent with X_{NH3} = 0 %. In order to calculate selectivities to organic nitrogen-containing compounds based on ammonia, molar flow rates of NH_3 were derived from the ideal gas (see chapter 7).

3.4.2 Gas chromatographic analysis: GC-FID (*online*)

The formation of organic products during the Fischer-Tropsch experiments was observed and recorded using two gas chromatographs equipped with flame ionization detector (GC-FID) and mass spectrometer (GC-MS).

A HP 6890 gas chromatograph with equipped with a FID and an Agilent HP Plot Q capillary column was used to analyze all *n*-paraffins and 1-olefins in the range from C_1 - C_9 formed during the catalytic experiments (Figure 3.2). The injection of the samples was performed *online* using a 6-way valve with a 1 mL sample loop. Unlike the GC-MS analysis, where peaks of lower hydrocarbons from C_1 - C_2 overlap with inorganic gases such as CO, H_2, Ar and CO_2, they can be nicely separated with the GC-FID.

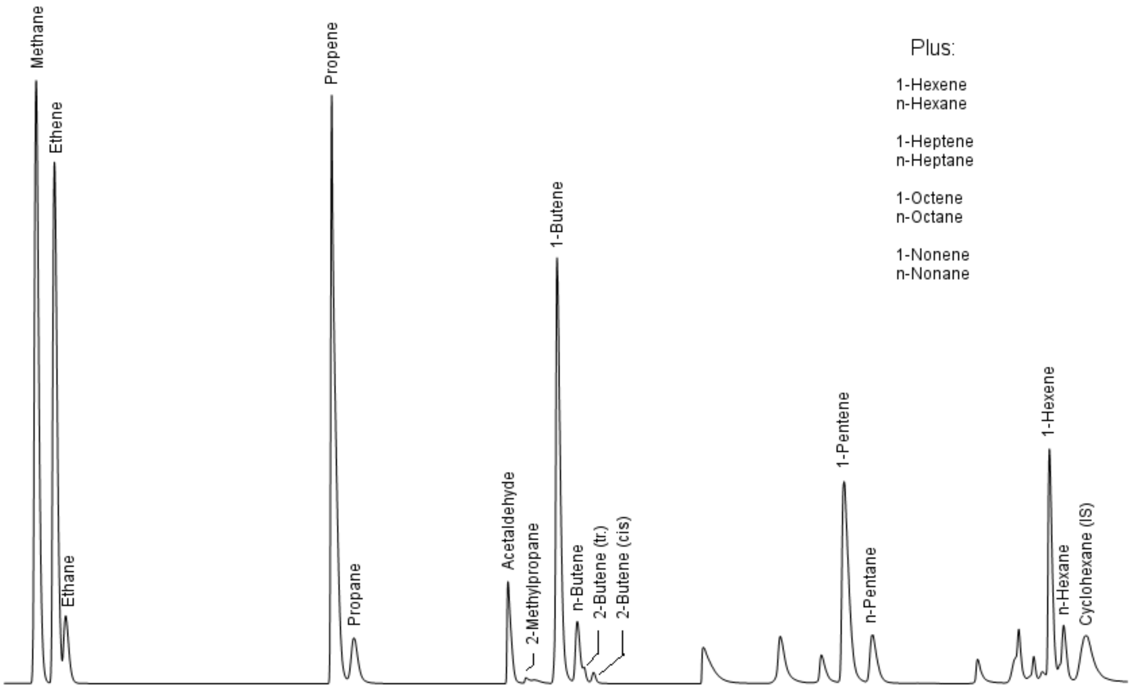

Figure 3.2: Gas chromatogram for FT products (Y-scale: intensity and X-scale: retention time are not displayed) on a potassium promoted iron catalyst in the absence of NH_3 obtained from *online* sampling on the HP 6890 GC-FID (Peaks for C_6 - C_9 1-olefins and *n*-paraffins ar not shown).

The Agilent HP Plot Q capillary column has the benefit to separate light hydrocarbon such as methane, ethane or ethene even at higher oven temperatures and no cooling of the GC oven to temperatures below 40 °C is necessary (Table 3.6). Due to better separation or the availability of the compound for calibration of the GC-MS (chapter 3.4.3), acetaldehyde, 2-methylpropane and 2-butene were analyzed with the GC-FID, too.

Table 3.6: Parameter for the analysis of organic compounds on a HP 6890 GC-FID.

Gas chromatograph	Hewlett Packard 6890 (*online*)
Detector	Flame ionization detector (FID) $T_{Detector}$ = 250 °C
Column	Agilent HP Plot Q (15 m, 0.32 mm I.D., 0.20 μm film thickness)
Stationary phase	Diviniybenzene/-styrol
Carrier gas	Hydrogen
Flow rate	3 mL/min for 1 min at 1 mL/min^2 to 1 mL/min
Column head pressure	1.4 bar
Injector	Split $T_{Injector}$ = 230 °C Split ratio 1:1
Temperature program	40 °C, 3 min isothermal at 8 °C/min to 120 °C, 5 min isothermal at 8 °C/min to 230 °C, 10 min isothermal

When using a flame ionization detector for the analysis of organic compounds, carbon atoms get ionized in a flame which results in a response signal from the detector. This response is linear but detection of carbon atoms at different oxidation states (oxygenates) results in a lower response signal. This can be compensated using response factors $f_{FID,i}$ for the quantification of oxygenates such as acetaldehyde:

$$f_{FID,i} = \frac{N_C}{N_{C\,(No\,O)} + N_{C\,(with\,O)}} \tag{3.5}$$

Here N_C represents the number of all carbon atoms and the response of carbon atoms which are not bonded to an oxygen atom is 1. The response of carbon atoms connected to an oxygen atom via a single bond is 0.55 and carbon atoms with a C=O double bond are considered to give no signal. All hydrocarbons detected by the FID in this work have the response factor of 1 whereas acetaldehyde as an oxygenate shows an exception with a $f_{FID,acetaldehyde} = 2$.

From the response factor $f_{FID,i}$, the carbon number N_i, the areas A_i and the molar flow rate of cyclohexane $\dot{n}_{CHx}$, the molar flow rates of an organic compound i can be calculated using cyclohexane as an internal standard:

$$\dot{n}_i = \left(\frac{N_{CHx}}{N_i}\right) \cdot \left(\frac{f_{FID,i} \cdot A_i}{f_{FID,CHx} \cdot A_{CHx}}\right) \cdot \dot{n}_{CHx} \qquad (3.6)$$

with

$$\dot{n}_i = \frac{\chi_{CHx} \cdot \dot{V}_{IS}}{V_A} \qquad (3.7)$$

where χ_{CHx} represents the concentration of cyclohexane in the mixture argon/cyclohexane.

3.4.3 Gas chromatographic analysis: GC-MS (*online*)

During the Fischer-Tropsch synthesis with additional NH_3 in the synthesis gas feed, N-containing compounds such as amines and nitriles can be formed [12][94]. To indentify and quantify this new compound class during Fischer-Tropsch synthesis a HP 6890 gas chromatograph equipped with a mass spectrometer (GC-MS). Other organic products such as oxygenated compounds and 2-olefins were analyzed by GC-MS, as well. The obtained mass spectra of the organic compounds then were compared with a database (National Institute of Standards and Technology, NIST).

Figure 3.3 shows the organic products in the range from C_2 - C_9, derived from Fischer-Tropsch experiments in the absence of ammonia, which were indentified and analyzed using a GC-MS (1-olefins and *n*-paraffins in brackets are analyzed with a HP 6890 GC-FID). During the gas chromatographic analysis, oxygenates and N-containing compounds showed longer retention times than paraffins or olefins from the same C fraction. For example, ethanol does not elute within the C_2 fraction but rather can be found within C_5 Fischer-Tropsch products. From this point of view, it is easy to quantify these compound classes by GC-MS since there are not affected by the regulations described in section 3.4.2. However, the retention times of organic nitrogen-containing compounds, which are not shown in Figure 3.3 and other organic products, are attached in the appendices (chapter 7).

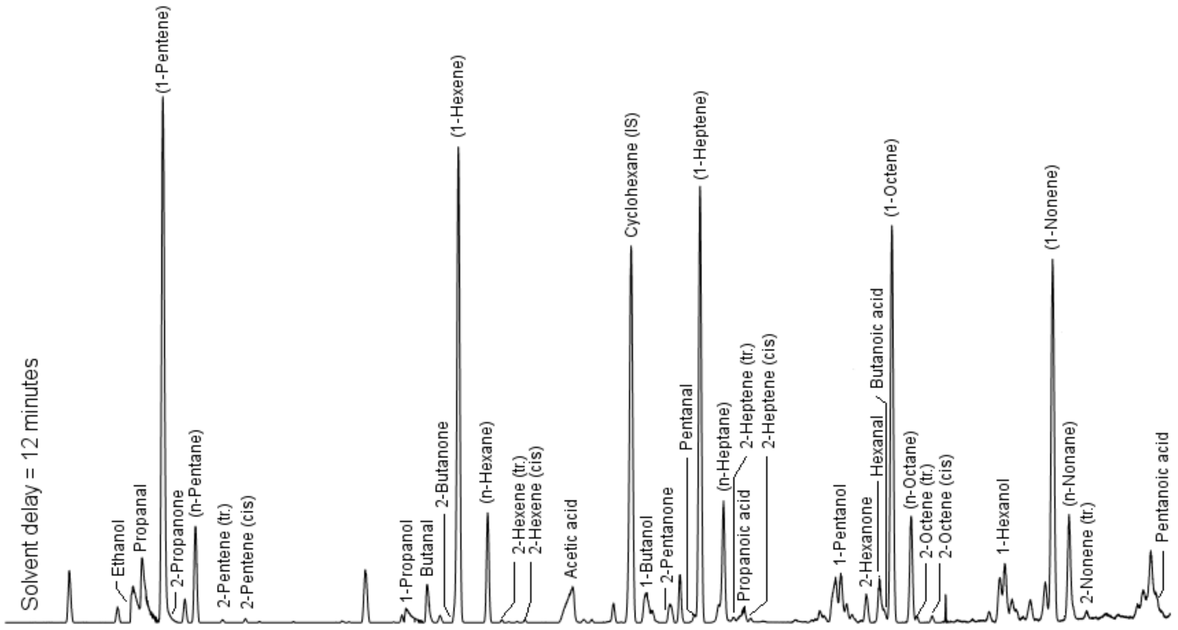

Figure 3.3: Gas chromatogram for FT products (Y-scale: intensity and X-scale: retention time are not displayed) on a potassium promoted iron catalysts in the absence of NH_3 obtained from *online* sampling on the HP 6890/5973 GC-MS (1-olefins and *n*-paraffins in brackets are analyzed on a HP 6980 GC-FID).

The injection of the samples was performed *online* using a 6-way valve with a 1 mL sample loop. For an accurate separation of the long chain FT products the GC oven was cooled with liquid nitrogen at -40 °C. To prevent any damages because of the filaments due to large amounts of inorganic gases such as CO, H_2, Ar and CO_2, a solvent delay of 12 minutes for the analysis of each sample was used.

Table 3.7: Parameter for the analysis of organic compounds on a HP 6890/5973 GC-MS.

Mass spectrometer	Hewlett Packard 5973
Detector	Mass selective detector (MSD) $T_{Detector}$ = 150 °C $T_{Transfer\ line}$ = 200 °C
Mode	Electron-impact (EI) T_{Source} = 230 °C
Scan range	12 – 300 amu @ 4.83 scans/sec
Gas chromatograph	Hewlett Packard 6890 (*online)*
Column	Optima 1 MS Accent (60 m, 0.25 mm I.D., 0.25 μm film thickness)
Stationary phase	Dimethylpolysiloxane
Carrier gas	Helium
Flow rate	2.7 mL/min
Column head pressure	1.18 bar
Injector	Split $T_{Injector}$ = 230 °C Split ratio 1:1
Temperature program	-40 °C, 3 min isothermal at 8 °C/min to 120 °C, 5 min isothermal at 8 °C/min to 230 °C, 10 min isothermal
Solvent delay	12 minutes

During the Fischer-Tropsch synthesis, a broad product spectra, consisting of paraffins, olefins or oxygenates is typically produced making it difficult to separate and identify. It gets even more complicated when adding ammonia to the synthesis gas feed and the product spectra is enlarged due the formation of N-containing compounds. Here the GC-MS technique has an advantage where characteristic ions from the organic molecules can be extracted and the separation of several peaks becomes possible (Figure 3.4). A list of the extracted ions m/z used in this work can be found in Table 7.3 within the appendices.

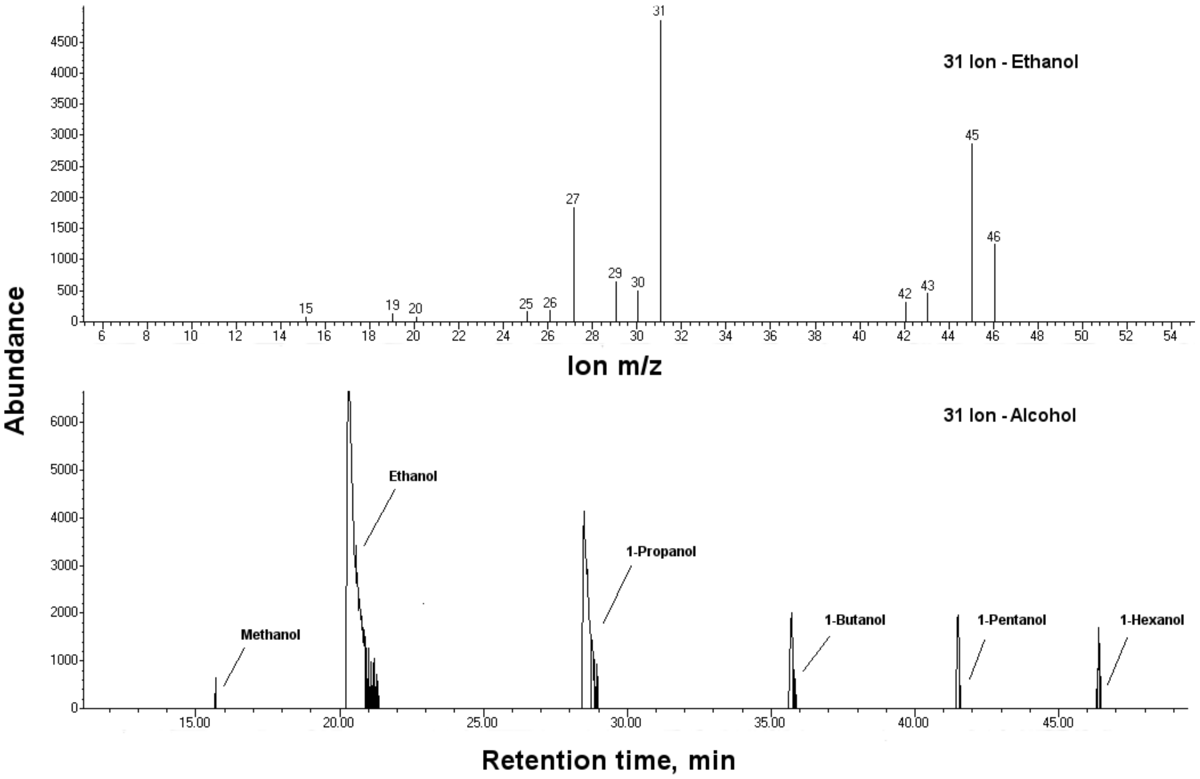

Figure 3.4: Mass spectra (EI) of ethanol and extracted ion chromatogram for ion m/z = 31 (alcohols) from a FT experiment in the absence of ammonia.

However, the analysis of organic compounds with a mass spectrometer is more complicated than with a flame ionization detector because a mass spectrometer does not show a linear response signal with different concentrations. All organic products which are going to be quantified by the GC-MS had to be calibrated (chapter 7.2). Due to the prices or the availability of branched chemicals such as 3-methylpentane for example, this compound class could not be calibrated on the GC-MS. Thus, branched hydrocarbons with the exception of 2-methylpropane (taken from GC-FID) were not included in the calculations for the selectivity of organic products derived from the Fischer-Tropsch experiments in this work.

From the extracted ions and an internal standard cyclohexane, which is not a product from the Fischer-Tropsch synthesis, calibration factors A and B can be derived (chapter 7.2) and the molar flow rate of an organic compound $\dot{n}_i$ can be calculated:

$$\dot{n}_i = \left(A_{MS,i} \left(\frac{A_i}{A_{CHx}} \right)^2 + B_{MS,i} \left(\frac{A_i}{A_{CHx}} \right) \cdot \dot{n}_{CHx} \right) \tag{3.8}$$

The calibration factors $A_{MS,i}$ and $B_{MS,i}$ are obtained from a polynomial 2nd order from the calibration of an organic compound i with cyclohexane.

3.4.4 Gas chromatographic analysis: GCxGC-TOF (*offline*)

Many different compound classes can be obtained in the organic product from Fischer-Tropsch synthesis. The result is a complex mixture consisting of polar and nonpolar organic compounds. When ammonia is added to the synthesis gas feed the situation becomes more complex and the use of two-dimensional gas chromatography (GCxGC) is a powerful analytical instrument to solve this issue. Here, after first separation on a first column, the analyte is going to be analyzed on a second column with a different polarity after a couple of seconds.

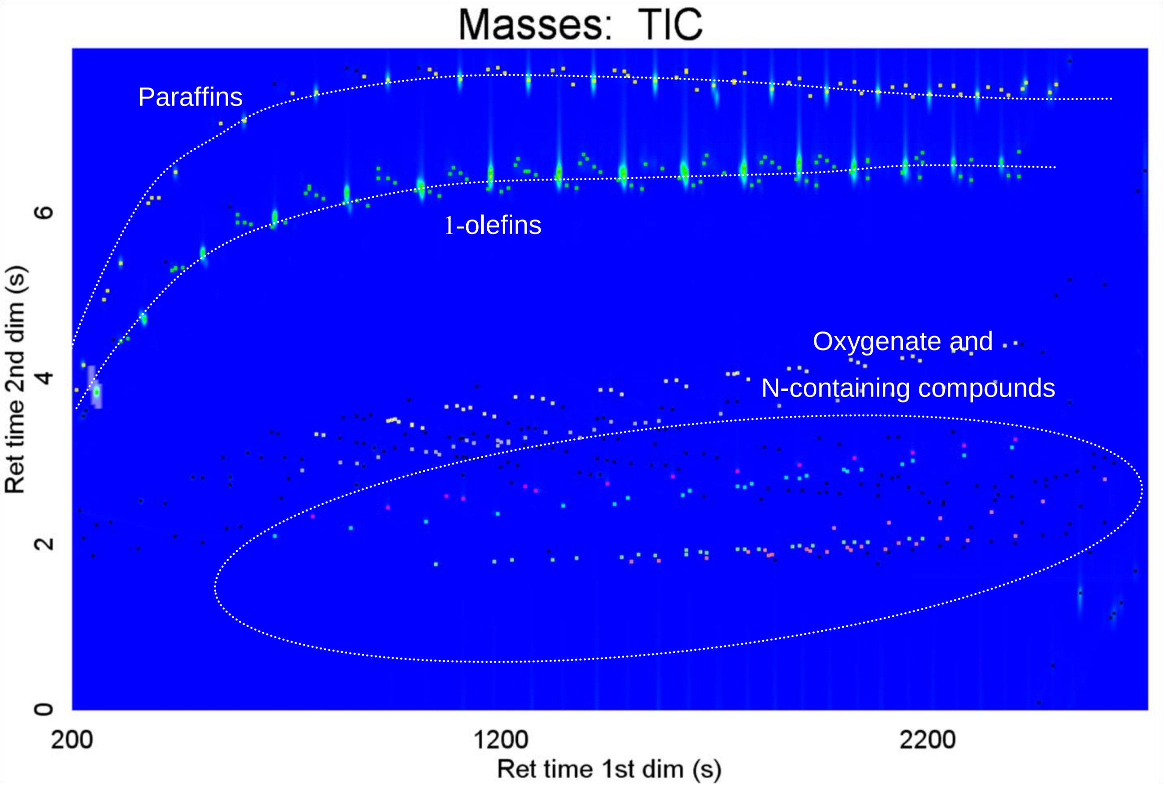

Figure 3.5: Chromatogram obtained from *offline* two-dimensional gas chromatographic analysis (GCxGC-TOF) of organic products from FT and NH_3-FT synthesis on a potassium promoted bulk iron catalyst.

The organic analyte then can be identified with a mass spectrometer (Time-of-Flight detector, TOF). Every single organic compound gives characteristic mass spectra which can be compared with a database (National Institute of Standards and Technology, NIST) in order to identify the peaks (Figure 4.24). This gas chromatographic analysis, in the further progress of the work referred as ‘GCxGC-TOF’, was performed by Mr. Christian de Vries at the University of Cape Town.

Table 3.8: Parameter for the analysis of organic compounds on an Agilent 7890/GCxGC-TOF.

Mass spectrometer	Leco Pegasus 4D
Detector	Time-of-Flight (TOF) $T_{\text{Transfer line}}$ = 250 °C
Gas chromatograph	Agilent 7890 (*offline)*
Modulator	$T_{\text{Modulation}}$ = 8 s
Injector	Split T_{Injector} = 225 °C Split ratio 80:1
Column 1	CP-Wax 52CB (30 m, 0.25 mm I.D., 0.20 µm film thickness)
Stationary phase	Polyethylene glycol
Carrier gas	Helium
Flow rate	0.6 mL/min
Column head pressure	1.19 bar
Temperature program	40 °C, 1 min isothermal at 4.5 °C/min to 215 °C, 5 min isothermal
Column 2	CP-Sil 8 CB (1.8 m, 0.1 mm, 0.10 µm film thickness)
Stationary phase	Polyphenylmethylsiloxane
Carrier gas	Helium
Flow rate	0.6 mL/min
Temperature program	72.50 °C, 1 min isothermal at 4.5 °C/min to 250 °C, 5 min isothermal

Liquid phase samples taken from the hot trap after the experiments (see chapter 3.3.2), were dissolved in *n*-hexane and injected *offline*. During GCxGC-TOF analysis in this study, the focus was on solely the qualitative identification of nitrogen-containing compounds such as amines, nitriles and amides.

The injected samples were analyzed on two different columns. The first peak separation step is performed on a polar CP-Wax 52CB capillary column (Table 3.8) and second separation was performed on a nonpolar CP-Sil 8 CB capillary column. A thermal modulator exists between the two columns which consist of jets to create two trapping zones by using liquid and gaseous nitrogen. After the analyte has passed the first capillary column, the liquid nitrogen holds back the injected sample in order to achieve accurate separation of the products before it is injected on the second capillary column.

3.4.5 Calculations

With the molar flow rates of the Fischer-Tropsch educts and organic products in the gas phase it is possible to calculate conversions and selectivities. The conversion of a reactant CO or H_2 towards organic products or CO_2 can be derived as followed:

$$X_{\mathrm{reactant}} = 1 - \frac{(\dot{n}_{\mathrm{reactant}})_{\mathrm{out}}}{(\dot{n}_{\mathrm{reactant}})_{\mathrm{in}}} \qquad (3.9)$$

To calculate the selectivity $S_{i(C)}$ to an organic product i on a carbon basis one have to consider the stoichiometry ν of the reaction:

$$S_{i,(C)} = \frac{\dot{n}_i}{(\dot{n}_{CO})_{\mathrm{in}} - (\dot{n}_{CO})_{\mathrm{out}}} \cdot \frac{|\nu_{CO}|}{\nu_i} \qquad (3.10)$$

Selectivities to nitrogen-containing compounds i based on ammonia as a reactant are calculated with equation 3.11:

$$S_{i,(N)} = \frac{\dot{n}_i}{(\dot{n}_{NH3})_{in} - (\dot{n}_{NH3})_{out}} \cdot \frac{|\nu_{NH3}|}{\nu_i} \tag{3.11}$$

The selectivity to an organic product i within organic compounds in the gas phase samples can be calculated from:

$$S_i = \frac{\dot{n}_i}{\sum \dot{n}_i} \tag{3.12}$$

Equation 3.12 can be modified towards a selectivity based on a carbon number n from an organic product i. As an example, the alcohol selectivity with a carbon number n is given in equation 3.13:

$$S_{alcohol,n} = \frac{\dot{n}_{alcohol,n}}{\dot{n}_{alcohol,n} + \dot{n}_{lin.\ hydrocarbons,n}} \tag{3.13}$$

4 Results and discussion

4.1 Catalyst characterization

Bulk iron based catalysts were used in previous studies by Sango [111] during his Fischer-Tropsch experiments in the presence of ammonia. For further studies on the topic of the ammonia co-feeding during Fischer-Tropsch synthesis, this catalyst material can be used and therefore more information about the catalyst (e.g. reduction behaviour, morphology, composition and particle size) is necessary.

The bulk iron- and cobalt-containing catalyst materials prepared from the precipitation of their metal nitrates with ammonia hydroxide (see section 3.1) were investigated with different methods at the Carl von Ossietzky Universität Oldenburg and the University of Cape Town (chapter 3.2) and results from the catalyst characterization are discussed here.

4.1.1 Atomic adsorption spectroscopy

The potassium promoted iron catalysts were analyzed by means of atomic adsorption spectroscopy (AAS) and results are presented in Table 4.1 (unpromoted iron and cobalt catalysts are also listed in Table 4.1).

Table 4.1: Nominal potassium content and content found by AAS (per g_{Fe}) of promoted iron catalysts.

Catalyst	**Nominal K content** (wt%)	**K content found by AAS** (wt%)
Fe-0K [1]	0.00	-
Fe-2K	2.00	1.52
Fe-5K	5.00	5.84
Co-0K [1]	0.00	-

[1] Catalysts Fe-0K and Co-0K were not analyzed by AAS since their K content is already 0.00 wt%.

It can be seen that the promotion with potassium was successful and K contents differ slightly from the theoretically calculated values of 2 and 5 wt%. From the results it may be speculated that an inhomogeneous potassium distribution on iron catalysts was obtained. Since only small amounts of potassium promoted catalyst samples were analyzed, they might not reflect the actual potassium content and are only screenshot of the average potassium distribution. Therefore, the use of higher amounts of catalyst materials during AAS would probably lead to more accurate results.

4.1.2 Temperature programmed reduction

The reduction behavior of the unpromoted/promoted bulk iron and cobalt catalyst materials were investigated by means of temperature programmed reduction (TPR). The metal oxides were reduced with hydrogen (5 vol% H_2 in Ar) to 900 °C and the reduction profiles are presented in Figure 4.1.

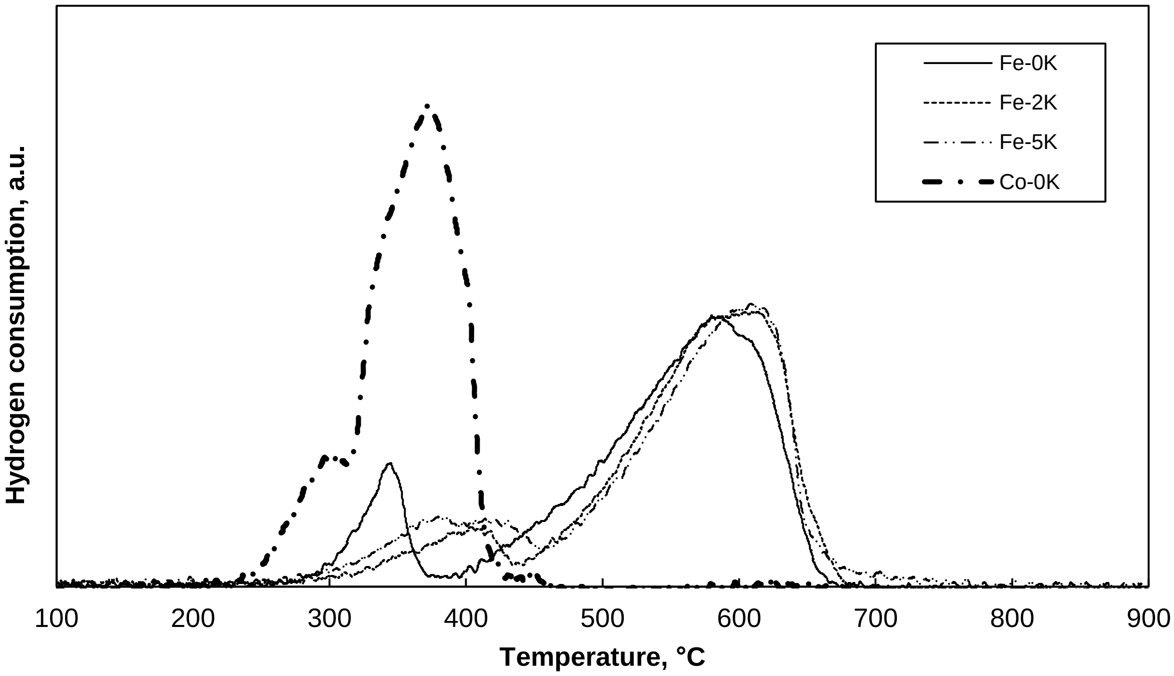

Figure 4.1: H_2-TPR profiles of calcined iron and cobalt catalyst samples.

The unpromoted iron oxides Fe-0K shows two distinct peaks indicating the two steps reduction of hematite (Fe_2O_3) to magnetite (Fe_3O_4) at 343 °C (Equation 4.1) and to metallic iron Fe at 588 °C (Equation 4.1) [40][116]. The transformation of magnetite to metallic iron is a slow process which is exhibited by the broad hydrogen consumption peak [117][118].

$$3\ Fe_2O_3 + H_2 \rightarrow 2\ Fe_3O_4 + H_2O \tag{4.1}$$

$$2\ Fe_3O_4 + 8H_2 \rightarrow 6\ Fe + 8\ H_2O \tag{4.2}$$

With the addition of potassium to bulk iron catalyst samples the reduction curves change slightly. For catalysts Fe-2K and Fe-5K the peak position of the first reduction step shifted approximately 45 - 60 °C to higher temperatures, while for the reduction to metallic iron the temperature increased to 607 °C. Furthermore this hindrance can be seen during the reduction from Fe_2O_3 to Fe_3O_4, where a broader peak results.

Compared to bulk iron oxides the reduction profile of cobalt oxide is different. Here, peak positions for the two reduction steps from cobalt(II,III) oxide (Co_3O_4) and cobalt(II) oxide (CoO) to metallic cobalt (Equation 4.3 and 4.4) occur at lower temperatures [19][87]. The first maximum appears at 291 °C and the second at 374 °C.

$$Co_3O_4 + H_2 \rightarrow 3\ CoO + H_2O \tag{4.3}$$

$$3\ CoO + 3H_2 \rightarrow 3\ Co + 3\ H_2O \tag{4.4}$$

From the H_2-TPR curves of all four prepared catalysts it can be seen that second reduction peaks are in accordance with the stoichiometry of the reactions and more hydrogen is consumed during the second reduction step.

4.1.3 X-ray diffraction spectroscopy

The results of X-ray diffraction spectroscopy (XRD) on the calcined unpromoted/promoted bulk iron and cobalt catalysts are shown in Figure 4.2 where it can be seen that catalysts have been prepared and calcined successfully. The metal hydroxides were transferred into the oxide phases Fe_2O_3 (hematite) and Co_3O_4, and XRD patterns match very well with the reference spectra. In case of catalyst Fe-5K a peak at 2 Theta = 31.6 ° appears which cannot be found on the other iron oxide samples. However, this peak is not related to either potassium or potassium oxide and, in turn, it is similar to the XRD pattern for iron oxyhydroxide (FeO(OH)).

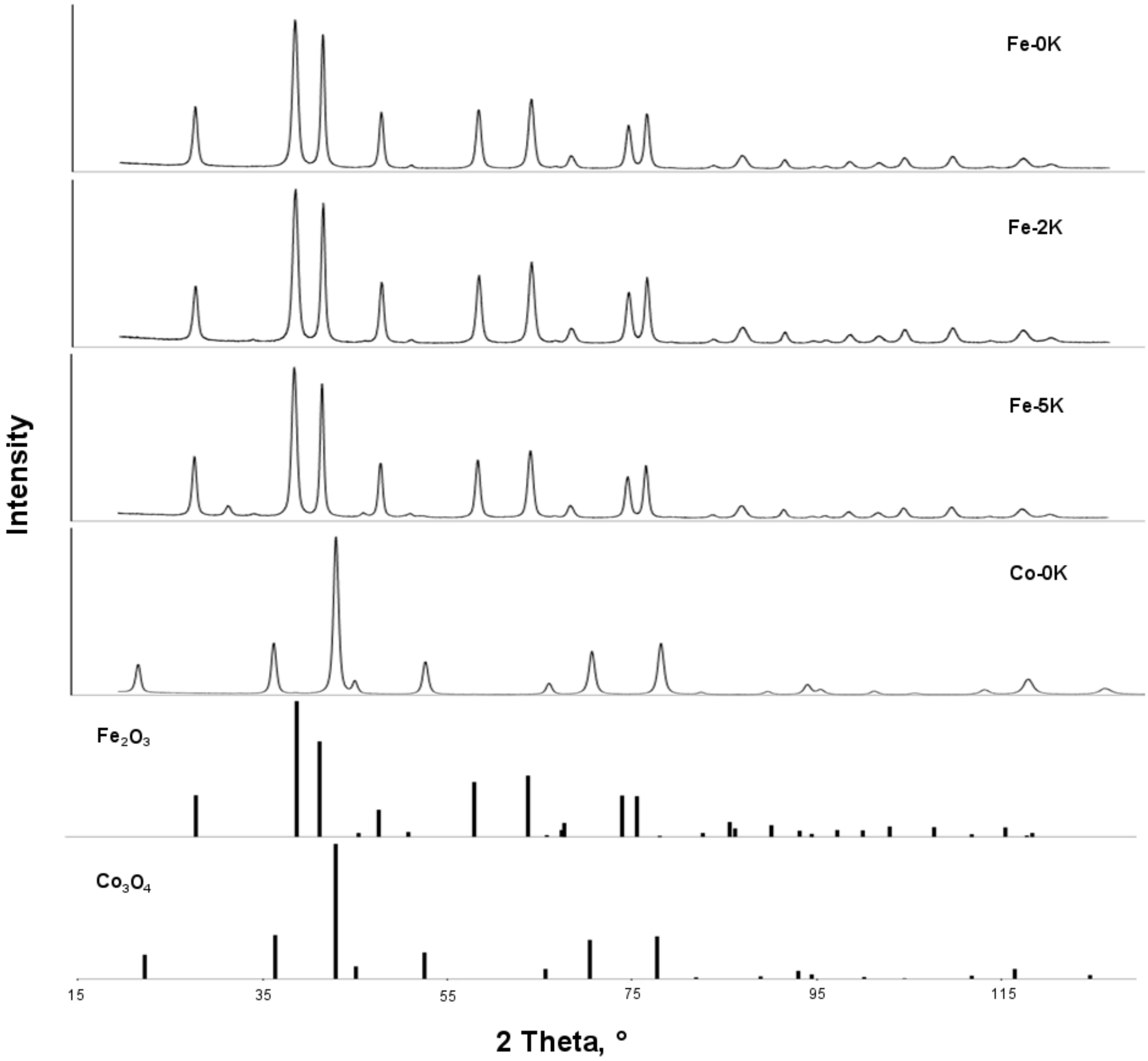

Figure 4.2: XRD patterns of calcined bulk iron/cobalt catalysts with different potassium loading and reference pattern (taken from International Centre for Diffraction Data PDF-2 database).

The average particle size of the catalysts was estimated using the Debye-Scherer equation (Equation 3.1), where the FWHM was calculated from main reflexes for Fe_2O_3 at 2 Theta = 38.6 ° and for Co_3O_4 at 2 Theta = 43 °. All catalyst materials exhibited an average diameter of 14-15 nm independent of the catalyst metal (Table 4.2). This was also with no consequence to the average iron oxide particle size upon the addition of potassium.

Table 4.2: Average particle size of calcined iron and cobalt catalysts estimated using the Debye-Scherer equation.

Catalyst	**Average particle size** (nm)
Fe-0K	14.63
Fe-2K	14.19
Fe-5K	14.86
Co-0K	14.84

4.1.4 Transmission electron microscopy

TEM micrographs of the calcined iron- and cobalt-containing catalysts (metal oxides) are displayed in Figure 4.3. As discussed in the XRD results, the average particle size for all materials was in the range of 14 to 15 nm. Although the particles are shaped uniformly, this average size estimate reasonably agrees with what appeared in the TEM images and, again, there appeared to be no influence on the iron catalyst with the addition of potassium. For bulk cobalt oxides, randomness in the morphology can be observed from the TEM images and some of the particles show nanorod-like structures [130].

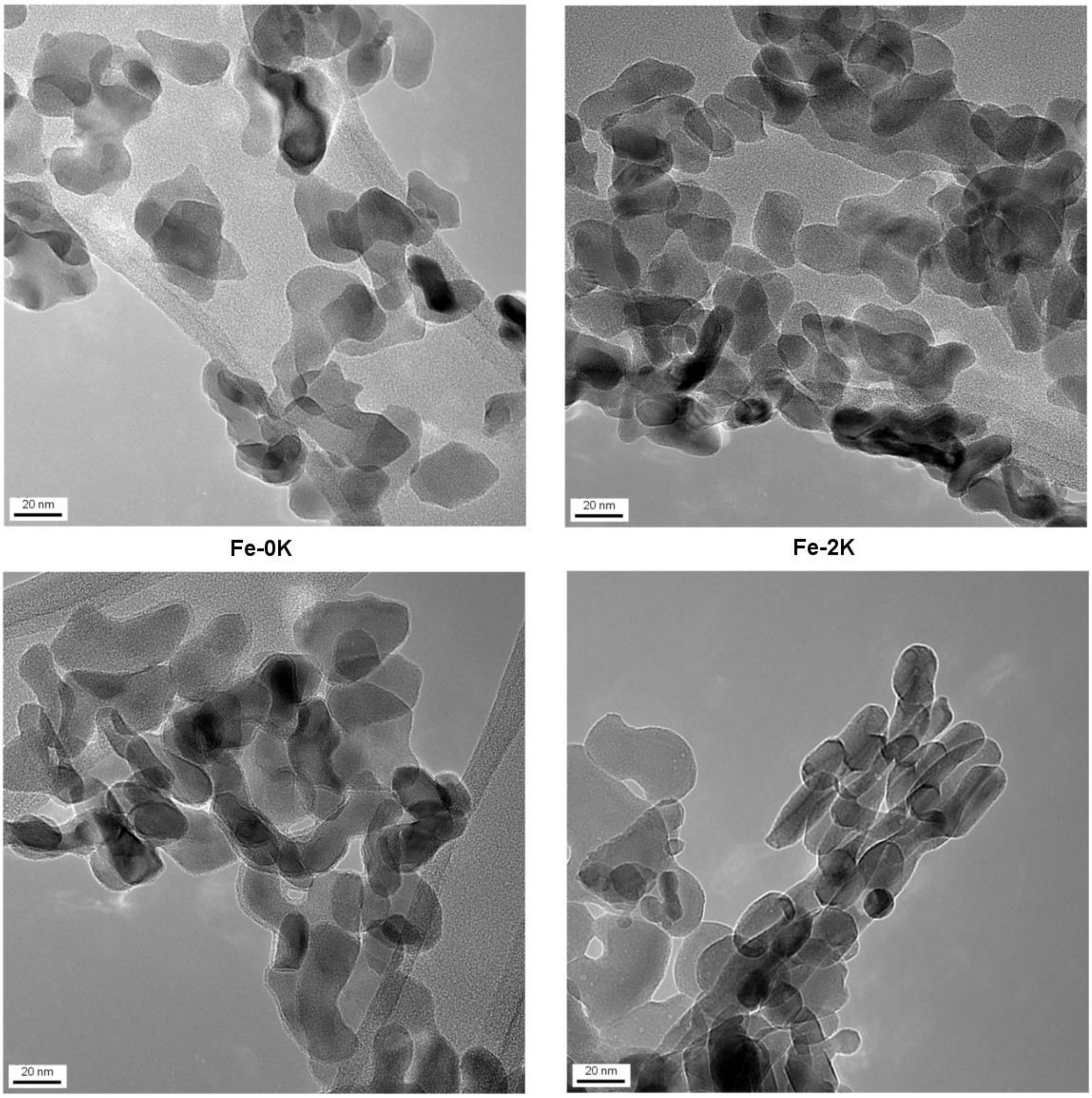

Fe-0K Fe-2K

Fe-5K Co-0K

Figure 4.3: TEM micrographs of the prepared iron and cobalt oxides.

4.1.5 Chemical analysis of spent catalysts

After 240 min of time on stream ammonia was added to the Fischer-Tropsch experiments in this study. In order to determine if any nitrides have been formed from the reaction in the presence of ammonia small amounts of spent catalysts were investigated for their nitrogen content. Table 4.3 shows nitrogen contents in bulk iron and cobalt catalysts after they have been exposed to ammonia-containing synthesis gas during the reaction.

Table 4.3: Results of N – Analysis for NH_3 co-feed experiments on iron and cobalt catalysts.

Catalyst	**H_2:CO ratio during experiment**	**p_{NH3} in synthesis gas** (bar)	**Duration NH_3 co-feed** (h)	**Nitrogen content** (wt%)
Fe-0K	2:1	0.2	4	0.07
Fe-2K	2:1	0.2	4	0.13
Fe-5K	2:1	0.2	4	0.11
Co-0K	1:1	0.2	4	0.08

Only small nitrogen contents were detected during the analysis of spent iron- and cobalt-based catalysts. From the results in Table 4.3, no statement can be given if metal nitrides were formed during Fischer-Tropsch experiments in the presence of ammonia. The nitrogen could also belong to residues from catalyst preparation where iron and cobalt nitrates were used (chapter 3.1.1).

4.1.6 Summary

Little is known about ammonia co-feeding during Fischer-Tropsch synthesis and the influence of catalysts onto the performance of the reaction. The literature which is available gives not sufficient information about the catalysts used for reactions. In this work, bulk iron- and cobalt catalysts were chosen to study the influence of ammonia on the Fischer-Tropsch synthesis. In general cobalt catalysts are supported on metal oxides in order to increase their catalytic activity but here catalytic performance was tested without any influence of a support and will be compared with the results from the experiments on iron-containing catalysts. However, for further investigations in the field of ammonia co-feeding during Fischer-Tropsch synthesis the composition, reduction behaviour, particle size and morphology of unpromoted/promoted bulk iron and cobalt catalysts were investigated.

It could be shown by means of XRD that metal oxide phases were successfully obtained from the catalyst preparation step. Impregnation of iron oxides with different potassium loadings, determined by AAS, had an influence on the H_2 reduction profile (TPR) where broader peaks were observed and a shift towards higher temperatures occurred. An average catalyst particle size between 14 and 15 nm was determined using the Debye-Scherer equation, whereas it was not possible to characterize particle sizes by means of TEM due to the non-inform shape of the particles. From the chemical analysis of spent catalysts from Fischer-Tropsch experiments in the presence of ammonia, small nitrogen contents were found. However, no statement can be given if the observations are related to the formation of metal nitrides during the reaction or if the nitrogen belongs to residue from catalysts preparation.

4.2 Catalytic Fischer-Tropsch experiments with ammonia

In this chapter the results of the ammonia addition to the synthesis gas (CO + H_2) feed during the Fischer-Tropsch (FT) experiments will be presented. It was reported in literature that the addition of ammonia to the synthesis gas feed during Fischer-Tropsch synthesis on transition metal based catalysts lead to the formation of N-containing compounds such as amines, amides and nitriles (for further information and other literature see also chapter 2.5) [6][10][11][12]. Amines, nitriles or amides are key chemicals and are used as pharmaceuticals, agricultural chemicals, solvents or intermediates in a number of industrial applications [5][6][7][8]. The Fischer-Tropsch with its huge production capacities and feedstock based on coal, natural gas or biomass could be beneficial for the production of such N-containing compounds.

Most of the publications are found in patents and little is known about the influence of NH_3 on the catalytic performance of transition metal based catalysts during conventional FT synthesis or the reaction mechanisms which could explain the formation of amines, nitriles or amides. In order to aid the fundamental understanding in this regard, catalytic experiments were conducted in a fixed-bed reactor using unpromoted and potassium promoted bulk iron catalysts (section 3.3). Reactions were also carried out on bulk cobalt catalysts and the results will be used to explain and support the findings from the experiments on iron catalysts. However, detailed information about the catalytic performance of bulk cobalt catalysts during Fischer-Tropsch experiments at different ammonia partial pressures can be found in chapter 7.4.4.

Prior to the catalytic Fischer-Tropsch experiments the metal oxides, Fe_2O_3 and Co_3O_4, were reduced *in situ* to the pure metal phase with hydrogen (see chapter 3.3.2). After the reduction was completed, the reaction was started by switching the gas flow to synthesis gas and ammonia was added to the Fischer-Tropsch reaction after 240 minutes of time of stream. In the further progress of this work these ammonia co-feed runs are also referred as ‘NH_3-FT’ experiments, catalytic experiments without ammonia as ‘FT’ experiments and catalytic tests at two different ammonia partial pressures (p_{NH3} = 0.0 and 0.2 bar) as ‘FT/NH_3-FT’ experiments.

Gaseous organic and inorganic products as well as reactants obtained from the reactions were analyzed by means of *online* gas chromatographic analysis (section 3.4) using different detectors (GC-TCD, GC-MS and GC-FID). An exception is the analysis of selected liquid phase samples which was performed *offline* by means of two-dimensional gas chromatography coupled with a mass spectrometer (GCxGC-TOF).

4.2.1 Experiments on unpromoted/promoted bulk iron catalysts

It was reported in literature that the addition of ammonia during the Fischer-Tropsch synthesis can improve the conventional FT product selectivity and high selectivities towards valuable olefins could be obtained [6][112]. The addition of ammonia to freshly reduced transition metal based catalysts can result in the formation of metal nitrides which show a better catalytic performance during Fischer-Tropsch reactions with CO and H_2 [105][113][114]. Here, increased olefin and C_{5+} hydrocarbon contents were found. Moreover, the catalysts showed an enhanced resistance against oxidation and carbon deposition onto the catalyst surface.

When ammonia is added to the Fischer-Tropsch synthesis, the formation of valuable nitrogen-containing compounds such as amines, nitriles or amides can be observed [6][10][11] [111]. The reactions can be carried out on unpromoted or potassium promoted transition metal catalysts and some authors reported about increased selectivities to these compounds with high potassium loadings [95][96].

While potassium is known to have beneficial promotional effects during the Fischer-Tropsch and the ammonia synthesis [3][39][40][63][72], little information is available on how the conventional Fischer-Tropsch product selectivity is affected when both potassium and ammonia are present [6][111].

From this point of view, a series of FT/NH_3-FT experiments on bulk iron catalysts with different potassium loadings was conducted and the results of the investigations will be presented in this section. Due to the complexity of the Fischer-Tropsch reaction, the results from the ammonia co-feeding will be discussed in more detail in chapter 4.2.1.10.

4.2.1.1 Catalytic activity

The catalytic activity during the Fischer-Tropsch synthesis is represented by the conversion of carbon monoxide to organic products and, on iron catalysts, carbon dioxide. Since the influence of ammonia on the catalytic performance of iron catalysts within this work was tested, this section also shows the conversion of ammonia and its influence on hydrogen consumption during FT/NH_3-FT experiments.

Carbon monoxide conversion

In Figure 4.4 the overall conversion of CO (organic products plus carbon dioxide) is presented.

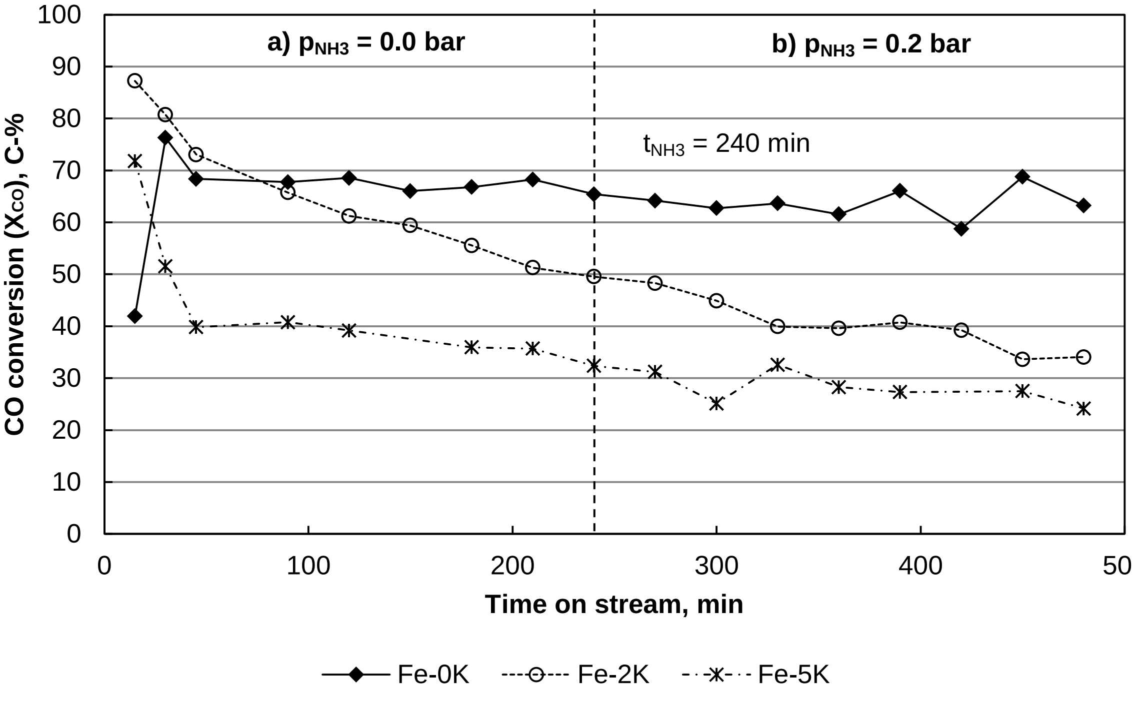

Figure 4.4: CO conversion (X_{CO}, C-%, organic products plus CO_2) during FT/NH_3-FT runs on iron catalysts with different potassium loadings in: a) the absence of NH_3 and b) the presence of NH_3 ($T_{Reactor}$ = 270 °C, P_{Total} = 4 bar, p_{NH3} = 0.0 - 0.2 bar, GHSV = 1920 h^{-1}, H_2:CO = 2:1).

The influence of potassium on the conversion of CO during the ammonia-free FT experiments (region a) in Figure 4.4) can be seen. With increasing potassium content in the iron catalysts, a decline in the CO conversion can be observed. Measurements in the beginning of the reactions up to 50 minutes of time on stream show fluctuations that are considered to result from establishing certain FT regimes (chapter 2.4.3). However, decreasing CO conversion with higher amounts of potassium could be related to catalyst deactivation due to the formation of free surface carbon from the Boudouard reaction (equation 2.3) [15][17]. An electron donor effect of potassium leads to enhanced CO dissociation and beside a mixture of different iron carbides and magnetite, free surface carbon could also be formed (Figure 2.5) [15]. These carbon species can block active sites for the reaction and conversion of CO is lowered [128]. Potassium itself also has the ability to block active sites of the catalysts which could lead to catalyst deactivation [41].

When ammonia is added to the synthesis gas feed, it appears that the CO conversion drops slightly in case of the NH_3-FT experiments on unpromoted iron catalysts and the decrease in conversion for the catalysts Fe-2K and Fe-5K continuous. Although ammonia is known as a catalyst poison which could lead to catalyst deactivation [13], the decrease of X_{CO} for the potassium promoted catalyst series could be still related to a deactivation process caused by surface carbon and is possibly not induced by ammonia. This would be in agreement with the results from Sango [111]. He conducted Fischer-Tropsch experiments in the presence of ammonia using similar potassium promoted bulk iron catalysts as within this work. Sango [111] observed that CO conversion is only affected at higher ammonia concentrations in the synthesis gas feed (10 to 35 vol%).

In case of catalyst Fe-5K, which has the highest potassium loading, it may be hypothesized that CO conversion becomes stabilized at a partial pressure of $p_{NH3} = 0.2$ bar. In this context Dry *et al.* [119] found that additional ammonia in the synthesis gas feed inhibits the Boudouard reaction and consequently catalyst deactivation due to carbon deposition on the catalyst surface is lowered. A decrease in carbon deposition was also reported by Shultz *et al.* [113] during Fischer-Tropsch experiments on iron nitrides used as catalysts.

However, the different behaviour in CO conversion at an ammonia partial pressure of $p_{NH3} = 0.2$ bar during the NH_3-FT experiments on unpromoted/promoted iron catalysts will be discussed in chapter 4.2.1.10.

Hydrogen conversion

The hydrogen consumption for the conducted FT/NH_3-FT experiments is shown in Figure 4.5. Highest H_2 conversion (X_{H2}) can be observed at $p_{NH3} = 0.0$ bar for unpromoted iron catalysts, followed by iron catalysts with increasing potassium content.

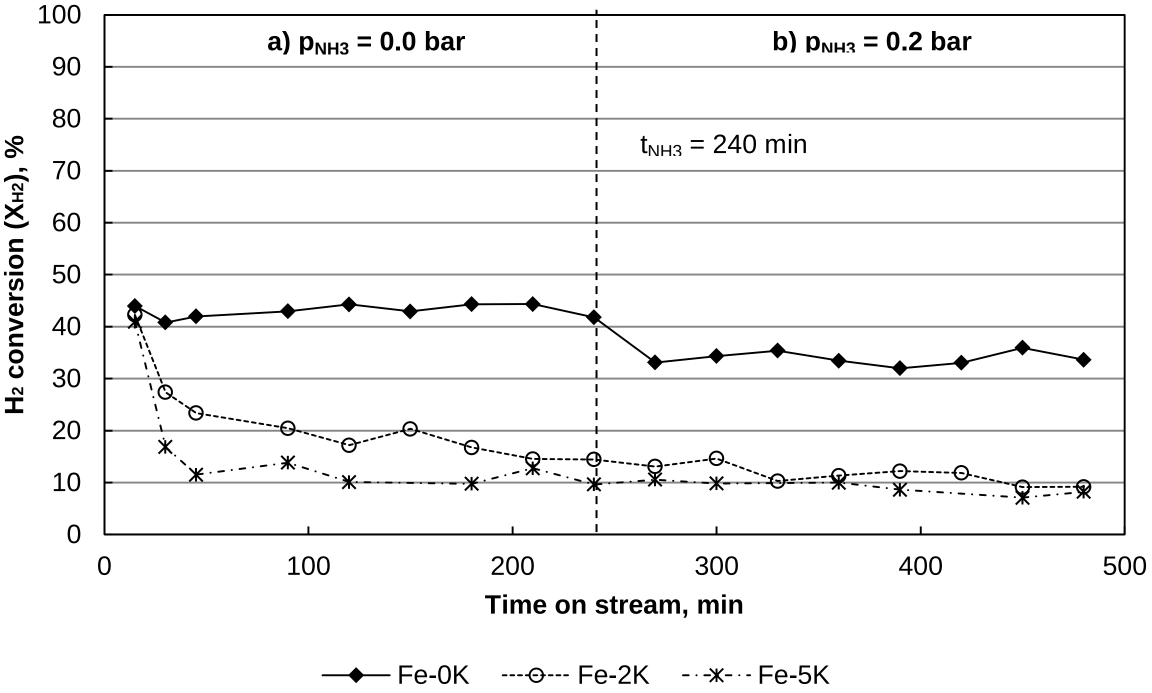

Figure 4.5: H_2 conversion (X_{H2}, %) during FT/NH_3-FT runs on iron catalysts with different potassium loadings in: a) the absence of NH_3 and b) the presence of NH_3 ($T_{Reactor}$ = 270 °C, P_{Total} = 4 bar, p_{NH3} = 0.0 - 0.2 bar, GHSV = 1920 h^{-1},H_2:CO = 2:1).

When ammonia is added to the system after 240 minutes of time on stream, the hydrogen consumption on unpromoted iron catalysts is still the highest but is mostly affected by the presence of NH_3 and X_{H2} declines by approximately 10 %. In contrast to that, the hydrogen conversion in case of FT/NH_3-FT experiments on potassium promoted iron catalysts decrease only slightly. Similar results were observed by Sango [111] during his NH_3-FT experiments conducted in a slurry reactor and using potassium promoted iron catalysts. The hydrogen conversion was influenced by low ammonia concentrations in the synthesis gas feed (2 - 5 vol%) and only ammonia concentrations up to 20 vol% led to decreased hydrogen conversion.

However, possible reasons for reduced hydrogen conversion in the presence of ammonia and the different behaviour between the catalysts will be discussed in the further progress of this work based on other results (chapter 4.2.1.10).

Ammonia conversion

Ammonia does not only act as a catalyst poison when exposed to transition metal catalysts and it can undergo chemical reactions which can affect the ammonia conversion during the NH_3-FT experiments in this work. When ammonia is added to the synthesis gas feed during Fischer-Tropsch synthesis, it can be converted to organic products such as amines, nitriles or amides (chapter 2.5) [10][11][12]. Other side reactions such as the formation of ammonium carbonate or ammonium bicarbonate could take place, too [98][111]. Transition metal catalysts (e.g. iron or cobalt) are also known to catalyze the endothermic decomposition reaction of ammonia to N_2 and H_2 (chapter 2.6.2) [72][73][74]. Furthermore, the parallel reaction of the NH_3 decomposition could take place and metal nitrides may be formed [113][114].

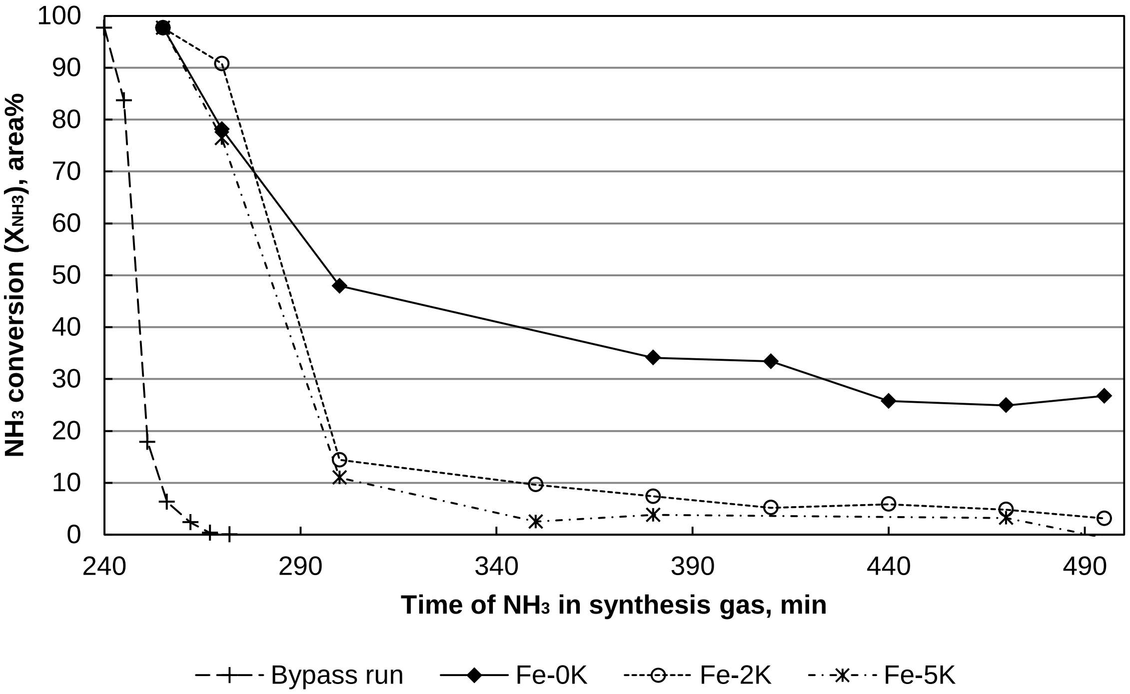

Figure 4.6: NH_3 conversion (X_{NH3}, area%) during NH_3-FT runs on iron catalysts with different potassium loadings ($T_{Reactor}$ = 270 °C, P_{Total} = 4 bar, p_{NH3} = 0.2 bar, GHSV = 1920 h^{-1}, H_2:CO = 2:1).

However, the conversion of ammonia (X_{NH3}) during NH_3-FT experiments on bulk iron catalysts with different potassium loadings is presented in Figure 4.6. In the beginning of the ammonia co-feeding, high values for NH_3 conversion (X_{NH3}) are observed which decrease with time on stream until they are stabilized after approximately 340 minutes. To explain initial high ammonia consumption, a blind run with the ammonia-containing synthesis gas feed was performed. Here, it can be observed that high ammonia conversion in the initial phase is related due to low ammonia contents. The amount of ammonia detected by the GC-TCD is correlating with the residence time of ammonia from the mass flow controllers (MFCs) to the GC-TCD. During the NH_3-FT experiments this residence time is increased due to the big volume of the hot trap which is mounted after the reactor (chapter 3.3.1). Consequently full detection of the theoretical ammonia flow rate is achieved at higher time on stream compared to bypass runs. However, from Figure 4.6 it is shown that an increase in potassium loading, result in a decrease in conversion of NH_3. More precisely, values for X_{NH3} can be found which are four times higher for NH_3-FT reactions on unpromoted iron catalysts compared to K doped catalysts. From these results it appears that potassium has an influence on ammonia consumption during NH_3-FT experiments. A possible reason can be found in literature [72] where lowered populations of adsorbed ammonia on iron catalyst surfaces are reported in the presence of potassium. Based on the results presented in the following chapters, a more detailed explanation for the different ammonia conversion will be given in chapter 4.2.1.10.

4.2.1.2 Formation of carbon dioxide

The formation of carbon dioxide (CO_2) from the Water-Gas Shift (WGS) and the Boudouard reaction is possible in the FT synthesis (equations 2.2 and 2.3 in chapter 2.1.2) [2][17][18]. Iron catalysts show a high activity towards the formation of carbon dioxide during the Fischer-Tropsch process [18] and the presence of potassium in the iron catalysts increases the CO_2 formation rates during FT reactions [15][128].

Figure 4.7 shows CO_2 selectivities for all three FT/NH_3-FT experiments on bulk iron catalysts with different potassium loadings. Since carbon dioxide was calibrated using mass flow controllers instead of a commercial calibration mixture the calibration factor $f_{TCD,CO2}$ is probably too high and CO_2 selectivities above 50 C-% were observed. From that point of view, CO_2 selectivities in this work will only show a trend and the Y-scale will be displayed dimensionless.

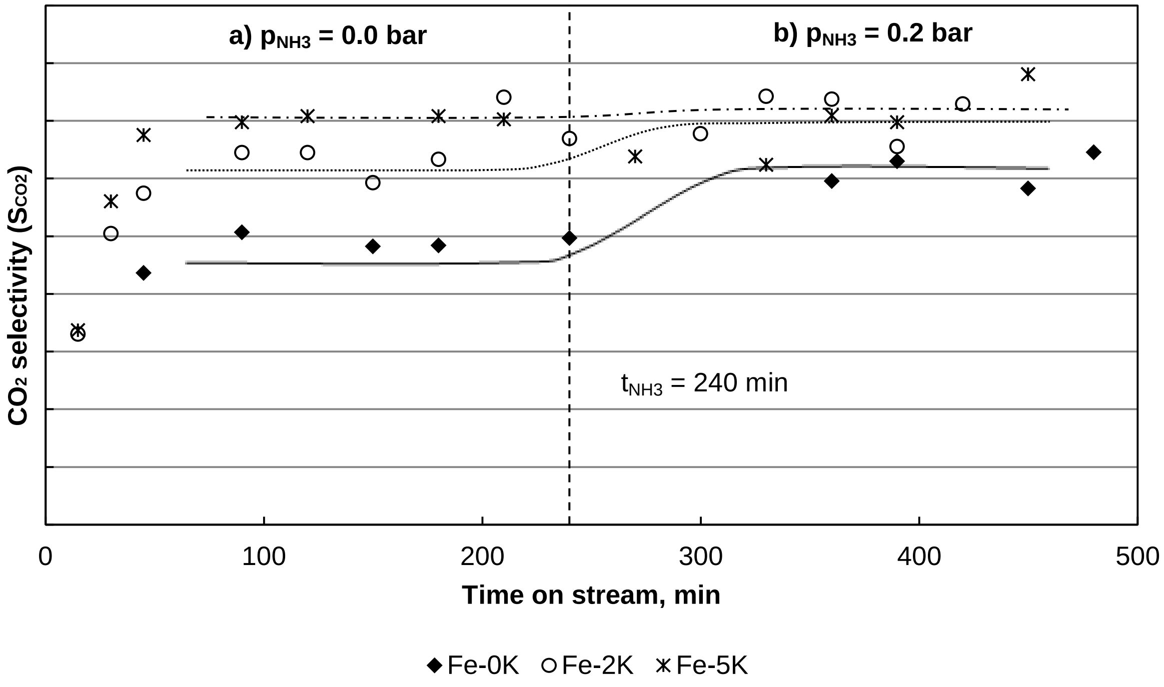

Figure 4.7: CO_2 selectivity (S_{CO2}) during FT/NH_3-FT runs on iron catalysts with different potassium loadings in: a) the absence of NH_3 and b) the presence of NH_3 ($T_{Reactor}$ = 270 °C, P_{Total} = 4 bar, p_{NH3} = 0.0 - 0.2 bar, GHSV = 1920 h^{-1}, H_2:CO = 2:1).

It can be seen from Figure 4.7 that in case of potassium doped iron catalysts, higher CO_2 selectivities compared to unpromoted iron catalysts are achieved (p_{NH3} = 0.0 bar). It appears that with increasing potassium content the tendency to form carbon dioxide is enhanced. This can be as a result of higher Boudouard and WGS reaction rates since potassium facilitates CO adsorption and dissociation (chapter 2.1.2 and chapter 2.4.1) [15][128]. Lower carbon monoxide and hydrogen conversion due to possible carbon deposition and WGS reactions during FT experiments on potassium promoted iron catalyst were already observed in this work at an ammonia partial pressure of 0.0 bar (Figure 4.4 and Figure 4.5) and would support the findings.

When ammonia is added to the synthesis gas feed, a gain in CO_2 selectivity can be observed during NH_3-FT runs on all tested iron catalysts. This effect is more pronounced for non potassium doped iron catalysts and decreases with increasing potassium loading.

Since it was reported by Dry *et al.* [119] or Shultz *et al.* [113] that additional NH_3 in the synthesis gas feed or the use of metal nitrides can inhibit the Boudouard reaction and a lower H_2 conversion was observed during FT/NH_3-FT experiments on unpromoted iron catalysts in this work (Figure 4.5), it seems that the gain in CO_2 selectivity could be more related to an enhanced WGS reaction. However, this can be only speculated and nor the WGS and the Boudouard reaction as a reason for high CO_2 selectivities can be excluded.

From the results, it appears that additional ammonia in the synthesis gas feed has a similar effect on the CO_2 selectivity to that of potassium as a promoter in iron catalysts and higher CO_2 selectivities can be obtained during the NH_3-FT experiments. In this context, a correlation between the potassium loading, different CO_2 formation rates and different ammonia conversions during NH_3-FT experiments on unpromoted/promoted iron catalysts (Figure 4.6) can be hereby assumed and this will be discussed in section 4.2.1.10.

4.2.1.3 Formation of methane

From all organic products methane is the most unwanted but the thermodynamically most favored product during Fischer-Tropsch synthesis [32]. In general it is tried to keep the methane selectivity as low as possible and in commercial applications, CH_4 selectivities between 4 and 8 C-% can be found [31]. Therefore, in the FT synthesis on iron catalysts, potassium is added to the catalyst in order to lower its activity towards methane. It is believed that methane is formed via associative desorption of a methyl species and surface hydrogen. Moreover, the methyl unit can also act as a chain initiator (Figure 4.8).

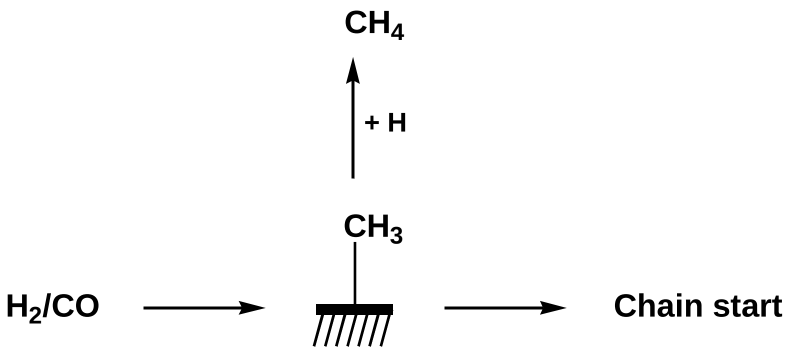

Figure 4.8: Scheme of the formation of methane or chain start from a methyl surface species in the FT synthesis(adapted from [32]).

The methane selectivities (S_{CH4}) in C-% for FT/NH_3 experiments on unpromoted and potassium promoted bulk iron catalysts are shown in Figure 4.9 (obtained from GC-TCD analysis). Highest methane selectivities (up to 20 C-% after 240 minutes) at an ammonia partial pressure of 0.0 bar can be observed when the reaction was carried out on potassium-free iron catalysts (Fe-0K). In case of the iron catalysts with a potassium content of 2 and 5 wt%, less methane was formed (approximately 5 C-% after 240 minutes) during the FT reactions. These effects of potassium are known in literature [15][31] and could be explained using Figure 4.8. There, it can be seen that methyl surface species and additional hydrogen is necessary for the formation of methane. This methyl surface species could be formed via the addition of hydrogen to a ‘CH_2’ monomer as it was described in the most accepted alkyl mechanism (Figure 2.1) [16][24]. Potassium in the catalyst metal is lowering the hydrogen-metal binding strength [15] and consequently less hydrogen or methyl units are populated on the catalyst surface which results in a lower methane selectivity.

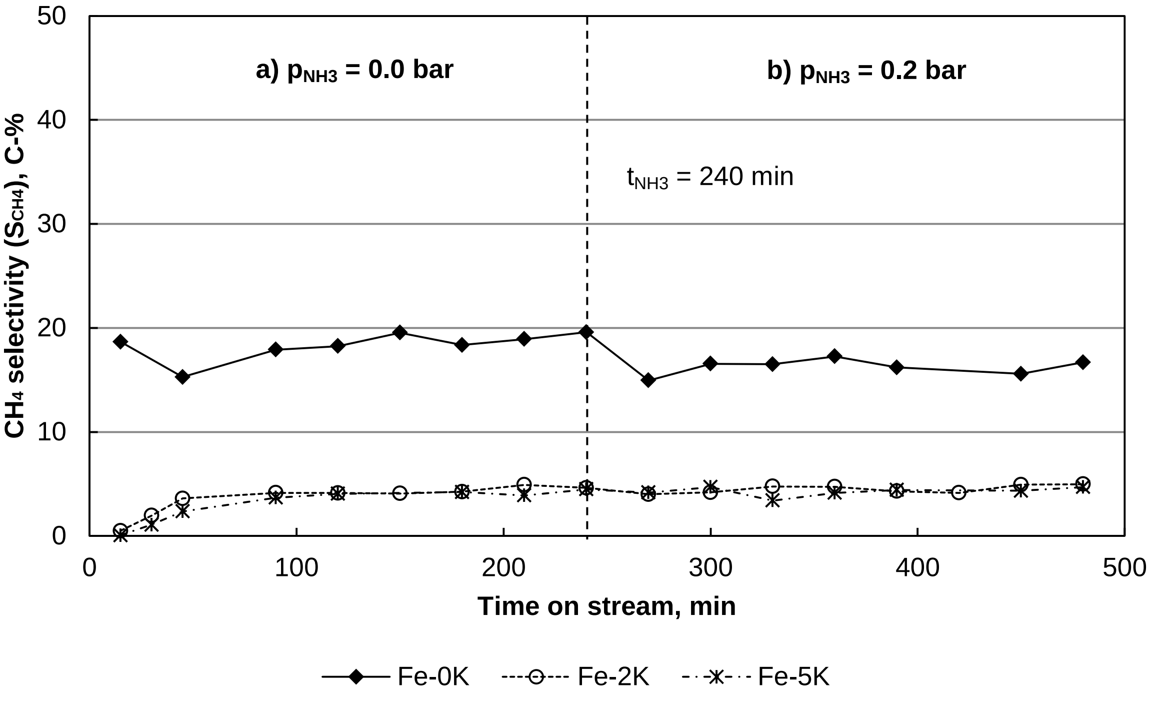

Figure 4.9: CH_4 selectivity (S_{CH4}, C-%) calculated from overall X_{CO} (CO_2 and organic products) during FT/NH_3-FT runs on iron catalysts with different potassium loadings in: a) the absence of NH_3 and b) the presence of NH_3 ($T_{Reactor}$ = 270 °C, P_{Total} = 4 bar, p_{NH3} = 0.0 - 0.2 bar, GHSV = 1920 h^{-1}, H_2:CO = 2:1).

In the presence of ammonia (p_{NH3} = 0.2 bar) the methane selectivity during NH_3-FT experiments on unpromoted iron catalysts decrease, whereas S_{CH4} remains unaffected on the potassium doped catalysts Fe-2K and Fe-5K (Figure 4.9).

From the results in this chapter it appears that additional ammonia in the synthesis gas feed during Fischer-Tropsch experiments on potassium-free iron catalysts shows similar promotional effects to that of potassium which can decrease the methane selectivity during FT synthesis. In contrast to this, with the use of potassium promoted iron catalysts, S_{CH4} is not altered by additional ammonia.

Similar results were found by Sango [111] during his FT/NH_3-FT experiments in a slurry reactor. The observed methane selectivities of approximately 4 C-% were not altered by the presence of ammonia in the synthesis gas feed using potassium promoted bulk iron catalysts during the studies. When the used catalysts are not doped with potassium, positive effects of ammonia on the methane selectivity can be found in this work, too (Table 4.14). Similar observations during FT/NH_3-FT experiments on supported cobalt catalysts in a slurry reactor were found by Rausch [6]. Ammonia also had an indirect effect on the methane selectivity during Fischer-Tropsch experiments performed by Lapidus *et al.* [105]. When ammonia was added to cobalt metals after the reduction, cobalt nitrides were formed, which showed lower formation rates of methane during their Fischer-Tropsch experiments.

However, a possible explanation for this behaviour will be given in section 4.2.1.10 based on further results.

4.2.1.4 Chain growth

The Fischer-Tropsch synthesis is a surface polymerization reaction as it was described in chapter 2.3. Surface species ‘Sp’ can undergo hydrogenation reactions to form paraffins or react further to longer chain hydrocarbons (Figure 2.3). This chain growth probability α can be described by the Anderson-Schulz-Flory (ASF) distribution (equation 2.4) assuming a carbon number independency. In this context, it is known that potassium can increase the C_{5+} product selectivity during Fischer-Tropsch synthesis and higher values for α can be found [15][31].

Table 4.4: Chain growth probability α during FT/NH_3-FT runs on iron catalysts at different NH_3 partial pressures and potassium loadings ($T_{Reactor}$ = 270 °C, P_{Total} = 4 bar, p_{NH3} = 0.0 - 0.2 bar, GHSV = 1920 h^{-1}, H_2:CO = 2:1).

Catalyst	**K loading** (wt%)	**Chain growth probability**	
		α_{C3-C8} (p_{NH3} = 0.0 bar)	α_{C3-C8} (p_{NH3} = 0.2 bar)
Fe-0K	0	0.45	0.50
Fe-2K	2	0.64	0.64
Fe-5K	5	0.66	0.67

From the results of FT/NH_3-FT experiments on iron catalysts in this work, the chain growth probability α (for linear hydrocarbons in the range from C_3 - C_8 where a linear behaviour could be found) is presented in Table 4.4. At ammonia partial pressures of 0.0 bar, α increases from 0.45 (Fe-0K) to 0.66 (Fe-5K), indicating the formation of long chain organic products when potassium is used as chemical promoter. These α values would be in agreement with the work of Cairns [14] and Sango [111] who carried out Fischer-Tropsch experiments using similar potassium promoted bulk iron catalysts.

It is speculated that chain growth during Fischer-Tropsch synthesis could occurs according to the alkyl mechanism where surface 'CH_2' units are believed to act as chain growth monomers [16][24]. When potassium is used as a promoter in iron catalysts, the bond between adsorbed 'CH_2' species and the catalyst surface could be strengthened and high numbers of the chain growth monomers could be populated on the catalyst surface. Furthermore, due to the same interactions of the promoter with the 3d-band of the metal, higher CO coverages can be achieved which could produce more 'CH_2' units [15]. At the same time the hydrogen-metal binding strength is lowered and less hydrogenation reactions to methyl surface units or methane could take place. It should be noted that this explanation is not the only reaction mechanism for chain growth during FT synthesis and that there are other possibilities, too. Additionally to 'CH_2' as chain growth monomers, olefins or alcohols were reported to have the ability to initiate chain growth or can get incorporated into the chain [21][34].

When NH_3 is added to the synthesis gas feed after 240 minutes of time on stream, α values remain unaffected during the reaction on potassium doped bulk iron catalysts. In contrast to this finding, increased chain growth probabilities α can be found (α_{C3-C8} = 0.50) when NH_3-FT reactions are carried out on unpromoted iron catalysts. From these results one could speculate if additional ammonia in the synthesis gas feed during the FT/NH_3-FT experiments shows similar promotional effects to that of potassium. Moreover, as it was shown in the chapters before, potassium doped iron catalysts are somehow resistant to additional ammonia and its influence.

In this context, increased chain growth probabilities were also found during FT/NH_3-FT experiments on bulk cobalt catalysts in this work (Table 4.14), too. Here, α values of 0.63 at an ammonia partial pressure of 0.0 bar were obtained which rise in the presence of ammonia to 0.71. During FT/NH_3-FT experiments on supported cobalt catalysts, Rausch [6] observed increased chain growth with additional ammonia in the synthesis gas feed whereas α values remained constant during FT/NH_3-FT experiments on potassium promoted bulk iron catalysts performed by Sango [111]. Similar results can be obtained when cobalt nitrides are used during the reaction. Here, increased α values were found by Lapidus *et al.* [105] during conventional FT experiments.

A more detailed discussion about the observed influence of ammonia on the chain growth probability during the Fischer-Tropsch experiments within this work can be found in chapter 4.2.1.10.

4.2.1.5 Formation of olefins

The main primary organic products of the Fischer-Tropsch synthesis are 1-olefins and they are formed via a β-H elimination reaction of a surface alkyl species before hydrogenation reactions towards paraffins can take place [23]. However, olefins can re-adsorb and undergo hydrogenation, double bond shift isomerisation, chain branching or can be incorporated into growing chains (Figure 4.11) [34][21][35]. In this context, potassium is known to suppress mainly these secondary reactions and increased olefin selectivities can be found when metal catalysts are doped with potassium [3].

Formation of 1- and 2-olefins

The olefin content (1- and 2-olefins), formed during FT experiments can be derived from diagrams showing the fraction of olefins in the total linear hydrocarbon products (olefins and *n*-paraffins). In Figure 4.10, olefin mole fractions in linear hydrocarbons (olefins and *n*-paraffins) for FT/NH_3-FT runs on iron catalysts with different potassium loadings are presented.

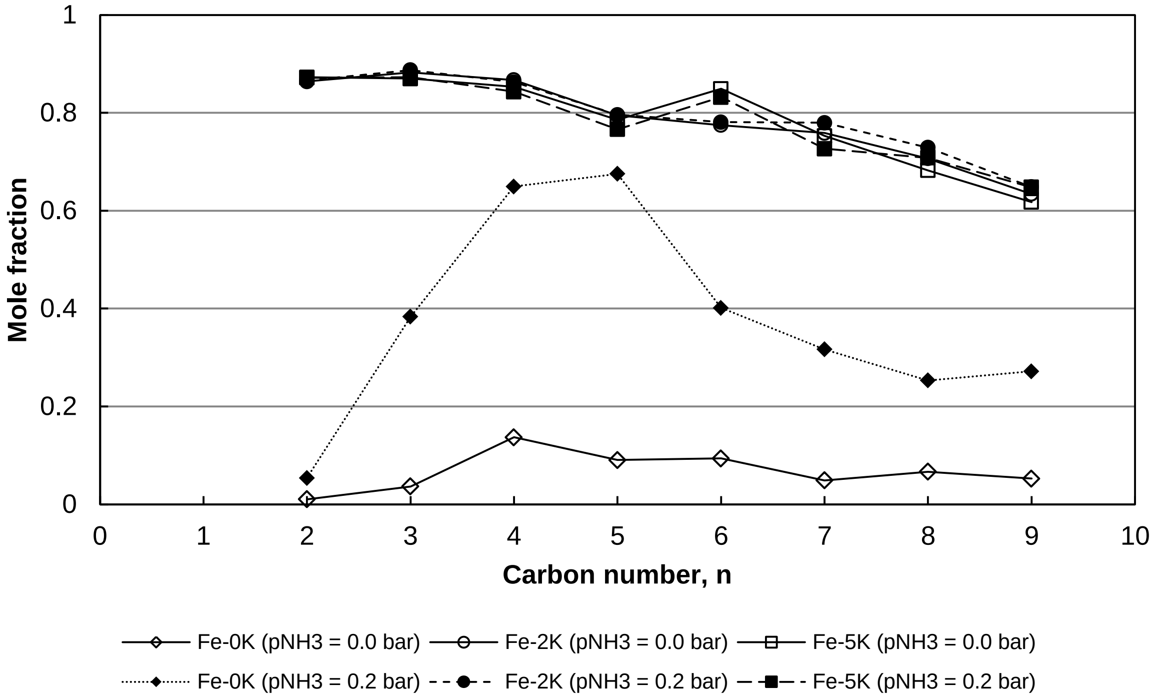

Figure 4.10: Mole fraction of olefins in all linear hydrocarbons (olefins and *n*-paraffins) during FT/NH_3-FT runs on iron catalysts at different NH_3 partial pressures and potassium loadings ($T_{Reactor}$ = 270 °C, P_{Total} = 4 bar, p_{NH3} = 0.0 - 0.2 bar, GHSV = 1920 h^{-1}, H_2:CO = 2:1).

Generally, on promoted iron catalysts olefin contents of around 70 – 90 mol % are found and indicate primary olefin selectivity [35]. Within this work, this is found for olefins in the carbon number range of C_2 - C_9 during FT runs on potassium promoted iron catalysts with K loadings of 2 and 5 wt % in the absence of NH_3. Olefin mole fractions between 0.84 and 0.87 (C_2 - C_3) are observed and with increasing chain length, the olefin content decreases (0.61 - 0.64 for C_9). In contrast to this, during FT experiments on unpromoted iron catalysts maximum olefin contents of 0.14 (C_4) are found and mainly *n*-paraffins are synthesized. This difference in molar olefin fractions between promoted and unpromoted iron catalysts is contributed to the properties of potassium which is able to force back secondary reactions such as the hydrogenation to the corresponding paraffin [3]. Due to lower hydrogen-metal binding strengths, less hydrogen is available on the catalyst surface to hydrogenate olefins to the corresponding paraffins [15].

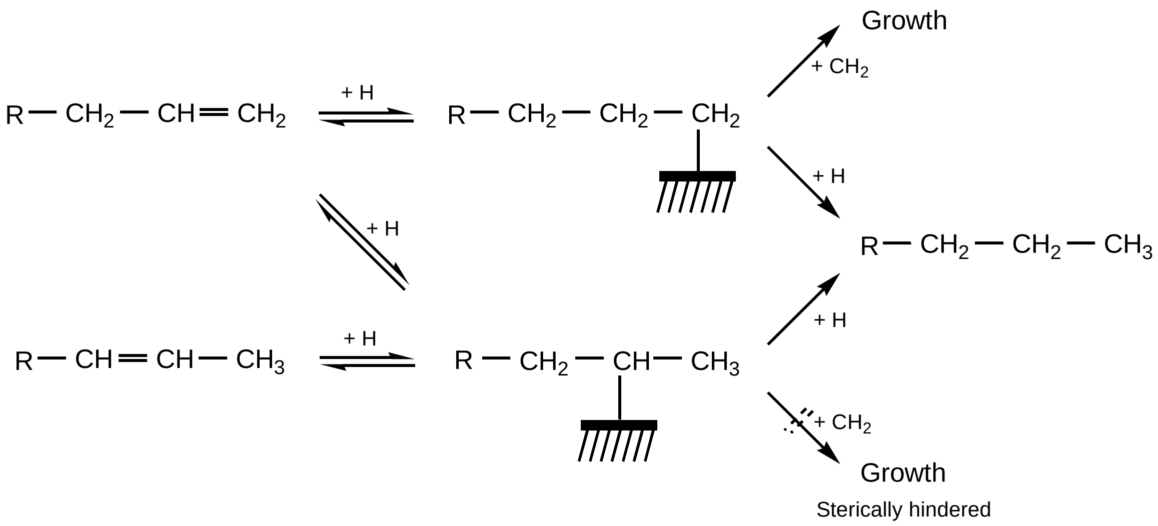

Figure 4.11: Scheme of secondary reactions from olefins in the FT synthesis (adapted from [35]).

It is notable that during FT/NH_3-FT experiments in this work high mole fractions of ethene can be found when the reactions are carried out on potassium promoted catalysts (at $p_{NH3} = 0.0$ and 0.2 bar). Due to the high reactivity of ethene to undergo hydrogenation reactions or further chain growth, low olefin contents are often found for C_2 fractions [34][35]. This could be as a result of a low surface coverage with atomic hydrogen since potassium is lowering the strength of metal-hydrogen [15]. However, with increasing carbon number of the olefins, there is an increased possibility that olefins remain on the catalyst surface to undergo side reactions (e.g. hydrogenation to the corresponding paraffin, double bond shift isomerisation, chain branching or incorporation into growing chains). Enhanced secondary reactions of long chain olefins were reported by Iglesia *et al.* [36] and were be explained by diffusion limitations.

After 240 minutes of time on stream and the addition of ammonia to the synthesis gas feed, the mole fractions of olefins do not change during NH_3-FT experiments on potassium promoted iron catalysts (Figure 4.10) while increased olefin contents in the presence of NH_3 on potassium-free iron catalysts can be observed. For example, for C_4 hydrocarbons the mole fraction of produced olefins increases from 0.14 (p_{NH3} = 0.0 bar) to approximately 0.65 (p_{NH3} = 0.2 bar). Only a small gain of ethene contents can be observed and over the range for the C_2-C_9 olefins, a maximum appears at C_5 (mole fraction of 1-pentene = 0.68). After the carbon number n = 5 less olefins are produced and the curve declines.

It seems that ammonia in the synthesis gas feed has promotional effects on the olefin selectivity since increased olefin contents are observed during NH_3-FT compared to the FT experiments on unpromoted iron catalysts. In contrast to this, the formation of olefins is not influenced by ammonia when additional potassium is present in the iron catalysts. From the results of FT/NH_3-FT reactions on cobalt catalyst in this work, a gain in the olefin selectivity of 59.1 mol% (for carbon numbers C_2 - C_9) was observed (Table 4.14).

Similar results during FT/NH_3-FT experiments on supported iron-and cobalt-containing catalysts were found by Rausch *et al.* [6][112]. During FT/NH_3-FT experiments in a fixed-bed and slurry reactor, he could clearly show, that on cobalt catalysts olefin contents increased significantly during the addition of ammonia. When the reaction was carried out on supported iron catalysts, ammonia influenced the formation rates of long chain olefins (C_7 - C_{10}) only slightly. With the use of potassium promoted bulk iron catalysts during FT/NH_3-FT studies, the mole fraction of olefins is not affected by low ammonia concentrations in the synthesis gas feed (2 - 10 vol%) as it was reported by Sango [111]. After ammonia concentrations were raised between 20 and 35 vol%, the amount of olefins increased, too. Increased olefin selectivities were observed by Yeh *et al.* [114], too, when iron nitrides as catalysts were used during conventional Fischer-Tropsch experiments.

Formation of 1-olefins

1-olefins are the main products formed during Fischer-Tropsch synthesis and they can undergo secondary reactions such as double bond shift isomerisation. As a result, a mixture of 1- and 2-olefins can be obtained (Figure 4.11) and mole fractions of 1-olefins in all total olefins for carbon numbers C_4 - C_9 are presented in Figure 4.12.

From Figure 4.12 it can be seen that high amounts of valuable 1-olefins are obtained during FT runs (p_{NH3} = 0.0 bar) on potassium promoted iron catalysts. 2-olefins could be obtained from re-adsorption of 1-olefins (Figure 4.11) and it is known in literature that potassium is forcing back this side reaction [3]. Due to its interaction with the 3d-band of the iron catalyst, the CO binding strength is increased and consequently the coverage of the catalyst surface with CO is increased. Re-adsorption of 1-olefins is possibly hindered since carbon monoxide may block active sites of the catalyst. In case of FT experiments on unpromoted iron catalyst low amounts of 1-olefins in the range of C_4 - C_6 are produced. Low chain 1-olefins are may be too reactive and can easily re-adsorb onto the catalyst surface to form 2-olefins.

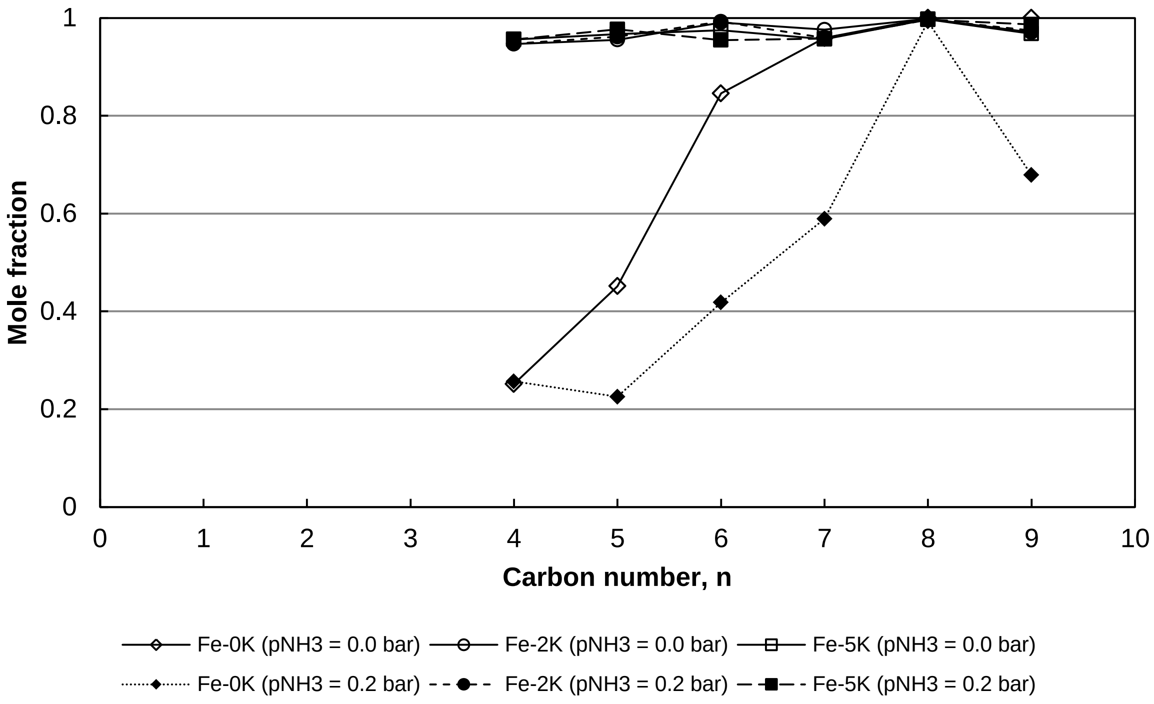

Figure 4.12: Mole fraction of 1-olefins in all linear olefins (1- and 2-olefins) during FT/NH_3-FT runs on iron catalysts at different NH_3 partial pressures and potassium loadings ($T_{Reactor}$ = 270 °C, P_{Total} = 4 bar, p_{NH3} = 0.0 - 0.2 bar, GHSV = 1920 h^{-1}, H_2:CO = 2:1).

The presence of ammonia (p_{NH3} = 0.2 bar) does not alter the 1-olefin content in case of NH_3-FT experiments on potassium-containing catalysts Fe-2K and Fe-5K, whereas smaller concentrations of 1-olefins are synthesized on potassium-free iron catalysts. A low value for 1-nonene (Fe-0K at p_{NH3} = 0.2 bar) which can be seen in Figure 4.12, can be led back to an analytical error since product peaks become more difficult to integrate with higher organic products during gas chromatographic analysis.

From the results in this chapter it could be seen that ammonia in the synthesis gas feed can change the olefin selectivity during FT/NH_3-FT experiments on potassium-free iron catalysts. It appears that the catalytic performance of potassium promoted iron catalysts is not influenced to the effects caused by ammonia as it was already described in the chapters before and possible reasons will be discussed in chapter 4.2.1.10.

4.2.1.6 Formation of branched products

During Fischer-Tropsch synthesis the formation of branched hydrocarbons is feasible and two possible routes are believed to be involved (Figure 4.13). Branched hydrocarbons can be obtained from secondary reactions of 1-olefins (1) as it was shown by Schulz *et al.* [60] with co-feeding experiments of ^{14}C-labelled propene molecules. The re-adsorption of 2-olefins followed by chain growth to branched compounds was concluded to occur only in initial periods where the intrinsic selective inhibitions of the FT system are not yet developed [35]. Another pathway towards branched hydrocarbons is the combination of an alkylidene with a methyl species (2) via primary product formation [101][102]. When transition metal catalysts (e.g. iron) for the Fischer-Tropsch reactions are doped with potassium, the formation of branched hydrocarbons can be suppressed [3][23].

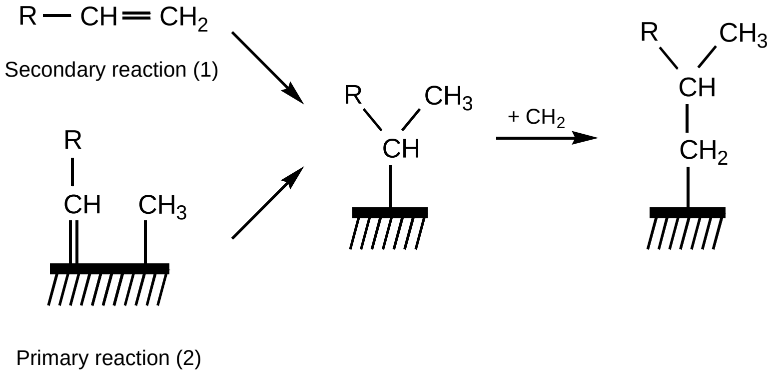

Figure 4.13: Scheme of the formation of branched hydrocarbons during Fischer-Tropsch synthesis via different mechanisms (adapted from [23]).

For the reasons described in chapter 3.4.3, it was abstained to calculate molar flow rates for branched hydrocarbons for carbon numbers C_{5+}. To describe the influence of promoters such as potassium and the influence of ammonia onto the formation of branched hydrocarbons the C_4 fraction was chosen. Here 2-methylpropane could be identified using a GC-FID (chapter 3.4.2) and shall represent the degree of branching in this work.

Figure 4.14 attempts to show the molar ratio of branched C_4 hydrocarbon/linear C_4 hydrocarbons (iso/lin) during FT/NH_3-FT experiments on bulk iron catalysts with different potassium loadings (in wt%). When comparing the formation of 2-methylpropane for FT reactions in the absence of NH_3 the influence of potassium as a promoter can be clearly seen. The molar ratio of branched to linear hydrocarbons decreases from around 0.09 (Fe-0K) to

0.02 (Fe-2K) when the iron catalyst was impregnated before with potassium. Promotion of iron catalyst with alkali metals is known to reduce side reactions during the Fischer-Tropsch synthesis [3]. Considering that the formation of branched hydrocarbons takes place via a secondary reaction as proposed by Schulz *et al.* [60], the decrease of iso/lin could be explained. Potassium as a base can neutralize acid sites on the catalyst surface which could catalyze the isomerisation of re-adsorbed olefins [23]. Normally these acidic sites are introduced by supports such as alumina [15]. The bulk iron catalysts used in this work are not supported and no information of the acid sites on this catalyst system is available. Moreover, in chapter 4.2.1.5 it was argued that re-adsorption of 1-olefins is hindered and less 2-olefins were formed when potassium as a promoter is present in the iron catalyst. From this point of view, it is assumed that the formation of branched hydrocarbons via secondary reactions seems to be unlikely during this study.

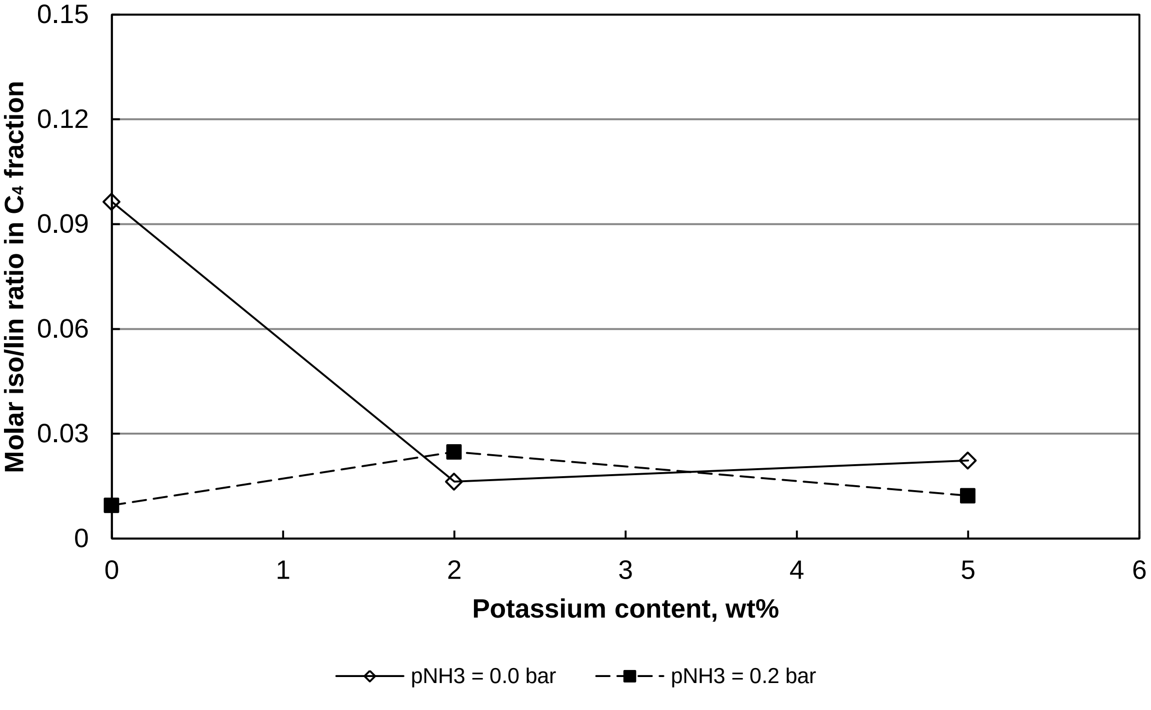

Figure 4.14: Molar iso/lin hydrocarbon ratio in C_4 fraction during FT/NH_3-FT runs on iron catalysts at different ammonia partial pressures and potassium loadings ($T_{Reactor}$ = 270 °C, P_{Total} = 4 bar, p_{NH3} = 0.0 - 0.2 bar, GHSV = 1920 h^{-1}, H_2:CO = 2:1).

When branched hydrocarbons are formed via a primary route, i.e. through the combination of an alkylidene with a methyl species, the results from chapter 4.2.1.3 and 4.2.1.4 could explain the decrease of the ratio of iso/lin hydrocarbons. There it was argued that potassium lowers the methane selectivity and increase the chain growth probability α because instead of hydrogenating reactions, more 'CH_2' species are formed. The CH_3 species which is required for the formation of branched hydrocarbons would be consequently less populated on the catalyst surface.

After 240 minutes of time on stream, ammonia is added to the synthesis gas feed and the ratio of 2-methylpropane/linear C_4 hydrocarbons drops in case of NH3-FT runs on unpromoted iron catalysts. The degree of branching at a partial pressure of ammonia of 0.2 bar remains unchanged when NH_3-FT reactions were carried out on potassium promoted bulk iron catalysts. During FT/NH_3-FT experiments, performed on bulk cobalt catalysts, similar results were observed. Here, the degree of branching (for C_4) also drops in the presence of ammonia (Table 4.14).

The Fischer-Tropsch experiments in this work are only screening experiments and time on stream is completed after 8 hours. Thus, high degrees of branching have been obtained during the initial stages of Fischer-Tropsch reactions and are believed to be due to a less dense population of the metal surface with surface species [35]. To verify, if ammonia causes the decrease of the molar ratio of branched and linear hydrocarbons, the degree of branching for the C_4 fraction before the addition of NH_3 is plotted in Figure 4.15.

From the ammonia-free runs in the initial phase of the Fischer-Tropsch experiments it can be seen that the molar ratio of branched/linear hydrocarbons for the C_4 fraction does not drop before the addition of NH_3 to the synthesis gas feed. This indicates and verifies that ammonia is able to force back the formation of branched hydrocarbons when potassium-free iron catalysts were used during the reaction. It seems that the catalytic performance of potassium promoted iron catalysts is not influenced by the addition of ammonia during the conducted FT/NH_3-FT experiments since the degree of branching remains the same with these catalysts (catalysts Fe-2K and Fe-5K in Figure 4.14). This would be in agreement with the studies of Sango [111]. During his FT/NH_3-FT runs on potassium promoted bulk iron catalysts in a slurry reactor, the degree of branching for the C_5 carbon number fraction is not influenced over a wide range of different ammonia concentrations. However, a more detailed argumentation about possible reasons for these findings will be given in chapter 4.2.1.10.

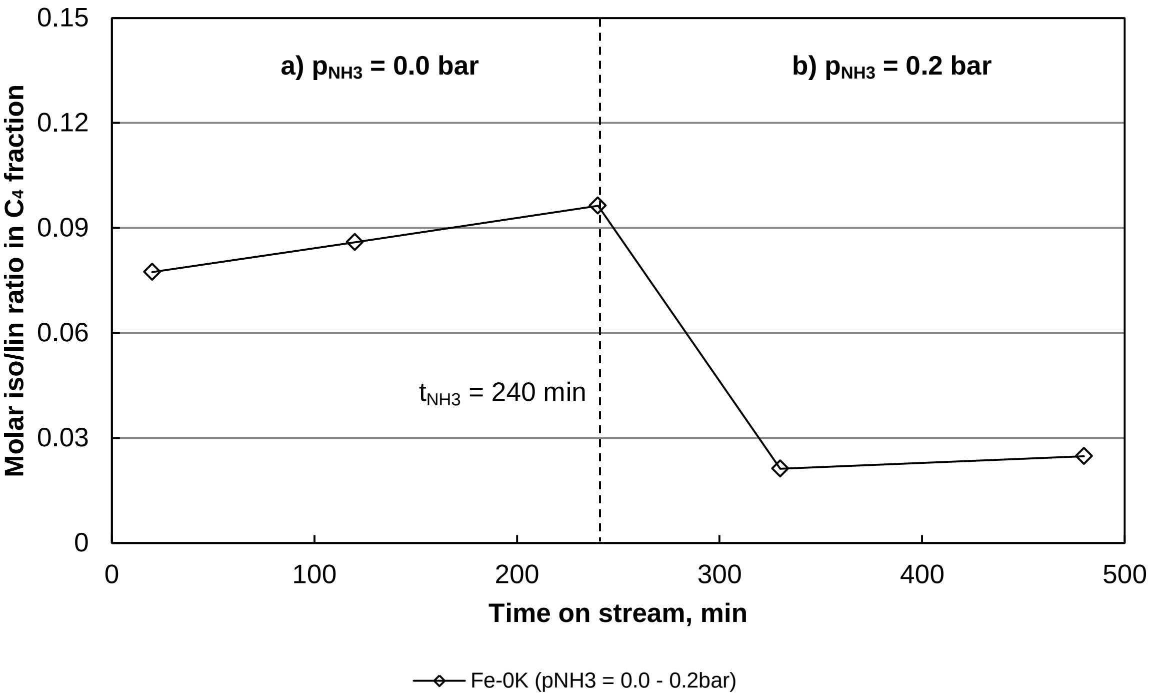

Figure 4.15: Molar iso/lin hydrocarbon ratio in C_4 fraction during FT/NH_3-FT experiments on unpromoted iron catalysts in: a) the absence of NH_3 and b) the presence of NH_3 ($T_{Reactor}$ = 270 °C, P_{Total} = 4 bar, p_{NH3} = 0.0 - 0.2 bar, GHSV = 1920 h^{-1}, H_2:CO = 2:1).

4.2.1.7 Formation of oxygenated products

As it was described in chapter 2.2.2, it is feasible to obtain oxygenates such as alcohols, aldehydes, carboxylic acids and methyl-ketones along with other hydrocarbons formed during the Fischer-Tropsch synthesis. In general, mainly aldehydes and alcohols and to a smaller extend methyl-ketones and carboxylic acids are formed [16]. Iron catalysts are known to produce large amounts of oxygenates during Fischer-Tropsch synthesis [4]. When metal catalysts are doped with potassium, this molar content can be increased further due to suppressed secondary reactions of the oxygenated compounds [3][16][35] or due to higher concentrations of the required surface intermediates for oxygenates [15]. Little is known about the formation of oxygenates during Fischer-Tropsch synthesis and in this work, mainly the reaction mechanisms proposed by Pichler and Schulz. [25] and Johnston *et al.* [30] will be used for the argumentation of the results.

Formation of alcohols, aldehydes and carboxylic acids

Alcohols, aldehydes and carboxylic acids are believed to be formed via CO insertion (**5**) into an alkyl-metal bond (**4**) or through an addition of a hydroxyl group (**2**) to an adsorbed alkylidene group (**1**) [25][30]. From the surface intermediates (**3**) and (**6**) alcohols or aldehydes are formed in a chain termination step with additional surface hydrogen. However, the addition of an OH group to the acyl surface species (**6**) yields to the formation of carboxylic acids. The alcohols, aldehydes and carboxylic acids can re-adsorb on the catalyst surface again and have the ability to readily interact which each other [14][61].

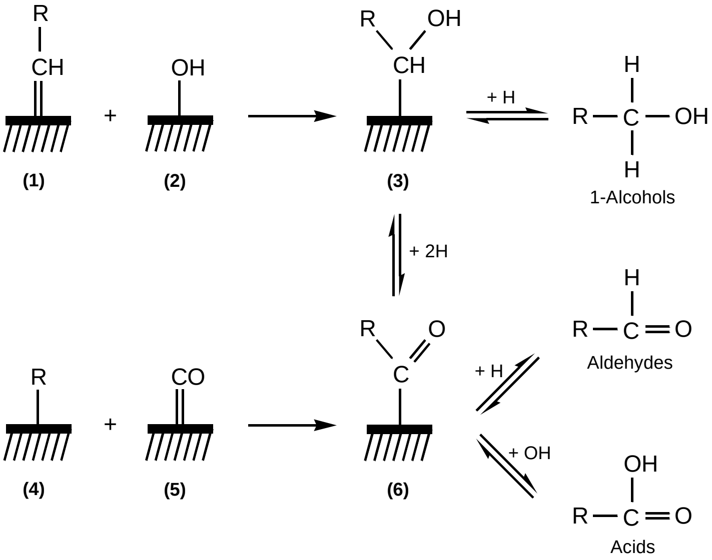

Figure 4.16: Reaction scheme of the formation of alcohols, aldehydes and carboxylic acids (adapted from [14]).

However, the mole fraction of the C_1 - C_6 oxygenates (with the exception of methyl-ketones) in the total linear organic products formed during FT/NH_3-FT reactions on unpromoted/promoted bulk iron catalysts is presented in Figure 4.17.

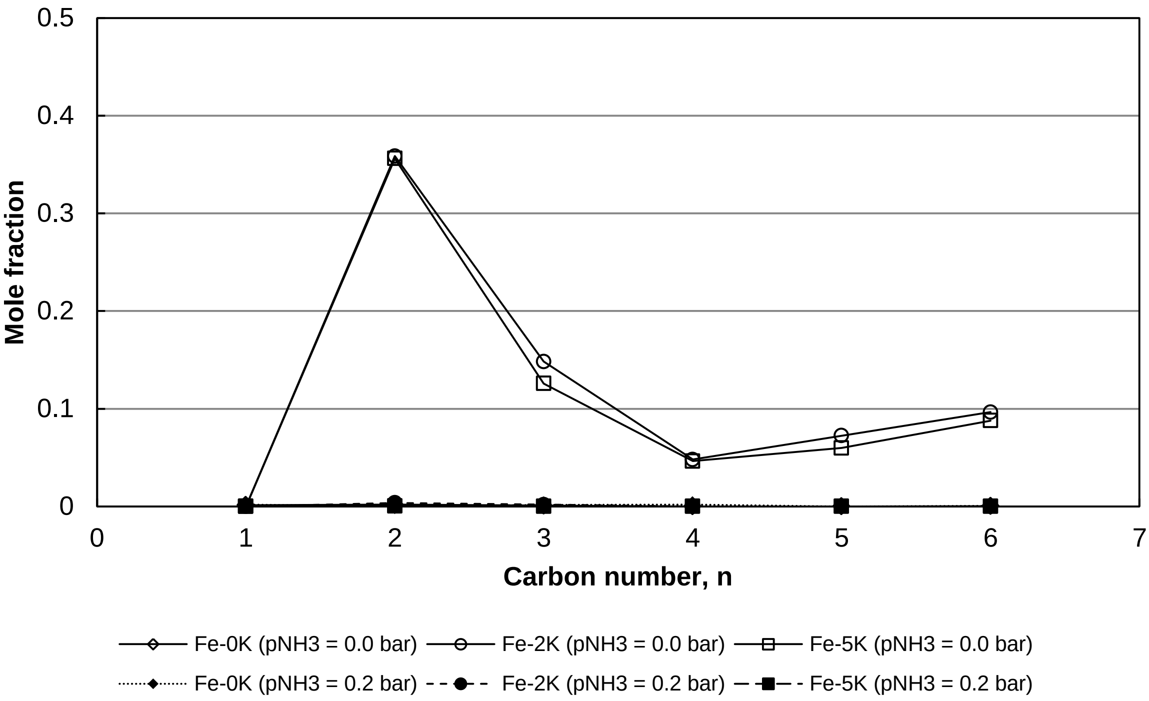

Figure 4.17: Mole fraction of oxygenates (with the exception of methyl-ketones) in all linear (plus C_1) organic products during FT/NH_3-FT runs on iron catalysts at different NH_3 partial pressures and potassium loadings ($T_{Reactor}$ = 270 °C, P_{Total} = 4 bar, p_{NH3} = 0.0 - 0.2 bar, GHSV = 1920 h^{-1}, H_2:CO = 2:1).

In case of FT experiments on unpromoted iron catalysts, almost no oxygenates can be found in the organic products. No aldehydes and carboxylic acids for carbon numbers ranging from C_2 - C_6 can be detected (Table 4.7 and Table 4.8) and methanol, ethanol and 1-propanol are obtained as the only oxygenates (not shown). However, these compounds are synthesized in small concentrations and if it is compared to the formation rates of the hydrocarbons from C_1-C_3, these values are negligible. In the absence of ammonia (p_{NH3} = 0.0 bar), oxygenates such as alcohols, aldehydes and carboxylic acids are only produced in higher quantities during FT experiments on potassium promoted iron catalysts (Fe-2K, Fe-5K). Here, mole fractions of alcohols, aldehydes and carboxylic acids up to 0.36 are obtained (C_2) and oxygenate fractions show a minimum on both promoted catalysts at C_4. It should be noted that methanol is the only C_1 oxygenate which is formed during the Fischer-Tropsch experiments and the formation of formic acid and formaldehyde is not observed during all three experiments. The presence of hexanoic acid, however, can barely be detected in the gas phase product. Due to its high boiling point of 205 °C hexanoic acid is probably condensed in the hot trap (chapter 3.3).

From these findings, the influence of potassium as a promoter for iron catalysts with respect to the formation of oxygenates can be seen. Due to the presence of potassium, secondary reactions of oxygenated compounds (namely hydrogenation to form a paraffin and incorporation into growing chains) could be suppressed as it was described before in literature [16][35]. Moreover, through an electron donor effect of potassium, the bond of adsorbed 'CO' units on the catalyst surfaces could be also strengthened and the density of the intermediates on the catalyst surface, which are required for the reaction pathways described in Figure 4.16, could be increased [15]. Dissociation of chemisorbed carbon monoxide due to the presence of potassium, leads to the formation of surface oxygen which could react further with hydrogen to generate OH groups [16]. The addition of the hydroxyl to an adsorbed alkylidene group leads to surface intermediate (**3**) in Figure 4.16 which could act as a precursor for the formation of alcohols, aldehydes and carboxylic acids [14][61]. Despite to the fact that the reaction mechanism proposed by Johnston *et al.* [30] was often used to explain the formation of oxygenated compounds, it is believed that population of OH groups on catalyst surfaces is supposed to be low [125]. These findings are based on DFT (Density Functional Theory = DFT) calculations using Co(0001) catalysts. However, another possibility to generate oxygenated compounds could lead via the CO insertion mechanism [16][25]. Adsorption of CO is mainly taking place due to the interaction of the filled 5σ-orbital and the double degenerated 2π*-orbital of carbon monoxide and the centre of the metal d-band [121][122][123]. In the presence of potassium in the catalyst, enhanced CO insertion might take place and more surface acyl intermediates (**6**) in Figure 4.16 could be formed. As a consequence, more oxygenated compounds could be generated during the reaction.

The oxygenated compounds formed during FT experiments on potassium promoted iron catalysts mainly consist of aldehydes (Table 4.7). From this result, it can be hypothesized that in this study, oxygenates are predominantly formed through the CO insertion mechanism and hydrogenation reactions of the acyl species to form the corresponding alcohol are low. The fact that carboxylic acids were detected in the organic products would support this hypothesis, too. These compounds are thought to be generated via an addition of hydroxyl groups to acyl intermediates [14]. A low hydrogenation tendency during FT experiments in this work was already shown in chapter 4.2.1.5 where high formation rates of ethene or olefins at all and low methane selectivities were observed during FT reactions on potassium promoted iron catalysts

Fe-2K and Fe-5K (Figure 4.9 and Figure 4.10). This could be as a result of a low surface coverage with atomic hydrogen since potassium lowers the strength of the metal-hydrogen bond [15].

However, a correlation between CO_2 partial pressure and the formation rate of carboxylic acids which was described by Dry [31] is not observed in this work. The findings in section 4.2.1.2 (Formation of CO_2) showed higher CO_2 selectivities in the absence of ammonia with increasing potassium loading, but the selectivities towards carboxylic acids remain the same (

Table 4.8).

Table 4.5: Selectivity (mol%) to oxygenates (with the exception of methyl-ketones) as a percentage of the detected linear C_2 - C_6 organic products ($T_{Reactor}$ = 270 °C, P_{Total} = 4 bar, p_{NH3} = 0.0 - 0.2 bar, GHSV = 1920 h^{-1}, H_2:CO = 2:1).

	Fe-0K		Fe-2K		Fe-5K	
	p_{NH3} = 0.0 bar	p_{NH3} = 0.2 bar	p_{NH3} = 0.0 bar	p_{NH3} = 0.2 bar	p_{NH3} = 0.0 bar	p_{NH3} = 0.2 bar
C_2 - C_4	0.1	0.0	21.4	0.2	20.5	0.0
C_5 - C_6	0.0	0.0	1.1	0.0	1.0	0.0
C_2 - C_6	0.1	0.0	22.5	0.2	21.5	0.0

Table 4.6: Selectivity (mol%) to alcohols as a percentage of the detected linear C_2 - C_6 organic products ($T_{Reactor}$ = 270 °C, P_{Total} = 4 bar, p_{NH3} = 0.0 - 0.2 bar, GHSV = 1920 h^{-1}, H_2:CO = 2:1).

	Fe-0K		Fe-2K		Fe-5K	
	p_{NH3} = 0.0 bar	p_{NH3} = 0.2 bar	p_{NH3} = 0.0 bar	p_{NH3} = 0.2 bar	p_{NH3} = 0.0 bar	p_{NH3} = 0.2 bar
C_2 - C_4	0.1	0.0	4.7	0.2	2.1	0.0
C_5 - C_6	0.0	0.0	0.4	0.0	0.1	0.0
C_2 - C_6	0.1	0.0	5.1	0.2	2.2	0.0

Table 4.7: Selectivity (mol%) to aldehydes as a percentage of the detected linear C_2 - C_6 organic products ($T_{Reactor}$ = 270 °C, P_{Total} = 4 bar, p_{NH3} = 0.0 - 0.2 bar, GHSV = 1920 h^{-1}, H_2:CO = 2:1).

	Fe-0K		Fe-2K		Fe-5K	
	p_{NH3} = 0.0 bar	p_{NH3} = 0.2 bar	p_{NH3} = 0.0 bar	p_{NH3} = 0.2 bar	p_{NH3} = 0.0 bar	p_{NH3} = 0.2 bar
C_2 - C_4	0.0	0.0	12.7	0.0	14.3	0.0
C_5 - C_6	0.0	0.0	0.7	0.0	0.8	0.0
C_2 - C_6	0.0	0.0	13.4	0.0	15.1	0.0

Table 4.8: Selectivity (mol%) to carboxylic acids as a percentage of the detected linear C_2 - C_6 organic products ($T_{Reactor}$ = 270 °C, P_{Total} = 4 bar, p_{NH3} = 0.0 - 0.2 bar, GHSV = 1920 h^{-1}, H_2:CO = 2:1).

	Fe-0K		Fe-2K		Fe-5K	
	p_{NH3} = 0.0 bar	p_{NH3} = 0.2 bar	p_{NH3} = 0.0 bar	p_{NH3} = 0.2 bar	p_{NH3} = 0.0 bar	p_{NH3} = 0.2 bar
C_2 - C_4	0.0	0.0	3.9	0.0	4.1	0.0
C_5 - C_6	0.0	0.0	0.0	0.0	0.0	0.0
C_2 - C_6	0.0	0.0	3.9	0.0	4.1	0.0

When ammonia is added (p_{NH3} = 0.2 bar) to the synthesis gas feed after 240 minutes of time on stream, the mole fraction of alcohols, aldehydes and carboxylic acids decrease significantly during Fischer-Tropsch reactions on potassium promoted iron catalysts (Table 4.5). Whereas small amounts of alcohols are still found in the linear organic products (Table 4.6), all of the aldehydes and carboxylic acids disappear when ammonia is added (Table 4.7 and

Table 4.8). During NH_3-FT experiments on unpromoted iron catalysts, no changes can be observed compared to the FT experiments in absence of ammonia and no alcohols, aldehydes and carboxylic acids are observed (with an exception of methanol).

Decreased selectivities in the presence of ammonia were also found during FT/NH_3-FT reactions on cobalt catalysts in this work. Alcohols, which were formed at an ammonia partial pressure of 0.0 bar, disappeared when ammonia was added to the synthesis gas feed (Table 4.14). These findings would be in agreement with the results of Rausch [6] who carried out FT/NH_3-FT reactions on cobalt catalysts in a slurry reactor. The amount of oxygenates such as alcohols, aldehydes and carboxylic acids which were formed before during conventional

FT experiments, dropped in the presence of ammonia, too [6]. During FT experiments on aluminum oxide supported copper catalysts conducted by Gredig *et al.* [91], methanol was generated and disappeared when ammonia was added to the synthesis gas feed (Figure 2.10). In contrast to these results, the formation of oxygenated compounds such as alcohols and carboxylic acids was still feasible during Fischer-Tropsch experiments in the presence of ammonia performed by Rottig [10] and Kölbel and Trapper [11]. This was also observed by Sango [111] during his Fischer-Tropsch experiments on bulk iron catalysts. Alcohols, aldehydes and carboxylic acids which were formed during the reaction, were reduced after the addition of ammonia to the synthesis gas feed and small concentrations of alcohols and aldehydes could be still observed.

At this point it should be noted that product sampling by means of using *online* gas chromatography in this work is a big advantage. Sango [111] and Cairns [14] reported about a loss on carboxylic acids during their *offline* analysis using glass ampoules due to strong adsorption of carboxylic acids with the glass surface. This led to a low carboxylic acid contents during the gas chromatographic analysis of the organic FT products.

Formation of methyl-ketones

It is believed in literature, that the addition of an alkyl group to the acyl species (**1**) as it is shown in Figure 4.18 yields methyl-ketones via chain termination [61][14]. The obtained methyl-ketone can hydrogenate in a secondary reaction to form a secondary alcohol.

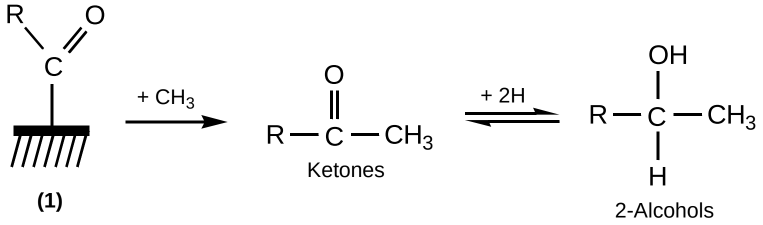

Figure 4.18: Scheme of the formation of methyl-ketones from an acyl intermediate and secondary reaction to secondary alcohols (adapted from [14]).

Along alcohols, aldehydes and carboxylic acids, the formation of methyl-ketones was observed during the Fischer-Tropsch experiments within this work and the mole fraction of methyl-ketones in the total linear organic products as a function of carbon number is presented in Figure 4.19.

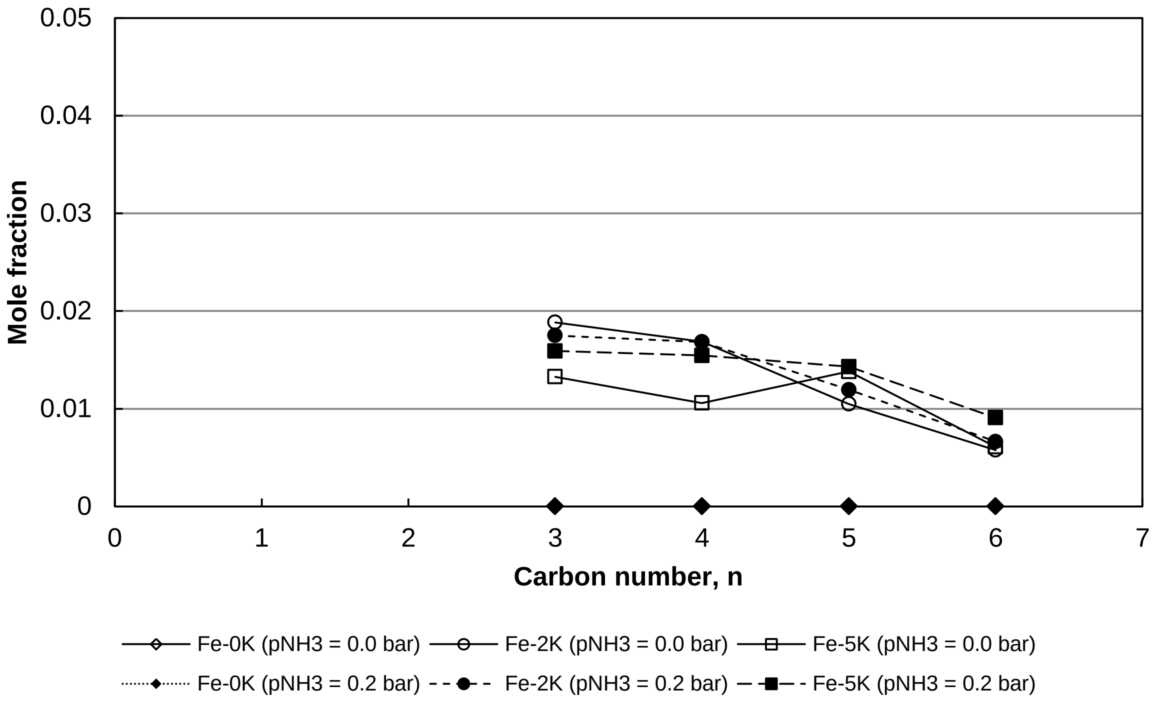

Figure 4.19: Mole fraction of methyl-ketones in all linear organic products during FT/NH_3-FT runs on iron catalysts at different NH_3 partial pressures and potassium loadings ($T_{Reactor}$ = 270 °C, P_{Total} = 4 bar, p_{NH3} = 0.0 - 0.2 bar, GHSV = 1920 h^{-1}, H_2:CO = 2:1).

Small amounts of methyl-ketones (mole fractions up to 0.02 for C_3) are obtained from the ammonia-free Fischer-Tropsch reactions on potassium promoted catalysts and the mole fraction of methyl-ketones decreases with increasing carbon number. When the reaction are carried out on unpromoted iron catalysts, almost no methyl-ketones are detected.

A possibility that no methyl-ketones were found during the reaction on unpromoted iron catalysts could be due to increased secondary reactions of oxygenated compounds in the absence of potassium [35][16]. Oxygenated compounds can re-adsorb and be hydrogenated to paraffins or incorporated into growing chains. When potassium is used as a promoter these secondary reactions are suppressed and the formation of methyl-ketones can be observed in the organic FT product (Figure 4.19). Potassium could also interact with the 3d-band of the iron catalyst and increases adsorption of carbon monoxide [15]. Since it is believed that methyl-ketones are generated through an acyl intermediate as proposed by Schulz [61] and Cairns [14], the number of acyl intermediates on the catalyst surface could be increased and higher formation rates of methyl-ketones could be obtained.

When increasing the ammonia partial pressure from 0.0 to 0.2 bar, methyl-ketones can still be found in the product spectra (for catalysts Fe-2K and Fe-5K). The mole fraction of methyl-ketones does not seem to be affected by addition of NH_3 to the synthesis gas feed. This was also affirmed by Sango [111] by adding ammonia during Fischer-Tropsch synthesis in a slurry reactor. The amount of methyl-ketones formed during conventional Fischer-Tropsch experiments was not affected when ammonia was added to the synthesis gas feed after 240 minutes. However, further reactions of methyl-ketones to secondary alcohols could not be detected during FT/NH_3-FT runs in this work and this is possibly due to very low molar flow rates of methyl-ketones. Moreover, beneficial effects resulting from the ammonia co-feeding during NH_3-FT experiments on potassium-free iron catalysts, as it was shown in the chapters before, could not be observed.

It is not clear how ammonia is suppressing the formation of oxygenates such as alcohols, aldehydes and carboxylic acids in case of NH_3-FT experiments on K promoted iron catalysts. From Figure 2.2 and Figure 4.16 it is shown that for the formation of alcohols and carboxylic acids, an adsorbed OH group could be involved in the reaction mechanism as proposed by Johnston *et al.* [30]. The adsorption of H_2O and NH_3 on iron oxides occurs on the same active sites, i.e. the Lewis sites [126]. Hydroxyl groups could adsorb on these active sites during the Fischer-Tropsch synthesis, too and from ligand field theory and the spectrochemical series, it is known that NH_3 is a stronger Lewis base than H_2O or OH groups [127]. Ammonia could adsorb onto the catalyst surface and dissociate into NH_2 and surface hydrogen (Figure 2.14). During the next step, hydroxyl groups could be replaced with amino groups and water could be formed from the reaction of surface hydrogen with surface hydroxyl groups (Figure 4.20). This could explain why methyl-ketones can still be found during NH_3-FT runs since they are formed via an addition of methyl groups to an acyl intermediate (Figure 4.18) [14].

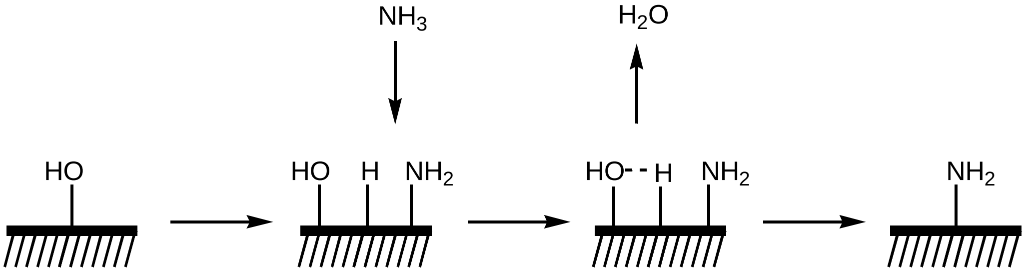

Figure 4.20: Scheme the formation of H_2O from an adsorbed hydroxyl group and ammonia.

During NH_3-FT experiments on potassium promoted iron catalysts increased CO_2 selectivities were observed (Figure 4.7) and it sounds reasonable that more water could be formed as illustrated in Figure 4.20, and consequently the WGS reaction would be enhanced due to the increased partial pressure of water (Equation 2.2). This hypothesis cannot be excluded but due to low flow rates of ammonia during the co-feeding tests (2 mL/min) and low ammonia conversions (Figure 4.6), the formation rates of additional water from reactions of ammonia would be low. Moreover, CO_2 formation could also take place via the Boudouard reaction (equation 2.3). As described in literature [125], it is believed that population of OH groups on catalyst surfaces is supposed to be low and it was postulated that the formation of oxygenates mainly occurs via CO insertion under the reaction conditions used in this work. From this point of view, suppressed formation rates of alcohols, aldehydes and carboxylic acids have to be explained differently and will be discussed in the next chapters.

4.2.1.8 Formation of organic nitrogen-containing products

It was reported that the addition of ammonia during Fischer-Tropsch experiments could lead to the formation of nitrogen or N-containing compounds. The reactions were carried out on iron, cobalt, copper or molybdenum catalysts and it was feasible to obtain amines, nitriles and amides from the reaction [6][10][91][98]. Along with these organic nitrogen-containing compounds, conventional Fischer-Tropsch products such as olefins and paraffins could be synthesized, too. Oxygenated compounds such as alcohols, aldehydes or carboxylic acids formed during the Fischer-Tropsch synthesis at an ammonia partial pressure of 0.0 bar were reported to decrease significantly when ammonia was added to the synthesis gas feed [6][91][111]. In this context, a correlation between the formation of N-containing compounds and oxygenates is speculated by some authors [6][89][91][111]. This involves the presence of surface intermediates which are required for the formation of oxygenates or the ability of oxygenates to re-adsorb onto the catalyst surface and react further with adsorbed nitrogen-containing surface species. It is therefore hypothesized that the formation of organic nitrogen-containing compounds could occur in a primary or secondary synthesis step. However, the reaction mechanisms for the formation of organic nitrogen-containing compounds during Fischer-Tropsch synthesis are still unclear. From this point of view, only the results from the gas chromatographic analysis with respect to amines, nitriles and amides will be presented in this chapter. Possible reaction pathways will be discussed in chapter 4.2.3 based on results from FT/NH_3-FT experiments at different reaction conditions (chapter 4.2.2).

Formation of amines and nitriles

After 240 minutes of time on stream during the Fischer-Tropsch experiments, some of the nitrogen was replaced by ammonia (chapter 3.3.2). The use of GC-MS techniques (*online* analysis on a HP 6890/5973 GC-MS) could show the evidence of aliphatic and terminal amines as well as nitriles in the Fischer-Tropsch product. Since it is possible to extract molecule specific ions from the complex FT gas chromatograms using the GC-MS, terminal aliphatic amines and nitriles (in the further progress of this work also referred as ‘amines’ and ‘nitriles’) could be indentified and quantified (chapter 3.4.3). These extracted ion chromatograms for amines (m/z = 30) and nitriles (m/z = 41) obtained from Fischer-Tropsch runs on a potassium promoted iron catalyst with p_{NH3} = 0.2 bar are presented in Figure 4.21.

The nitriles for carbon numbers between C_2 - C_6 can be identified when comparing the obtained mass spectra with the NIST database (chapter 3.4.3). It is difficult to separate the terminal aliphatic amine, which often show a tendency for a ‘tailing’ during gas chromatographic analysis. Therefore, it was tried to perform a better gas chromatographic analysis using an Optima 5 Amin capillary column in the beginning of the studies. However, separation of other Fischer-Tropsch products such as alcohols, methyl-ketones or carboxylic acids was hindered using this column. Additionally, due to low GC oven temperatures (-40 °C) in the initial phase of every single GC-MS analysis, the stationary phase of the Optima 5 Amin capillary column was not yet activated. As a result, the separation of amines during Fischer-Tropsch experiments was about the same as using an Optima 1 MS Accent capillary column. Here, ‘tailing’ effects were observed, too and gas chromatographic analysis using the GC-MS was performed on an Optima 1 MS Accent capillary column again. In order to calculate molar flow rates of amines, which were formed during FT/NH_3-FT experiments, a mixture of amines was prepared and injected using the same conditions for the GC-MS analysis as during the experiments. The elution time of every single amine was recorded and used for the FT/NH_3-FT experiments afterwards.

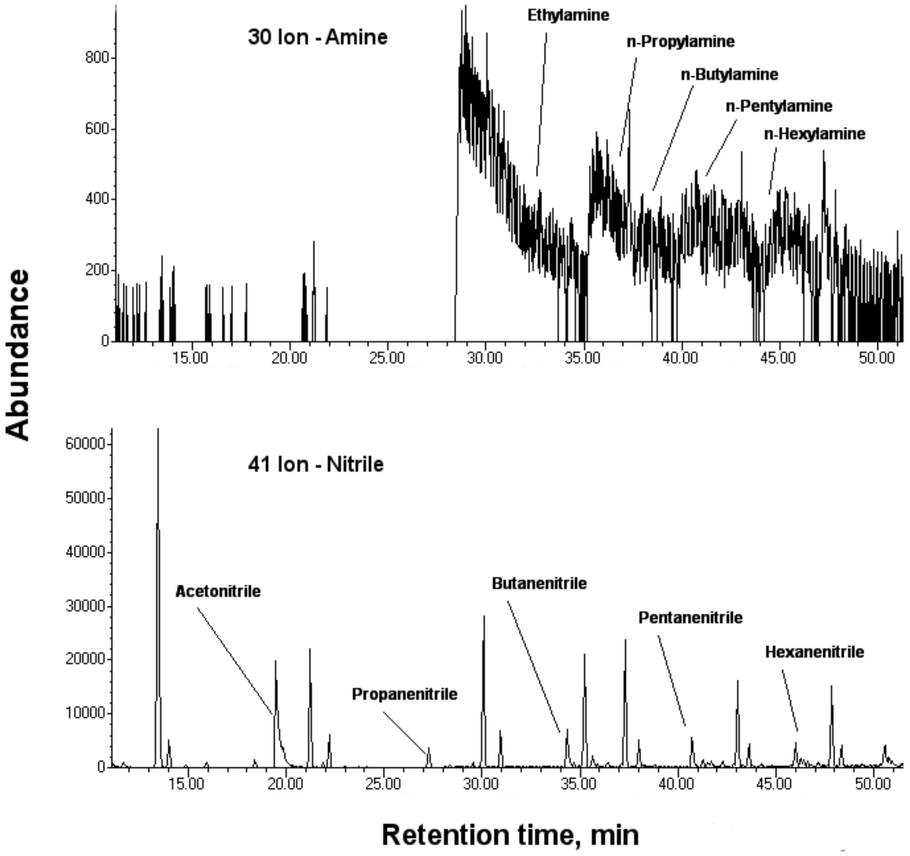

Figure 4.21: Extracted ion chromatograms for terminal aliphatic amines and nitriles and their corresponding ion m/z from NH_3-FT runs on catalyst Fe-2K (note that the ion m/z = 41 for *n*-propanenitrile overlaps with 2-methylpentene and the ion m/z = 54 was chosen for *n*-propanenitrile).

The mole fraction of amines and nitriles along the total linear organic products for C_1 - C_6 as a function of carbon number for NH_3-FT experiments on unpromoted/promoted iron catalysts is shown in Figure 4.22. Iron catalysts without potassium as a promoter show no activity towards amines and nitriles during the Fischer-Tropsch reaction with ammonia. Only a small content of organic nitrogen-containing compounds is detected, with the exception of for carbon numbers C_5 and C_6 where small concentrations of nitriles are found in the organic product. However, these amounts are too small as they would be noticeable in the mole fraction in all linear organic products. Moreover, these findings could be related to an error during GC analysis. During NH_3-FT experiments using potassium promoted bulk iron catalysts, the presence of amines and nitriles can be detected. For a carbon number of C_2, potassium promoted iron catalysts show highest mole fractions (up to 0.23) towards amines and nitriles.

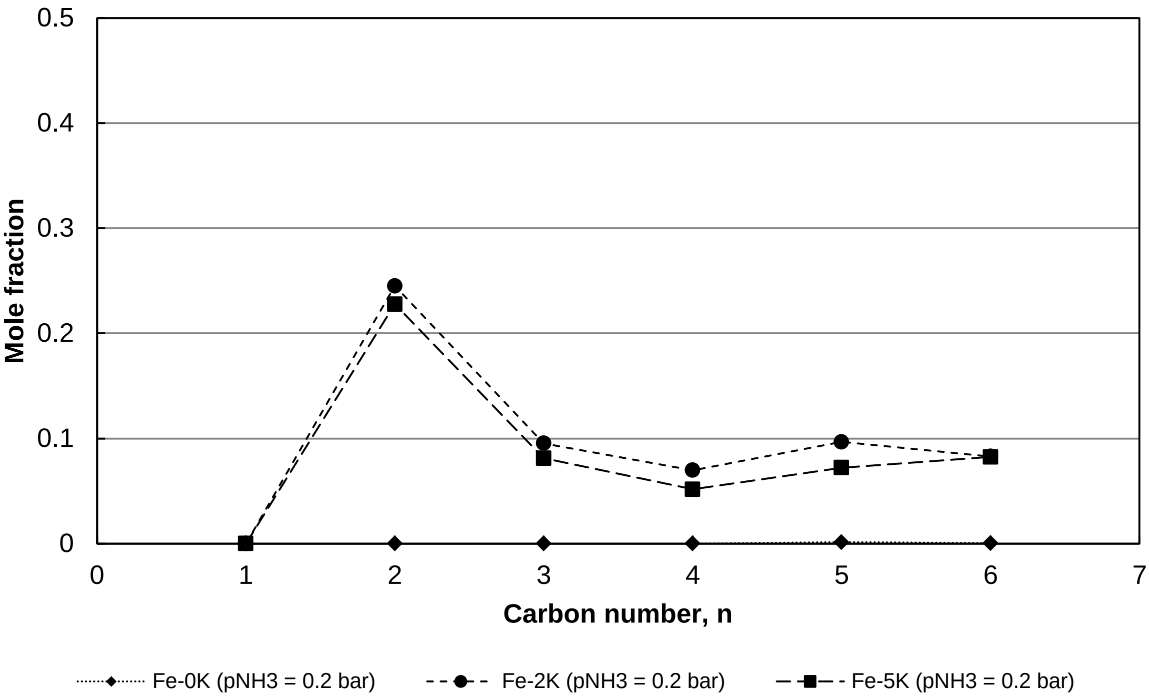

Figure 4.22: Mole fraction of amines and nitriles in all linear (plus C_1) organic products during NH_3-FT runs on iron catalysts at different NH_3 partial pressures and potassium loadings
($T_{Reactor}$ = 270 °C, P_{Total} = 4 bar, p_{NH3} = 0.2 bar, GHSV = 1920 h^{-1}, H_2:CO = 2:1).

After carbon number C_2 the mole fraction of amines and nitriles in all linear organic products drop significantly to around 0.09 and stabilizes on this level to a carbon number of C_6. From two-dimensional *offline* GC analysis of selected liquid phase samples, the presence of nitriles up to a carbon number of C_{17} was observed whereas no amines were found using this *offline* GC technique. These polar compounds probably accumulated in the water phase of the product (cold trap) and were therefore not found in the in the liquid phase samples collected from the hot trap. However, the water phase collected from the cold trap could not be separated and analyzed due to its low amount.

During the Fischer-Tropsch experiments with the co-feed of ammonia, on unpromoted/promoted iron catalysts no amines or nitriles with the carbon number of C_1 such as methylamine or hydrogen cyanide could be detected. The existence of secondary or tertiary amines such as diethylamine and triethylamine, for example, could not be confirmed but cannot be excluded. A possible explanation could be that due to apparently low concentrations and difficulties (‘tailing’ of amines) during *online* gas chromatographic analysis, these compounds could not be identified in this work.

Table 4.9: Selectivity (mol%) to N-containing compounds (amines and nitriles) as a percentage of the detected linear C_2 - C_6 organic products ($T_{Reactor}$ = 270 °C, P_{Total} = 4 bar, p_{NH3} = 0.0 - 0.2 bar, GHSV = 1920 h^{-1}, H_2:CO = 2:1).

	Fe-0K		Fe-2K		Fe-5K	
	p_{NH3} = 0.0 bar	p_{NH3} = 0.2 bar	p_{NH3} = 0.0 bar	p_{NH3} = 0.2 bar	p_{NH3} = 0.0 bar	p_{NH3} = 0.2 bar
C_2 - C_4	0.0	0.0	0.0	14.4	0.0	13.0
C_5 - C_6	0.0	0.0	0.0	1.4	0.0	1.1
C_2 - C_6	0.0	0.0	0.0	15.8	0.0	14.1

Table 4.10: Selectivity (mol%) to amines as a percentage of the detected linear C_2 - C_6 organic products ($T_{Reactor}$ = 270 °C, P_{Total} = 4 bar, p_{NH3} = 0.0 - 0.2 bar, GHSV = 1920 h^{-1}, H_2:CO = 2:1).

	Fe-0K		Fe-2K		Fe-5K	
	p_{NH3} = 0.0 bar	p_{NH3} = 0.2 bar	p_{NH3} = 0.0 bar	p_{NH3} = 0.2 bar	p_{NH3} = 0.0 bar	p_{NH3} = 0.2 bar
C_2 - C_4	0.0	0.0	0.0	4.0	0.0	2.1
C_5 - C_6	0.0	0.0	0.0	0.4	0.0	0.0
C_2 - C_6	0.0	0.0	0.0	4.4	0.0	2.1

Table 4.11: Selectivity (mol%) to nitriles as a percentage of the detected linear C_2 - C_6 organic products ($T_{Reactor}$ = 270 °C, P_{Total} = 4 bar, p_{NH3} = 0.0 - 0.2 bar, GHSV = 1920 h^{-1}, H_2:CO = 2:1).

	Fe-0K		Fe-2K		Fe-5K	
	p_{NH3} = 0.0 bar	p_{NH3} = 0.2 bar	p_{NH3} = 0.0 bar	p_{NH3} = 0.2 bar	p_{NH3} = 0.0 bar	p_{NH3} = 0.2 bar
C_2 - C_4	0.0	0.0	0.0	10.4	0.0	10.8
C_5 - C_6	0.0	0.0	0.0	1.0	0.0	1.1
C_2 - C_6	0.0	0.0	0.0	11.4	0.0	11.9

In Table 4.9, Table 4.10 and Table 4.11 the selectivities (mol%) to N-containing compounds (amines and nitrile) for different carbon numbers can be seen. Additionally, the selectivities towards these compounds are also given for an ammonia partial pressure of 0.0 bar. Nitriles are making up the bulk of the organic nitrogen-containing compounds and the selectivities to both organic nitrogen-containing compound classes (amines and nitriles) decline with increasing carbon number as it was already shown in Figure 4.22. However, a discussion why mostly nitriles were formed instead of amines during the NH_3-FT experiments will be given in chapter 4.2.3.

From the results, one could see that it was only possible to obtain amines and nitriles during the NH_3-FT experiments when iron catalysts were doped with potassium. This would be in agreement to results in literature where it was reported that amines or nitriles were generated from the co-feeding of ammonia, monomethylamine (MMA) or dimethylamine (DMA) during Fischer-Tropsch synthesis on potassium promoted metal catalysts (see also chapter 2.5) [10][89][95][96][111]. Moreover, additional alkali or alkaline earth metals in the catalysts were reported to result in a further increase in selectivities towards acetonitrile [95]. In contrast to that, o*nline* gas chromatographic analysis of the product stream during NH_3-FT experiments on cobalt catalysts within this work showed the presence of peaks with the extracted ion m/z = 30. These peaks possibly belong to amines but due to low concentrations no further identification or quantification was possible. However, these bulk cobalt catalysts were not impregnated with potassium. In contrast to the results described above, it was shown in literature that potassium does not necessarily has to be present in the catalyst to generate amines or nitriles from Fischer-Tropsch experiments in the presence of ammonia [6][90][91].

It is therefore not clear on how potassium affects the formation of organic nitrogen-containing compounds during NH_3-FT synthesis. An explanation could be found in literature where several authors assume reaction pathways to the formation of N-containing compounds via oxygenates or oxygen-containing precursors [6][89][91][111]. Based on this assumption, the reaction would take place in a primary or a secondary reaction step. The amount of organic nitrogen-containing formed during NH_3-FT experiments would be dependent on the activity of the catalyst to produce oxygenates such as alcohols, aldehydes or carboxylic acids. However, possible reaction mechanism to amines and nitriles during Fischer-Tropsch synthesis in the presence of ammonia will be discussed in chapter 4.2.3.

Formation of amides

As first authors, Rausch [6] and Sango *et al.* [12][111] reported about the formation of amides during NH_3-FT experiments in a slurry reactor using cobalt and iron catalysts respectively. The concentration of this compound class within the organic product was small as observed using *offline* GC-MS techniques. During NH_3-FT experiments in a fixed-bed reactor within this work, it was not possible to detect amides using *online* GC-MS techniques and *offline* two-dimensional gas chromatography (GCxGC-TOF) was used instead (chapter 3.4.4).

Figure 4.23 attempts to show the evidence of amides during NH_3-FT experiments on potassium promoted iron catalysts. Along with amides, the presence of nitriles and oxygenated compounds such as 1-alcohols, methyl-ketones and carboxylic acids can be observed, too.

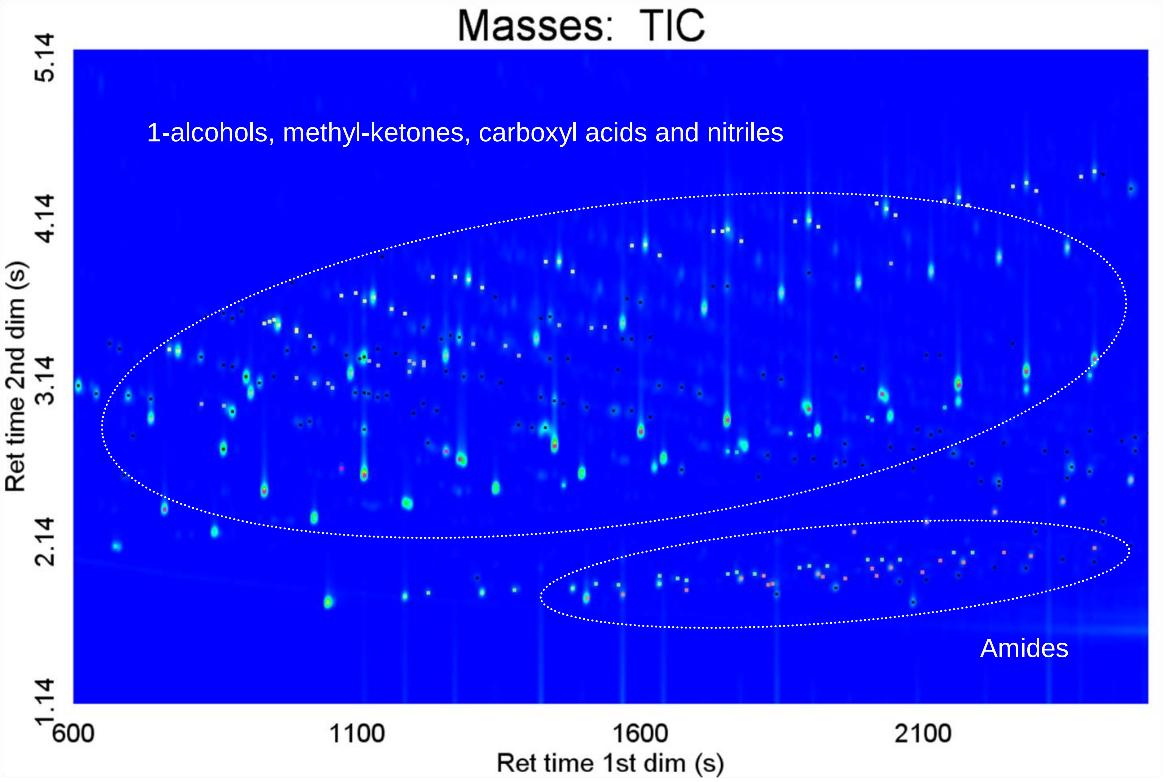

Figure 4.23: Chromatogram obtained from *offline* two-dimensional gas chromatographic analysis (GCxGC-TOF) of organic products from FT and NH_3-FT synthesis on a potassium promoted bulk iron catalyst ($T_{Reactor}$ = 270 °C, P_{Total} = 4 bar, p_{NH3} = 0.2 bar, GHSV = 1920 h^{-1}, H_2:CO = 2:1).

A library/database (NIST) was used to identify the obtained mass spectra of the products. Mainly the formation of linear amides in the range from C_3 - C_6 is observed and concentrations of these compounds are in general low. Products were found where the mass spectra could indicate the formation of N-alkylated acetamide, but an accurate classification is not possible due to low concentrations of these compounds.

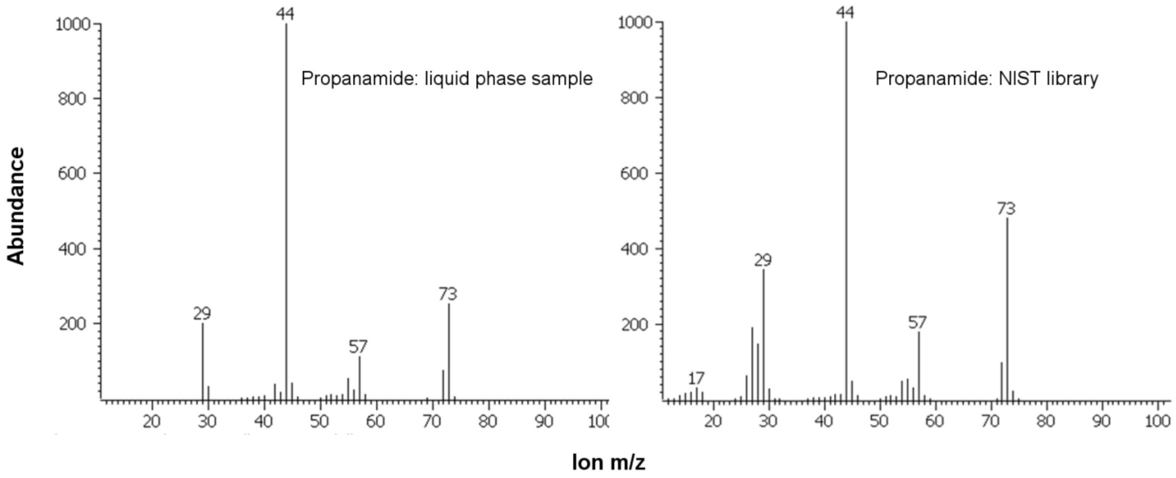

Figure 4.24: MS histogram for propanamide (left: liquid phase sample obtained from NH_3-FT run, right: NIST library).

4.2.1.9 Formation of inorganic nitrogen-containing compounds

During NH_3-FT experiments in this work, promoted bulk iron catalysts showed a different catalytic performance compared to unpromoted iron catalysts. Iron catalysts without potassium are not active to yield organic N-containing compounds such as amines and nitriles as it was shown in Figure 4.22. Despite of this observation, it is remarkable that highest ammonia conversion X_{NH3} was observed during NH_3-FT experiments on unpromoted iron catalysts (Figure 4.6).

Table 4.12: NH_3 conversion (area%) and selectivity based on NH_3 (mol%) to amines and nitriles (C_2 - C_6) during NH_3-FT experiments on iron catalysts with different potassium loadings.

Potassium loading (wt%)	X_{NH3} (area%)	$S_{amines, nitriles(N)}$ (mol %)
0	26.7	0.0
2	4.8[1]	13.3
5	3.2[1]	10.3

[1] X_{NH3} was taken 15 minutes earlier compared to NH_3-FT runs on catalyst Fe-0K.

Table 4.12 shows the ammonia conversion (X_{NH3}) and the selectivity to amines and nitriles based on ammonia. Here, areas for ammonia detected by the TCD were converted into molar flow rates using the ideal gas law. Consequently, the difference in ammonia conversion could be associated to other reactions than the formation of amines, nitriles or amides. However, possible side reactions of ammonia during NH_3-FT experiments will presented in this chapter. The selectivities based on ammonia to organic nitrogen-containing compounds during NH_3-FT experiments on potassium promoted iron catalysts are also low (Table 4.12). This is related to the fact that only amines and nitriles up to carbon number C_6 were detected during *online* gas chromatographic analysis. Moreover, nitriles up to C_{17} and amides were only observed during *offline* gas chromatographic analysis of selected liquid phase samples, and therefore these compounds are not included within the calculation of the selectivity. Additionally, it should be noted that side reactions of NH_3 during the NH_3-FT experiments on potassium promoted iron catalysts cannot be excluded, too.

Formation of ammonium carbonate/bicarbonate

When ammonia is added to the synthesis gas feed during Fischer-Tropsch synthesis, the formation of ammonium carbonate [98] or ammonium bicarbonate [111] is possible (chapter 2.5.4). Water and carbon dioxide, which can be formed during the Fischer-Tropsch reaction (chapter 2.1.1 and chapter 2.1.2) could undergo a side reaction with ammonia (equation 2.5 and 2.6).

During NH_3-FT at $p_{NH3} = 0.2$ bar experiments on iron catalysts in this work, an additional peak with a main characteristic ion m/z = 44 is found during GC-MS analysis (Figure 4.25) in the product. It may be speculated that this peak belongs to ammonium carbonate or ammonium bicarbonate. To verify this assumption, an extracted ion chromatogram (m/z = 44) from NH_3-FT reactions on bulk cobalt catalysts in the presence of ammonia is also shown in Figure 4.25. Cobalt catalysts are not active for CO_2 formation from WGS or Boudouard reactions [17][22] and consequently no ammonium carbonate or ammonium bicarbonate can be detected during the NH_3-FT experiments. It should be noted that the peaks in Figure 4.25a) belong to aldehydes, which disappear in the presence of ammonia ((b)). However, the peak in Figure 4.25b) is very broad since the used capillary column is not capable to separate inorganic salts.

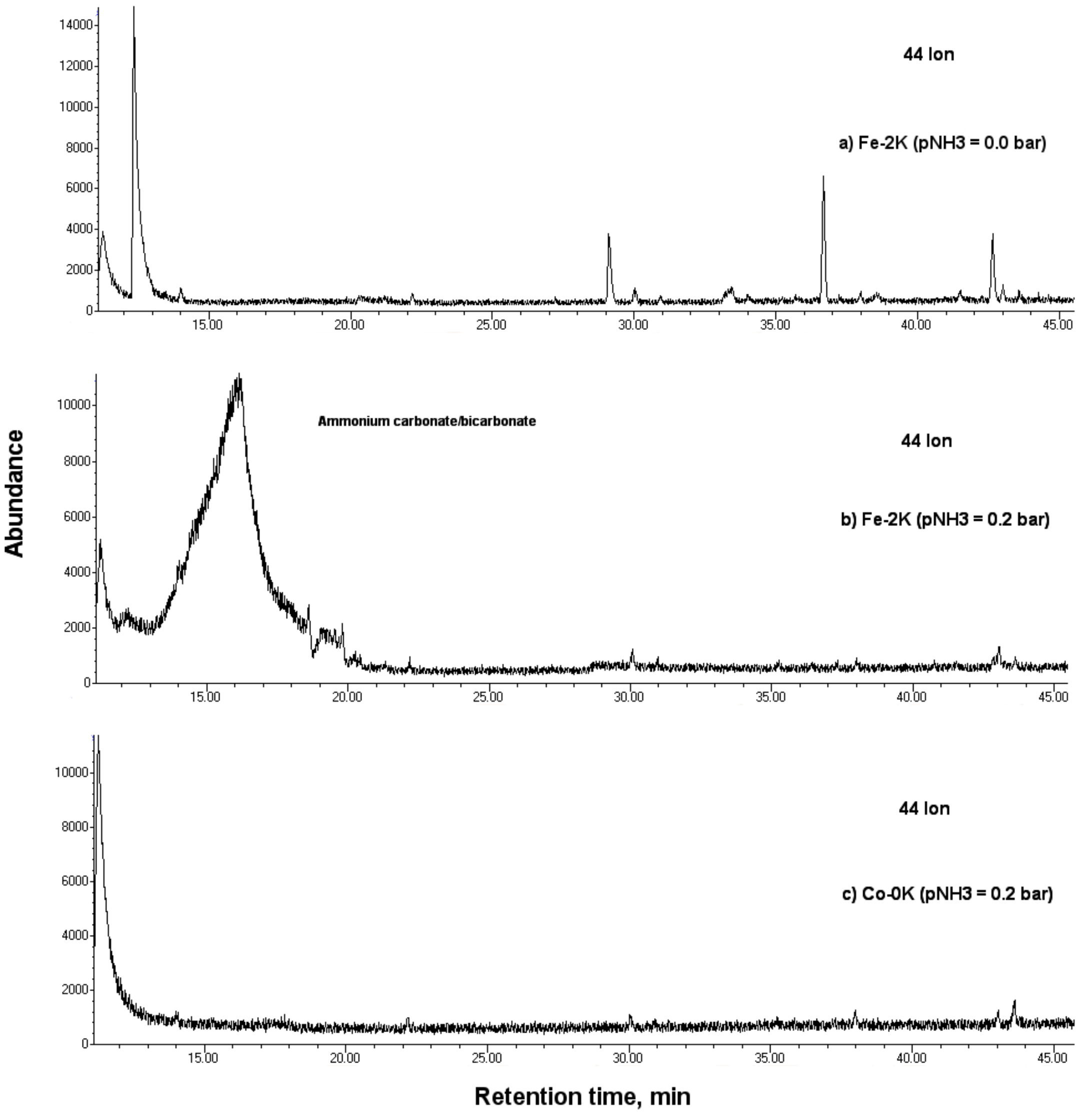

Figure 4.25: Extracted ion chromatograms for ion m/z = 44: a) FT on Fe-2K at p_{NH3} = 0.0 bar, b) NH_3-FT on Fe-2K at p_{NH3} = 0.2 bar, c) NH_3-FT on Co-0K at p_{NH3} = 0.2 bar.

Since no comparable mass spectra for either ammonium carbonate or ammonium bicarbonate could be found in the NIST database, an aqueous solution of ammonium bicarbonate was injected in the GC-MS. Ammonium bicarbonate shows also the main characteristic ion m/z = 44 and the retention time is slightly shifted (by 0.9 minutes) but would match with that of the unknown peak. Ammonium carbonate was not available and could not be analyzed using the GC-MS. Due to the same anion CO_3^{2-} to that of ammonium bicarbonate it could be speculated that ammonium carbonate shows the ion m/z = 44 during GC-MS analysis, too. However, this could not be verified and in the further progress of this work, this peak is referred as ‘ammonium carbonate/bicarbonate’.

It was tried to ‘quantify’ the content of ammonium carbonate/bicarbonate using the area ratios of the extracted ion of ammonium carbonate/bicarbonate (m/z = 44) and the internal standard cyclohexane (m/z = 84, Figure 4.13).

Table 4.13: Area ratio of the extracted ion m/z of ammonium carbonate/bicarbonate and cyclohexane (A_{44}/A_{84}) during FT/NH_3-FT runs on iron catalysts with different potassium loadings ($T_{Reactor}$ = 270 °C, P_{Total} = 4 bar, p_{NH3} = 0.0 - 0.2 bar, GHSV = 1920 h^{-1}, H_2:CO = 2:1).

Time (min)	**Fe-0K**	**Fe-2K**	**Fe-5K**
	Ion area ratio m/z = A_{44}/A_{84}	Ion area ratio m/z = A_{44}/A_{84}	Ion area ratio m/z = A_{44}/A_{84}
240 (FT)	-	-	-
480 (NH_3-FT)	9.67	6.16	1.01

According to Table 4.13, ammonium carbonate/bicarbonate is synthesized in smaller amounts during NH_3-FT reactions on potassium promoted iron catalysts. Along the tested iron catalyst series, contents of ammonium carbonate/bicarbonate decrease with increasing potassium loadings. A relation with different CO_2 selectivities (and consequently different water concentrations) observed during the NH_3-FT experiments (Figure 4.7) and the formation of ammonium carbonate/bicarbonate can be hereby assumed. But without further investigations, the decrease of ammonium carbonate/bicarbonate as shown in Table 4.13 cannot be explained.

However, it seems that the difference in the formation rates of ammonium carbonate/bicarbonate during NH_3-FT reactions on unpromoted and potassium promoted iron catalysts is little. Moreover, the ammonia conversion observed during NH_3-FT experiments on catalyst Fe-2K almost matches with that of catalyst Fe-5K (Table 4.12) and therefore, the ion ratios m/z = A_{44}/A_{84} should be the same, too. From this point view, it is more likely that other side reactions might take place as well which could be responsible for the high ammonia conversion on catalyst Fe-0K.

Formation of molecular nitrogen

In literature it is known that ammonia can decompose to nitrogen and hydrogen on transition metal catalysts at higher temperatures (Figure 2.15) [73][78][80]. After the addition of ammonia during Fischer-Tropsch synthesis on potassium-free iron catalysts, high conversion of ammonia and lower hydrogen consumption compared to conventional FT runs was observed (Figure 4.5). It could be speculated if these observations are related to the formation of hydrogen from the decomposition of NH_3.

Despite of the fact that during Fischer-Tropsch synthesis iron catalysts are readily converted into a mixture of magnetite and iron carbides (chapter 2.4.3), it can be assumed that NH_3 decomposition takes place. In this context, it was reported in literature that iron carbides could also catalyze the decomposition of ammonia [129]. The rate-limiting step for the decomposition of ammonia to molecular nitrogen and hydrogen is the re-combinative desorption of N_2 [75]. When potassium is present in the catalyst, the decomposition rate of NH_3 could be affected. The use of additional potassium in the iron catalysts facilitates dissociative chemisorption of nitrogen as it was shown on Fe(111) and Fe(110) surfaces by Strongin and Somorjai [72]. Potassium also decreases the population of adsorbed NH_3 on the catalyst surface via decreasing the adsorption energy of ammonia. It is also known in literature that the N-H bond is dilating when ammonia adsorbs on potassium-free iron surfaces [77]. Due to these facts, possible NH_3 decomposition to N_2 and H_2 is hindered. This could result in low ammonia conversions, when NH_3-FT reactions were carried out on potassium promoted iron catalysts Fe-2K and Fe-5K (Figure 4.6 and Table 4.12). These findings agree well with the results of Arabczyk and Zamlynny [84] who reported lower decomposition rates on iron catalysts when potassium was present on the catalyst surface. Based on these facts and results within this work, it seems likely that high ammonia conversion on unpromoted bulk iron catalysts could be related to an enhanced NH_3 decomposition to H_2 and N_2.

Formation of metal nitrides

When exposing freshly reduced transition metal catalysts to ammonia at temperatures between 400-495 °C, metal nitrides can be obtained [105][113][114]. These metal nitrides showed improved catalytic performance during Fischer-Tropsch synthesis and similar promotional effects (e.g. lower methane contents, higher olefin selectivities and higher C_{5+}

selectivities) to that of potassium were found [105][113][114]. During NH_3-FT reactions on unpromoted iron catalysts within this work, decreased conversion of CO and H_2 (chapter 4.2.1.1) as well as higher CO_2 (Figure 4.7) and lower methane selectivities compared to ammonia-free FT experiments were observed (Figure 4.9). Furthermore, more olefins were produced (Figure 4.10), the degree of branching declines (Figure 4.14) and increased chain growth probabilities (Table 4.4) were found when ammonia was added to the synthesis gas feed. With an exception of CO_2 formation, similar results are observed when cobalt catalysts are used for the reaction (Table 4.14). It may be speculated if metal nitrides were formed during the NH_3-FT experiments which could result in large ammonia conversions during NH_3-FT runs on potassium-free iron catalysts (Figure 4.6).

Despite this similarity (i.e. the improved catalytic performance of catalyst Fe-0K), it seems unlikely that metal nitrides were formed within this work. The conversion of ammonia during the NH_3-FT experiments does not indicate bulk iron nitride formation (Figure 4.6). A maximum of X_{NH3}, which appeared in the initial phase of the ammonia co-feeding, was contributed due to long residence times of NH_3 in the hot trap (chapter 4.2.1.1). The ammonia conversion seems to be stabilized after the total amount of untreated ammonia has reached the GC-TCD and no extensive NH_3 consumption can be contributed to nitriding processes. From a thermodynamic point of view, the formation of bulk metal nitrides could be unfavorable under the used reaction conditions within this work, too [99][109]. Small amounts of hydrogen are sufficient to suppress nitriding processes and when cobalt as the catalytic metal is used, ammonia has to be present in excess [6][106]. In this context, it was also found by Baiker [104] during hydroamination experiments that the formation of metal nitrides strongly depends on the presence of hydrogen. Hummel *et al.* [97] reported that when iron nitrides were used in the FT synthesis, no bulk iron nitrides were found in the spent catalyst and iron nitrides were converted to iron carbides during the reaction within minutes. This could be in agreement with findings from chemical analysis where spent iron and cobalt catalysts were investigated on their nitrogen content (chapter 4.1.5). Only small traces of nitrogen were found and it was therefore assumed that the nitrogen is either related to the formation of metal nitrides or to residues from the catalyst preparation where metal nitrates were used (chapter 3.1). Moreover, since nitriding processes are endothermic reactions, high temperatures are required [99][105][108][114]. Therefore, the temperatures applied in this work could be too low. From these facts, formation of metal nitrides during NH_3-FT experiments appears to be unlikely.

Table 4.14: Effect of ammonia on the catalytic performance of unpromoted cobalt and iron catalysts during FT/NH_3-FT synthesis [1].

	Co-0K		Fe-0K	
	p_{NH3} = 0.0 bar	p_{NH3} = 0.2 bar	p_{NH3} = 0.0 bar	p_{NH3} = 0.2 bar
S_{CH4} (C-%)	17.3	11.6	19.6	16.7
α	0.63	0.71	0.45	0.50
$S_{olefin,C2-C9}$ (mol%)	17.0	76.1	4.3	30.5
iso/lin ratio, C_4	0.11	0.01	0.10	0.01
$S_{oxy,C1-C6}$ (mol%)	2.4	0.0	0.1	0.1

[1] Reaction conditions are listed in Table 3.4.

4.2.1.10 Discussion

During Fischer-Tropsch experiments in the presence of ammonia, a different catalytic behaviour was observed when unpromoted or potassium promoted iron catalysts were used (chapter 4.2.1.1 to 4.2.1.9). On potassium-free iron catalysts, conversion of carbon monoxide and hydrogen dropped compared to conventional FT runs and higher olefin and CO_2 selectivities as well as higher chain growth probabilities were found. Furthermore, the formation of methane and side reactions such as chain branching were reduced in the presence of ammonia. Similar results were found when cobalt catalysts were used during FT/NH_3-FT experiments (Table 4.14). Here, an exception can be found for the CO_2 formation since cobalt is not active for the WGS or the Boudouard reaction [17][22]. In contrast to that, the changes described above were not observed during NH_3-FT experiments on the potassium promoted iron catalysts Fe-2K or Fe-5K. Here, only the selectivity to CO_2 was increased slightly in the presence of ammonia.

From the results, it may be speculated if ammonia is acting as a catalyst poison and blocks active sites for the Fischer-Tropsch reaction [13]. This could explain low CO and H_2 conversion, low methane selectivities or reduced side reactions but not increased CO_2 selectivities or chain growth probabilities α which were observed during NH_3-FT experiments on catalyst Fe-0K.

Another possibility for the observed effects could be the formation of bulk metal nitrides during the conducted NH_3-FT experiments. It was found by Yeh *et al.* [114] that nitrogen in iron nitrides could interact with the 3d band of iron. As a consequence, bulk iron nitrides showed improved catalytic performance during Fischer-Tropsch synthesis and similar effects to that within this work (e.g. lower methane contents, higher olefin selectivities and higher C_{5+} selectivities) were observed [105][113][114]. The formation of bulk nitrides within this work could possibly explain the improved catalytic performance of catalyst Fe-0K (chapter 4.2.1.1 to 4.2.1.6) but there are some aspects which would disagree with this hypothesis (chapter 4.2.1.9). From a thermodynamic point of view, the formation of bulk iron nitrides seem to be unlikely under the reaction conditions applied in this work. Small amounts of hydrogen are sufficient to suppress nitriding processes and when cobalt as the catalytic metal is used, ammonia has to be present in excess [6][106]. The temperature of 270 °C which was used during the NH_3-FT experiments could be too low and for the endothermic formation of iron nitrides, higher temperatures could be required [99][105][108][114]. Moreover, no extensive NH_3 consumption could be contributed to nitriding processes during the reaction and X_{NH3} appears to be constant over the time on stream (chapter 4.2.1.1). From this, the formation of bulk metal nitrides seems to be unlikely and a different explanation for the improved catalytic performance of the potassium-free iron catalyst has to be found.

Another explanation for the improved product performance during NH_3-FT experiments on unpromoted iron catalysts could be related to ammonia itself which could interact with the 3d band of the iron catalyst. The basic properties of ammonia could induce an electron donor effect on the catalyst as it was proposed by Rausch [6]. Similar electron donor effects were described for potassium as a promoter and bulk metal nitrides during Fischer-Tropsch synthesis (e.g. [15][63] [105][113][114]). The use of additional ammonia in the synthesis gas feed may result in similar promotional effects to that of potassium or bulk metal nitrides (examples for promotional effects are given in chapter 2.4.1 and 2.6.3).

During NH_3-FT experiments on potassium-free iron catalyst Fe-0K, higher ammonia conversions were observed compared to the experiments using potassium doped iron catalysts (Figure 4.6). It was assumed during NH_3-FT experiments using unpromoted iron catalysts that high ammonia conversion is related to enhanced ammonia decomposition processes to N_2 and H_2 (chapter 4.2.1.9). Before the formation of molecular nitrogen in a re-combinative desorption step, atomic nitrogen is bonded with high concentrations on the catalysts surface [81]. These surface species could act as ‘surface nitrides’ and therefore, also be responsible for the improved catalytic performance of catalyst Fe-0K during the NH_3-FT experiments. The presence of surface nitrides was also proposed by Löffler and Schmidt [85] during ammonia decomposition reactions. They found that the reaction proceeds faster when metal nitrides were used instead of conventional metal catalysts. Since the authors could not find any evidence for bulk metal nitrides after the reaction, they proposed the presence of surface metal nitrides as a form of adsorbed and dissolved nitrogen near to the catalyst surface [85].

When potassium as a promoter for the Fischer-Tropsch reaction is used in the iron catalyst, less NH_3 is adsorbed on the catalyst surface [72] during NH_3-FT experiments and less NH_3 decomposition could take place [84]. Assuming that ammonia itself or surface bonded nitrogen atoms are responsible for enhanced electron donor effects, conventional Fischer-Tropsch parameters should be influenced only little. The results of FT/NH_3-FT experiments on potassium promoted catalysts Fe-2K and Fe-5K affirmed that the catalytic performance was mostly not affected by the presence of ammonia in the synthesis gas feed (chapter 4.2.1.1 to 4.2.1.6). Here, the conversion of CO and H_2 as well as the selectivities to methane, olefins or branched hydrocarbons were not influenced by ammonia. Moreover, chain growth probabilities remained unchanged and the selectivity to CO_2 was increased only slightly. An exception is the disappearance of alcohols, aldehydes or carboxylic acids and the presence of amines, nitriles and amides in the organic product when ammonia was added to the FT reaction (chapter 4.2.1.7 and 4.2.1.8). This would be in agreement with the results from Sango [111]. During his NH_3-FT experiments with similar NH_3 concentrations of 5 vol% in the synthesis gas feed on potassium promoted iron catalysts, the described conventional Fischer-Tropsch parameters were not changed as well. During the studies of Sango [111] and Sango *et al.* [12], alcohols, aldehydes and carboxylic acids disappeared, too.

It seems that the promotion of iron catalysts with potassium has an indirect effect on the formation of organic nitrogen-containing compounds (4.2.1.8). During Fischer-Tropsch experiments on potassium promoted bulk iron catalysts, the formation of alcohols, aldehydes and carboxylic acids was observed (chapter 4.2.1.7). These compounds disappeared when ammonia was added to the synthesis gas feed and the formation of amines, nitriles and amides was observed instead. Almost no organic oxygen- and no nitrogen-containing compounds were detected during FT/NH_3-FT experiments on potassium-free iron catalysts. Therefore, a correlation between the formation of these two compound classes was assumed based on other literature [6][89][91][111]. However, a more detailed discussion on this topic will be given in chapter 4.2.3 based on the results from chapter 4.2.2.

4.2.1.11 Summary

The influence of ammonia on the catalytic performance of bulk cobalt and unpromoted/potassium promoted bulk iron catalysts during Fischer-Tropsch experiments was investigated. The experiments were conducted in a fixed-bed reactor and the reactant as well as the product gas stream was analyzed by means of *online* gas chromatography (GC-TCD, GC-FID and GC-MS). Selected liquid phase samples were analyzed using two-dimensional *offline* gas chromatography (GCxGC-TOF).

In the absence of NH_3 during Fischer-Tropsch experiments, it could be seen that additional potassium in iron catalysts has an impact on the catalytic performance compared to the use of potassium-free iron catalysts. Lower CO and H_2 conversion, lower methane selectivities and increased formation rates of CO_2 were observed when FT experiments were carried out on potassium promoted iron catalysts. Moreover, increased olefin and oxygenate contents were observed while side reactions such as chain branching were suppressed. When potassium was present in the catalyst, chain growth probabilities were enhanced and therefore, the selectivity to long chain hydrocarbons was increased. This influence can be explained by an electron donor effect of potassium which can interact with the 3d band of the iron catalyst. However, higher potassium loadings up to 5 wt% had no further effect with an exception of the CO conversion which was lower compared to experiments on iron with a potassium loading of 2 wt%. During FT experiments on bulk cobalt catalysts, mainly the formation of hydrogenated products such as paraffins was observed and small amounts of alcohols were found in the organic product.

When the ammonia partial pressure was raised from 0.0 to 0.2 bar, a different catalytic behaviour of promoted and unpromoted metal catalysts during the reaction was observed. During NH_3-FT experiments on potassium-free iron catalysts, the conversion of carbon monoxide and hydrogen decreased. Additionally, higher olefin and CO_2 selectivities as well as higher chain growth probabilities were found. The formation of methane and side reactions such as chain branching were reduced during experiments in the presence of ammonia. With the exception of CO_2 formation, similar results were obtained when FT/NH_3-experiments were carried out on bulk cobalt catalysts. During NH_3-FT runs on potassium promoted iron catalysts, ammonia had no influence on most of the FT products (e.g. olefins, methane and branched hydrocarbons). Furthermore, chain growth probabilities and conversion of CO and H_2 were not affected by the presence of ammonia. The selectivity to CO_2 increased slightly with additional ammonia in the synthesis gas feed and this gain was less pronounced with increasing potassium content in the iron catalyst. The different catalytic performance of unpromoted and potassium promoted metal catalysts during NH_3-FT experiments could be explained by the adsorption properties of ammonia or side reactions such as the decomposition of ammonia to N_2 and H_2. It was speculated that ammonia itself or surface bonded nitrogen atoms could act as ‘surface nitrides’ and induce an electron donor effect. Potassium in addition, can decrease the concentration of adsorbed ammonia or atomic nitrogen on the catalyst surface. As a consequence, potassium promoted iron catalysts are mostly influenced by potassium itself as a promoter for the Fischer-Tropsch reaction and changes of the catalytic performance in the presence of ammonia are less pronounced.

While no organic nitrogen-containing compounds could be detected during NH_3-FT experiments using unpromoted iron catalysts, the formation of terminal aliphatic amines and large amounts of nitriles was observed. The use of *offline* 2-dimensional gas chromatography ensured the presence of amides and nitriles up to carbon numbers of C_{17}. Similar results were obtained during Fischer-Tropsch experiments (p_{NH3} = 0.0 - 0.2 bar) on cobalt catalysts but only amines could be found in the product. Before the addition of ammonia to the synthesis gas feed during the reaction on cobalt and potassium promoted iron catalysts, alcohols, aldehydes or carboxylic acids were detected in the organic product. These compounds were suppressed in the presence of ammonia and a correlation between oxygenates and nitrogen-containing compounds was assumed. Nitrogen-containing products from NH_3-FT experiments may be formed via oxygen-containing precursors or oxygenates in a primary or secondary reaction step.

4.2.2 Influence of reaction parameters

Organic nitrogen-containing compounds such as amines, nitriles and amides are important and valuable organic products and a variety of different commercial synthesis routes are available nowadays (for further information and literature see also chapter 2.5) [5][49][50]. Due to the high demand of these compounds and their feedstock based on limited crude oil reserves, the focus should shift to alternative production routes. In this context, the scientific literature reported that amines, nitriles and amides can be obtained during Fischer-Tropsch synthesis with additional ammonia [6][90][96][112].

Alcohols, aldehydes or carboxylic acids which were formed during conventional FT synthesis in this work (chapter 4.2.1), disappeared when ammonia was added to the synthesis gas feed. During NH_3-FT experiments, the formation of amines, nitriles and amides was observed instead. From the results of FT/NH_3-FT experiments in chapter 4.2.1 and other literature [6][89][91][111], a correlation between the formation of oxygenates such as alcohols, aldehydes or carboxylic acids and organic nitrogen-containing compounds (e.g. amines, nitriles and amides) is hereby assumed. Organic nitrogen-containing products could be therefore formed from oxygenates or oxygen-containing precursors via a secondary or primary reaction step (a more detailed description of possible reaction mechanisms can be found in chapter 4.2.3). From this point of view, it must be possible to steer the selectivity towards organic nitrogen-containing compounds by changing the content of alcohols, aldehydes and carboxylic acids during the reaction. In this context it is known in literature that the formation rate of oxygenates can be varied using different Fischer-Tropsch reaction parameters such as temperature, H_2:CO ratio or space velocity [3][23].

Little is known about synthesis conditions or the formation of organic nitrogen-containing products during NH_3-FT synthesis. Due to different reaction conditions used, these results are difficult to compare (chapter 2.5). In this context, results from hydroamination experiments of alcohols with nitrogen sources (e.g. ammonia and amines) could help to understand or explain the results from NH_3-FT experiments within this study. This reaction is somewhat related to the Fischer-Tropsch synthesis since similar catalyst are employed and experimentally identified surface reactions as well as hypothesized reaction mechanisms show similarities. During the reaction, ammonia or amines are co-fed with an alcohol and amines or nitriles can be obtained as products.

In order to steer the selectivity to oxygenated compounds and organic N-containing products during FT/NH_3-FT synthesis, a series of experiments at different reaction parameters (e.g. temperature, H_2:CO ration and space velocity) was conducted using potassium promoted iron catalysts (catalyst Fe-2K). It should be noted that the *online* gas chromatographic analysis of organic nitrogen-containing during these experiments was limited to amines and nitriles (chapter 4.2.1.8). No liquid phase samples were taken for *offline* two-dimensional gas chromatographic analysis with the GCxGC-TOF and the formation of amides during the NH_3-FT experiments in this chapter could not be ensured (chapter 4.2.1.8). Moreover, the conversion of CO and H_2, chain growth probabilities as well as selectivities to conventional FT products (e.g. methane, olefins, branched hydrocarbons, methyl-ketones and CO_2) during FT/NH_3-FT on potassium promoted iron catalysts remained unaffected or were only changed slightly by additional ammonia in the synthesis gas feed (chapter 4.2.1). From this point of view, conversions and selectivities of or to these compounds are attached in the appendices (chapter 7.4) and this chapter will focus only on the formation of alcohols, aldehydes, carboxylic acids, amines and nitriles.

4.2.2.1 Variation of the reaction temperature

In a number of Fischer-Tropsch experiments on potassium doped iron catalysts the influence of temperature on the product selectivity was investigated. From Table 2.1 it can be seen that with increasing temperature in the FT synthesis, the selectivity to oxygenated compounds decreases (chapter 2.3.2) [3][23]. In order to vary the oxygenate selectivity and consequently the selectivity to amines and nitriles, the temperature was raised from 250 °C to 300 °C (Table 4.15).

Table 4.15: Reaction conditions during FT/NH_3-FT runs in a fixed-bed reactor on an iron catalyst doped with 2 wt% potassium at different temperatures.

	Temperature (°C)	**Pressure** (bar)	**p_{NH3}** (bar)	**GHSV** (h^{-1})	**H_2:CO**
Experiment 1	250	4	0.0 - 0.2	1920	2:1
Experiment 2	270	4	0.0 - 0.2	1920	2:1
Experiment 3	300	4	0.0 - 0.2	1920	2:1

The influence of the reaction temperature on the selectivity to oxygenate (with the exception of methyl-ketones) and organic nitrogen-containing products is presented in Figure 4.26.

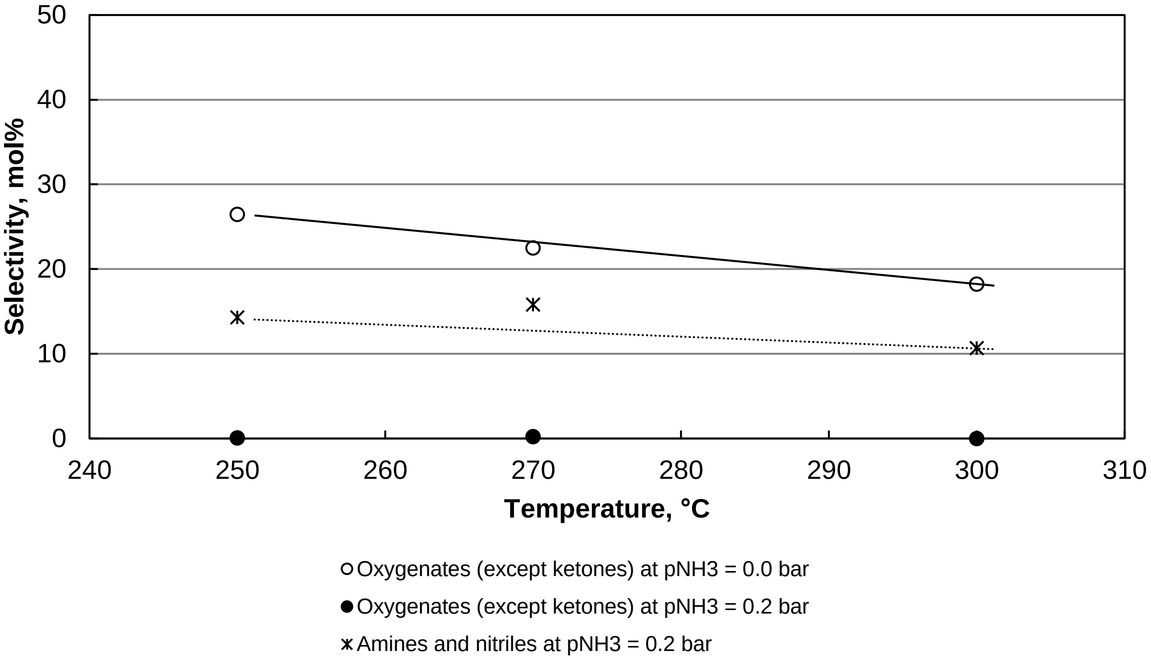

Figure 4.26: Selectivity (mol%) to oxygenates (with the exception of methyl-ketones) and amines plus nitriles as a percentage of all linear organic products (C_2 - C_6) at different temperatures ($T_{Reactor}$ = 250 - 300 °C, P_{Total} = 4 bar, p_{NH3} = 0.0 - 0.2 bar, GHSV = 1920 h^{-1}, H_2:CO = 2:1, catalyst = Fe-2K).

During FT experiments at a temperature of 250 °C, selectivities to alcohols, aldehydes and carboxylic acids of 26.4 mol% can be obtained (C_2 - C_6) and with increasing temperature, the selectivity drops to approximately 18 mol%. In the presence of ammonia, oxygenated compounds (with the exception of methyl-ketones) disappear and the formation of amines and nitriles is observed instead. Similar to alcohols, aldehydes and carboxylic acids, the selectivity to amines and nitriles is also decreasing when the temperature is raised to 300 °C during the reaction. Assuming that oxygenate or oxygen-containing precursors are involved in the formation organic nitrogen-containing products, it is noticeable that the selectivity to amines and nitriles is lower compared to the selectivity to alcohols, aldehydes and carboxylic acids. This could be related to the fact that not all organic nitrogen-containing products could be detected using *online* gas chromatographic analysis (chapter 4.2.1.8). Amides were only analyzed by means of *offline* two-dimensional gas chromatographic analysis (GCxGC-TOF) and selectivities to amides are, therefore, not considered within the calculations of the selectivity.

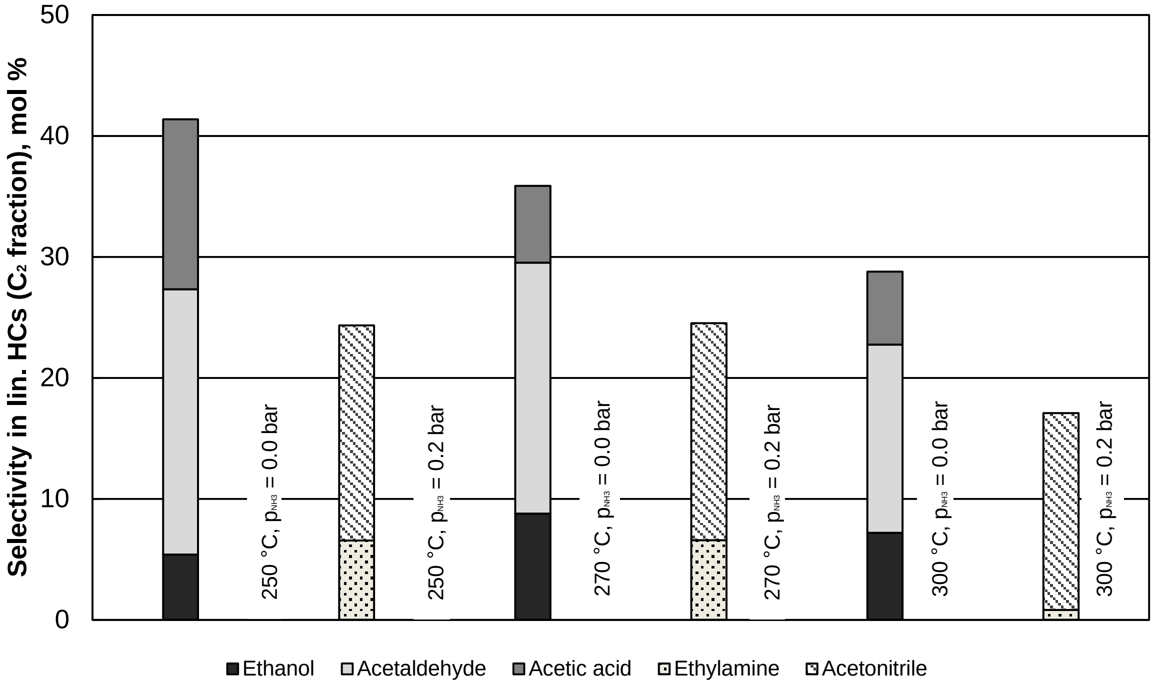

Figure 4.27: Selectivity (mol%) to oxygenates and amines plus nitriles as a percentage of all linear C_2 organic products at different temperatures ($T_{Reactor}$ = 250 - 300 °C, P_{Total} = 4 bar, p_{NH3} = 0.0 - 0.2 bar, GHSV = 1920 h^1, H_2:CO = 2:1, catalyst = Fe-2K).

To illustrate the deviation of alcohols, aldehydes and carboxylic acids in linear organic products during FT experiments in this work, the selectivity to the C_2 fraction of these products at temperatures between 250 °C and 300 °C is presented in Figure 4.27. High contents of acetic acid and lower ethanol selectivities are observed when the FT reaction is carried out at 250 °C. With increasing the reaction temperature to 300 °C, lower formation rates of acetic acid and acetaldehyde can be observed and compared to that, the amount of ethanol is slightly increases.

At an ammonia partial pressure of 0.2 bar, low selectivities to ethylamine and acetonitrile are observed when NH_3-FT experiments were carried out at 300 °C (Figure 4.27). Moreover, almost no ethylamine is found at this temperature and mainly acetonitrile is formed during the reaction.

The observations shown in Figure 4.26 and Figure 4.27 could be explained with results in literature [6][9][14]. At an ammonia partial pressure of 0.0 bar, alcohols, aldehydes and carboxylic acids can readily interact with each other (Figure 2.2) [14][61]. Assuming the formation of organic nitrogen-containing compounds from oxygenates at an ammonia partial pressure of 0.2 bar, amines and nitriles could be obtained then from re-adsorbed alcohol or aldehyde molecules (Figure 2.6) [6][9]. Moreover, with increasing temperature, side reactions were enhanced and higher selectivities towards acetonitrile and hydrocarbons were found [6]. The nitrile intermediate **(4)** shown in Figure 2.6 could be populated in high concentrations on the catalyst surface during NH_3-FT experiments at 300 °C. After desorption of this nitrile intermediate and loss of 3 hydrogen atoms, increased acetonitrile contents could be explained (Figure 4.27). However, low selectivities to amines and nitriles at temperatures of 300 °C compared 250 °C could be explained by likewise low oxygenate selectivities (e.g. to alcohols, aldehydes and carboxylic acids) or enhanced hydrocarbon formation from re-adsorbed oxygenated compounds [6].

Table 4.16: NH_3 conversion (area%) and selectivity based on NH_3 (mol%) to amines and nitriles (C_2 - C_6) during NH3-FT experiments on iron catalysts doped with 2 wt% potassium at different temperatures.

Reaction temperature (°C)	**X_{NH3}** (area%)	**$S_{amines,nitriles,(N)}$** (mol%)
250	2.2	21.2
270	4.8 [1]	13.3
300	6.1	3.6

[1] X_{NH3} was taken 15 minutes earlier compared to the other experiments.

Table 4.16 shows the conversion of ammonia (area%) for NH_3-FT runs at different temperatures. The conversion of ammonia at 250 °C is very low and slightly increases from 2.2 area % (250 °C) with increasing temperature (6.1 area % at 300 °C). In contrast to that, highest selectivities to amines and nitriles (based on X_{NH3}) in the carbon number range between C_2 - C_6 can be found at a reaction temperature of 250 °C. However, high NH_3 conversion and low selectivities to amines and nitriles could be related due to the existence of side reactions of ammonia including the possible formation of N_2 and H_2 or ammonium carbonate/bicarbonate (for further information and literature see also chapter 4.2.1.9 and chapter 2.6.2) [73][78][80]. The decomposition of ammonia to molecular nitrogen and hydrogen is an endothermic process and high temperatures will increase the rate of decomposition [80].

4.2.2.2 Variation of the synthesis gas composition

It was reported in literature [3][23] that the oxygenate content during Fischer-Tropsch synthesis can be changed when different H_2:CO ratios are used. With hydrogen-rich synthesis gas, oxygenates or oxygenate surface intermediates can be hydrogenated to paraffins and lower oxygenate selectivities are observed. Based on these findings three Fischer-Tropsch experiments were conducted using a different synthesis gas composition (H_2:CO = 1:1, 2:1, 4:1) in expectation to achieve high amine and nitrile selectivities (Table 4.17).

Table 4.17: Reaction conditions during FT/NH_3-FT runs in a fixed-bed reactor on an iron catalyst doped with 2 wt% potassium at different H_2:CO ratios.

	Temperature (°C)	**Pressure** (bar)	p_{NH3} (bar)	**GHSV** (h^{-1})	**H_2:CO**
Experiment 1	270	4	0.0 - 0.2	1920	1:1
Experiment 2	270	4	0.0 - 0.2	1920	2:1
Experiment 3	270	4	0.0 - 0.2	1920	4:1

At an ammonia partial pressure of p_{NH3} = 0.0 bar alcohols, aldehydes and carboxylic acids in all linear organic products can be detected during FT synthesis on potassium promoted iron catalysts (Figure 4.28). With increasing H_2:CO ratio the selectivity to oxygenated compounds in the carbon number range from C_2 - C_6 declines from 30.1 mol% to 16.8 mol% and formation of these compounds is suppressed when NH_3 is added to the synthesis gas feed. Similar as it was reported in literature [6][89][91][111] or shown in the chapters before (chapter 4.2.1 and chapter 4.2.2.1), amines and nitriles are generated instead. Since increased formation rates of amines and nitriles are evident when a H_2:CO ratio of 1:1 was used during the reaction (Figure 4.28), a correlation between the formation of oxygen- and nitrogen-containing products can be hereby assumed, too. As it was described in chapter 4.2.2.1, lower selectivities to amines and nitriles are observed compared to the selectivities to alcohols, aldehydes and carboxylic acids during the FT/NH_3-FT experiments. This could be related to the fact that not all organic nitrogen-containing compounds were detected during *online* gas chromatographic analysis (chapter 4.2.1.8).

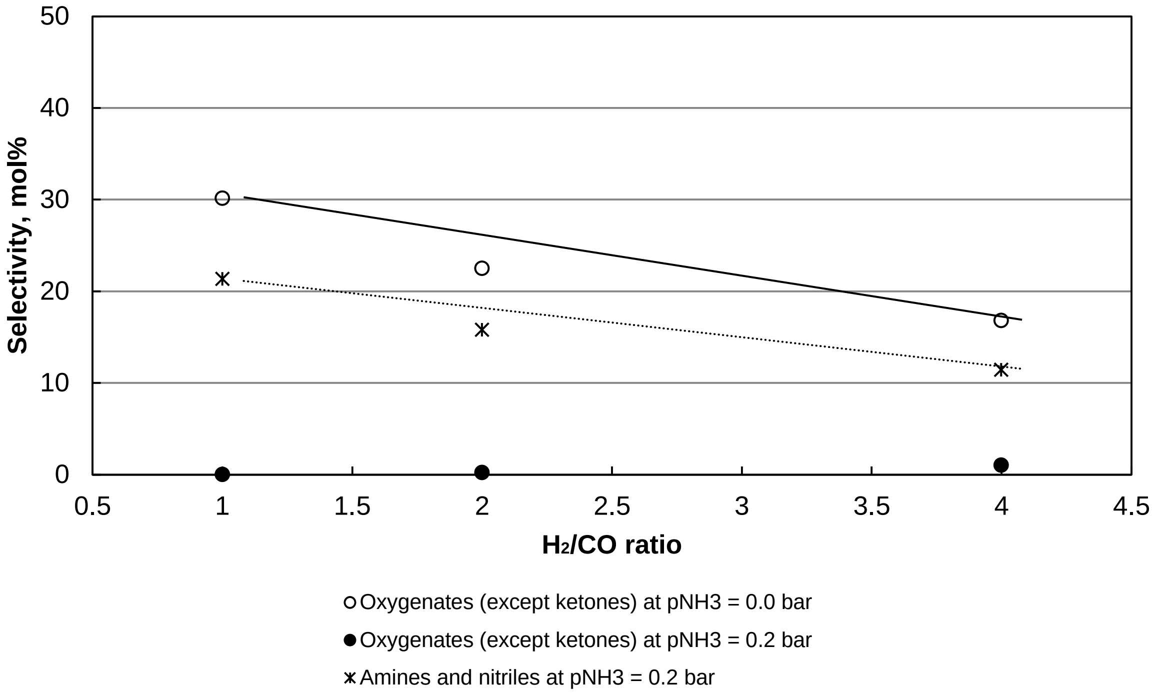

Figure 4.28: Selectivity (mol%) to oxygenates (with the exception of methyl-ketones) and amines plus nitriles as a percentage of all linear organic products (C_2 - C_6) at different H_2:CO ratios ($T_{Reactor}$ = 270 °C, P_{Total} = 4 bar, p_{NH3} = 0.0 - 0.2 bar, GHSV = 1920 h^{-1}, H_2:CO = 1:1, 2:1, 4:1, catalyst = Fe-2K).

A more detailed description of the diversity of the obtained O- and N-containing products is given in Figure 4.29. Here again, the C_2 fraction is chosen to illustrate the influence of different H_2:CO ratios on the product selectivity. During FT experiments at H_2:CO ratios of 1:1, mainly acetaldehyde and acetic acid are formed. By changing the synthesis gas composition to H_2:CO 4:1, formation rates of these products are reduced and more ethanol is generated. At ammonia partial pressures of 0.2 bar, the amount of ethylamine within linear organic products in the C_2 fraction slightly increases as more hydrogen is available in the synthesis gas mixture and in contrast to that, the selectivity to acetonitrile decreases.

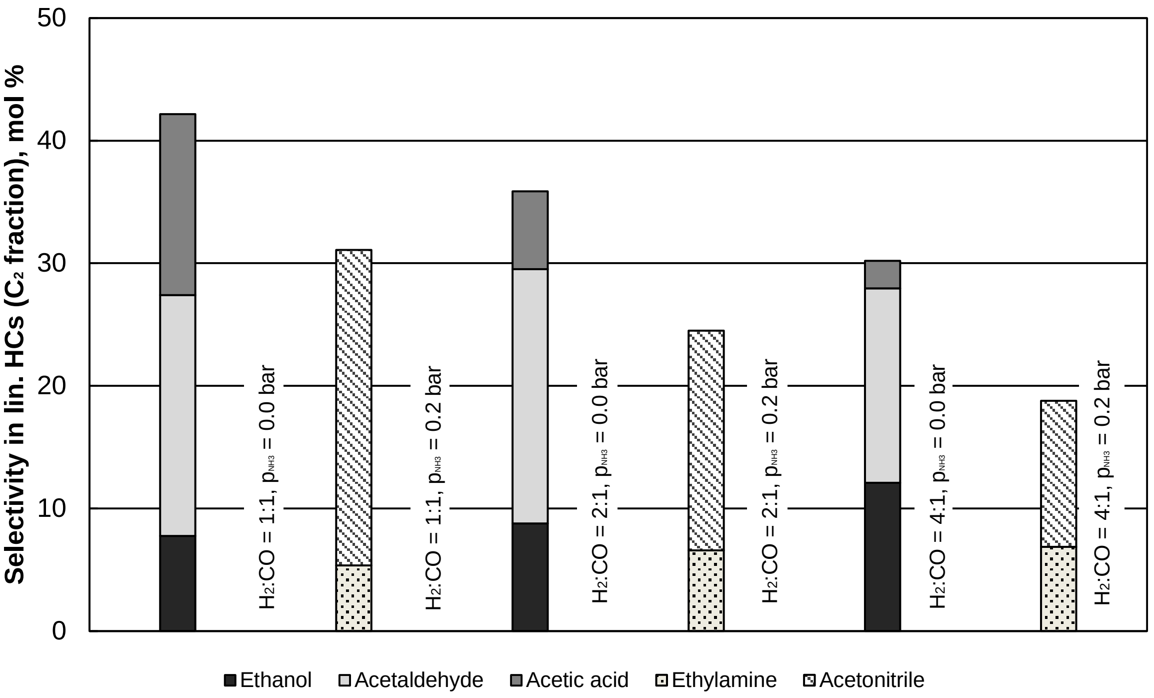

Figure 4.29: Selectivity (mol%) to oxygenates and amines plus nitriles as a percentage of all linear C_2 organic products at different H_2:CO ratios ($T_{Reactor}$ = 270 °C, P_{Total} = 4 bar, p_{NH3} = 0.0 – 0.2 bar, GHSV = 1920 h^{-1}, H_2:CO = 1:1, 2:1, 4:1, catalyst = Fe-2K).

It is known from hydroamination experiments that nitriles can re-adsorb onto the catalyst surface and can undergo hydrogenation to the corresponding amine [9]. In this context, hydrogen-rich atmospheres were reported to have beneficial effects on the amine selectivity [6]. Assuming that nitriles can also re-adsorb during NH_3-FT synthesis, a lower coverage of the iron catalyst surface with adsorbed hydrogen at a synthesis gas composition of 1:1 could reduce this secondary reaction. This would explain the lower ratio of ethylamine/acetonitrile during NH_3-FT experiments at H_2:CO ratios of 1:1 compared to experiments at a H_2:CO ratio of 4:1.

Compared to the experiments in the previous section, no trend of X_{NH3} or $S_{amines,\ nitriles(N)}$ according to different H_2:CO ratios is noticeable and the values remain almost the same. Moreover, the experiment with a synthesis gas composition of H_2:CO = 2:1 probably shows an ammonia conversion which is too low and could be related to an error from GC-TCD analysis. Assuming this, the selectivity $S_{amines,\ nitriles(N)}$ would be also lowered in this case. However, only a small amount of ammonia is converted to amines and nitriles within the C_2 - C_6 fraction. This could be related to limitations during *online* gas chromatographic analysis (chapter 3.4). Here, only amines and nitriles in the carbon number range between C_2 - C_6 and no amides could be analyzed (similar to all the other chapters).

Table 4.18: NH_3 conversion (area%) and selectivity based on NH_3 (mol%) to amines and nitriles (C_2 - C_6) during NH3-FT experiments on iron catalysts doped with 2 wt% potassium and different H_2:CO ratios.

H_2:CO ratio	**X_{NH3}** (area%)	**$S_{amines,nitriles,(N)}$** (mol%)
1:1	7.9	6.8
2:1	4.8 [1]	13.3
4:1	7.5	9.6

[1] X_{NH3} was taken 15 minutes earlier compared to the other experiments.

No information is available on how much moles of amines or nitriles with high carbon numbers or amides have been formed during the reaction. For example, *offline* two-dimensional gas chromatographic analysis revealed the presence of nitriles up to carbon number of C_{17} (chapter 4.2.1.8). Therefore, values for $S_{amines,\ nitriles(N)}$ in Table 4.18 do not display the whole amount of amines and nitriles formed during the NH_3-FT experiments and different selectivities (based on ammonia) to these compounds could be expected. Additionally, similar to the NH_3-FT runs presented in chapter 4.2.1 and chapter 4.2.2.1, side reactions such as the decomposition of NH_3 or the formation of ammonium carbonate/bicarbonate cannot be excluded. From that point of view, unlike as in the previous chapter where a trend of X_{NH3} and $S_{amines,\ nitriles(N)}$ can be assumed, it is not possible to interpret the results shown in Table 4.18.

4.2.2.3 Variation of the gas hourly space velocity

From Table 2.1 it can be seen that the amount of oxygenates formed during Fischer-Tropsch synthesis can be influenced by the residence time of the gas flow over the catalyst bed [3][23]. The residence time can be expressed as gas hourly space velocity (GHSV) which can be calculated by dividing the actual gas flow (mL/min) by the volume of the catalyst bed (mL). In this work, the GHSV was calculated in h^{-1} and further information to flow rates used during the reactions can be found in Table 3.4.

The selectivity to oxygenates and nitrogen-containing compounds was studied in dependency of the gas hourly space velocity. Since the flow rate of ammonia at a partial pressure of 0.2 bar was already very low (2 mL/min) and no accurate lower flow rates could be ensured, the volume of the catalyst bed was varied for the experiments instead (Table 4.19). For a better understanding and handling, the GHSV was also converted into the contact time which is the reciprocal value of the GHSV. In the further progress of this work this term, will also be used for the presentation and interpretation of the results.

Table 4.19: Reaction conditions during FT/NH_3-FT runs in a fixed-bed reactor on an iron catalyst doped with potassium (2 wt%) at different gas hourly space velocities (GHSV, h^{-1}) or contact times (s).

	Temperature (°C)	**Pressure** (bar)	**p_{NH3}** (bar)	**GHSV** (h^{-1})	**Mass catalyst** (g)	**Contact time** (s)
Experiment 1	270	4	0.0 - 0.2	3840	0.50	0.94
Experiment 2	270	4	0.0 - 0.2	1920	1.00	1.88
Experiment 3	270	4	0.0 - 0.2	1280	1.50	2.88

The formation rates of oxygenate and nitrogen-containing compounds in the range from C_2 - C_6 organic products are not strongly influenced by changing the GHSV or contact time of the reactants over the catalyst bed (Figure 4.30). Only a slight decrease in selectivity to these compounds (oxygenates at p_{NH3} = 0.0 bar, nitriles and amines at p_{NH3} = 0.2 bar) can be seen with increasing contact time to 2.88 s. It could be possible that these differences are related to GC analysis errors. Selectivities during FT/NH_3-FT experiments were calculated based on molar flow rates in domains of 10^{-5} and 10^{-11} mol/min (chapter 7.4.5) and errors or deviations during GC analysis cannot be excluded. From this point of view, it appears that variation of the GHSV or contact time has no influence on the selectivity to oxygenate and N-containing compounds.

In experiment 3, not all of the oxygenated compounds are suppressed in the presence of ammonia and small concentrations of ethanol, 1-propanol and 1-butanol can still be found in the organic product. During this experiment, highest amounts of catalyst were used in order to achieve a contact of 2.88 s and the observations could be explained by high formation rates of organic products (e.g. oxygenates and hydrocarbons). Assuming that organic nitrogen-containing compounds are formed from oxygenates or oxygen-containing precursors, the ammonia partial pressures could be too low. Consequently, not all oxygenates (with the exception of methyl-ketones) or oxygen-containing precursors could be converted to organic nitrogen-containing products. Similar results were reported by Sango [111] during FT/NH_3-FT experiments on potassium promoted iron catalysts. At low ammonia concentration (2 vol%) in the synthesis gas feed, alcohols were still found in the product and this content declined with increasing ammonia partial pressure.

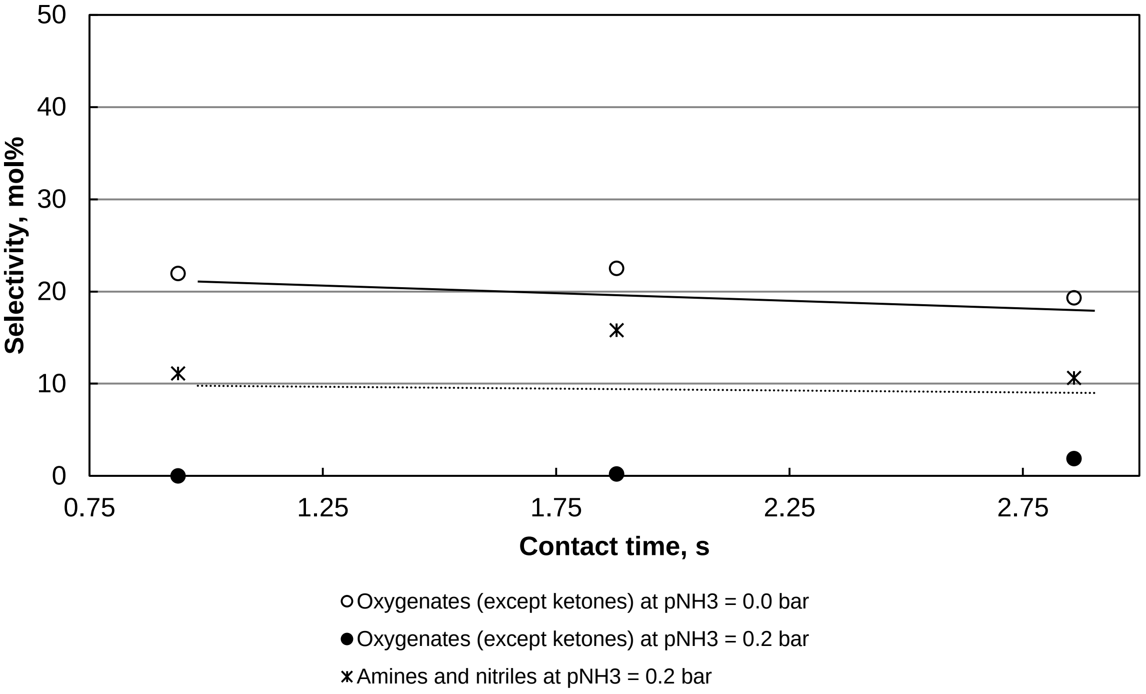

Figure 4.30: Selectivity (mol%) to oxygenates (with the exception of methyl-ketones) and amines plus nitriles as a percentage of all linear organic products (C_2 – C_6) at different contact times ($T_{Reactor}$ = 270 °C, P_{Total} = 4 bar, p_{NH3} = 0.0 - 0.2 bar, GHSV = 1280 - 3840 h^{-1}, H_2:CO = 2:1, catalyst = Fe-2K).

Organic products at carbon number C_2 represent the diversity of oxygenate and nitrogen-containing compounds during FT/NH_3-FT experiments in Figure 4.31. The use of larger catalyst amounts with constant reactant flow rates at an ammonia partial pressure of 0.0 bar shift the ethanol selectivity towards higher values (from 5.5 mol% at 0.94 s to 10.8 mol% at 2.88 s) while contents of acetaldehyde and acetic acid decrease (by 6.1 and 2.5 mol% respectively). In the presence of ammonia (p_{NH3} = 0.2 bar), the selectivity to ethylamine and acetonitrile seem not to be influenced by different gas hourly space velocities. Here, the ratio ethylamine/acetonitrile remains the same during the experiments at GHSV between 0.94 - 2.88 s.

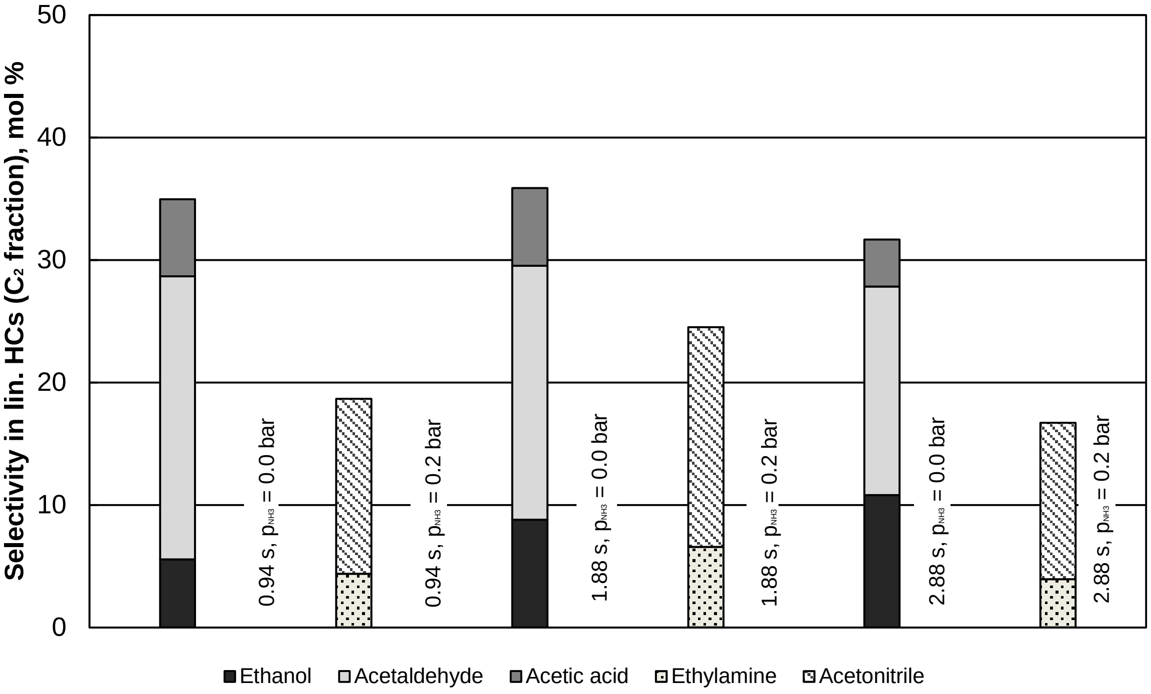

Figure 4.31: Selectivity (mol%) to oxygenates and amines plus nitriles as a percentage of all linear C_2 organic products at different contact times ($T_{Reactor}$ = 270 °C, P_{Total} = 4 bar, p_{NH3} = 0.0 - 0.2 bar, GHSV = 1280 - 3840 h^{-1}, H_2:CO = 2:1, catalyst = Fe-2K).

In this context, Rausch [6] found that equilibrium between ethylamines (MEA, DMA, TMA) and acetonitrile was achieved after short contact times of reactants (i.e. ethanol and ammonia) on the catalyst surface. With higher contact times after 0.2 s, acetonitrile almost disappeared in the product and mainly the formation of MEA, DMA, TMA and hydrocarbons was observed during the hydroamination experiments. If amines and nitriles can interact during NH_3-FT synthesis, the equilibrium conditions between amines and nitriles can be expected to be different due to a different type of reaction. Moreover, increased formation rates of ethanol at contact times of 2.88 s in the ammonia-free FT runs, could be related to enhanced secondary reactions of acetaldehyde or acetic acid. This would also explain why the content of these compounds declines (Figure 4.31). During NH_3-FT experiments, the ratio of ethylamine/acetonitrile was not affected by different contact times and it could be hypothesized that the re-adsorption of acetonitrile to form the corresponding amine via hydrogenation is hindered. Here, large amounts of surface hydrogen are required (Figure 2.6) [9] and this reaction might only take place at high hydrogen partial pressures.

Table 4.20: NH_3 conversion (area%) and selectivity based on NH_3 (mol%) to amines and nitriles (C_2 - C_6) during NH3-FT experiments on iron catalysts doped with 2 wt% potassium and different contact times (s).

Contact time (s)	X_{NH3} (area%)	$S_{amines,nitriles,(N)}$ (mol%)
0.94	4.7	4.6
1.88	4.8 [1]	13.3
2.88	9.6	7.9

[1] X_{NH3} was taken 15 minutes earlier compared to the other experiments.

According to Table 4.20, no clear tendency in matters of ammonia conversion and selectivity to amines and nitriles based on ammonia is noticeable. One could expect that due to fewer catalyst amounts, less NH_3 is adsorbed on the catalyst surface resulting in lower X_{NH3} values. But instead, same conversion for ammonia at two different contact times (0.94 s and 1.88 s) can be seen. It is more likely that X_{NH3} is lower in experiment 1 but from GC analysis incorrect areas for ammonia were obtained. This would automatically result in higher selectivities towards amines and nitriles. However, only small amounts of ammonia are converted to organic nitrogen-containing products during NH_3-FT experiments at different gas hourly space velocities. Possible reasons could be found from the interpretation of the results in the chapters above. Only amines and nitriles between C_2 - C_6 were detected during *online* gas chromatographic analysis and no organic nitrogen-containing compounds after carbon number C_6 are included within the calculation of $S_{amines,\ nitriles(N)}$. Furthermore, no amides are included within these calculations, too. However, side reactions such as ammonia decomposition or formation of ammonium carbonate/bicarbonate could also take place and cannot be excluded. Similar to chapter 4.2.2.2, it is therefore not possible to interpret the results shown in Table 4.20.

4.2.2.4 Summary

During FT/NH_3-FT synthesis on transition metal catalyst the formation of alcohols, aldehydes or carboxylic acids is suppressed and nitrogen-containing compounds such as amines and nitriles can be obtained instead. Therefore, a correlation between the formation of organic oxygen- and nitrogen-containing compounds was hypothesized. Amines and nitriles are may be formed from oxygenates or oxygen-containing precursor in a secondary or primary reaction step.

The variation of reaction conditions such as temperature, H_2:CO ratio and gas hourly space velocity during FT/NH_3-FT experiments could show that the selectivity to amines and nitriles can be increased along with higher molar flow rates of alcohols, aldehydes and carboxylic acids. The use of low temperatures and low H_2:CO ratios during the reaction has beneficial effects for the synthesis of oxygenates and consequently of nitrogen-containing compounds. Here highest selectivities towards these products were observed. It appears that a change of the gas hourly space velocity has no influence on the selectivity to these compounds and the selectivities remained unchanged. Moreover, the formation of the hydrogen-leaner product (e.g. aldehydes and nitriles) is affected by different reaction conditions, too. In this context, the C_2 product fraction could show that the ratio of ethanol/acetaldehyde and ethylamine/acetonitrile decreases with high temperatures or low H_2:CO ratios. It appears that the variation of gas hourly space velocity or contact time has no effect on the product selectivity to nitrogen-containing compounds. While increased alcohol formation was observed with higher contact times, ratios of ethylamine/acetonitrile remained the same.

However, aldehydes and nitriles were making up the bulk within oxygenate and nitrogen-containing compounds during all experiments. Furthermore, the selectivity to N-containing compounds was always lower than compared to that of alcohols, aldehydes and carboxylic acids. This could be related to the fact that not all nitrogen-containing products such as amides could be detected using *online* gas chromatographic analysis.

From the results some similarities between hydroamination and NH_3-FT experiments could be observed. The use of high temperatures during hydroamination of alcohols with ammonia also leads to the formation of mainly nitriles. Moreover, hydrogen-rich atmospheres were found to have positive effects on the amine/nitrile ratio, too.

Low ammonia conversions were observed during the conducted NH_3-FT experiments. Side reactions such as the formation of ammonium carbonate/bicarbonate or the decomposition of ammonia to nitrogen and hydrogen could take place. Whereas no statement about the formation rate of ammonium bicarbonate could be made, high temperatures may enhance the endothermic decomposition process of NH_3.

4.2.3 Mechanistic discussion for N-containing compounds

During NH_3-FT experiments on potassium promoted iron catalysts, the formation of amines, nitriles and amides could be observed (chapter 4.2.1 and 4.2.2). Little is known about the formation of organic nitrogen-containing compounds during Fischer-Tropsch synthesis with ammonia added to the synthesis gas feed. Therefore, reaction mechanisms for the synthesis of these compound classes are not developed and verified yet.

It is reported in literature that amines or nitriles could be formed from the reaction of ammonia or cyanides with olefins (amination of alkenes, Ritter reaction) and ammonia with methyl-ketones during reductive amination reactions [6][55][56][57]. Within this study, there are no indications that amines, nitriles and amides were generated via these reactants (e.g. olefins and methyl-ketones). During FT experiments on potassium promoted iron catalysts, the selectivities to olefins or methyl-ketones were not changed when ammonia was added to the synthesis gas feed (chapter 4.2.1.5 and 4.2.1.7). Moreover, increased olefin formation was observed during the addition of ammonia on unpromoted iron and cobalt catalysts (Table 4.14). Due to these observations, other possible formation routes for the synthesis of amines, nitriles and amides have to be found.

During FT/NH_3-FT experiments within this work (chapter 4.2.1.7 and 4.2.2), alcohols, aldehydes and carboxylic acids were suppressed in the presence of ammonia (Figure 4.32). Furthermore, almost no C_1 oxygenated compounds and no C_1 N-containing products were detected during gas chromatographic analysis. It should be also noted that no oxygenates and no organic nitrogen-containing compounds were detected when FT/NH_3-FT experiments were carried out on unpromoted iron catalysts. The variation of reaction conditions such as temperature, H_2:CO ratio and gas hourly space velocity (GHSV) during FT experiments (chapter 4.2.2), led to different selectivities to alcohols, aldehydes and carboxylic acids. The use of low temperatures and low H_2:CO ratios resulted in increased formation rates of these compounds. When ammonia was added to the synthesis gas feed, similar results could be observed. Here as well, increased selectivities to amines and nitriles could be observed when low temperatures and low H_2:CO ratios were used during the reaction. Therefore, a correlation between the formation of oxygen and nitrogen-containing compounds can be assumed as it was reported by some authors before [6][89][91][111]. Organic nitrogen-containing compounds may be formed from oxygenates such as alcohols, aldehydes or carboxylic acids or their oxygen-containing precursors.

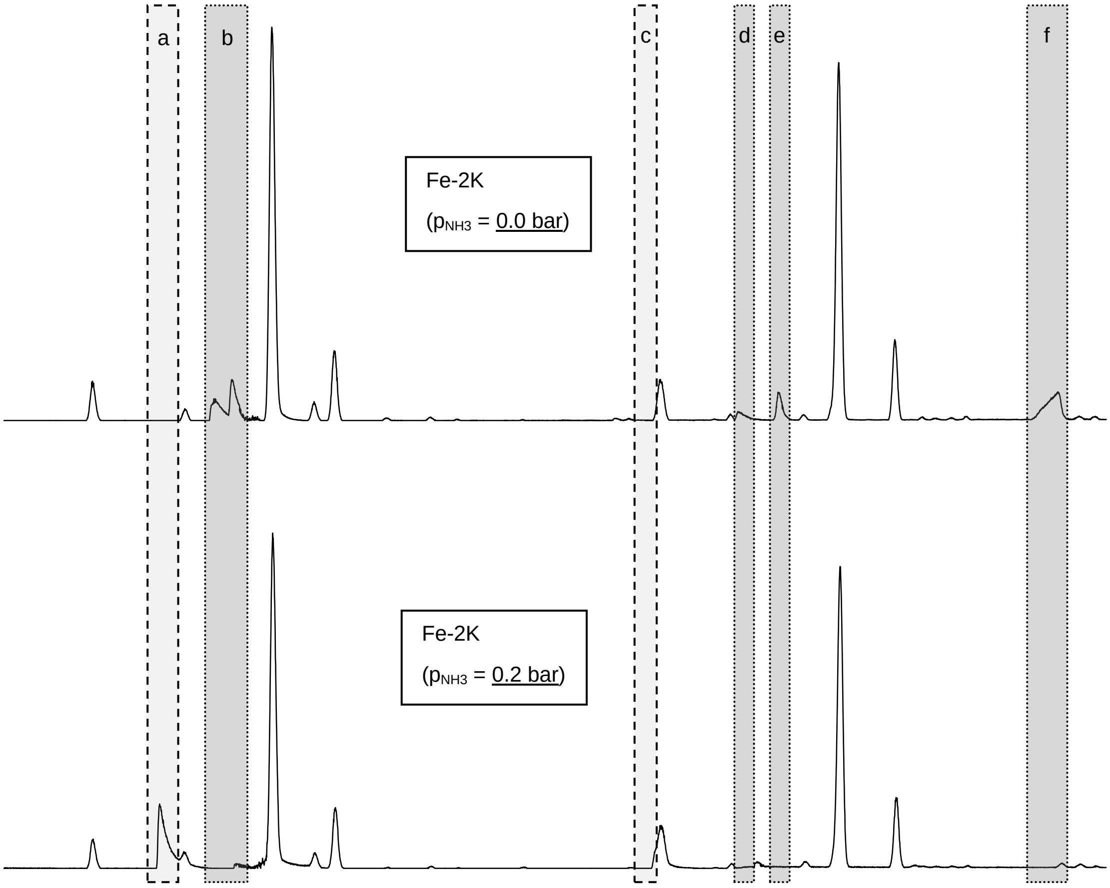

Figure 4.32: Snapshot of two gas chromatograms (no extracted ions, Y-scale: intensity and X-scale: retention time are not displayed) in the lower organic product regions during Fischer-Tropsch reactions on potassium promoted iron catalysts at different ammonia partial pressures ($T_{Reactor}$ = 270 °C, P_{Total} = 4 bar, p_{NH3} = 0.0 - 0.2 bar, GHSV = 1920 h^{-1}, H_2:CO = 2:1). The letters a – f represent: a = acetonitrile, b = ethanol and propanal, c = propanenitrile, d = 1-butanol, e = butanal, f = acetic acid.

Assuming the formation of organic nitrogen-containing compounds via a secondary reaction step from re-adsorbed oxygenates, findings from hydroamination experiments of alcohols with ammonia (chapter 2.5.1) can be used to explain the results from FT/NH_3-FT experiments. According to the reaction mechanism proposed by Jones *et al.* [9], alcohols can adsorb on transition metal surfaces and react further with adsorbed amino groups to yield amines (Figure 2.6). Aldehydes and nitriles can be obtained from this kind of reaction, too. During Fischer-Tropsch experiments on potassium promoted iron catalysts within this work, a mixture of alcohols, aldehydes, carboxylic acids and methyl-ketones was formed. Aldehydes and carboxylic acids may re-adsorb onto the catalyst surface to form a hydroxyl species **(2)** from an acyl intermediate **(1)** via hydrogen addition (Figure 4.33) [14].

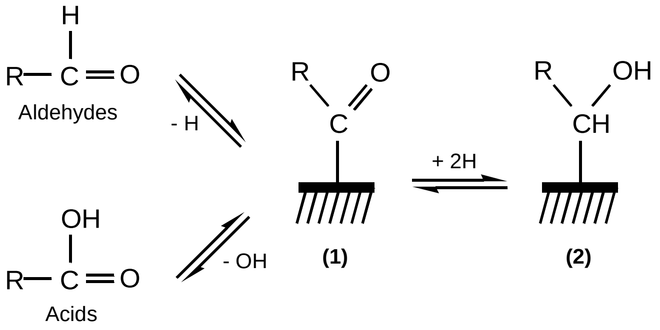

Figure 4.33: Re-adsorption of aldehydes and carboxylic acids and formation of a hydroxyl surface species (adapted from [14]).

Further reaction to amines or nitriles could take place via surface species (**2**) in Figure 4.33 through an alkylidene surface species which may be involved in oxygenate formation as it was proposed by Jones *et al.* [9]. From this the disappearance of aldehydes and carboxylic acids during NH_3-FT experiments could be explained. Cairns [14] reported that re-adsorption of methyl-ketones does not lead to the surface intermediates (**1**) or (**2**) in Figure 4.33. Since the selectivity to methyl-ketones was not altered in the presence of ammonia (Figure 4.19) no formation of nitrogen-containing products could be expected from these compounds. Therefore, a formation route of amines, nitriles and amides via a secondary reaction step cannot be excluded but there are some indications which show evidence for a primary reaction step via oxygen-containing precursors.

During the FT and NH_3-FT experiments on potassium promoted bulk iron catalysts within this work, only little hydrogenation tendencies could be observed. High selectivities to olefins, aldehyde and nitriles were obtained when FT/NH_3-FT experiments were carried out on catalysts Fe-2K and Fe-5K. From that point of view, it appears to be unlikely that acyl intermediate shown in Figure 4.33 get hydrogenated to form surface species (**2**). Despite that oxygenates are very reactive, no statement can be made if 100 mol% of the alcohols, aldehydes or carboxylic acids can re-adsorb onto the catalyst surface to generate nitrogen-containing compounds. During Fischer-Tropsch reactions, the catalyst surface is mainly covered with CO and possible re-adsorption sites could be blocked. Moreover, when potassium as a promoter is added to FT catalysts, secondary reactions such as hydrogenation to paraffins are suppressed [16][35]. This would also reduce the possibility that alcohols, aldehydes and carboxylic acids re-adsorb onto the catalysts surface to generate organic nitrogen-containing compounds.

Based on these results it is questionable if amines, nitriles or amides are only formed via a secondary reaction step. A primary route via oxygen-containing precursors as it was suggested by Gredig *et al.* [91] cannot be excluded and may occur currently with the secondary reaction step. The findings of Gredig *et al.* [91] are based on a postulated reaction mechanism of Baiker *et al.* [92][104] and Vedage *et al.* [93] where it is thought that an aldehyde surface intermediate is involved in the reaction pathway to nitrogen-containing compounds.

Based on the ligand field theory and the spectrochemical series, it was discussed in chapter 4.2.1.7 [127] if ammonia can replace surface hydroxyl groups. From the ethylidene mechanism by Jones *et al.* [9] it is known that after abstraction of a hydroxyl group from the adsorbed alcohol, an amino group is added instead. This reaction step also could take place in a primary reaction step and surface species (**3**) in Figure 4.34 could be formed. Similar to the formation of alcohols (chapter 2.2.2), hydrogen can be added to the amino surface species **(3)** and amines are generated via hydrogen addition in a chain termination step.

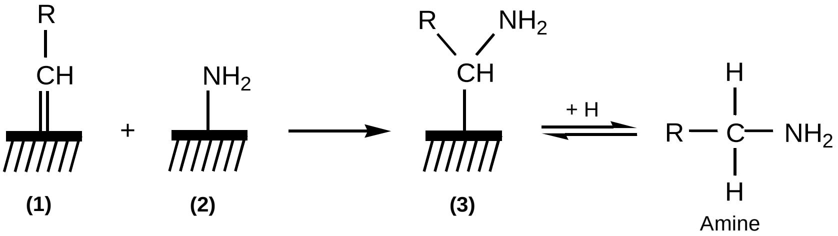

Figure 4.34: Formation of amines from an alkylidene and amino group in a primary synthesis step with chain termination.

From co-feeding experiments with methylamine during Fischer-Tropsch synthesis, it could be shown that amines can adsorb on the catalyst surface to form nitriles [94]. This could explain the presence of nitriles in this work during NH_3-FT experiments. But similar to the ability of alcohols, aldehydes and carboxylic acids to re-adsorb on the catalyst surface [14], this tendency may expected to be low and the large amounts of nitriles which were formed during NH_3-FT experiments cannot be explained.

During the experiments, several indications were found that the density of acyl surface units on the catalyst surface is possibly very high. High contents of aldehydes during the ammonia-free runs were detected which could be formed via the CO insertion mechanism (chapter 2.2.2 and 4.2.1.7). It might be speculated that these acyl intermediates are still present when ammonia was added to the synthesis gas feed since the content of methyl-ketones remained unchanged compared to experiments at $p_{NH3} = 0.0$ bar (Figure 4.19). In this context, large amounts of nitriles were formed during the reaction ($p_{NH3} = 0.2$ bar) and it might be possible that nitriles could be generated via this ‘aldehyde’ precursor as it was postulated in literature [91][92][93][104].

However, three different reaction mechanisms for the formation of nitriles can be hypothesized where nitriles are formed in a chain termination step under the loss of water (Figure 4.35). The reaction mechanisms would be dependent on the degree of hydrogenation of the oxygen-containing precursors on the catalyst surface (Figure 4.35). Moreover, the resulting reaction mechanism would be also dependent on which surface species after the dissociation of ammonia are available. From Figure 2.14 it can be seen that a mixture of ‘NH_2’, ‘NH’ and ‘N’ units is adsorbed on the catalyst surface [74]. However, all the required surface species shown in Figure 4.35, could be dependent on the reaction conditions or the catalytic metal used during the reaction.

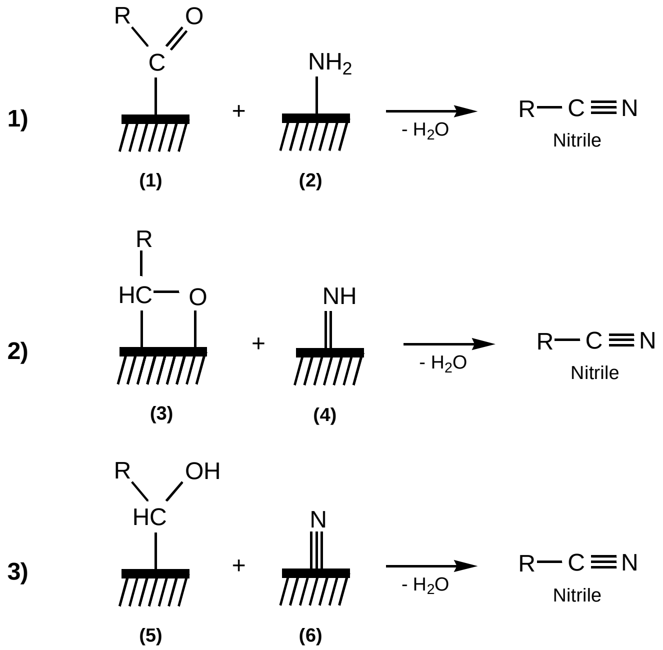

Figure 4.35: Formation of nitriles from different precursors in a primary synthesis step with chain termination and formation of water (reaction pathway 3) is adapted from Sango [111]).

It has been proposed in literature that acyl surface intermediates are involved in the formation of carboxylic acids in the FT synthesis, too [14]. A hydroxyl group is added to an acyl species and carboxylic acids can be obtained (Figure 4.16). Analogous to the formation of amines, the presence of amides (chapter 4.2.1.8) could be explained by the addition of an amino instead of a hydroxyl group to the acyl intermediate (Figure 4.36).

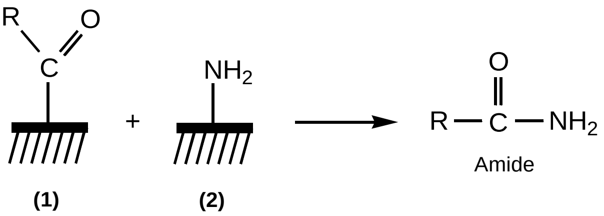

Figure 4.36: Formation of amides from an acyl intermediate and amino group in a primary synthesis step with chain termination (adapted from [111]).

It may be speculated that the reaction mechanisms are influenced by the reaction conditions as it was shown in this work. The findings in chapter 4.2.2 can be explained by the variation of the required oxygen-containing precursors since different reaction parameters such as temperature, H_2:CO ratio and gas hourly space velocities (GHSV) were applied.

The use of other metal catalysts than iron could influence the selectivity to amines, nitriles or amides. Before the addition of ammonia during FT experiments on bulk cobalt catalysts, mainly the formation of alcohols was observed. The alcohols disappeared in the presence of ammonia in the synthesis gas feed (Table 4.14) and the formation of amines could be detected instead. In contrast to NH_3-FT experiments on potassium promoted iron catalysts, no evidence for the formation of nitriles could be observed. High hydrogenation tendencies of cobalt catalysts were reported in this context before [31] and this could also the influence selectivities to organic nitrogen-containing compounds such as amines. The use of slurry instead of fixed-bed reactors could affect the selectivity to amines or nitriles. In this context, Sango [111] and Sango *et al.* [12] mainly found amines within the organic nitrogen-containing product during their NH_3-FT experiments.

From the results in this work, it cannot be stated exclusively if the formation of organic nitrogen-containing compounds takes place via a primary or secondary reaction mechanism and it cannot be excluded that both mechanisms are involved.

5 Summary

Within the present work, the influence of ammonia on the catalytic activity and product distribution during Fischer-Tropsch experiments on bulk unpromoted/potassium promoted iron and unpromoted cobalt catalysts was investigated.

The catalyst materials have been prepared and characterized by means of AAS, TPR, XRD and TEM. All FT/NH_3-FT experiments were conducted in a fixed-bed reactor and gas chromatographic analysis of gaseous samples was performed *online* using 6-way valves. Different detectors and columns ensured identification and quantification of organic products (GC-MS and GC-FID). Methane and reactants such as carbon monoxide, hydrogen and ammonia were analyzed using a GC-TCD. Selected liquid phase samples were analyzed *offline* by means of two-dimensional gas chromatography (GCxGC-TOF) in order to achieve a better separation of the complex product spectra for the identification of nitrogen-containing compounds.

During Fischer-Tropsch experiments on unpromoted iron catalysts in the absence of ammonia (p_{NH3} = 0.0 bar), mainly paraffins were synthesized and only small concentrations of olefins and oxygenated compounds were detected within the organic products. When bulk cobalt catalysts were used, mainly the formation of hydrogenated products such as paraffins was observed, and additionally alcohols were found in the organic product. A different catalytic behaviour was observed when FT reactions (at p_{NH3} = 0.0 bar) were carried out on potassium promoted bulk iron catalysts. Due to the presence of potassium in the iron catalysts, lower CO and H_2 conversion and high formation rates of olefins and CO_2 were observed. The selectivity towards methane or branched hydrocarbons declined and a higher chain growth probability was found. Oxygenated compounds such as alcohols, carboxylic acids, methyl-ketones and in large amounts, aldehydes were formed. These effects are related to potassium which can interact with the 3d band of iron and induce an electron donor effect to the catalyst.

When ammonia (p_{NH3} = 0.2 bar) was added during Fischer-Tropsch synthesis, a different catalytic behaviour of promoted and unpromoted metal catalysts was observed. On potassium-free iron catalysts, increased olefin and CO_2 selectivities as well as higher chain growth probabilities were found, whereas selectivity to methane and the degree of branching declined. Additionally, the conversions of CO and H_2 declined with additional ammonia in the synthesis gas feed. With the exception of CO_2 formation, similar results were obtained when FT/NH_3-experiments were carried out on bulk cobalt catalysts. In contrast to that, the addition of ammonia had no influence on most of the conventional FT products (e.g. olefins, methane and branched hydrocarbons) in case of potassium promoted iron catalysts. Furthermore, chain growth probabilities and conversion of CO and H_2 were not affected with additional ammonia in the synthesis gas feed. The selectivity to CO_2 increased only slightly and this gain was less pronounced with increasing potassium content in the iron catalyst.

The different catalytic performance of unpromoted and potassium promoted metal catalysts during NH_3-FT experiments could be explained by the adsorption properties of ammonia or by side reactions such as the decomposition of ammonia to N_2 and H_2. It was hypothesized that ammonia or surface bonded nitrogen atoms could act as ‘surface nitrides’ and induce an electron donor effect on the catalyst. Potassium in addition, can decrease the concentration of adsorbed ammonia or atomic nitrogen on the catalyst surface. In this context, ammonia conversions during NH_3-FT experiments on unpromoted iron catalysts were found to be four times higher than compared to reactions on potassium promoted iron catalysts. As a consequence, potassium promoted iron catalysts are mostly influenced by potassium itself as a promoter for the Fischer-Tropsch reaction and changes of the catalytic performance in the presence of ammonia are less pronounced.

When ammonia was added (p_{NH3} = 0.2 bar) during the FT experiments on potassium promoted iron catalysts, oxygenated compounds such as alcohols, aldehydes and carboxylic acids disappeared and nitrogen-containing compounds were formed. From *online* gas chromatographic analysis and the use of a mass spectrometer (GC-MS), the formation of terminal aliphatic amines and large amounts of nitriles was observed. While no evidence for the formation of methylamine, hydrogen cyanide or branched amines could be detected, nitriles with chain length to C_{17} were synthesized. *Offline* two-dimensional gas chromatography coupled with a mass spectrometer (GCxGC-TOF) ensured the presence of linear amides up to carbon numbers C_6 within selected liquid phase samples. While almost no organic oxygen- and no nitrogen-containing products were detected using unpromoted iron catalysts, similar result were obtained during Fischer-Tropsch experiments on cobalt catalysts.

Here, alcohols, which were formed before the addition of ammonia, disappeared in the presence of ammonia and amines were detected instead. During FT/NH_3-FT experiments on potassium promoted iron catalysts, process parameters such as temperature and the synthesis gas composition were varied at different ammonia partial pressures (p_{NH3} = 0.0 and 0.2 bar). During these tests, it was possible to increase or decrease the selectivities towards organic oxygen- and nitrogen-containing compounds in the same manner. In this context, low temperatures and hydrogen-poor synthesis gas seem to be beneficial for the production of these compounds. Moreover, the ratios between hydrogenated/dehydrogenated products (alcohol/aldehyde and amine/nitrile) could be changed during these experiments. Here, at low temperatures and high H_2:CO ratios, the formation of alcohols (p_{NH3} = 0.0 bar) or amines (p_{NH3} = 0.2 bar) is preferred.

Based on these results, a correlation between the formation of organic oxygen- and nitrogen-containing compounds was hypothesized. Since alcohols, aldehydes and carboxylic acids can re-adsorb onto metal surfaces, the organic nitrogen-containing products could be generated analogous to hydroamination experiments via a secondary reaction step from oxygenates. Another possibility is that amines, nitriles and amides are formed via a primary reaction step via oxygen-containing precursors. However, no differentiation between these two reactions mechanisms could be made. Although some indications for a primary synthesis step were found, it is possible that both reaction mechanisms are involved in the formation of organic nitrogen-containing compounds. Moreover, the use of different reaction conditions and catalysts could have an influence on the current reaction mechanism.

From these results, it appears that ammonia in low concentrations does not act as a catalyst poison on iron catalysts and more research could be invested on the ammonia co-feeding during Fischer-Tropsch synthesis. In order to increase selectivities towards nitrogen-containing compounds, higher pressures during the FT/NH_3-FT reaction could be applied. The use of catalysts which can produce large amounts of alcohols, aldehydes or carboxylic acids could lead to higher selectivities to organic nitrogen-containing compounds.

Zusammenfassung

In der vorliegenden Arbeit ist der Einfluss von Ammoniak auf die katalytische Aktivität und Produktverteilung von kaliumhaltigen und undotierten Eisen- und Kobaltkatalysatoren während der Fischer-Tropsch Synthese untersucht worden.

Die hergestellten Katalysatormaterialien sind mittels AAS, TPR, XRD und TEM untersucht und die FT/NH_3-FT Experimente in einem Festbettreaktor durchgeführt worden. Eine gaschromatographische Analyse der Edukte und Produkte erfolgte *online* mit Hilfe von 6-Wege-Ventilen. Verschiedene Detekortypen und Säulenmaterialien kamen zum Einsatz, um organische Produkte (GC-MS und GC-FID) zu identifizieren und zu quantifizieren. Methan und Edukte wie Kohlenmonoxid, Wasserstoff und Ammoniak wuden mit einem GC-TCD analysiert. Ausgewählte Flüssigproben wurden *offline* mittels zwei-dimensionaler Gaschromatographie (GCxGC-TOF) untersucht, um eine genauere Analyse der komplexen Fischer-Tropsch Produktspektren zu gewährleisten.

Während der Fischer-Tropsch Experimente an undotieren Eisenkatalysatoren in der Abwesenheit von Ammoniak (p_{NH3} = 0.0 bar) wurden hauptsächlich Paraffine und nur geringe Mengen an Olefinen und sauerstoffhaltigen Verbindungen synthetisiert. An Kobaltkatalysatoren wurden neben Paraffinen als Hauptprodukte, die Bildung von Alkoholen beobachtet. Ein unterschiedliches katalytisches Verhalten wurde beobachtet, wenn die FT Experimente (at p_{NH3} = 0.0 bar) an kaliumhaltigen Eisenkatalysatoren durchgeführt worden sind. Die Zugabe von Kalium zu dem Eisenkatalysator resultierte in geringeren CO- sowie H_2-Umsätzen und hohe Olefin- als auch Kohlenstoffdioxidselektivitäten wurden erziehlt. Die Selektivitäten zu Methan oder verzweigten Kohlenwasserstoffen verringerte sich und erhöhte Kettenwachstumswahrscheinlichkeiten wurden beobachtet. Darüber hinaus sind sauerstoffhaltige Verbindungen wie Alkohole, Carbonsäuren, Methylketone und Aldehyde synthetisiert worden. Die Beobachtungen lassen sich mit der Anwesenheit von Kalium erklären, welches mit dem 3d-Band des Eisen wechselwirken und einen Elektronen-Donor-Effekt ausüben kann.

Durch die Zugabe von Ammoniak (p_{NH3} = 0.2 bar) während der Fischer-Tropsch Synthese konnte ein unterschiedliches katalytisches Verhalten der undotierten und dotierten

Metallkatalysatoren beobachtet werden. Eisenkatalysatoren ohne Kalium zeigten geringere CO- und H_2-Umsätze sowie erhöhte Bildungsraten an Olefinen und CO_2. Während die Kettenwachstumswahrscheinlichkeit anstieg, wurden geringere Selektivitäten zu Methan und verzweigten Kohlenwasserstoffen beobachtet. Mit der Ausnahme der Kohlendioxidbildung wurden ähnliche Ergebnisse während FT/NH_3-FT Experimenten an Kobaltkatalysatoren erziehlt. Im Gegensatz zu den beschriebenen Resultaten hat die Zugabe von Ammoniak während der FT Synthese an kaliumhaltigen Eisenkatalysatoren keinen Effekt auf die Selektivität der meisten konventionellen Fischer-Tropsch Produkte wie Olefine, Methan und die verzweigten Kohlenwasserstoffe. Darüber hinaus wurden Kettenwachstumswahrscheinlichkeiten sowie die Umsätze an Kohlenmonoxid und Wasserstoff nicht beeinflusst. Die Selektivität zu CO_2 erhöhte sich nur geringfügig und diese Zunahme war weniger ausgeprägt je mehr Kalium in dem Eisenkatalysator eingesetzt worden ist.

Die Unterschiede in dem katalytischen Verhalten zwischen undotierten und mit Kalium dotierten Metallkatalysatoren können durch ein unterschiedliches Adsorptionsverhalten des Ammoniaks oder durch Nebenreaktionen wie der Zersetzung von Ammoniak zu N_2 und H_2 erklärt werden. Es wird vermutet, dass Ammoniak oder oberflächengebundene Stickstoffatome als „Oberflächennitride“ agieren und einen Elektronen-Donor-Effekt auf den Katalysator ausüben könnten. Zusätzliches Kalium in dem Katalysator kann diesbezüglich die Konzentration von adsorbierten Ammoniak oder atomarem Stickstoff auf der Katalysatoroberfläche herabsetzen. In diesem Zusammenhang sank der Ammoniakumsatz während der NH_3-FT Experimente an kaliumhaltigen Eisenkatalysatoren um ein Viertel im Vergleich zu den Experimenten an undotierten Eisenkatalysatoren. Daraus lässt sich schliessen, dass das katalytische Verhalten kaliumhaltiger Eisenkatalysatoren während der Fischer-Tropsch Experimente überwiegend durch das Alkalimetall als Promoter beeinflusst wird, und der Effekt von Ammoniak an diesen Katalysatoren geringer ist.

Sauerstoffhaltige Verbindungen wie Alkohole, Aldehyde und Carbonsäuren konnten in der Anwesenheit von Ammoniak (p_{NH3} = 0.2 bar) während der Fischer-Tropsch Synthese an kaliumhaltigen Eisenkatalysatoren nicht detektiert werden. Stattdessen wurde die Bildung von organischen stickstoffhaltigen Verbindundungen beobachtet. Mittels eines Massenspektrometers (GC-MS) konnte die Anwesenheit endständiger, aliphatischer Amine und

Nitrile nachgewiesen werden. Mit Hilfe von zwei-dimensionaler Gaschromatographie und eines weiteren Massenspektrometers (GCxGC-TOF) wurden Nitrile mit einer Kettenlänge bis C_{17} und lineare Amide in der Flüssigphase der FT Produkte detektiert. Während mit undotierten Eisenkatalysatoren keine organischen sauerstoff- und stickstoffhaltigen Produkte synthesisiert wurden, ist der Anteil der Alkohole während der Experimente an undotierten Kobaltkatalysatoren in Anwesenheit von Ammoniak gesunken, und es wurde die Bildung von Aminen beobachtet. Mittels unterschiedlicher Reaktionstemperaturen und H_2:CO Verhältnisse konnte während der FT/NH_3-FT Synthese an kaliumhaltigen Eisenkatalysatoren die Selektivität zu organischen sauerstoff- und stickstoffhaltigen Verbindungen in gleichem Maße verändert werden. Niedrige Reaktionstemperaturen und H_2:CO Verhältnisse begünstigten die Bildung dieser Verbindungen. Darüber hinaus konnte das Verhältins zwischen Alkohol/Aldehyd und Amin/Nitril mit Hilfe von niedrigen Reaktionstemperaturen und wasserstoffreichem Synthesegas erhöht werden.

Aufgrund dieser Ergebnisse wird ein Zusammenhang zwischen der Bildung von organischen sauerstoff- und stickstoffhaltigen Verbdindungen vermutet. Da Alkohole, Aldehyde und Carbonsäuren auf der Katalysatoroberfläche readsorbieren können, liegt es Nahe, dass stickstoffhaltige Verbindungen analog zu Hydroaminierungsreaktionen in einer Sekundärreaktion gebildet werden könnten. Eine weitere Möglichkeit stellt die Synthese dieser Komponenten in einem primären Reaktionsschritt über sauerstoffhaltige Intermediate dar. Anhand der Versuchsergebnisse sind Hinweise auf einen primären Reaktionsschritt gefunden und diskutiert worden, aber die Möglichkeit, dass beide Reaktionsmechanismen ablaufen, ist nicht auszuschliessen. Vielmehr wäre es möglich, dass die Wahl der Reaktionsbedingungen und des Katalysators einen Einfluss auf den jeweiligen Reaktionsmechanismus haben.

Ammoniak scheint in geringen Konzentrationen kein Katalysatorgift für Eisenkatalysatoren zu sein und die Forschung auf dem Gebiet der Ammoniakzugabe während der FT Synthese könnte intensiviert werden. Durch die Wahl von hohen Reaktionsdrücken während der FT Synthese oder Katalysatoren, die große Mengen an Oxygenaten bilden, wäre es möglich den Anteil an Aminen, Nitrilen oder Amiden in den Fischer-Tropsch Produkten zu erhöhen.

6 References

[1] Kühnle, A., Fischer-Tropsch-Wachse Synthese, Struktur, Eigenschaften und Anwendung, *Fett. Wiss. Technol.* **1982**, 84, 156 - 162.

[2] Dry, M., The Fischer-Tropsch process: 1950 – 2000, *Catal. Today* **2002**, 71, 227 - 241.

[3] Claeys, M., Selektivität, Elementarschritte und kinetische Modellierung bei der Fischer-Tropsch-Synthese, PhD thesis, Universität Fridericiana Karlsruhe (**1997**).

[4] Schulz, H., Short history and present trends of Fischer-Tropsch synthesis, *Appl. Catal. A: Gen.* **1999**, 186, 3 - 12.

[5] Hayes, K. S., Industrial processes for manufacturing amines, *Appl. Catal. A: Gen.* **2001**, 221, 187 - 195.

[6] Rausch, A., C-N-Kopplungen an heterogenen kobalthaltigen Katalysatoren, PhD thesis, Carl von Ossietzky Universität Oldenburg (**2008**).

[7] McKinney, R., J, DeVito, S. C., in: Kirk-Othmer Encyclopaedia of Chemical Technology, 5th Edition, John Wiley & Sons, New Jersey, **2006**.

[8] Reck, R. A., Nitrogen derivatives (amides, diamides, nitriles, primary amines and oxides), *J. Am. Oil Chemists´Soc.* **1979**, 56, 796 - 801.

[9] Jones, J. R., Sharratt, A. P., Jackson, S. D., Gladden, L. F., Webb, G., in: Allen, J. (ed.), Synthesis and applications of isotopically labeled compounds, Wiley & Sons, Vol. 5, New York, **1995**.

[10] Rottig, W., Catalytic hydrogenation of carbon monoxide with addition of ammonia or methylamine, U.S. Patent 2821537, **1958**.

[11] Kölbel., H., Trapper, J., Aliphatic amines from carbon monoxide, steam and ammonia, *Angew. Chem. Internat. Edit.* **1966**, 5, 843 - 844.

[12] Claeys, M., van Steen, E., Roessner, F., Sango, T., Process for the production of nitrogen or phosphorous containing compounds from synthesis gas, U.S. Patent 2011/0092728 A1, **2011**.

[13] Bartholomew, C. H., Mechanisms of catalyst deactivation, *Appl. Catal. A: Gen.* **2001**, 17 - 60.

[14] Cairns, P., Oxygenates in Iron Fischer-Tropsch Synthesis: is copper a selectivity promoter?, PhD thesis, University of Cape Town (**2008**).

[15] Dry, M. E., in: Anderson, J. R., Boudart, M. (eds.), Catalysis Science and Technology, Vol. 1, Springer Verlag, New York, **1981**, p. 159 - 255.

[16] Claeys, M., van Steen, E., in: Steynberg, A. P., Dry, M. E. (eds.), Fischer-Tropsch Technology, *Stud. Surf. Sci. Catal.*, Vol. 152, Elsevier, Amsterdam, **2004**, pp. 601.

[17] Dry, M. E., in: Steynberg, A. P., Dry, M. E. (ed.), Fischer-Tropsch Technology, *Stud. Surf. Sci. Catal.*, Vol. 152, Elsevier, Amsterdam, **2004**, pp. 533.

[18] Dry, M., Practical and theoretical aspects of the catalytic Fischer-Tropsch process, *Appl. Catal. A: Gen.* **1996**, 138, 319 - 344.

[19] Lögdberg, S., Tristantini, D., Borg, O., Ilver, L., Gevert, B., Järas, S., Blekkan, E. A., Holmen, A., Hydrocarbon production via Fischer-Tropsch synthesis from H_2-poor syngas over different Fe-Co/γ-Al_2O_3 bimetallic catalysts, *Appl. Catal. B: Environ.* **2009**, 89, 167 - 182.

[20] van der Laan, G. P., Beenackers, A. A. C. M., Intrinsic kinetics of the gas-solid Fischer-Tropsch and water gas shift reactions over a precipitated iron catalyst, *Appl. Catal. A: Gen.* **2000**, 193, 39 - 53.

[21] Davis, B. H., Fischer-Tropsch synthesis: current mechanism and futuristic needs, *Fuel Process. Technol.* **2001**, 71, 157 - 166.

[22] Newsome, D. S., The water-gas shift reaction, *Catal. Rev.-Sci. Eng.* **1980**, 21, 275 - 318.

[23] Mabaso, E. I., Nanosized iron crystallites for Fischer-Tropsch synthesis, PhD thesis, University of Cape Town (**2005**).

[24] Kaminsky, M. P., Winograd, N., Geoffroy, G. L., Vannice, M. A., Direct SIMS observation of methylidene, methylene, and methyl intermediates on a Ni(111) methanation catalyst, *J. Am. Chem. Soc.* **1986**, 108, 1315 - 1316.

[25] Pichler, H., Schulz, H., Neuere Erkenntnisse auf dem Gebiet der Synthese von Kohlenwasserstoffen aus CO und H_2, *Chem.-Ing. Techn.* **1970**, 42, 1162.

[26] Maitlis, P. M., Quyoum, R., Long, H. C., Turner, M. L., Towards a chemical understanding of the Fischer-Tropsch reaction: alkene formation, *Appl. Catal. A: Gen.* **1999**, 186, 363 - 374.

[27] Anderson, R. B., Hofer, L. J. E., Storch, H. H., Der Reaktionsmechanismus der Fischer-Tropsch-Synthese, *Chemie-Ing.-Techn.* **1958**, 9, 560 - 566.

[28] Anderson, K. G., Ekerdt, J. G., Study of Fischer-Tropsch synthesis over Fe/SiO_2: Effect of diethylamine on hydrocarbon and alcohol production, *J. Catal.* **1985**, 95, 602.

[29] Dry, M. E., The Fischer-Tropsch process – commercial aspects, *Catal. Today* **1990**, 6, pp. 183.

[30] Johnston, P., Joyner, R., in: Studies in Surface Science and Catalysis, Vol. 75, Elsevier, Budapest, **1993**., pp. 165.

[31] Dry, M. E., in: Steynberg, A. P., Dry, M. E. (ed.), Fischer-Tropsch Technology, *Stud. Surf. Sci. Catal.*, Vol. 152, Elsevier, Amsterdam, **2004**, pp. 196.

[32] Anderson, R. B., The Fischer-Tropsch Synthesis, Academic Press, New York, **1984**, pp. 26.

[33] Huff, G., Satterfield, C., Evidence for two chain growth probabilities on iron catalysts in the Fischer-Tropsch synthesis, *J. Catal.* **1984**, 85, 370 - 379.

[34] Tau, L., Dabbagh, H., Bao, S., Davis, B., Fischer-Tropsch synthesis. Evidence for two chain growth mechanisms, *Catal. Lett.* **1990**, 7, 127 - 140.

[35] Schulz, H., Claeys, M., Reactions of α-olefins of different chain length added during Fischer-Tropsch synthesis on a cobalt catalyst in a slurry reactor, *Appl. Catal. A: Gen.* **1999**, 186, 71 - 90.

[36] Iglesia, E., Reyes, S. C., Madon, R. J., Soled, S. L., Selectivity control and catalyst design in the Fischer-Tropsch synthesis: sites, pellets, and reactors, *Adv. Catal.* **1993**, 39, 221 - 302.

[37] Schulz, H., Claeys, M., Kinetic modeling of Fischer-Tropsch product distributions, *Appl. Catal. A: Gen.* **1999**, 186, 91 - 107.

[38] Vannice, M. A., The catalytic synthesis of hydrocarbons from H_2/CO mixtures over the group VIII metals, *J. Catal.* **1977**, 50, pp. 228.

[39] Bukur, D. B., Mukesh, D., Patel, S. A., Promoter effects on precipitated iron catalysts for Fischer-Tropsch synthesis, *Ind. Eng. Chem. Res.* **1990**, 29, 194.

[40] Raje, A. P., O´Brian, R. J., Davis, B. H., Effect of potassium promotion on iron-based catalysts for Fischer-Tropsch synthesis, *J. Catal.* **1998**, 180, 36 - 43.

[41] van Steen, E., Claeys, M., Fischer-Tropsch catalysts for the biomass-to-liquid (BTL)-process, *Chem. Eng. Technol.* **2008**, 31, 655- 666.

[42] De Klerk, A., in: Fischer-Tropsch Refining, Wiley-VCH Verlag & Co. KgaA, Weinheim, **2011**.

[43] Moulijn, J. A., van Diepen, A. E., Kapteijn, F., Catalysts deactivation: Is it predictable? What to do?, *Appl. Catal. A: Gen.* **2001**, 212, 3 - 16.

[44] Li, S., Krishnamoorthy, S., Li, A., Meitzner, G. D., Iglesia, E., Promoted iron-based catalysts for the Fischer-Tropsch synthesis: design, synthesis, site densities and catalytic properties, *J. Catal.* **2002**, 206, 202 - 217.

[45] Mansker, L. D., Jin, Y., Bukur, D. B., Datye, A. K., Characterization of slurry phase iron catalysts for Fischer-Tropsch synthesis, *Appl. Catal. A: Gen.* **1999**, 186, 277 - 296.

[46] Hilmen, A. M., Schanke, D., Hanssen, K. F., Holmen, A., Study of the effect of water on alumina supported cobalt Fischer-Tropsch catalysts, *Appl. Catal. A: Gen.* **1999**, 186, 169 - 188.

[47] Iglesia, E., Design, synthesis and use of cobalt-based Fischer-Tropsch synthesis catalysts, *Appl. Catal.* **1997**, 161, 59.

[48] van Steen, E., Claeys, M., Dry, M. E., van de Loosdrecht, J., Viljoen, E. L., Visagie, J. L., Stability of nano-crystals: Thermodynamics analysis of oxidation and re-reduction of cobalt in water/hydrogen mixtures, *J. Phys. Chem. B* **2005**, 109, 3575.

[49] Corbin, D. C., Schwarz, S., Sonnichsen, G. C., Methylamines synthesis: A review, *Catal. Today* **1997**, 37, 71 - 102.

[50] Turcotte, M. G., Johnson, T. A., in: Kroschwitz, I., Hoowe-Grant, M., Othmer, D. F. (eds.), Kirk-Othmer Encyclopedia of Chemical Technology 4th Edition, 2, John Wiley & Sons, New York, **1992**, 369 - 386.

[51] Chi, Y., Zhou, Y. G., Zhang, X., Highly enantioselective reductive amination of simple aryl ketones catalyzed by Ir-f-binaphane in the presence of titanium(IV) isopropoxide and iodine, *J. Org. Chem.* **2003**, 68, 4120 - 4122.

[52] Feng, S. G., Templeton, J. L., Stepwise reduction of acetonitrile in [Tp'(CO)(PhCCMe)W($NCCH_3$)][BF_4], *J. Am. Chem. Soc.* **1989**, 111, 6477 - 6478.

[53] Kazansky, V. B., Zaitsev, A. V., Borokov, V. Y., Lapidus, A., Infrared diffuse reflectance study of alkali promoted iron/alumina and cobalt/alumina Fischer-Tropsch catalysts prepared by decomposition of carbonyls, *Appl. Catal.* **1988**, 40, 17.

[54] Storch, H. H., Golumbic, N., Anderson, R. B., The Fischer-Tropsch and related Syntheses, John Wiley & Sons, New York, **1951**.

[55] Bini, L., Müller, C., Vogt, D., Mechanistic studies on hydrocyanation reactions, *ChemCatChem* **2010**, 2, 590 - 608.

[56] Grasselli, R. K., Selective oxidation and ammoxidation of olefins by heterogeneous catalysis, *J. Chem. Educ.* **1986**, 63, 216 - 221.

[57] Grasselli, R. K., *Advances and future trends in selective oxidation and ammoxidation catalysis* **1999**, 49, 141 - 153.

[58] Hull, D. C., Preparation of aliphatic nitriles, U.S. Patent 2,732,397, **1956**.

[59] Hagemeyer, H. J., Holmes, J. D., Preparation of nitriles, U.S. Patent 3,979,432, **1976**.

[60] Schulz, H., Rao, B. R., Elstner, M., ^{14}C-Studien zum Reaktionsmechanismus der Fischer-Tropsch-Synthese, *Erdöl und Kohle* **1970**, 22, pp. 651.

[61] Schulz, H., Molekülaufbau bei der Fischer-Tropsch-Synthese. Reaktionsschritte des Molekülaufbaus durch katalytische Umsetzung von Kohlenmonoxid und Wasserstoff, *Erdöl und Kohle* **1977**, Vol. 22, pp. 651.

[62] Blyholder, G., Lawless, M., Hydrogen-assisted dissociation of CO on a catalyst surface, *Langmuir* **1991**, 7, 140 - 141.

[63] Dry, M. E., Oosthuizen, G. J., The correlation between catalyst surface basicity and hydrocarbon selectivity in the Fischer-Tropsch synthesis, *J. Catal.* **1968**, 11, 18 - 24.

[64] Luo, M., Davis, B. H., Fischer-Tropsch synthesis: activation of low-alpha potassium promoted iron catalysts, *Fuel Process. Technol.* **2003**, 83, 49 - 65.

[65] Sewell, G., O´Connor, C., van Steen, E., Reductive amination of ethanol with silica-supported cobalt and nickel catalysts, *Appl. Catal. A.: Gen.* **1995**, 125, 99 - 112.

[66] Gardner, D. A., Clark, R. T., Catalytic process for preparing ethyl amines, U.S. Patent 4,255,357, **1981**.

[67] Moorthy, J. N., Singhal, N., Facile and highly selective conversion of nitriles to amides via indirect acid-catalyzed hydration using TFA or AcOH-H_2SO_4, *J. Org. Chem.* **2005**, 70, 1926 - 1929.

[68] Yamaguchi, K., Matsushita, M., Mizuno, N, Efficient hydration of nitriles to amides on water, catalyzed by ruthenium hydroxide supported on alumina, *Angew. Chem.* **2004**, 116, 1602 - 1606.

[69] Boudart, M., Kinetics and mechanism of ammonia synthesis, *Catal. Rev. - Sci. Eng.* **1981**, 23, 1 - 15.

[70] Raróg, W., Kowalczyk, Z., Sentek, J., Skladanowski, D., Szmigiel, D., Zieliñski, Decomposition of ammonia over potassium promoted ruthenium catalyst supported on carbon, *Appl. Catal. A: Gen.* **2001**, 208, 213 - 216.

[71] Liu, W., Tsong, T. T., Direct observation of reaction intermediates in catalytic synthesis of ammonia, *Surf. Sci.* **1986**, 165, 26 - 30.

[72] Strongin, D. R., Somorjai, G. A., The effects of potassium on ammonia synthesis over iron single-crystal surfaces, *J. Catal.* **1988**, 109, 51 - 60.

[73] Choudhary, T. V., Sivadinarayana, C., Goodman, D. W., Catalytic ammonia decomposition: CO_x-free hydrogen production for fuel cell applications, *Catal. Lett.* **2001**, 72, 197 - 201.

[74] Fastrup, B., Temperature programmed adsorption and desorption of nitrogen on iron ammonia synthesis catalysts, and consequences for the microkinetics analysis of NH_3 synthesis, *Top. Catal. 1* **1994**, 273 - 283.

[75] Tsai, W., Weinberg, W. H., Steady-state decomposition of ammonia on the Ru(001) surface, *J. Phys. Chem.* **1987**, 91, 5302 - 5307.

[76] Kielbasa, K., Pelka, R., Arabczyk, W., Studies of the kinetics of ammonia decomposition on promoted nanocrystalline iron using gas phases of different nitriding degree, *J. Phys. Chem. A* **2010**, 114, 4531 - 4534.

[77] Strongin, D., Mowlem, J., A NEXAFS study on the adsorption of ammonia on clean and potassium-promoted iron, *Surf. Sci. Lett.* **1991**, 247, 209 - 214.

[78] Yin, S. F., Xu, B. Q., Zhou, X. P., Au, C. T., A mini-review on ammonia decomposition catalysts for on-site generation of hydrogen for fuel cell applications, *Appl. Catal. A: Gen.* **2004**, 277, 1 - 9.

[79] Lendzion-Bielun, Z., Pelka, R., Arabczyk, W., Study of the kinetics of ammonia synthesis and decomposition on iron and cobalt catalysts, *Catal. Lett.* **2009**, 129, 119 - 123.

[80] Yin, S. F., Zhang, Q. H., Xu, B. Q., Zhu, W. X., Ng, C. F, Au, C. T., Investigation on the catalysis of CO_x-free hydrogen generation from ammonia, *J. Catal.* **2004**, 224, 384 - 396.

[81] Grunze, M., Golze, M., Driscoll, R. K., Dowben, P. A., Ammonia adsorption and decomposition on a Ni(110) surface, *J. Vac. Sci. Technol.* **1981**, 18, 611 - 615.

[82] Gundry, P. M., Haber, J., Tompkins, F. C., Surface potential measurements on nickel and iron films during the chemisorption of ammonia, nitrogen and hydrogen, *J. Catal.* **1962**, 363 - 371.

[83] Grabke, H. J., Reaktionen von Ammoniak, Stickstoff und Wasserstoff an der Oberfläche von Eisen I. Zur Kinetik der Nitrierung von Eisen mit NH_3-H_2-Gemischen und der Denitrierung, *Ber. Bunsen. Phys. Chem.* **1968**, 72, 533 - 541.

[84] Arabczyk, W., Zamlynny, J., Study of the ammonia decomposition over iron catalysts, *Catal. Lett.* **1999**, 60, 167 - 171.

[85] Löffler, D. G., Schmidt, L. D., Kinetics of NH_3 decomposition on iron at high temperatures, *J. Catal.* **1976**, 44, 244 - 258.

[86] Pommersheim, J. M., Coull, J., Reactions of monoehtylamine over porous copper in a closed recycling system, *AIChE Journal* **1971**, 17, 1075 - 1080.

[87] Freese, U., Mechanistische Aspekte zur heterogen katalysisierten Hydroaminierung von C_2 - Alkoholen, PhD thesis, Carl von Ossietzky Universität Oldenburg (**2001**).

[88] Knifton, J. F., Lin, J. J., Storm, D. A., Wong, S. F., New synthesis gas chemistry, *Catal. Today* **1993**, 18, 355 – 384.

[89] Kölbel, H., Abdulahad, I., Kanowski, S., Ralek, M., Formation of terminal secondary and tertiary alkylamines by single-step synthesis from carbon monoxide, steam and monomethylamine and dimethylamine, respectively, *React. Kinet. Catal. L.* **1974**, 1, 267 - 270.

[90] Gredig, S. V., Koeppel, R. A., Baiker, A., Synthesis of methylamines from CO_2, H_2 and NH_3. Catalytic behavior of various metal-alumina catalysts, *Appl. Catal. A: Gen.* **1997**, 162, 249 - 260.

[91] Gredig, S. V., Koeppel, R. A., Baiker, A., Comparative study of synthesis of methylamines from carbon oxides and ammonia over Cu/Al_2O_3, *Catal. Today* **1996**, 29, 339 - 342.

[92] Baiker, A., Caprez, W., Holstein, W. L., Catalytic amination of aliphatic alcohols in the gas and liquid phases: Kinetics and reaction pathway, *Ind. Eng. Chem. Prod. Res. Dev.* **1983**, 22, 217 - 225.

[93] Vedage, G. A., Herman, R. G., Klier, K., Chemical trapping of surface intermediates in methanol synthesis, *J. Catal.* **1985**, 95, 423 - 434.

[94] Olivé, G., Olivé, S., Process for preparing acetonitrile, U.S. Patent 4,058,548, **1977**.

[95] Auvil, S. R., Penquite, C. R., Process for preparing acetonitrile, U.S. Patent 4,272,452, **1981**.

[96] Gambelli, J. W., Auvil, S. R., Acetonitrile process with improved catalysts, U.S. Patent 4,272,451, **1981**.

[97] Hummel, A. A., Badani, M. V., Hummel, K. E., Delgass, W. N., Acetonitrile synthesis from CO, H_2 and NH_3 over iron catalysts, *J. Catal.* **1993**, 139, 392 - 405.

[98] Kim, K. N., Lane, A. M., The selective synthesis of acetonitrile from carbon monoxide, hydrogen and ammonia over Mo/SiO_2, *J. Catal.* **1992**, 137, 127 - 138.

[99] Baiker, A., Monti, D., Interaction of ammonia with metallic copper, nickel and cobalt catalysts studied by temperature programmed desorption, *Ber. Bunsenges. Phys. Chem.* **1983**, 87, 602 - 605.

[100] Wiberg, N., in: Lehrbuch der Anorganischen Chemie, 102. Auflage, de Gruyter, **2007**, p. 671.

[101] Fischer, F., Tropsch, H., The synthesis of petroleum at atmospheric pressures from gasification products from coal, *Brennstoff Chemie* **1926**, 7, 97 - 104.

[102] Craxford, S., Rideal, E., Die Fischer-Tropsch synthese von Kohlenwasserstoffen und einige verwandte Reaktionen, *Brennstoff Chemie* **1939**, 20, pp. 263.

[103] Espinoza, R. L., Steynberg, A. P., Jager, B., Vosloo, A. C., Low temperature Fischer-Tropsch synthesis from a Sasol perspective, *Appl. Catal. A: Gen.* **1999**, 186, 13 - 26.

[104] Baiker, A., Catalytic amination of aliphatic alcohols. The role of hydrogen as inhibitor for catalyst deactivation, *Ind. Eng. Chem. Prod. Res. Dev.* **1981**, 20, 615 - 618.

[105] Lapidus, A. L'Vovich, Krylova, A. J., Activation of hydrocarbon synthesis catalysts with hydrogen and ammonia, U.S. 6,337,353 B1, **2002**.

[106] Baiker, A., Monti, D., Fan, Y. S., Deactivation of copper, nickel and cobalt catalysts by interaction with aliphatic amines, *J. Catal.* **1984**, 88, 81 - 88.

[107] Baiker, A., Richarz, W., Catalytic amination of long chain aliphatic alcohols, *Ind. Eng. Chem. Prod. Res. Dev.* **1977**, 16, 261 - 266.

[108] Gardner, D. A., Clark, R. T., Catalytic process for preparing ethyl amines, U.S. Patent 4,255, 357, **1981**.

[109] Baiker, A., Kijenski, J., Catalytic synthesis of higher aliphatic amines from the corresponding alcohols, *Cat. Rev.-Sci. Eng.* **1985**, 27, 653 - 697.

[110] Pelka, R., Kielbasa, K., Arabczyk, W., The effect of iron nanocrystallites´ size in catalysts for ammonia synthesis on nitriding reaction and catalytic ammonia decomposition, *Cent. Eur. J. Chem.* **2011**, 9, 240 - 244.

[111] Sango, T., Master thesis, University of Cape Town (**2008**).

[112] Rausch, A., Roessner, F., Claeys, M., van Steen, E., Process for the production of hydrocarbons including olefins from synthesis gas, U.S. Patent 2011/0160510 A1, **2011**.

[113] Shultz, J. F., Hofer, L. J. E., Stein, K. C., Anderson, R. B., Carbides, nitrides and carbonitrides of iron as catalysts in the Fischer-Tropsch synthesis, Bureau of Mines **1963**, Bulletin 612.

[114] Yeh, E. B., Schwartz, L. H., Butt, J. B., Silica-supported iron nitride in Fischer-Tropsch Reactions, *J. Catal.* **1985**, 91, 241 - 253.

[115] Chen, G. M., Jaggi, N. K., Butt, J. B., Yeh, E. B., Schwartz, L. H., Mössbauer and magnetic studies of ε-Fe_xN, $2 < x < 3$, *J. Phys. Chem.* **1983**, 87, 5326 - 5332.

[116] Lin, H. Y., Chen, Y. W., Li, C., The mechanism of reduction of iron oxide by hydrogen, *Thermochim. Acta* **2003**, 400, 61 - 67.

[117] Bukur, D. B., Okabe, K., Rosynek, P., Li, C., Wang, D., Rao, K. R. P. M., Huffman, G. P., Activation studies with a precipitated iron catalyst for Fischer-Tropsch synthesis, *J. Catal.* **1995**, 155, 353 - 365.

[118] Jin, Y., Datye, A., Phase transformations in iron Fischer-Tropsch catalysts during temperature-programmed reduction, *J. Catal.* **2000**, 196, 8 - 17.

[119] Dry, M. E., Shingles, T., Boshoff, L. J., van H. Botha, C. S., Factors influencing the formation of carbon on iron Fischer-Tropsch catalysts, *J. Catal.* **1970**, 17, 347 - 354.

[120] Schulz, H., Gökcebay, H. in: Kosak, J., Dekker, M. (eds.), Catalysis of Organic Reactions, New York, **1984**, p. 153.

[121] Hoffmann, R., A chemical and theoretical way to look at bonding on surfaces, *Rev. Mod. Phys.* **1988**, 60, 601 - 628.

[122] Blyholder, G., Molecular orbital view of chemisorbed carbon monoxide, *J. Phys. Chem.* **1964**, 68, 2772 - 2777.

[123] Hammer, B., Morikawa, Y., Norskov, J. K., CO chemisorption at metal surfaces and overlayers, *Phys. Rev. Lett.* **1996**, 76, 2141 - 2144.

[124] van Daelen, M. A., Li, Y. S., Newsam, J. M., van Santen, R. A., Transition states for NO and CO dissociation on Cu(100) and Cu(111) surfaces, *Chem. Phys. Lett.* **1994**. 226, 100 - 105.

[125] Gong, X. Q., Raval, R., Hu, P., A density functional theory study on the water formation at high coverages and the water effect in the Fischer-Tropsch synthesis, *Mol. Phys.* **2004**, 102, 993 - 1000.

[126] Blyholder, G., Richardson, E. A., Infrared and volumetric data on the adsorption of ammonia, water and other gases on activated iron(III) oxide, *J. Phys. Chem.* **1962**, 66, 2597 - 2602.

[127] Janiak, C., in: Riedel, E. (ed.), Moderne Anorganische Chemie, de Gruyter, 3. Auflage, Berlin, **2007**.

[128] Koeken, Ard C. J., Galvis, H. M. T., Davidian, T., Ruitenbeek, M., de Jong, K. P., Suppression of carbon deposition in the iron-catalyzed production of lower olefins from synthesis gas, *Angew. Chem. Int. Ed.* **2012**, 51, 7190 - 7193.

[129] Uemiya, S., Uchida, M., Moritomi, H., Yoshiie, R., Nishimura, M., Ammonia Decomposition Catalyst with Resistance to Coexisting sulfur compounds, *Materials Transactions* **2005**, 46, 2709 - 2712.

[130] Tao, L., Zai, J., Wang, K., Zhang, H., Xu, M., Shen, J., Su, Y., Qian, X., Co_3O_4 nanorods/graphene nanosheets nanocomposites for lithium ion batteries with improved reversible capacity and cycle stability, *J. Power Sources* **2012**, 202, 230 - 235.

7 Appendices

7.1 List of chemicals and gases

Table 7.1: List of chemicals and gases used in this study.

Name (purity)	**Origin**	**Name (purity)**	**Origin**
Acetaldehyde (99.5 %)	Acros	2-Hexanone (98 %)	Sigma-Aldrich
Acetone (pure)	BI-Laborbedarfslager	*n*-Hexylamine (99 %)	Sigma-Aldrich
Acetic acid (90 %)	Aldrich	Helium 5.0	Air Liquide
Acetonitrile (99.5 %)	BI-Laborbedarfslager	Hexanoic acid (99.5)	Sigma-Aldrich
Argon 5.0	Air Liquide	Hexanal (98 %)	Unknown
Ammonia 2.8	Messer Griesheim	Hexanenitrile (98 %)	Sigma-Aldrich
Ammonium hydroxide (25 %)	BI-Laborbedarfslager	Hydrogen 5.0	Air Liquide
Ammonium bicarbonate (Unknown)	BI-Laborbedarfslager	Iron(III) nitrate nonahydrate	Sigma Aldrich
1-Butanol (99.9 %)	BASF	Methanol (99.9 %)	VWR
2-Butanone (for synthesis)	BI-Laborbedarfslager	Methylamine (98 %)	Unknown
n-Butylamine (Unkown)	Unknown	1-Nonene (pure)	Fluka
Butanal (99.9 %)	Riedel de Häen	Nitrogen 5.0	Air Liquide
Butanoic acid (98 %)	Fluka	1-Octene (99 %)	Acros
Carbon monoxide 2.5	Messer Griesheim	1-Pentene (95 %)	Aldrich
Carbon dioxide 5.0	Air Liquide	1-Pentanol (99 %)	BI-Laborbedarfslager
Cobalt(II) nitrate hexahydrate		1-Propanol (> 99 %)	Aldrich
Cyclohexane (for synthesis)	BI-Laborbedarfslager	2-Pentanone (Unknown)	Unknown
Ethanol (96 %)	BI-Laborbedarfslager	2-Propanone (Unknown)	BI-Laborbedarfslager
Ethylamine (70 %, aq.)	Unknown	*n*-Pentylamine (Unknown)	Unknown
1-Hexene (96 %)	Merck	*n*-Propylamine (99 %)	BI-Laborbedarfslager
1-Heptene (> 99 %)	Aldrich	Pentanoic acid (Unknown)	Unknown
1-Hexanol (98 %)	Sigma-Aldrich	Pentanal (Unknown)	Unknown
Pentanenitrile (Unknown)	Unknown	Propanenitrile (Unknown)	Unknown
Propanoic acid (Unknown)	Unknown	SiO_2 (K253)	Chemiewerk Bad Köstritz GmbH
Propanal (97 %)	Alfa Aesar		

7.2 Calibration factors

For all compounds which were detected and analyzed during the *online* gas chromatographic analysis using the GC-TCD, GC-MS and the GC-FID, calibration factors of the compounds had to be determined or calculated.

7.2.1 GC-TCD

In order to determine the response factors of the reactants (CO, H_2) and products such as CO_2 and CH_4, a mixture of these gases was prepared. Mass flow controllers (MFC) were used for mixing the gases with different concentrations in the gas flow. Argon as an internal standard was added to this mixture, too, and the calibration factors $f_{TCD,i}$ of an compound i was calculated using equation 3.4 in chapter 3.4.1. In Table 7.2 the obtained calibration factors are presented:

Table 7.2: Calibration factors $f_{TCD,i}$ for a compound i analyzed with the GC-TCD.

Compound	**Calibration factor $f_{TCD,i}$**
Hydrogen (H_2)	4.46
Argon (Ar)	1.00 [1]
Carbon monoxide (CO)	18.10
Methane (CH_4)	0.64
Carbon dioxide (CO_2)	14.05

[1] For argon a calibration factor of 1 was chosen.

7.2.2 GC-FID

All linear paraffins and 1-olefins in the carbon number range from C_1 - C_9 as well as acetaldehyde, 2-methylpropane and 2-butene were analyzed using the GC-FID. The calibration factors $f_{FID,i}$ of an organic compound i were calculated using equation 3.5 in chapter 3.4.2 and a more detailed explanation can be found in this section, too.

7.2.3 GC-MS

Compared to a flame ionization detector, a mass spectrometer does not show a linear response. In order to quantify most of the products during the Fischer-Tropsch synthesis with the GC-MS, a calibration with reference chemicals had to be done and a list of all calibrated compounds is given in Table 7.3.

Table 7.3: Chemicals used for the calibration of the GC-MS and their specific data.

Fraction	**Compound**	**Molecular formula**	**Specific ion m/z**	**Molar mass** (g/mol)	**Boiling point** (°C)
C_1	Methanol	CH_4O	31	32.04	65
	Methylamine [1]	CH_5N	30	31.06	-6
C_2	Ethanol	C_2H_6O	31	46.07	78
	Acetic acid	$C_2H_4O_2$	60	60.05	118
	Ethylamine [1]	C_2H_7N	30	45.08	17
	Acetonitrile	C_2H_3N	41	41.05	82
C_3	1-Propanol	C_3H_8O	31	60.10	97
	Propanoic acid	$C_3H_6O_2$	29	74.08	141
	Propanal	C_3H_6O	29	58.08	47
	2-Propanone	C_3H_6O	58	58.08	57
	n-Propylamine	C_3H_9N	30	59.11	48
	Propanenitrile	C_3H_5N	54	55.08	97
C_4	1-Butanol	$C_4H_{10}O$	31	74.12	118
	Butanoic acid	$C_4H_8O_2$	60	88.11	164
	Butanal	C_4H_8O	44	72.11	75
	2-Butanone	C_4H_8O	72	72.11	80
	n-Butylamine	$C_4H_{11}N$	30	73.14	77
	Butanenitrile	C_4H_7N	41	69.11	118

C_5	1-Pentene	C_5H_{10}	42, 55[2]	70.13	30
	1-Pentanol	$C_5H_{12}O$	31	88.15	137
	Pentanoic acid	$C_5H_{10}O_2$	60	102.13	186
	Pentanal	$C_5H_{10}O$	44	86.13	102
	2-Pentanone	$C_5H_{10}O$	43	86.13	101 – 105
	n-Pentylamine	$C_5H_{13}N$	30	87.16	104
	Pentanenitrile	C_5H_9N	41	83.13	139
C_6	1-Hexene	C_6H_{12}	41, 41[2]	84.16	63
	1-Hexanol	$C_6H_{14}O$	31	102.17	155 – 159
	Hexanoic acid	$C_6H_{12}O_2$	60	116.16	205
	Hexanal	$C_6H_{12}O$	44	100.16	119 – 124
	2-Hexanone	$C_6H_{12}O$	58	100.16	128
	n-Hexylamine	$C_6H_{15}N$	30	101.19	131 – 132
	Hexanenitrile	$C_6H_{11}N$	41	97.16	161 – 164
C_7	1-Heptene	C_7H_{14}	41, 41[2]	98.19	94
C_8	1-Octene	C_8H_{16}	41, 41[2]	112.24	121
C_9	1-Nonene	C_9H_{18}	56, 55[2]	126.24	146

[1] Due the low boiling point of this compound an aqueous solution was used for the calibration.

[2] The second m/z ion was used to calibrate 2-olefins.

Based on the Fischer-Tropsch C_5 fraction, examples of the calibration diagrams are given in Figure 7.1to Figure 7.9. For the calibration of the GC-MS, each analyte ‘a’ was injected thrice for 5 different volumes respectively (0.02 µL, 0.04 µL, 0.06 µL, 0.08 µL and 0.1 µL). The molar ratio n_a/n_{is} (n_{is} is the amount of substance for the **i**nternal **s**tandard cyclohexane taken from the GC-FID chromatograms for every sample) was plotted against the extracted ion area ratio m/z of the analyte and the internal standard cyclohexane. A polynomial 2nd order gives the calibration factors $A_{MS,i}$ and $B_{MS,i}$ which are required to calculate the molar flow rate (equation 3.8) of the specific organic compound formed during the Fischer-Tropsch reaction.

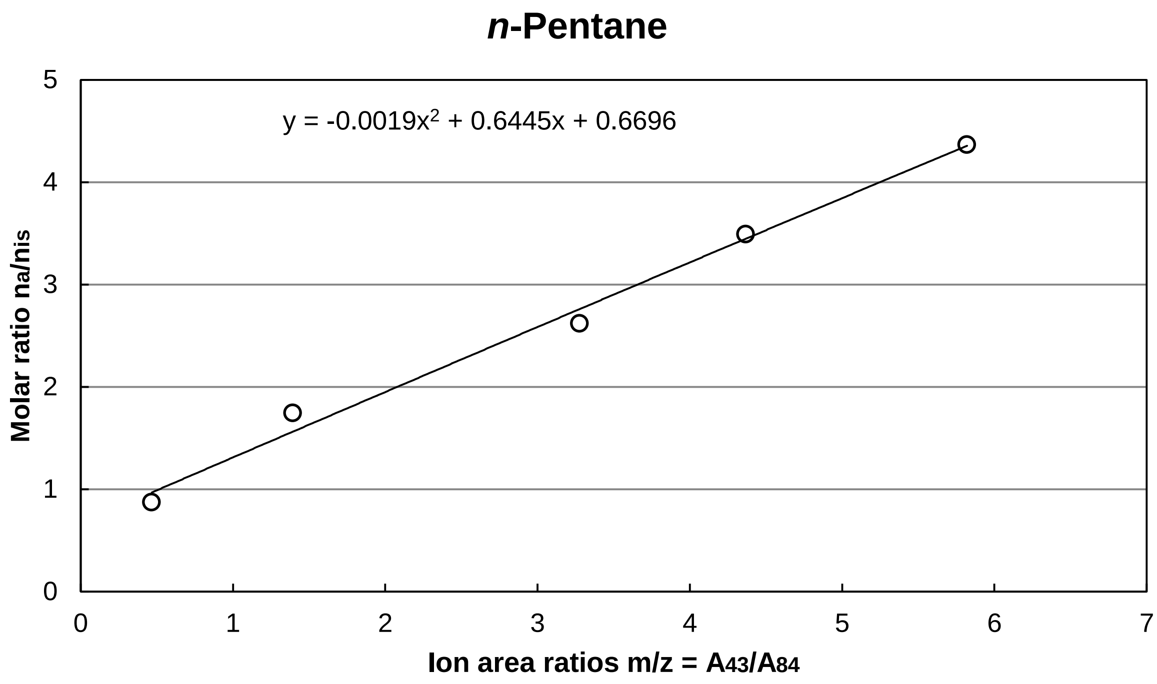

Figure 7.1: Calibration curve for *n*-pentane with the ion m/z = 43.

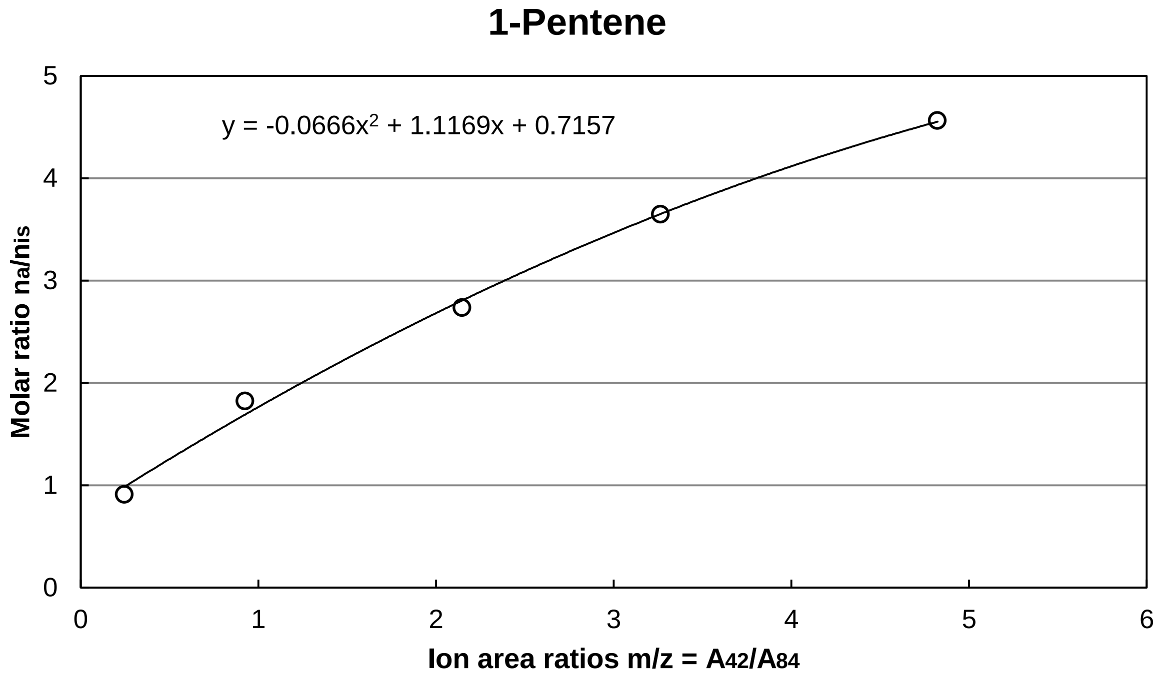

Figure 7.2: Calibration curve for 1-pentene with the ion m/z = 42.

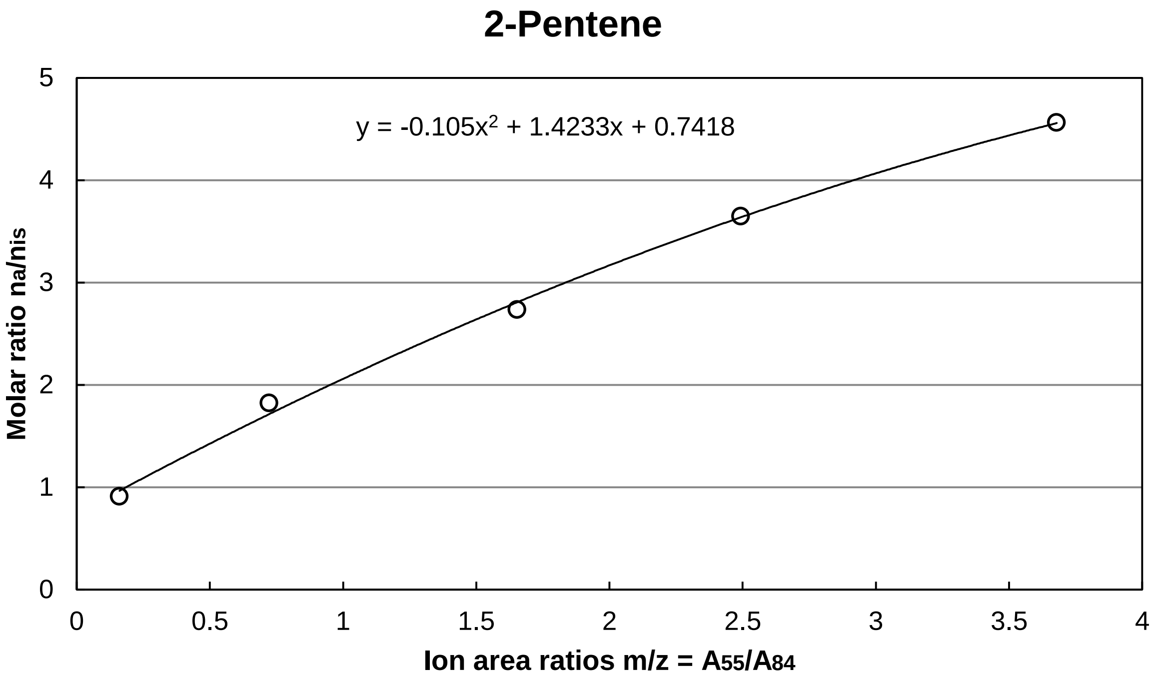

Figure 7.3: Calibration curve for 2-pentene with the ion m/z = 55.

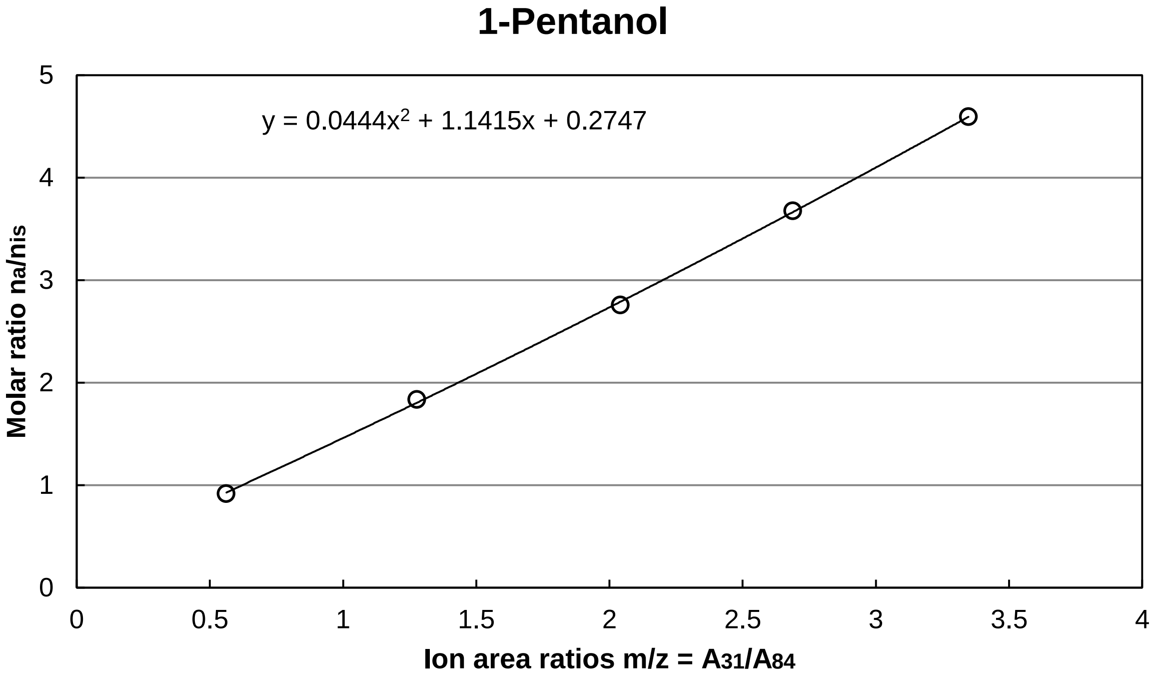

Figure 7.4: Calibration curve for 1-pentanol with the ion m/z = 31.

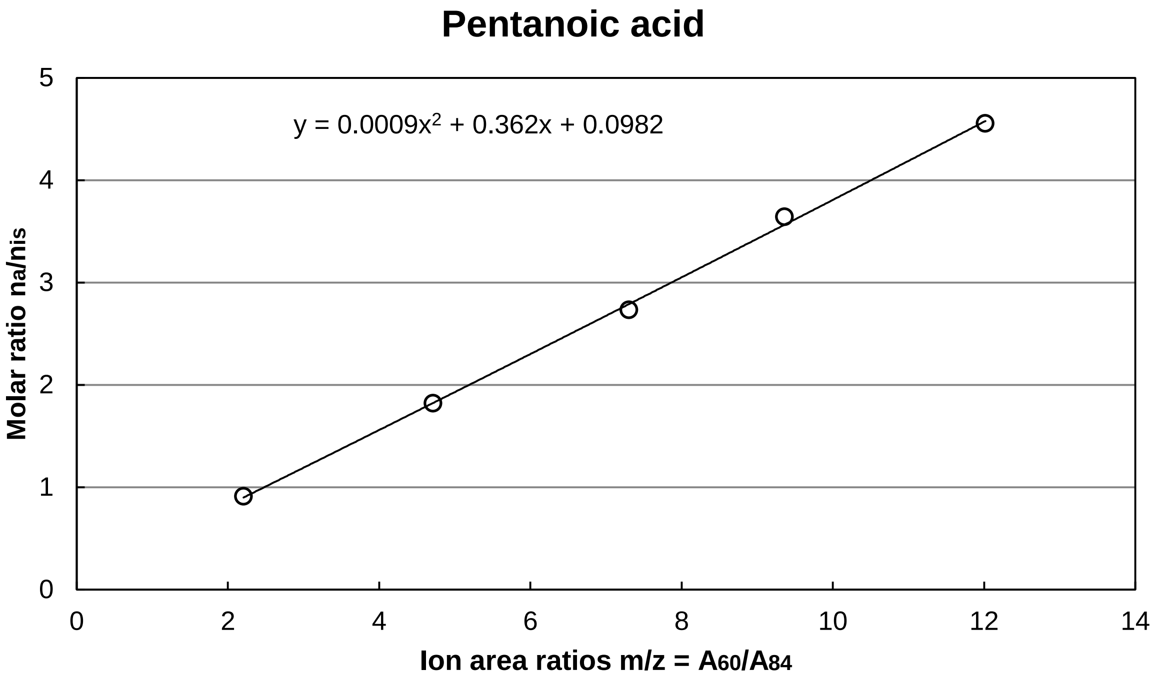

Figure 7.5: Calibration curve for pentanoic acid with the ion m/z = 60.

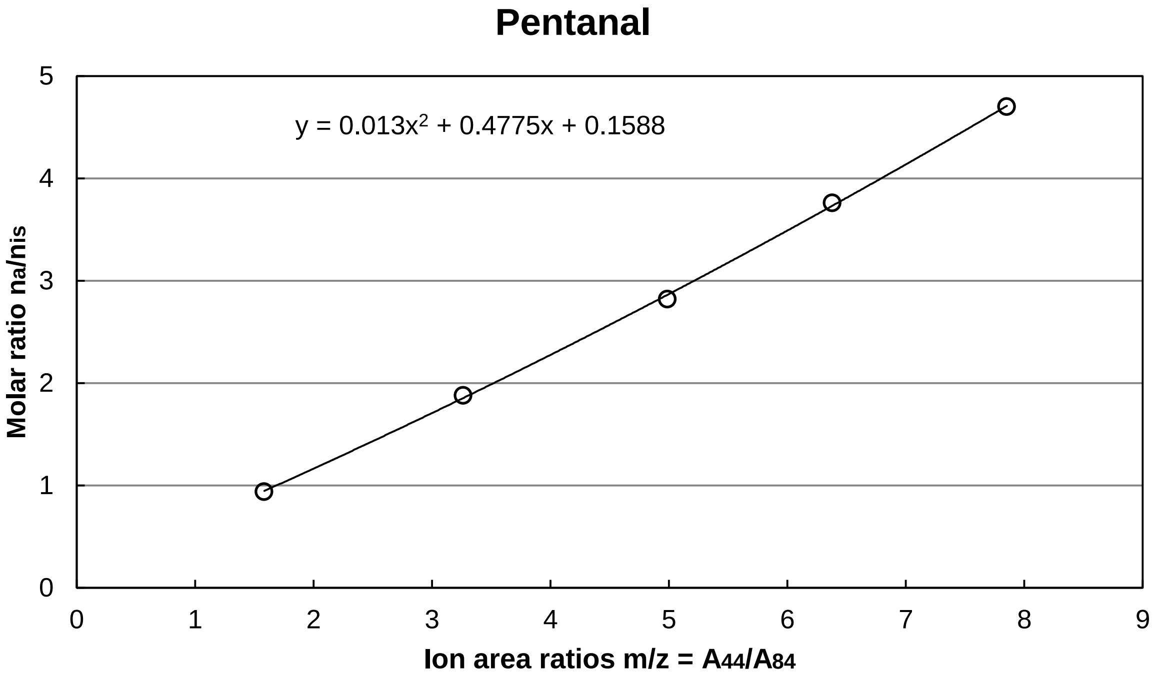

Figure 7.6: Calibration curve for pentanal with the ion m/z = 44.

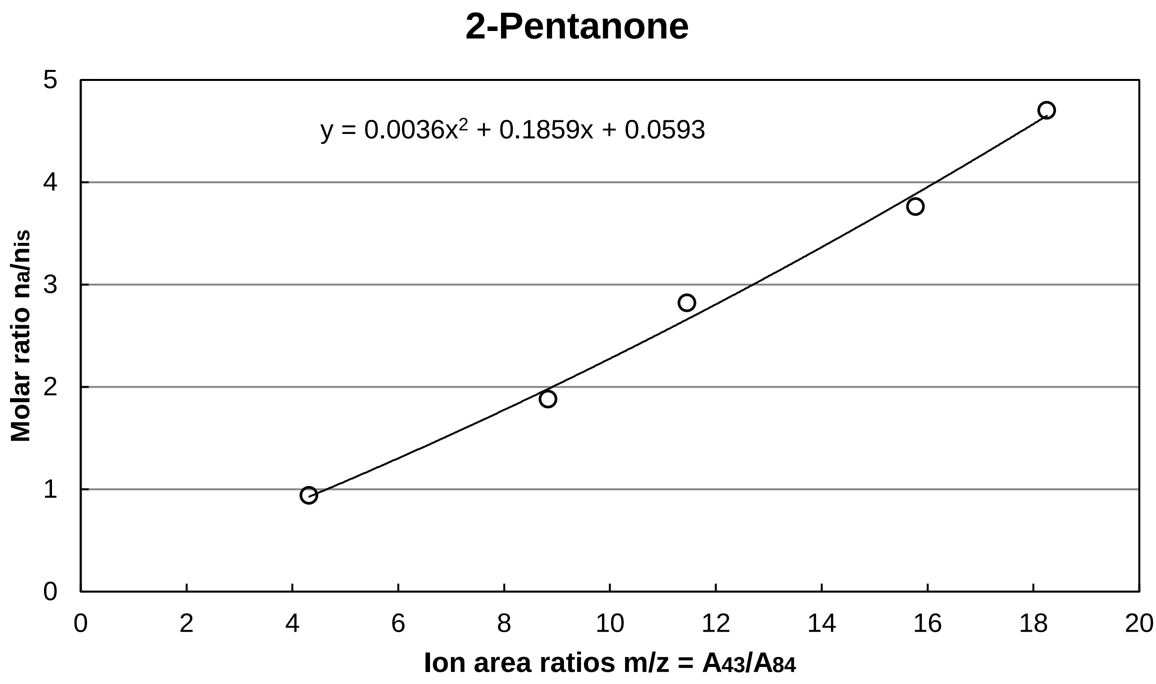

Figure 7.7: Calibration curve for 2-pentanone with the ion m/z = 43.

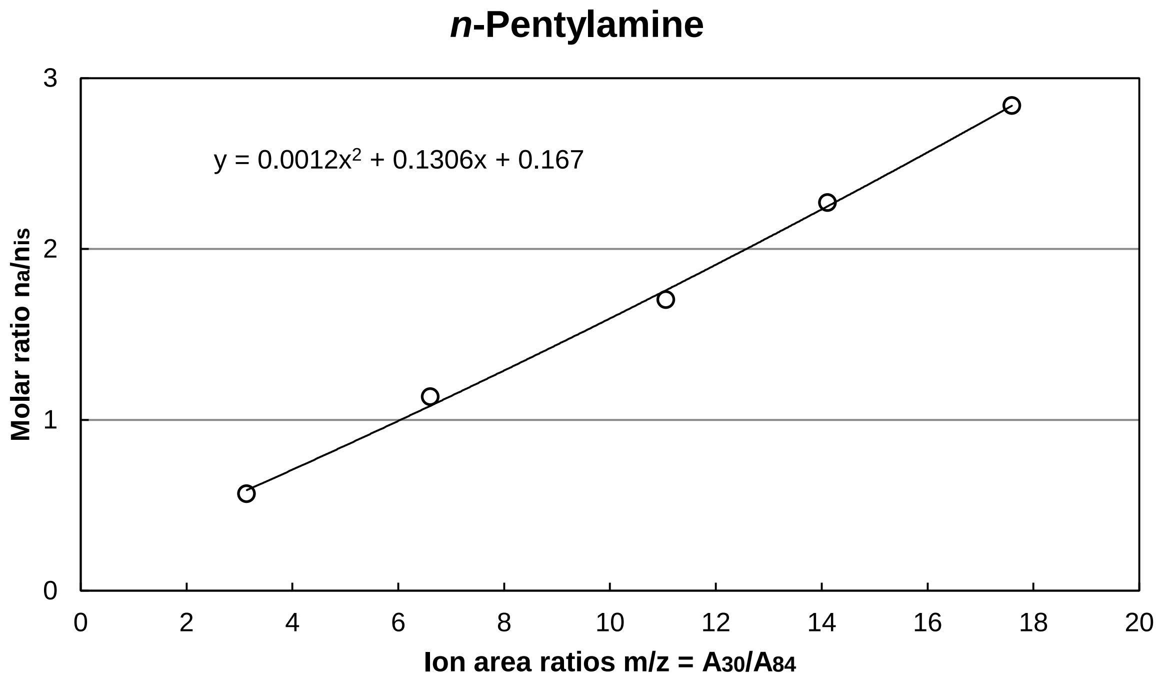

Figure 7.8: Calibration curve for *n*-pentylamine with the ion m/z = 30.

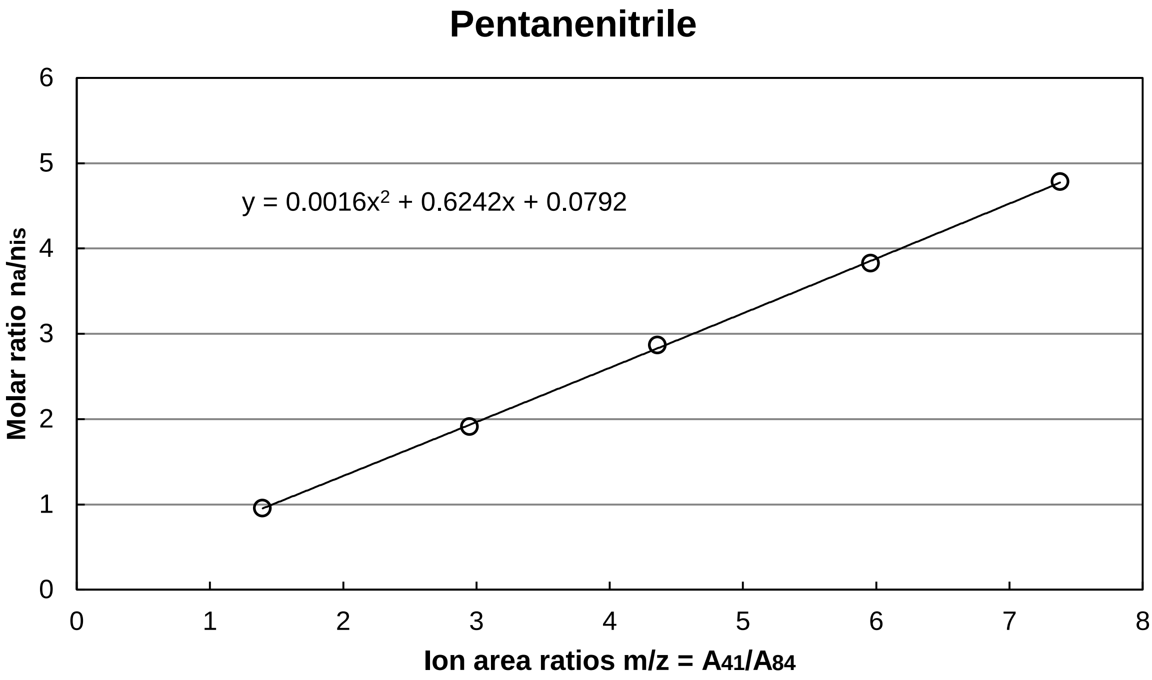

Figure 7.9: Calibration curve for pentanenitrile with the ion m/z = 41.

7.3 Retention times during *online* GC analysis

Table 7.4: Retention times (minutes) for compounds detected with the GC-TCD (argon was used as an internal standard on column 1).

Compound	**Retention time** (min)	**Column (stationary phase)**
Hydrogen	2.13	Column 1 (Carbosieve S-II)
Argon	3.66	Column 1 (Carbosieve S-II)
Carbon monoxide	4.45	Column 1 (Carbosieve S-II)
Methane	7.95	Column 1 (Carbosieve S-II)
Carbon dioxide	14.84	Column 1 (Carbosieve S-II)
Ammonia	2.14	Column 2 (Porapak P)

Table 7.5: Retention times (minutes) for compounds detected with the GC-FID (cyclohexane is not a Fischer-Tropsch product and was used as an internal standard).

Compound	**Retention time** (min)	**Compound**	**Retention time** (min)
Methane	0.75	1-Pentene	20.12
Ethene	1.19	*n*-Pentane	20.75
Ethane	1.45	1-Hexene	25.00
Propene	7.85	*n*-Hexane	25.31
Propane	8.34	Cyclohexane	25.85
Acetaldehyde	12.03	1-Heptene	28.30
2-Methylpropane	12.69	*n*-Heptane	28.52
1-Butene	13.25	1-Octene	30.98
n-Butane	13.69	*n*-Octane	31.15
2-Butene (tr.)	13.84	1-Nonene	33.66
2-Butene (cis)	14.07	*n*-Nonane	33.87

Table 7.6: Retention times (minutes) for compounds detected with the GC-MS (cyclohexane is not a Fischer-Tropsch product and was used as an internal standard).

Compound	**Retention time** (min)	**Compound**	**Retention time** (min)
Methanol	15.69	1-Heptene [2]	37.27
Acetonitrile [1]	19.53	*n*-Propylamine [1]	37.28
Ethanol	20.35	*n*-Heptane [2]	37.98
Propanal	20.58	2-Heptene (tr.)	38.27
2-Propanone	21.27	Propanoic acid	38.60
1-Pentene [2]	21.29	2-Heptene (cis)	38.85
n-Pentane [2]	22.27	Pentanenitrile [1]	40.75
2-Pentene (tr.)	22.99	1-Pentanol	41.51
2-Pentene (cis)	23.68	2-Hexanone	42.25
Propanenitrile [1]	27.29	Hexanal	42.66
1-Propanol	28.47	Butanoic acid	42.75
Butanal	29.10	1-Octene [2]	43.01
2-Butanone	29.96	*n*-Butylamine [1]	43.04
Ethylamine [1]	30.06	*n*-Octane [2]	43.60
1-Hexene [2]	30.40	2-Octene (tr.)	43.76
n-Hexane [2]	30.93	2-Octene (cis)	44.2
2-Hexene (tr.)	31.36	*n*-Pentylamine [1]	44.70
2-Hexene (cis)	32.52	Hexanenitrile [1]	46.03
Acetic acid	33.28	1-Hexanol	46.38
Butanenitrile [1]	34.37	*n*-Hexylamine [1]	47.22
Cyclohexane	35.22	1-Nonene [2]	47.83
1-Butanol	35.70	*n*-Nonane [2]	48.32
2-Pentanone	36.36	2-Nonene (tr.)	48.86
Pentanal	36.67	Pentanoic acid	50.84

[1] At an ammonia partial pressure p_{NH3} = 0.2 bar., [2] These compounds were quantified using the GC-FID.

7.4 Catalytic performance of bulk iron and cobalt catalysts

In this section the conversion of CO and H_2 as well as the selectivities to conventional Fischer-Tropsch products from the experiments on potassium promoted iron catalysts shown in chapter 4.2.2 are presented. Additionally, the results from the FT/NH_3-FT experiments conducted on bulk cobalt catalysts will be presented, too.

7.4.1 Variation of the reaction temperature

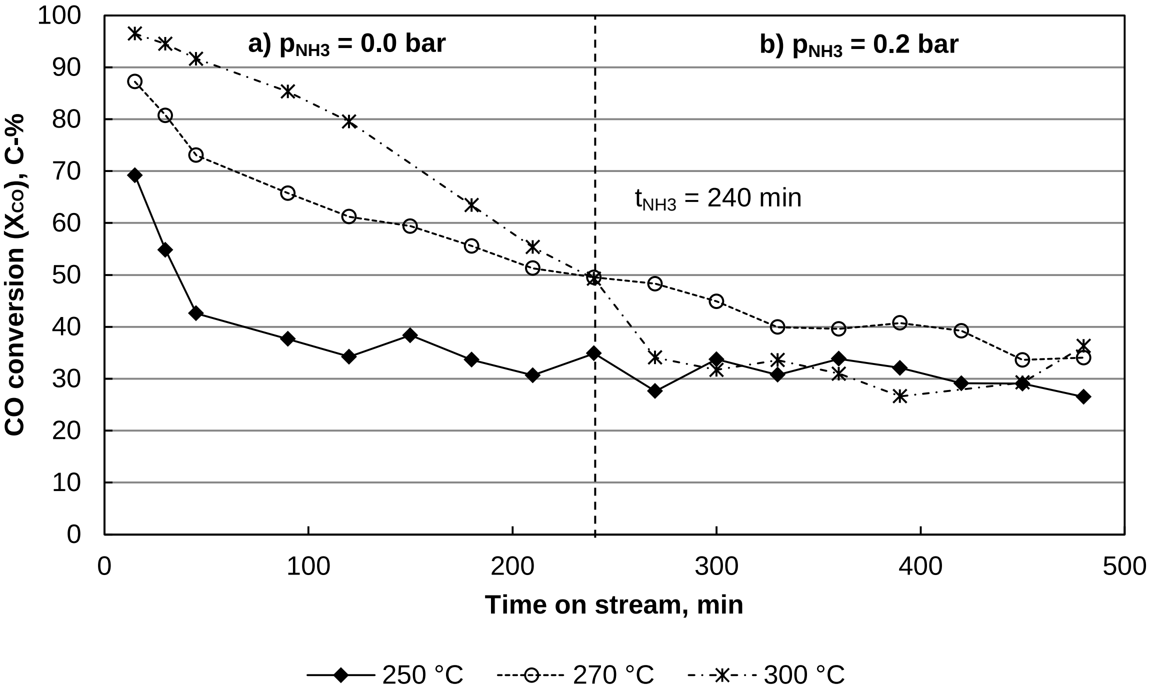

Figure 7.10: CO conversion (X_{CO}, C-%, organic products plus CO_2) during FT/NH_3-FT runs on iron catalysts doped with 2 wt% potassium in: a) the absence of NH_3 and b) the presence of NH_3 ($T_{Reactor}$ = 250 - 300 °C, P_{Total} = 4 bar, p_{NH3} = 0.0 - 0.2 bar, GHSV = 1920 h^{-1}, H_2:CO = 2:1).

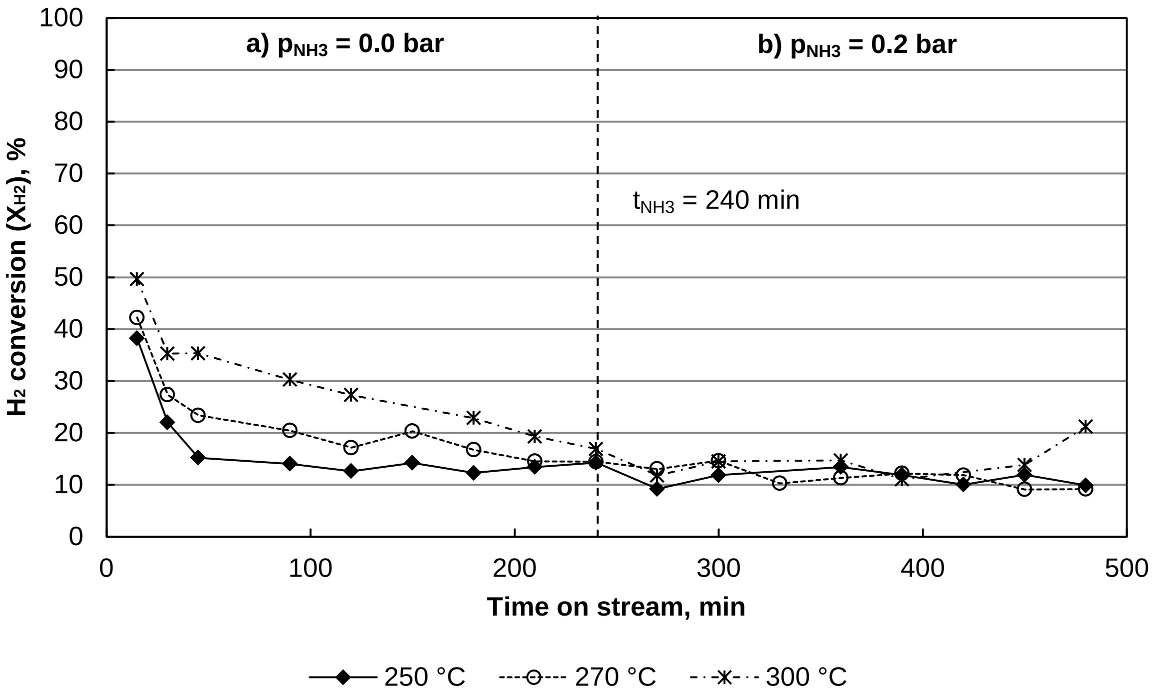

Figure 7.11: H_2 conversion (X_{H2}, %) during FT/NH_3-FT runs on iron catalysts doped with 2 wt% potassium in: a) the absence of NH_3 and b) the presence of NH_3 ($T_{Reactor}$ = 250 - 300 °C, P_{Total} = 4 bar, p_{NH3} = 0.0 - 0.2 bar, GHSV = 1920 h^{-1},H_2:CO = 2:1).

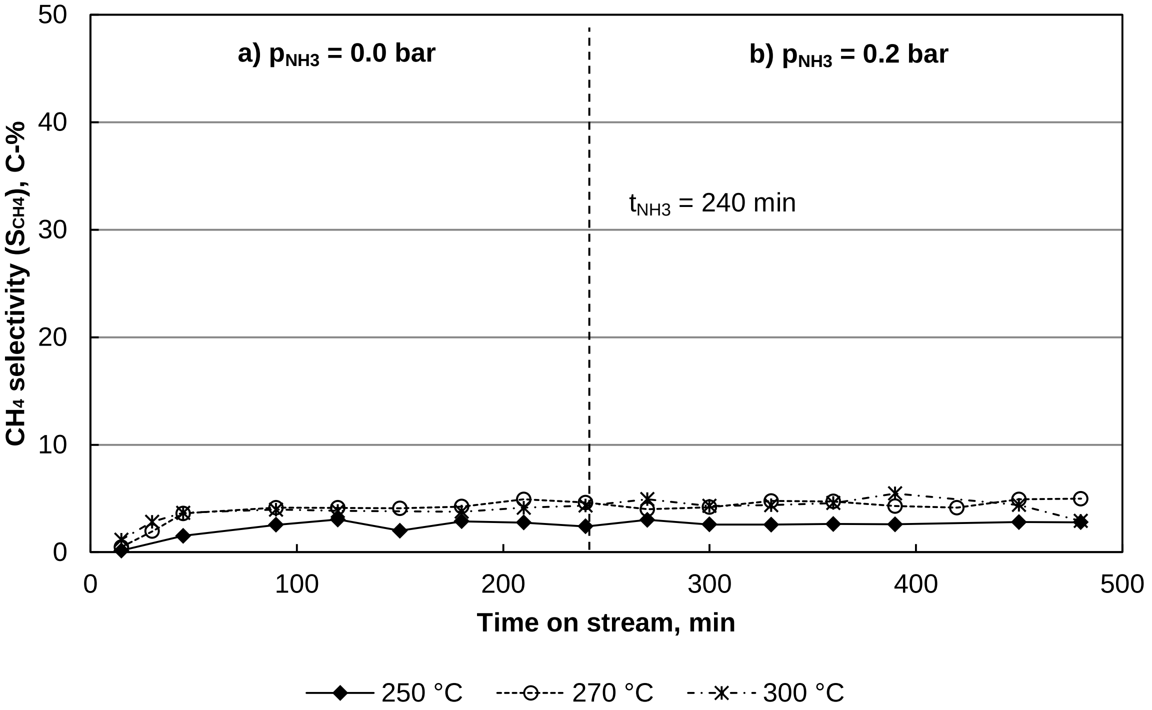

Figure 7.12: CH_4 selectivity (S_{CH4}, C-%) calculated from overall X_{CO} (CO_2 and organic products) during FT/NH_3-FT runs on iron catalysts doped with 2 wt% potassium in: a) the absence of NH_3 and b) the presence of NH_3 ($T_{Reactor}$ = 250 - 300 °C, P_{Total} = 4 bar, p_{NH3} = 0.0 - 0.2 bar, GHSV = 1920 h^{-1}, H_2:CO = 2:1).

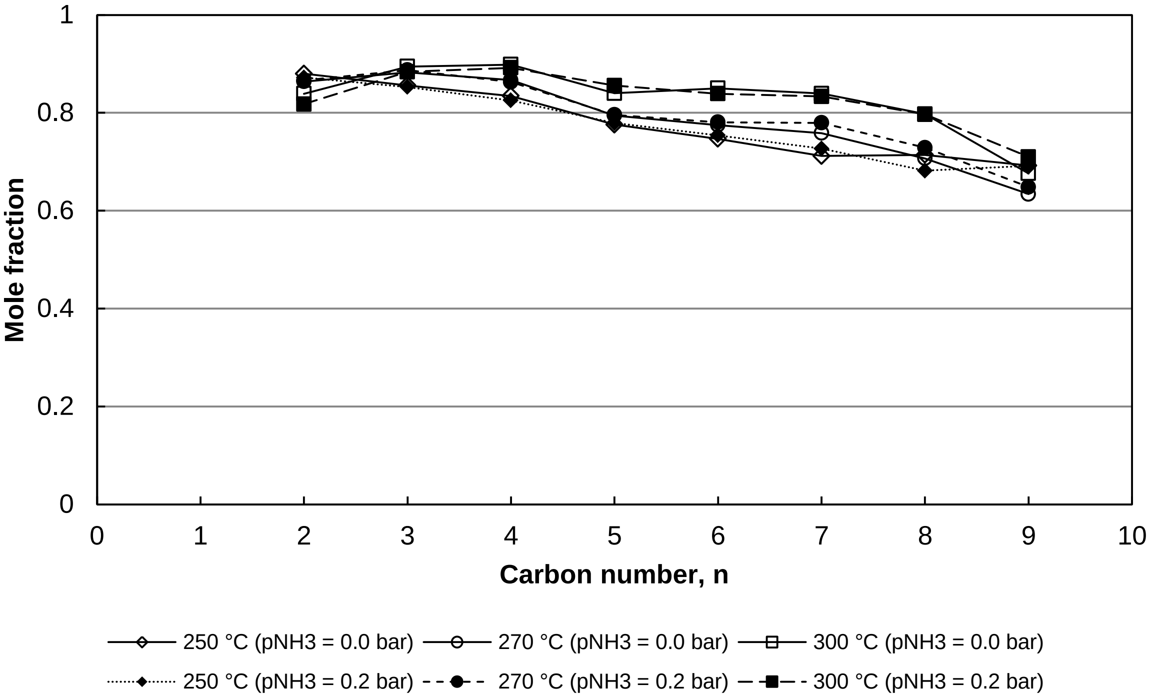

Figure 7.13: Mole fraction of olefins in linear hydrocarbons (olefins and *n*-paraffins) during FT/NH_3-FT runs on iron catalysts doped with 2 wt% potassium at different NH_3 partial pressures ($T_{Reactor}$ = 250 - 300 °C, P_{Total} = 4 bar, p_{NH3} = 0.0 - 0.2 bar, GHSV = 1920 h^{-1}, H_2:CO = 2:1).

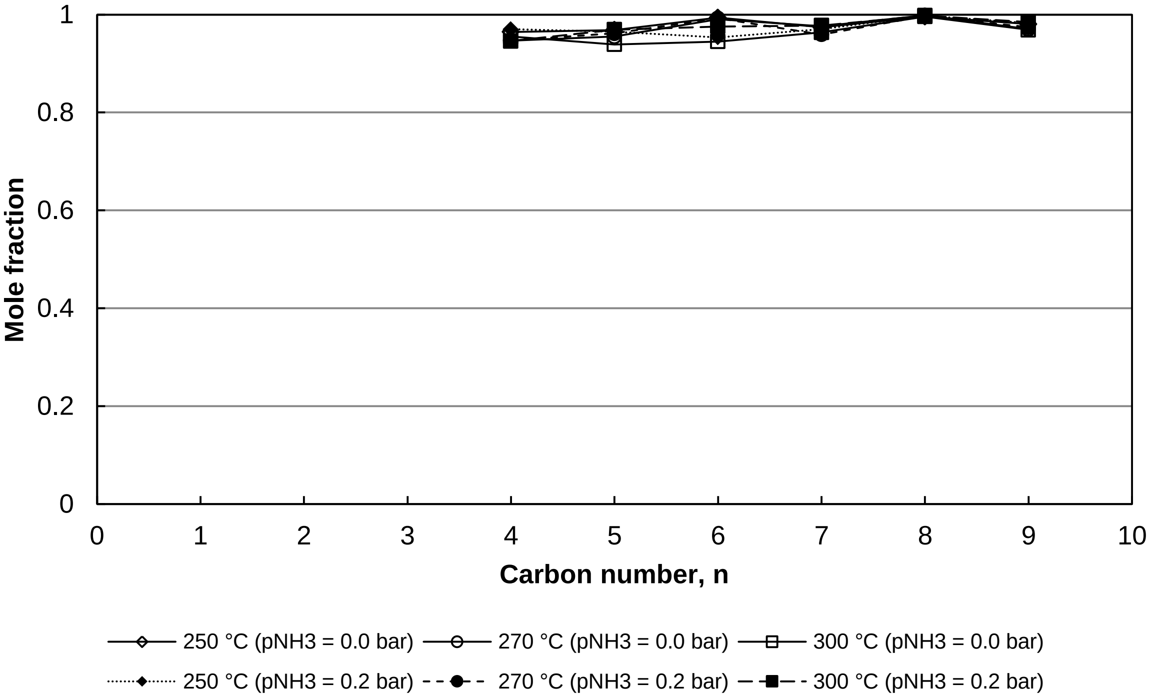

Figure 7.14: Mole fraction of 1-olefins in linear olefins (1- and 2-olefins) during FT/NH_3-FT runs on iron catalysts doped with 2 wt% potassium at different NH_3 partial pressures ($T_{Reactor}$ = 250 - 300 °C, P_{Total} = 4 bar, p_{NH3} = 0.0 - 0.2 bar, GHSV = 1920 h^{-1}, H_2:CO = 2:1).

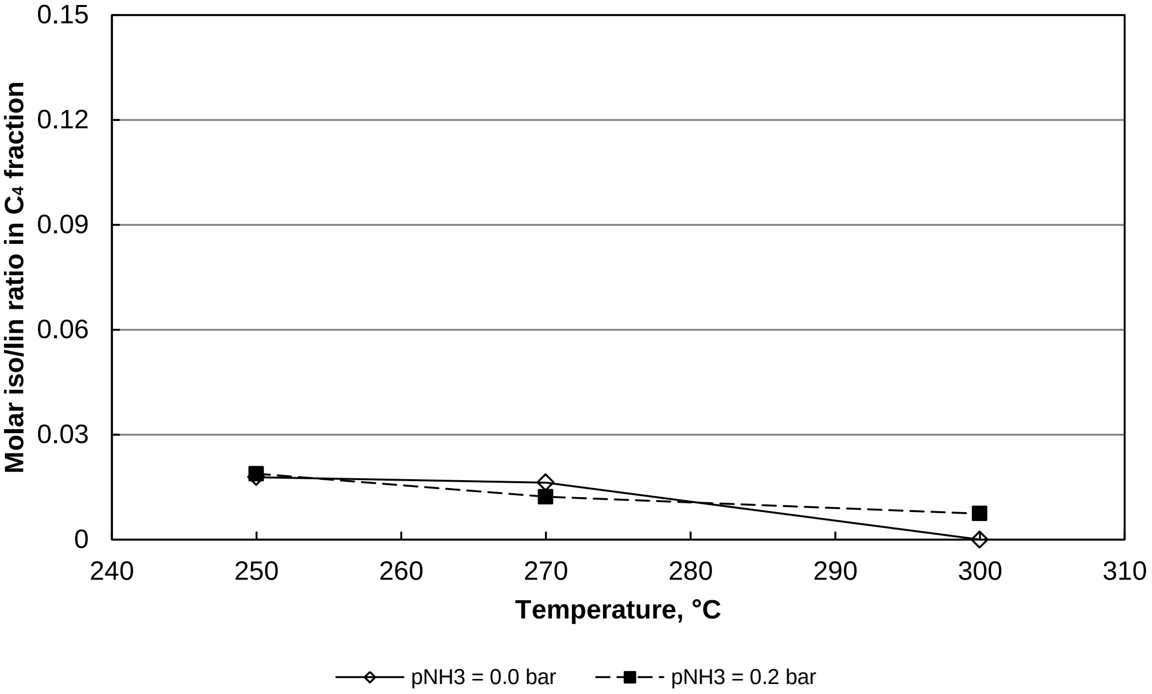

Figure 7.15: Molar iso/lin hydrocarbon ratio in C_4 fraction during FT/NH_3-FT runs on iron catalysts doped with 2 wt% potassium at different ammonia partial pressures ($T_{Reactor}$ = 250 - 300°C, P_{Total} = 4 bar, p_{NH3} = 0.0 - 0.2 bar, GHSV = 1920 h^{-1}, H_2:CO = 2:1).

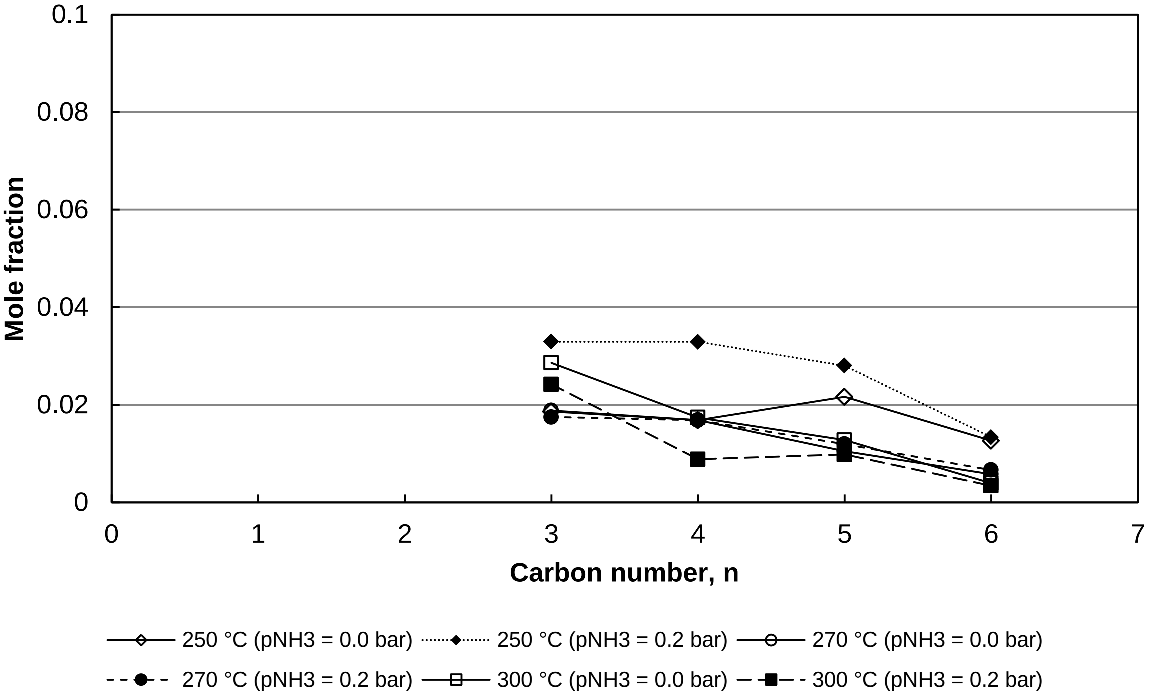

Figure 7.16: Mole fraction of methyl-ketones in all linear organic products during FT/NH_3-FT runs on iron catalysts doped with 2 wt% potassium at different NH_3 partial pressures ($T_{Reactor}$ = 250 - 300°C, P_{Total} = 4 bar, p_{NH3} = 0.0 - 0.2 bar, GHSV = 1920 h^{-1}, H_2:CO = 2:1).

Table 7.7: Chain growth probability α during FT/NH$_3$-FT runs on iron catalysts doped with 2 wt% potassium at different NH$_3$ partial pressures and temperatures (T$_{Reactor}$ = 250 - 300 °C, P$_{Total}$ = 4 bar, p$_{NH3}$ = 0.0 - 0.2 bar, GHSV = 1920 h^{-1}, H$_2$:CO = 2:1).

Temperature (°C)	**Chain growth probability**	
	α_{C3-C8} (p_{NH3} = 0.0 bar)	α_{C3-C8} (p_{NH3} = 0.2 bar)
250	0.69	0.65
270	0.64	0.64
300	0.70	0.70

7.4.2 Variation of the synthesis gas composition

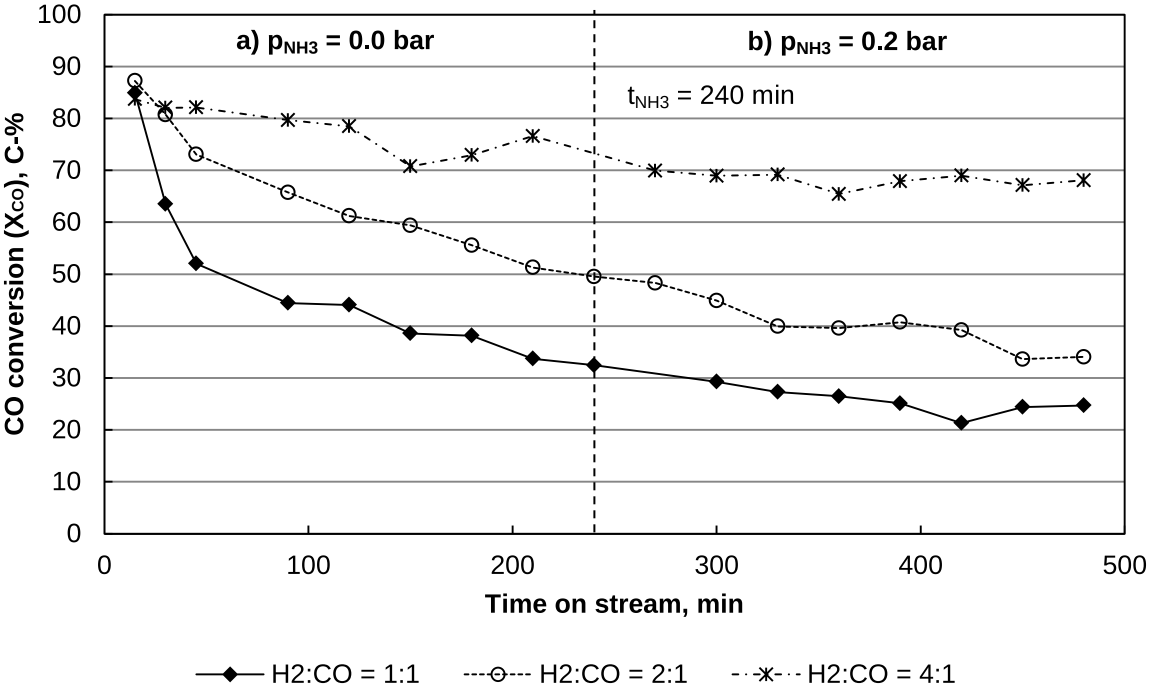

Figure 7.17: CO conversion (X$_{CO}$, C-%, organic products plus CO$_2$) during FT/NH$_3$-FT runs on iron catalysts doped with 2 wt% potassium in: a) the absence of NH$_3$ and b) the presence of NH$_3$ (T$_{Reactor}$ = 270 °C, P$_{Total}$ = 4 bar, p$_{NH3}$ = 0.0 - 0.2 bar, GHSV = 1920 h^{-1}, H$_2$:CO = 1:1, 2:1, 4:1).

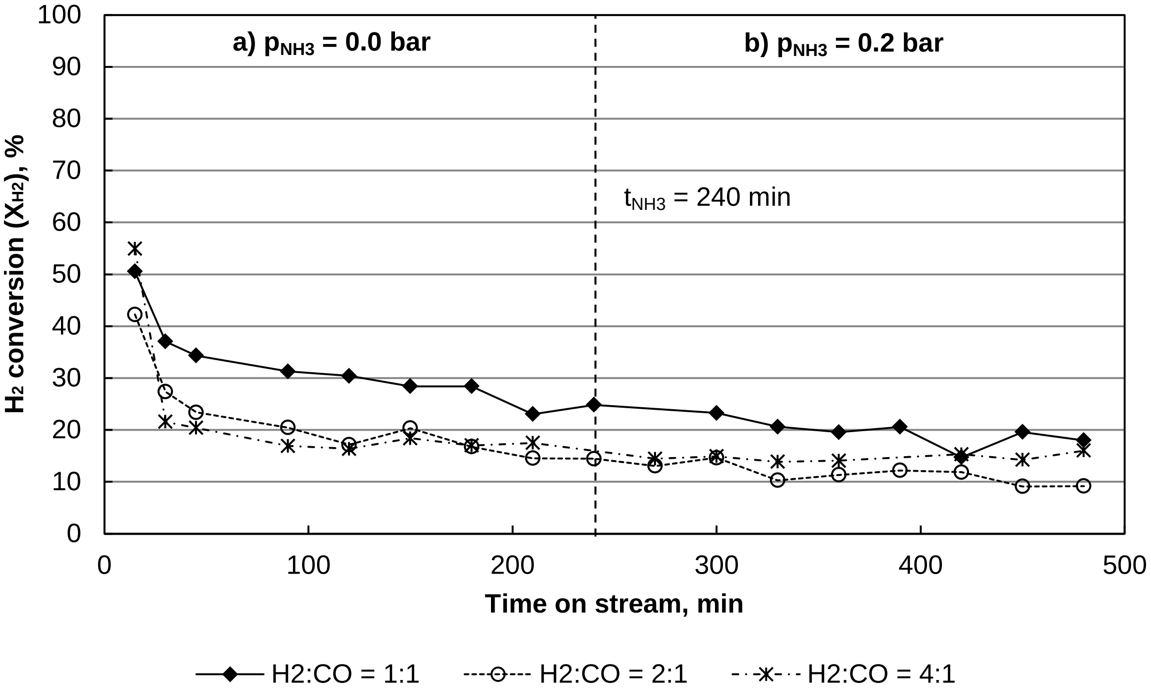

Figure 7.18: H_2 conversion (X_{H2}, %) during FT/NH_3-FT runs on iron catalysts doped with 2 wt% potassium in: a) the absence of NH_3 and b) the presence of NH_3 ($T_{Reactor}$ = 270 °C, P_{Total} = 4 bar, p_{NH3} = 0.0 - 0.2 bar, GHSV = 1920 h^{-1},H_2:CO = 1:1, 2:1, 4:1).

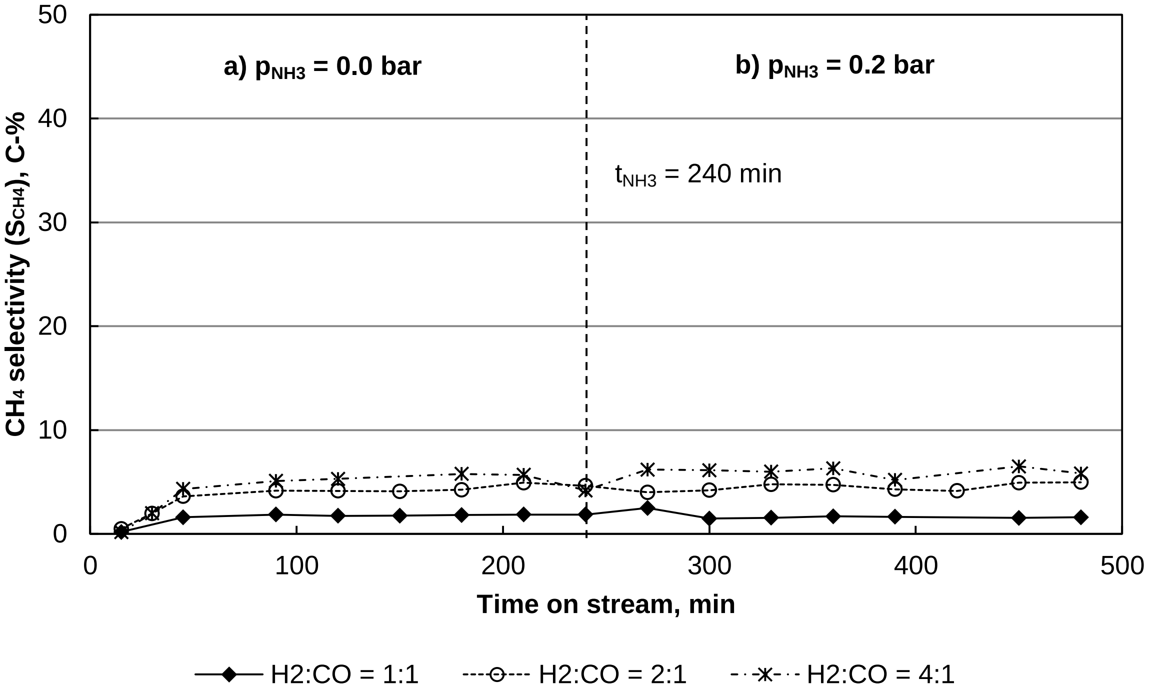

Figure 7.19: CH_4 selectivity (S_{CH4}, C-%) calculated from overall X_{CO} (CO_2 and organic products) during FT/NH_3-FT runs on iron catalysts doped with 2 wt% potassium in: a) the absence of NH_3 and b) the presence of NH_3 ($T_{Reactor}$ = 270 °C, P_{Total} = 4 bar, p_{NH3} = 0.0 - 0.2 bar, GHSV = 1920 h^{-1}, H_2:CO = 1:1, 2:1, 4:1).

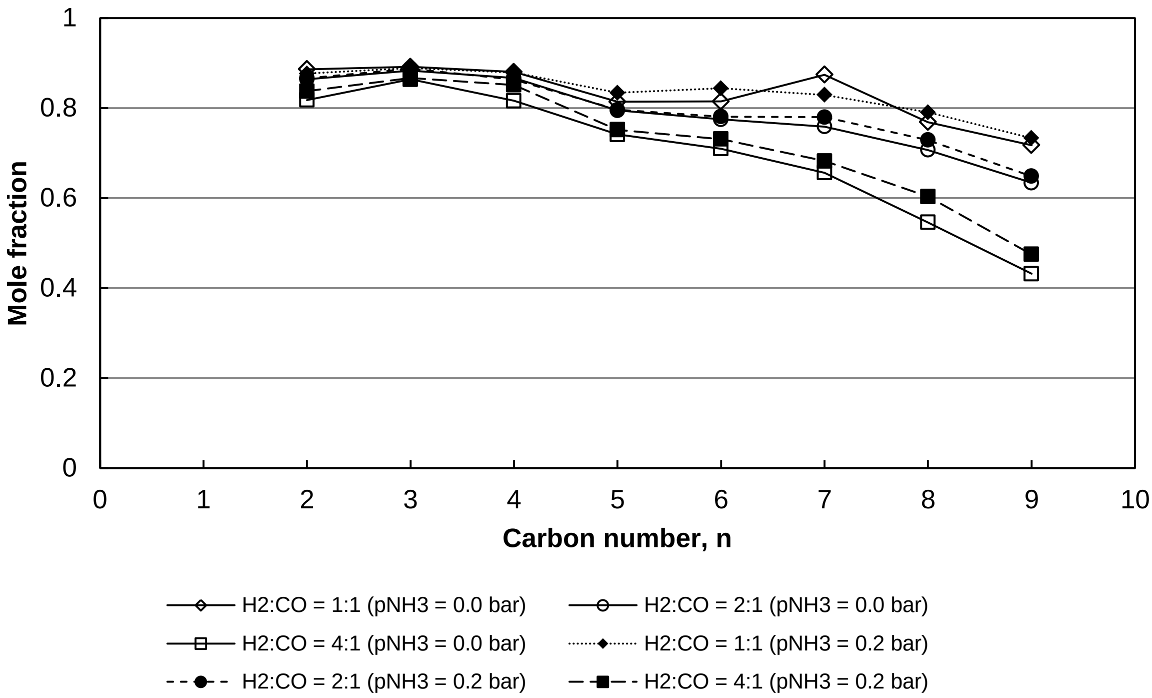

Figure 7.20: Mole fraction of olefins in linear hydrocarbons (olefins and *n*-paraffins) during FT/NH_3-FT runs on iron catalysts doped with 2 wt% potassium at different NH_3 partial pressures ($T_{Reactor}$ = 270 °C, P_{Total} = 4 bar, p_{NH3} = 0.0 - 0.2 bar, GHSV = 1920 h^{-1}, H_2:CO = 1:1, 2:1, 4:1).

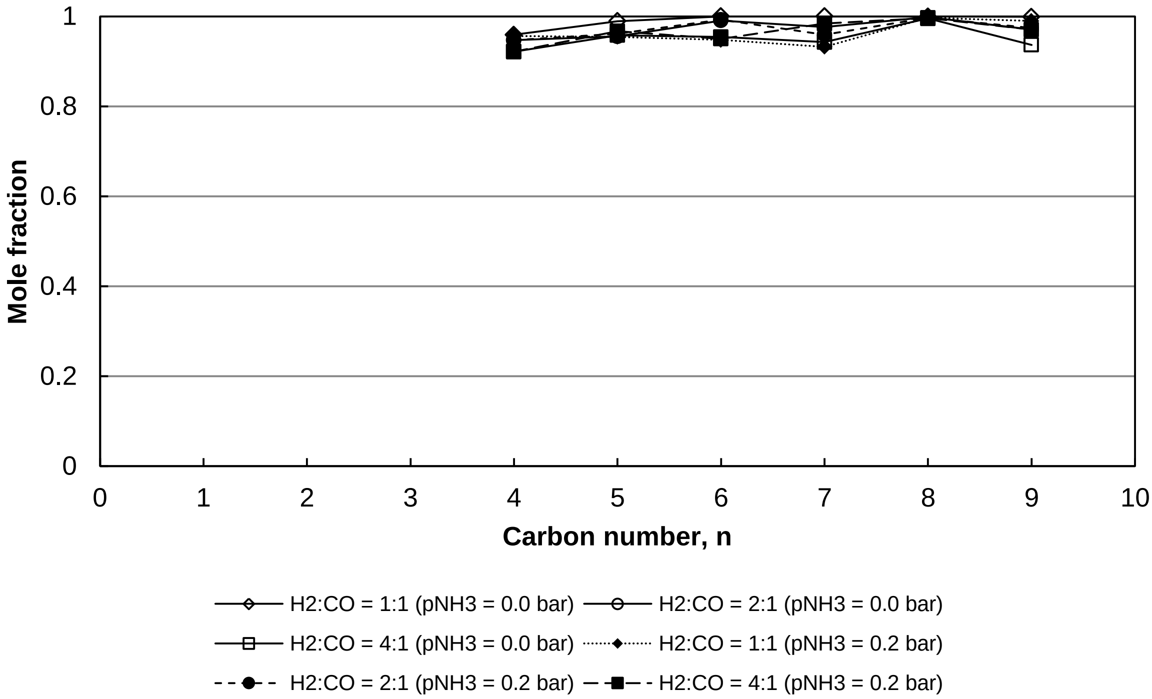

Figure 7.21: Mole fraction of 1-olefins in linear olefins (1- and 2-olefins) during FT/NH_3-FT runs on iron catalysts doped with 2 wt% potassium at different NH_3 partial pressures ($T_{Reactor}$ = 270 °C, P_{Total} = 4 bar, p_{NH3} = 0.0 - 0.2 bar, GHSV = 1920 h^{-1}, H_2:CO = 1:1, 2:1, 4:1).

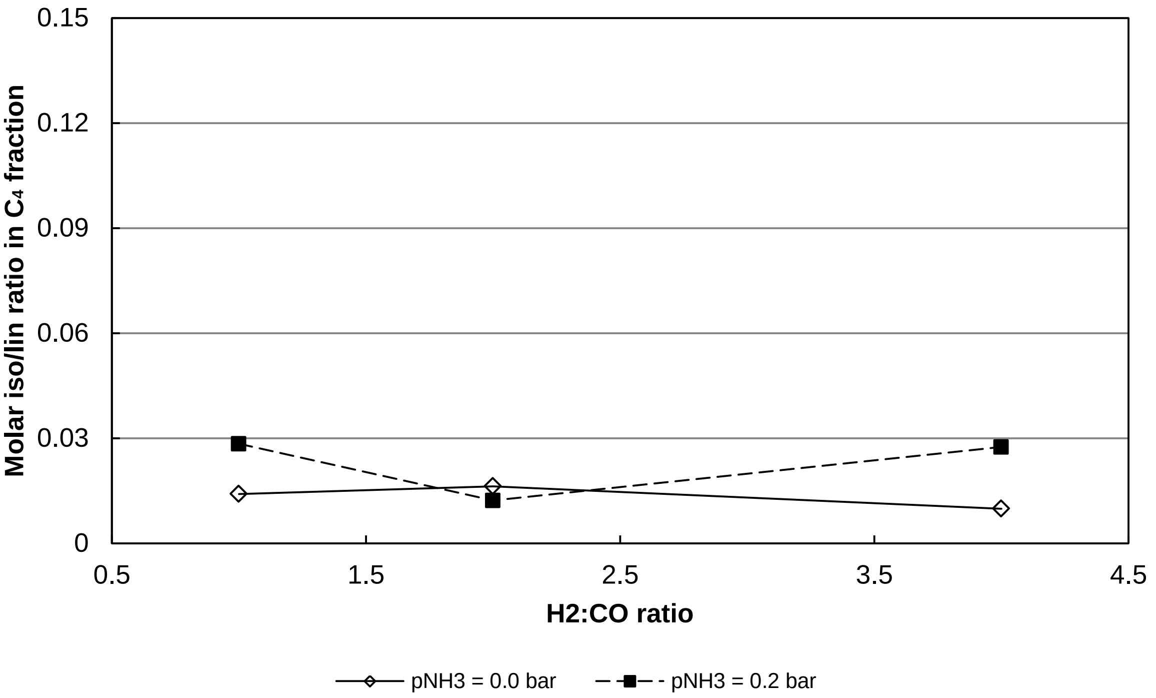

Figure 7.22: Molar iso/lin hydrocarbon ratio in C_4 fraction during FT/NH_3-FT runs on iron catalysts doped with 2 wt% potassium at different ammonia partial pressures ($T_{Reactor}$ = 270 °C, P_{Total} = 4 bar, p_{NH3} = 0.0 - 0.2 bar, GHSV = 1920 h^{-1}, H_2:CO = 1:1, 2:1, 4:1).

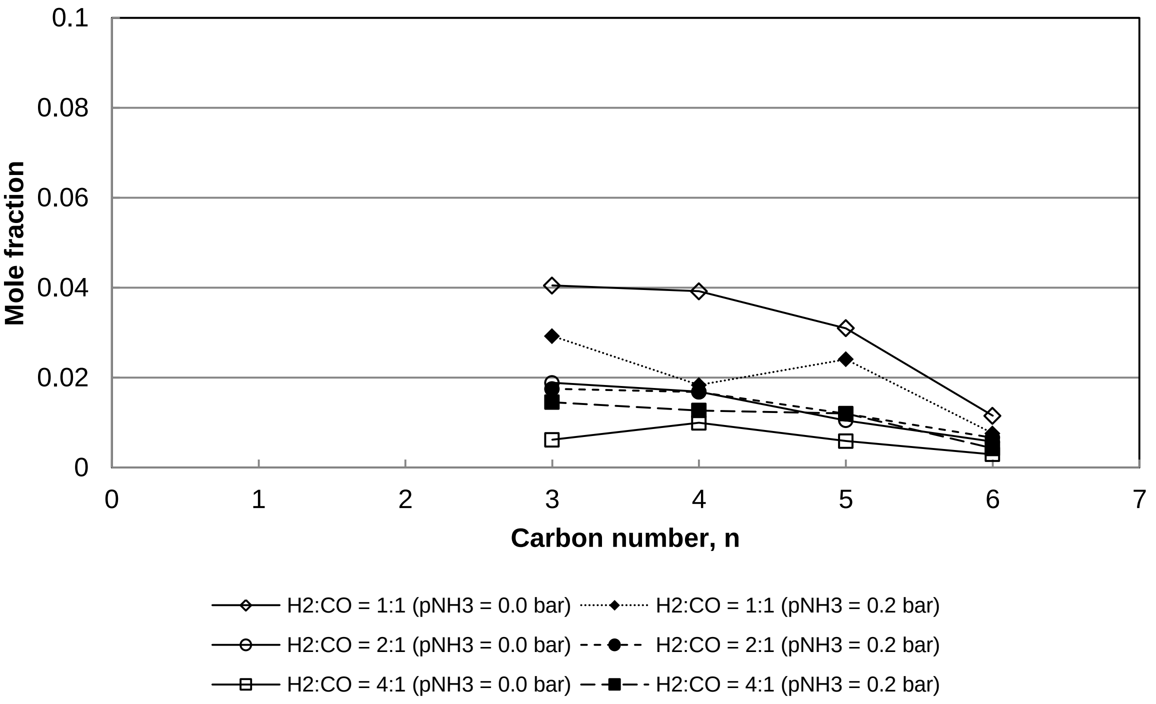

Figure 7.23: Mole fraction of methyl-ketones in all linear organic products during FT/NH_3-FT runs on iron catalysts doped with 2 wt% potassium at different NH_3 partial pressures ($T_{Reactor}$ = 270 °C, P_{Total} = 4 bar, p_{NH3} = 0.0 - 0.2 bar, GHSV = 1920 h^{-1}, H_2:CO = 1:1, 2:1, 4:1).

Table 7.8: Chain growth probability α during FT/NH_3-FT runs on iron catalysts doped with 2 wt% potassium at different NH_3 partial pressures and synthesis gas compositions ($T_{Reactor}$ = 270 °C, P_{Total} = 4 bar, p_{NH3} = 0.0 - 0.2 bar, GHSV = 1920 h^{-1}, H_2:CO = 1:1, 2:1, 4:1).

H_2:CO ratio	**Chain growth probability**	
	α_{C3-C8} (p_{NH3} = 0.0 bar)	α_{C3-C8} (p_{NH3} = 0.2 bar)
1:1	0.66	0.66
2:1	0.64	0.64
4:1	0.60	0.60

7.4.3 Variation of the gas hourly space velocity (GHSV)

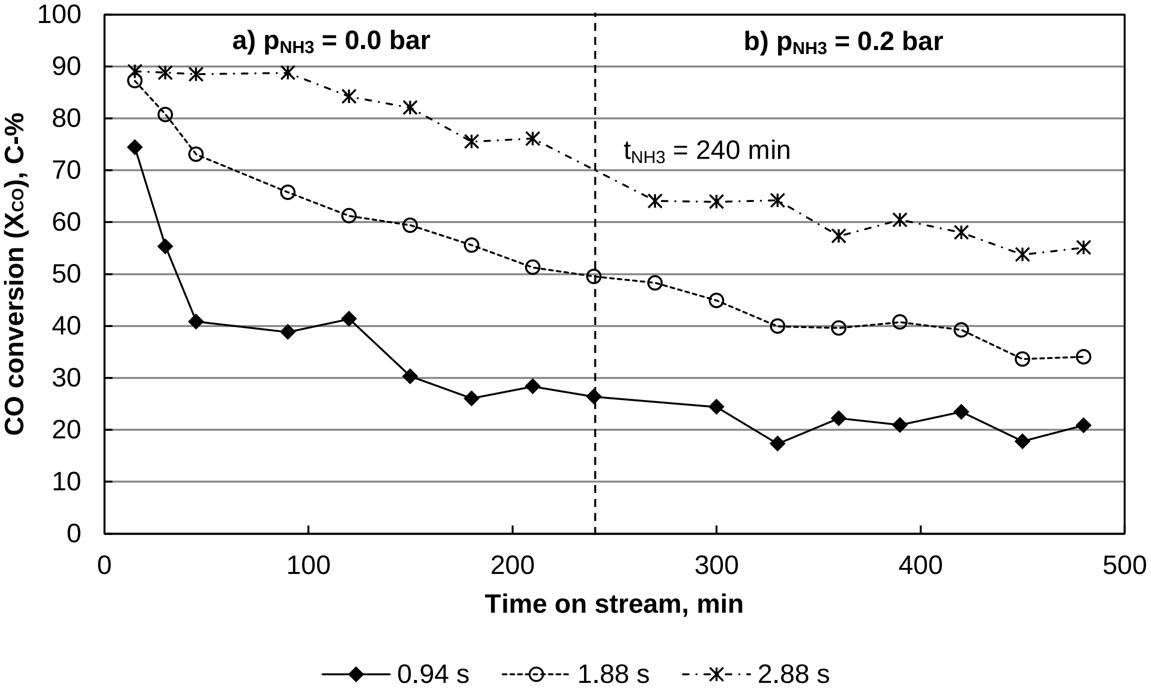

Figure 7.24: : CO conversion (X_{CO}, C-%, organic products plus CO_2) during FT/NH_3-FT runs on iron catalysts doped with 2 wt% potassium in: a) the absence of NH_3 and b) the presence of NH_3 ($T_{Reactor}$ = 270 °C, P_{Total} = 4 bar, p_{NH3} = 0.0 - 0.2 bar, GHSV = 1280 - 3840 h^{-1}, H_2:CO = 2:1).

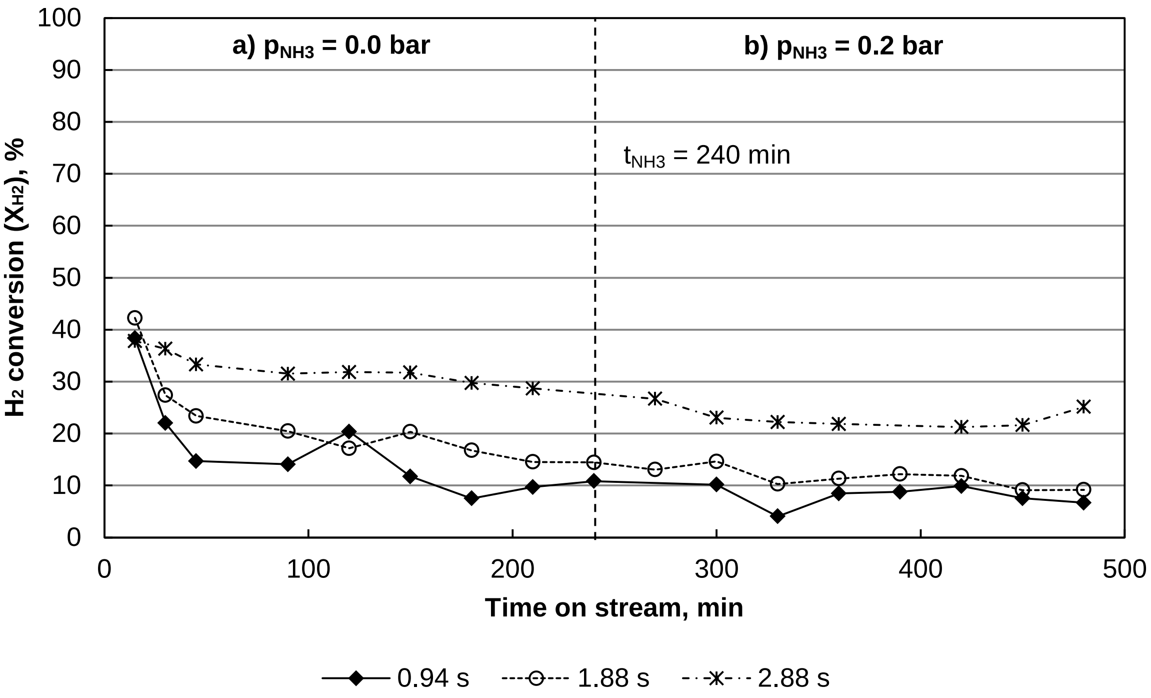

Figure 7.25: H_2 conversion (X_{H2}, %) during FT/NH_3-FT runs on iron catalysts doped with 2 wt% potassium in: a) the absence of NH_3 and b) the presence of NH_3 ($T_{Reactor}$ = 270 °C, P_{Total} = 4 bar, p_{NH3} = 0.0 - 0.2 bar, GHSV = 1280 - 3840 h^{-1},H_2:CO = 2:1).

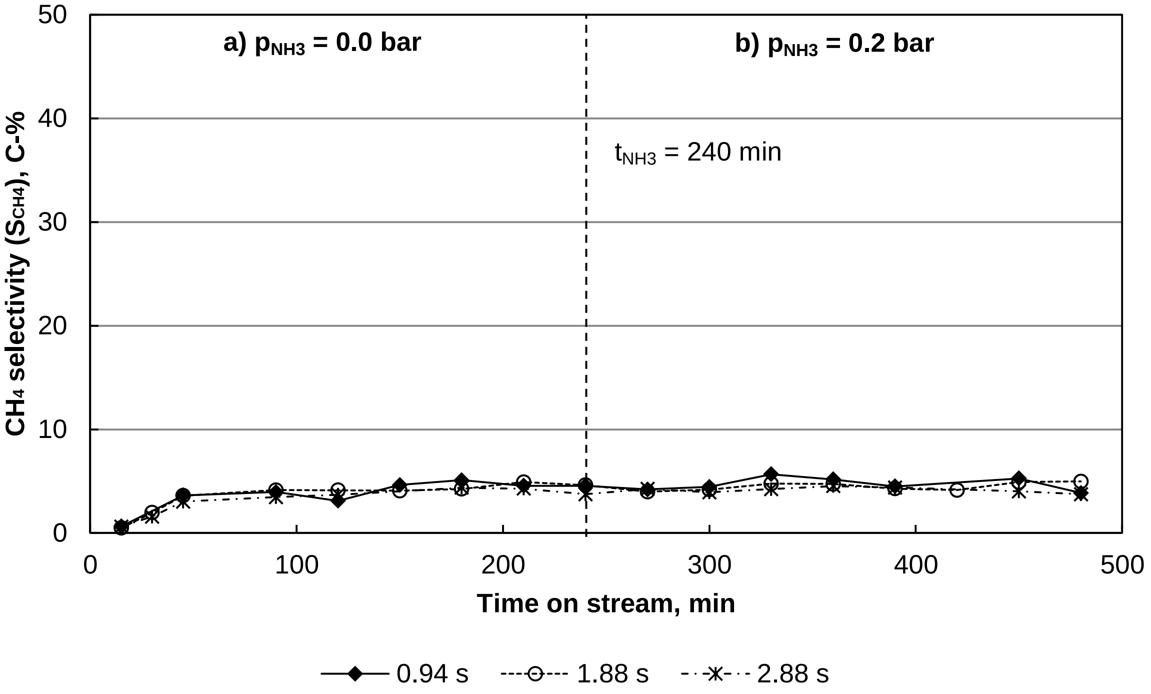

Figure 7.26: CH_4 selectivity (S_{CH4}, C-%) calculated from overall X_{CO} (CO_2 and organic products) during FT/NH_3-FT runs on iron catalysts doped with 2 wt% potassium in: a) the absence of NH_3 and b) the presence of NH_3 ($T_{Reactor}$ = 270 °C, P_{Total} = 4 bar, p_{NH3} = 0.0 - 0.2 bar, GHSV = 1280 - 3840 h^{-1}, H_2:CO = 2:1).

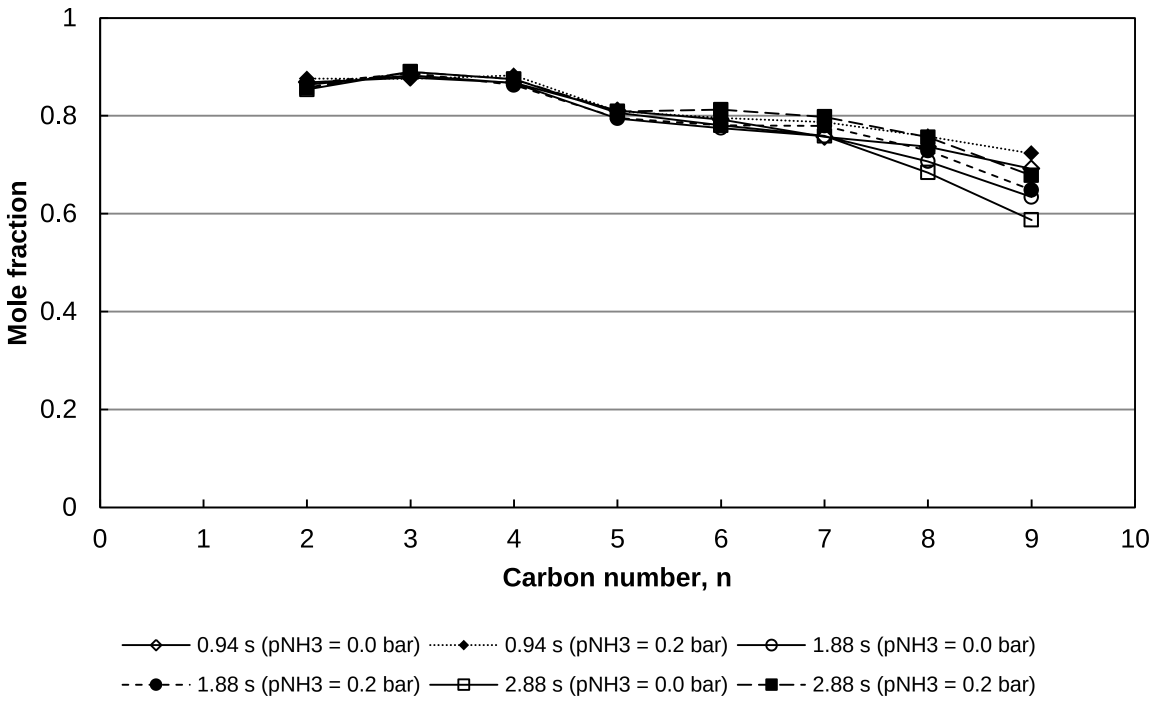

Figure 7.27: Mole fraction of olefins in linear hydrocarbons (olefins and *n*-paraffins) during FT/NH_3-FT runs on iron catalysts doped with 2 wt% potassium at different NH_3 partial pressures ($T_{Reactor}$ = 270 °C, P_{Total} = 4 bar, p_{NH3} = 0.0 - 0.2 bar, GHSV = 1280 - 3840 h^{-1}, H_2:CO = 2:1).

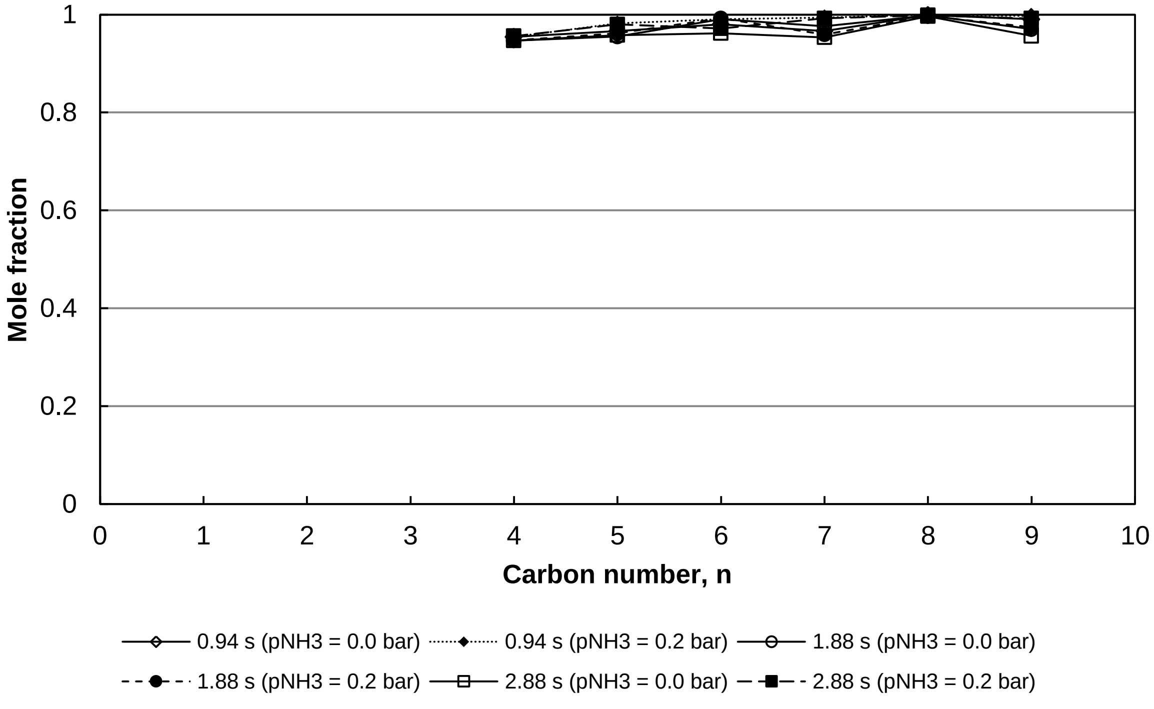

Figure 7.28: Mole fraction of 1-olefins in linear olefins (1- and 2-olefins) during FT/NH_3-FT runs on iron catalysts doped with 2 wt% potassium at different NH_3 partial pressures ($T_{Reactor}$ = 270 °C, P_{Total} = 4 bar, p_{NH3} = 0.0 - 0.2 bar, GHSV =1280 - 3840 h^{-1}, H_2:CO = 2:1).

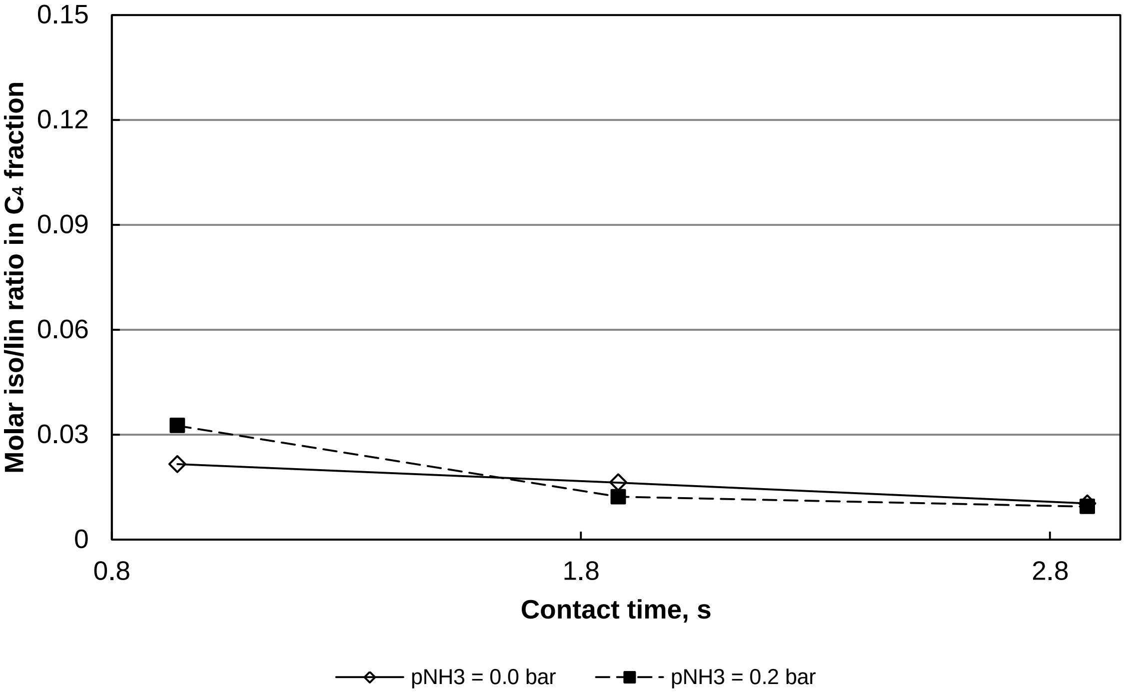

Figure 7.29: Molar iso/lin hydrocarbon ratio in C_4 fraction during FT/NH_3-FT runs on iron catalysts doped with 2 wt% potassium at different ammonia partial pressures ($T_{Reactor}$ = 270 °C, P_{Total} = 4 bar, p_{NH3} = 0.0 - 0.2 bar, GHSV = 1280 - 3840 h^{-1}, H_2:CO = 2:1).

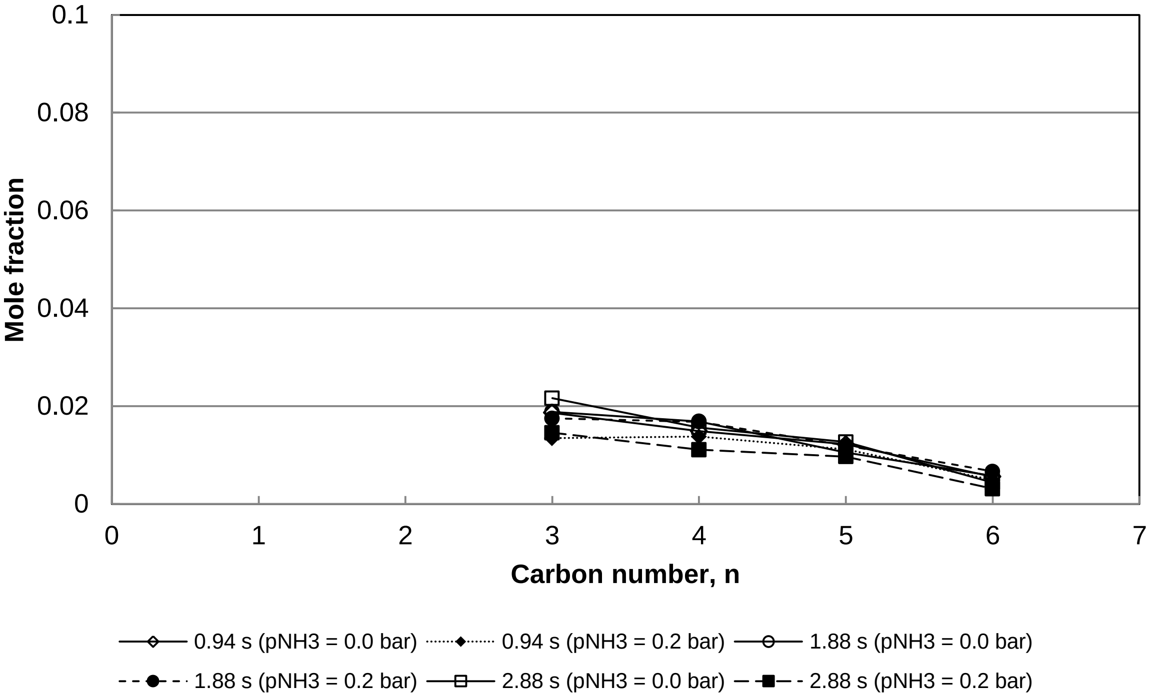

Figure 7.30: Mole fraction of methyl-ketones in all linear organic products during FT/NH_3-FT runs on iron catalysts doped with 2 wt% potassium at different NH_3 partial pressures ($T_{Reactor}$ = 270 °C, P_{Total} = 4 bar, p_{NH3} = 0.0 - 0.2 bar, GHSV = 1280 - 3840 h^{-1}, H_2:CO = 2:1).

Table 7.9: Chain growth probability α during FT/NH_3-FT runs on iron catalysts doped with 2 wt% potassium at different NH_3 partial pressures and synthesis gas compositions ($T_{Reactor}$ = 270 °C, P_{Total} = 4 bar, p_{NH3} = 0.0 - 0.2 bar, GHSV = 1280 - 3840 h^{-1}, H_2:CO = 2:1).

Contact time (s)	**Chain growth probability**	
	α_{C3-C8} (p_{NH3} = 0.0 bar)	α_{C3-C8} (p_{NH3} = 0.2 bar)
0.94	0.64	0.65
1.88	0.64	0.64
2.88	0.64	0.64

7.4.4 FT/NH_3-FT experiments on bulk cobalt catalysts

Table 7.10: Conversion of CO (C-%), H_2 (%) and NH_3 (area%) during FT/NH_3-FT runs at different ammonia partial pressures ($T_{Reactor}$ = 250 °C, P_{Total} = 4 bar, p_{NH3} = 0.0 - 0.2 bar, GHSV = 1920 h^{-1}, H_2:CO = 1:1).

Conversion	**p_{NH3} = 0.0 bar**	**p_{NH3} = 0.2 bar**
CO (C-%)	4.2	3.6
H_2 (%)	19.9	16.3
NH_3 (area%)	-	2.4

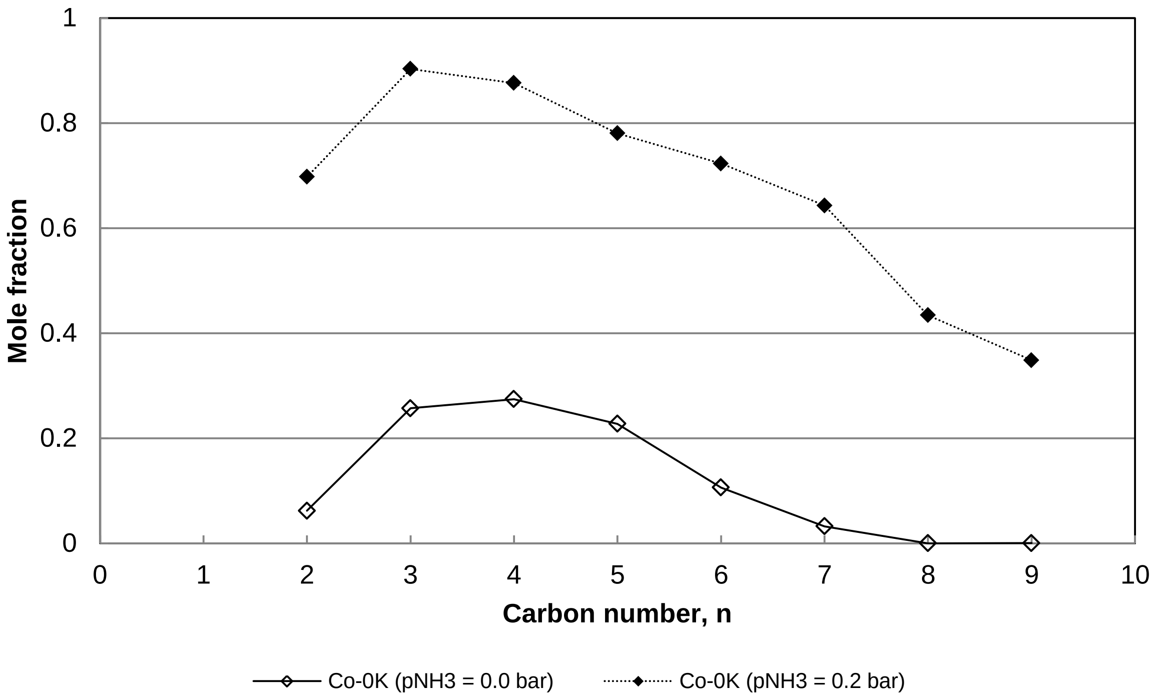

Figure 7.31: Mole fraction of olefins in linear hydrocarbons (olefins and *n*-paraffins) during FT/NH_3-FT runs on bulk cobalt catalysts at different NH_3 partial pressures ($T_{Reactor}$ = 250 °C, P_{Total} = 4 bar, p_{NH3} = 0.0 - 0.2 bar, GHSV = 1920 h^{-1}, H_2:CO = 1:1).

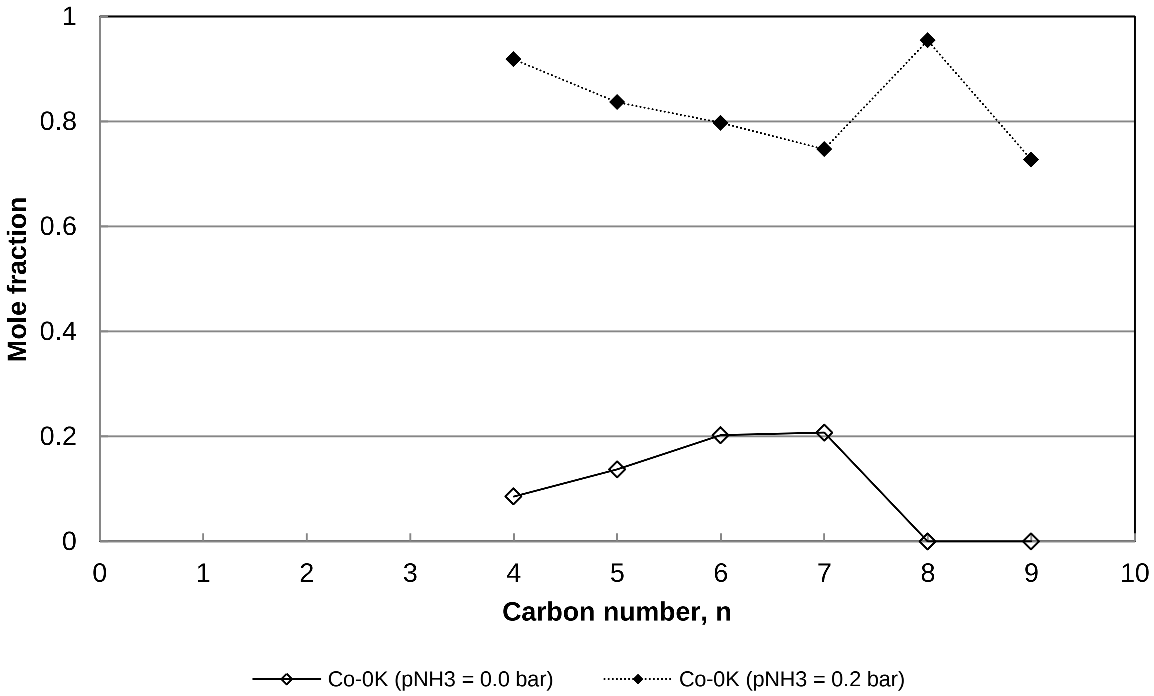

Figure 7.32: Mole fraction of 1-olefins in linear olefins (1- and 2-olefins) during FT/NH_3-FT runs on bulk cobalt catalysts at different NH_3 partial pressures ($T_{Reactor}$ = 250 °C, P_{Total} = 4 bar, p_{NH3} = 0.0 - 0.2 bar, GHSV =1920 h^{-1}, H_2:CO = 1:1).

7.4.5 Molar flow rates

Not all the rates obtained from the experiments will presented and as an example, the molar flow rates during FT experiments on iron catalysts doped with 2 wt% potassium (p_{NH3} = 0.0 bar) will be shown.

Table 7.11: Molar flow rates (mol/min) obtained from GC-TCD analysis during FT experiments on bulk iron catalysts doped with 2 wt% potassium in the absence of ammonia ($T_{Reactor}$ = 270 °C, P_{Total} = 4 bar, p_{NH3} = 0.0 bar, GHSV = 1920 h^{-1}, H_2:CO = 2:1).

Compound	**Molar flow rate** (mol/min) [1]
Hydrogen	7.7E-04
Argon	2.02E-04
Carbon monoxide	2.03E-04
Methane	9.2E-06
Carbon dioxide	1.3E-04

[1] Molar flow rates after 240 min of time on stream (TOS).

Table 7.12: Molar flow rates (mol/min) obtained from GC-FID analysis during FT experiments on bulk iron catalysts doped with 2 wt% potassium in the absence of ammonia ($T_{Reactor}$ = 270 °C, P_{Total} = 4 bar, p_{NH3} = 0.0 bar, GHSV = 1920 h^{-1}, H_2:CO = 2:1).

Compound	**Molar flow rate** (mol/min)	**Compound**	**Molar flow rate** (mol/min)
Methane	5.0E-06	1-Pentene	4.5E-07
Ethene	2.0E-06	*n*-Pentane	1.2E-07
Ethane	3.1E-07	1-Hexene	2.7E-07
Propene	1.4E-06	*n*-Hexane	7.8E-08
Propane	1.9E-07	Cyclohexane	2.6E-07
Acetaldehyde	7.4E-07	1-Heptene	1.8E-07
2-Methylpropane	1.5E-08	*n*-Heptane	5.8E-08
1-Butene	7.7E-07	1-Octene	1.2E-07
n-Butane	1.2E-07	*n*-Octane	5.2E-08
2-Butene (tr.)	2.2E-08	1-Nonene	1.0E-07
2-Butene (cis)	2.1E-08	*n*-Nonane	6.0E-08

Table 7.13: Molar flow rates (mol/min) obtained from GC-MS analysis during FT experiments on bulk iron catalysts doped with 2 wt% potassium in the absence of ammonia ($T_{Reactor}$ = 270 °C, P_{Total} = 4 bar, p_{NH3} = 0.0 bar, GHSV = 1920 h^{-1}, H_2:CO = 2:1).

Compound	**Molar flow rate** (mol/min)	**Compound**	**Molar flow rate** (mol/min)
Methanol	4.4E-10	2-Pentanone	6.8E-09
Ethanol	3.1E-07	Pentanal	2-8E-08
Propanal	2.0E-07	2-Heptene (tr.)	2.1E-09
2-Propanone	3.6E-08	Propanoic acid	5.4E-08
2-Pentene (tr.)	9.9E-09	2-Heptene (cis)	2.2E-09
2-Pentene (cis)	1.1E-08	1-Pentanol	1.7E-08
1-Propanol	3.0E-08	2-Hexanone	2.3E-09
Butanal	1.8E-08	Hexanal	2.4E-08
2-Butanone	1.7E-08	Butanoic acid	1.4E-08
2-Hexene (tr.)	2.1E-10	2-Octene (tr.)	9.9E-11
2-Hexene (cis)	7.7E-11	2-Octene (cis)	1.3E-10
Acetic acid	2.3E-07	1-Hexanol	1.3E-08
Cyclohexane	2.6E-07	2-Nonene (tr.)	2.3E-09
1-Butanol	1.2E-08	Pentanoic acid	1.3E-09

Selbstständigkeitserklärung

Hiermit erkläre ich, dass ich diese Arbeit selbstständig und ohne unerlaubte fremde Hilfe verfasst und keine anderen als die angegebenen Quellen und Hilfsmittel benutzt habe.

Robert Henkel

Oldenburg, 05. September 2012 Robert Henkel

Lebenslauf

Persönliche Daten

Name	Robert Henkel
Geboren am	27. April 1981 in Demmin
Staatsangehörigkeit	deutsch

Ausbildung

02/2008 - 12/2011	Promotionsstudium an der Carl von Ossietzky Universität Oldenburg in der Arbeitsgruppe Technische Chemie 2
01/2011 - 02/2011	Forschungsaufenthalt an der Suranaree University of Technology (Thailand) am Institute of Science
11/2010 - 12/2010	
09/2008 - 01/2009	Forschungsaufenthalte an der University of Cape Town (Südafrika) am Department of Chemical Engineering
10/2002 - 01/2008	Studium der Chemie an der Carl von Ossietzky Universität Oldenburg in der Arbeitsgruppe Technische Chemie 2
1993 - 2002	Kooperative Gesamtschule in Schneverdingen
1990 - 1993	Hans-Beimler-Oberschule in Bergen/Rügen
1987 - 1990	Grundschule in Dranske/Rügen

Robert Henkel

Oldenburg, den 05. September 2012 Robert Henkel